BULLETION OF THE MINERAL RESEARCH AND EXPLORATION

Foreign Edition 2015 150

CONTENTS

Bull. Min. Res. Exp. (2015) 150: 1-18

Bulletin of the
Mineral Research and Exploration

http://bulletin.mta.gov.tr

The GEOLOGY of GÖKÇEADA (ÇANAKKALE)

Ramazan SARI[a,*], Ahmet TÜRKECAN[b], Mustafa DÖNMEZ[b], Şahset KÜÇÜKEFE[a], Ümit AYDIN[c] and Öner ÖZMEN

[a] *Maden Tetkik ve Arama Genel Müdürlüğü Balıkesir Bölge Müdürlüğü*
[b] *Maden Tetkik ve Arama Genel Müdürlüğü Jeoloji Etütleri Dairesi Başkanlığı*
[c] *Maden Tetkik ve Arama Genel Müdürlüğü Maden Etüt ve Arama Dairesi Başkanlığı*

Keywords:
Gökçeada, Geology,
Volcanism, Magmatism

ABSTRACT

The geology and especially the magmatic rocks of Gökçeada, which is the biggest island of Turkey and located at 20 km's west of Biga Peninsula, constitute the subject of this study. Late Ediacaran/Early Paleozoic aged Çamlıca metamorphics which crop out with a tectonic uplift in a narrow area in northwest of Gökçeada are the oldest rocks of the island. Early Eocene aged Karaağaç Formation which is formed by submarine fan deposits unconformably overlies Çamlıca metamorphics. As for the Dağiçitepe volcanic member which is formed by rhyolitic lavas, tuff and tuffites emplaced into Karaağaç Formation cutting Çamlıca metamorphics is the oldest volcanic unit of the study area. On Karaağaç Formation, Koyunbaba Formation has unconformably been deposited which consists of Middle Eocene shallow marine sediments. Then it has conformably been overlain by Soğucak Formation which consists of SE-NW extending reefal limestone. Middle-Upper Eocene aged Ceylan Formation which conformably overlies the Soğucak Formation and the early Oligocene aged Mezardere Formation which conformably overlies Ceylan Formation have been deposited due to turbiditic currents in deep marine environment. Late Eocene(?) – Oligocene aged subvolcanics which cut Mesozoic and Eocene units and emplaced into Eocene aged sedimentary units in the form of crypto dome and dome form the recent rigid topography of the study area and are the second magmatic phase called the "Gökçeada Domes". Diorite-monzonites porphyry which crystallized in lower zones of subvolcanics on the other hand constitutes Mutludere intrusion. In eastern and southern parts of Gökçeada, Late Oligocene Gökçeada ignimbrites are located which are observed in the form of pumice flows on Mezardere Formation. These ignimbrites are then overlain by Early Miocene aged Kesmekaya volcanics which are formed by blocky ash flows. Middle Miocene aged Eşelek volcanics consisting of lava and pyroclastics with composition basaltic andesite and andesite are observed on a large area in east of Gökçeada. Upper Miocene aged Çanakkale Formation which is generally formed by the intercalation of poor consolidated conglomerate, sandstone, siltstone and marl crops out in narrow regions at east, southeast and south of Gökçeada. Quaternary alluvial deposits and debris composed of loose, unconsolidated sand, silt and other sediments unconformably overlie all previous units and complete the succession. Main tectonic structures of Gökçeada are formed by right lateral oblique faults which developed in Neo-tectonic period.

1. Introduction

Gökçeada is located at north of Aegean depression at southwest of Thrace and is approximately 20 km's away from Biga Peninsula (Figure 1). It belongs to Çanakkale Province, and is the biggest island of Turkey with an area of 289 km^2 and a coastal length of 92 km.

This study was made in order to prepare 1/25 000 scaled geological maps which will form a basis to polymetal researches in Gökçeada within scope of "Çanakkale-Balıkesir Ruhsat Etütleri" (Çanakkale-Balıkesir License Researches) subproject carried out between years 2008-2011 of the "Batı-Orta Anadolu Polimetal Maden Aramaları Projesi"

*Corresponding author: Ramazan Sarı, rsarimta@hotmail.com

(Project of West-Central Anatolian Polymetal Mineral Researches) of the General Directorate of Mineral Research and Exploration (MTA). Within this framework, geological maps previously prepared in Gökçeada were assessed, and the revision and/or detailed geological investigations at necessary areas were made. Paleontological, petrographical and mineralogical descriptions of samples were collected on field and their chemical analyses were performed in MTA labs. However, the geochronological dating were made in ActLab (Canada).

First significant geological investigations in Gökçeada have been realized by Akartuna (1950), Okut (1975), Akartuna and Atan (1978). However, especially the studies of Akartuna and Atan (1978) have been used during the preparation of geological maps. Later on; Ercan et al. (1995) have investigated the characteristics of Tertiary volcanism, and Kesgin and Varol (2003), Varol and Baykal (2008) have carried out studies related to the stratigraphy of sedimentary rocks. Ilgar et al. (2008), on the other hand have published 1/100.000 scaled geological map of the island. However, this island can merely be called as the "Land of Domes" because of their excessive domal structures forming the actual morphology. But, the magmatic rocks of Gökçeada have not been mentioned in any of these studies. However, an important magmatic activity in the island is in question. Therefore; the purpose of this investigation is to prepare geological maps in which magmatic rocks widely observed on the island were distinguished in detail, and contribute to researches related to reveal the geological evolution and mineral potential of the region.

2. Stratigraphy

In Gökçeada, metamorphic, magmatic and sedimentary rocks crop out ranging from Mesozoic to Quaternary. The formation names suggested in the book "Thrace Lithostratigraphical Units" (MTA, 2006) of the Stratigraphy Committee were used for the nomenclature of formations in which rocks have formed. The geological map of the island and generalized stratigraphical section of rocks were given in figures 1 and 2, respectively.

2.1. Çamlıca Metamorphics (Pєça)

This unit is composed of sericitic schist, chloritic schist, slate and marble layers. It was defined as "Çamlıca metamorphics" in Biga Peninsula by Okay et al. (1990) and in this study the same name was given to this unit. It crops out on Dağiçi Hill and in the stream located at west of Dağiçi Hill, in a very small area at northwest of Gökçeada (Figure 1).

More than 80% of Çamlıca metamorphics which form in sericitic and chloritic schists, slate and marble types are constituted by gray, dirty brown, greenish colored, well foliated, much micaeous, quartz-mica schists with carbonates in occasion. Petrographically; garnet-mica-quartz schist, and mica-quartz schist were detected in the unit. In addition to quartz and white mica minerals, calcite, biotite, albite, chlorite and garnet minerals are also widely present in these rocks.

The bottom of Çamlıca metamorphics does not appear in Gökçeada. These metamorphics have cropped out by faulting in the stream at west of Dağiçi Hill (Figure 3). The unit is while overlain by an angular discordance by Kuvizian-early Lutetian aged sediments (Figure 4), it is also crosscut by Eocene aged rhyolites and Oligocene aged subvolcanics.

The unit which was aged as Paleozoic by Akartuna and Atan (1978), though there was not found any fossils, is cut by Eocene and Oligo-Miocene granitoids in west of Karabiga town in Biga Peninsula (Ilgar et al., 2008). The age of metamorphism of the unit, using fengites in quartz-mica schists in Biga Peninsula, was determined as 65-69 My using Rb/Sr method (Okay and Satır, 2000). Recent studies carried out show that the primary depositional age of Çamlıca metamorphics is Late Ediacaran and/or Early Paleozoic (Tunç et al., 2012).

When the similarity of lithological and metamorphic characteristics of rocks in close vicinity is taken into consideration, it is thought that Çamlıca metamorphics resemble to Upper tectonical unit which is formed by quartz-mica schist and gneisses consisting of calc schist, marble and amphibolite interlayers in Rhodopian massive between Greece and Bulgaria (Papanikolau and Panagopulos, 1981; Barr et al., 1999; Okay and Satır, 2000; Duru et al., 2008).

2.2. Karaağaç Formation (Tek)

In west-northwest of Gökçeada, conglomerate, sandstone, claystone, marl intercalation and volcanic rocks in rhyolitic composition crop out between Gizli Harbor and Mutlu Stream. This unit was first introduced by Sfondrini (1961) in Thrace as "Karaağaç unit" and was named as Karaağaç Formation in Gökçeada within scope of this study.

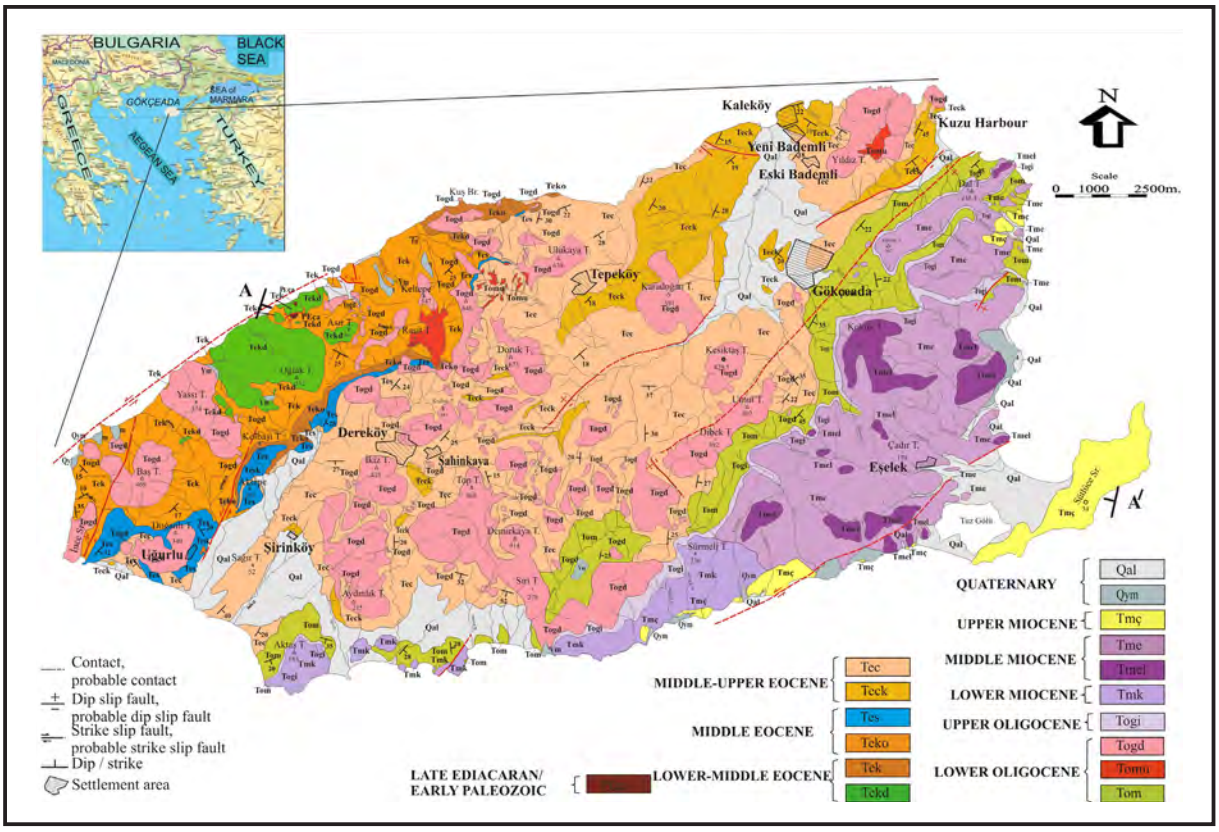

Figure 1- Geological map of Gökçeada (modified from Akartuna and Atan (1978)). Qal- Alluvial; Qym- debris; Tmç- Çanakkale Formation: sandstone, claystone, siltstone etc.; Tme- Eşelek volcanics: Basaltic andesite, andesitic pyroclastics; Tmel- Lava member: Gray-dark gray colored pyroxene andesitic lava; Tmk- Kesmekaya volcanics: Ash-block flow, lahar type pyroclastic flows; Togi- Gökçeada ignimbrite: Dark white colored pumice and pumice flow; Togd- Gökçeada domes: Porphyritic andesite; Tomu- Mutludere intrusion: Quartz monzonite, diorite-diorite porphyry; Tom- Mezardere Formation: Conglomerate, sandstone, siltstone, marl, etc.; Tec- Ceylan Formation: Claystone, sandstone, siltstone, shale, marl, etc.; Teck- sandstone member: Medium-thick bedded sandstone, siltstone; Tes- Soğucak Formation: Reefal limestones: Teko- Koyunbaba Formation: Conglomerate, sandstone, siltstone; Tek- Karaağaç Formation: sandstone, claystone, limestones, marl, conglomerate, etc.; Tekd- Dağiçitepe volcanic: Rhyolitic lava, tuff and tuffite; Pєça- Çamlıca metamorphics: Mica schist, sericitic schist, chloritic schists etc.

Karaağaç Formation begins with conglomerate at the bottom and consists of coarse and thick sandstone layers, rhyolitic tuffs and channel fill sediments towards upper parts. Thin bedded limestone layers take place at lower parts of the formation and consists of much nummulitic fossils. Lensoidal channel fill sediments form the uppermost layer of the succession and channel bottoms have abrasive surface. Within channels, mudstone pieces and mollusks of marine fossils are observed.

The lower contact of the unit unconformably overlies Çamlıca metamorphics in stream at west-northwest of Dağiçi Hill and is then overlain by Koyunbaba Formation.

Karaağaç Formation which has 900 m thickness in Aktaş locality (Kesgin and Varol, 2003) were interpreted as submarine fan deposits which become shallow in upper parts then grades into deltaic deposits (Ilgar et al., 2008).

In samples collected from lowermost parts of the formation which unconformably overlie Çamlıca Formation;

Assilina suteri SCHAUB, 1981,

Assilina tenuimarginata HEIM, 1908,

Assilina cuvillieri SCHAUB, 1981,

Assilina maior HEIM, 1908,

Nummulites praediscorbinus SCHAUB, 1981,

Nummulites cf *lehneri* SCHAUB, 1962,

Nummulites boussaci ROZLOZSNIK, 1924,

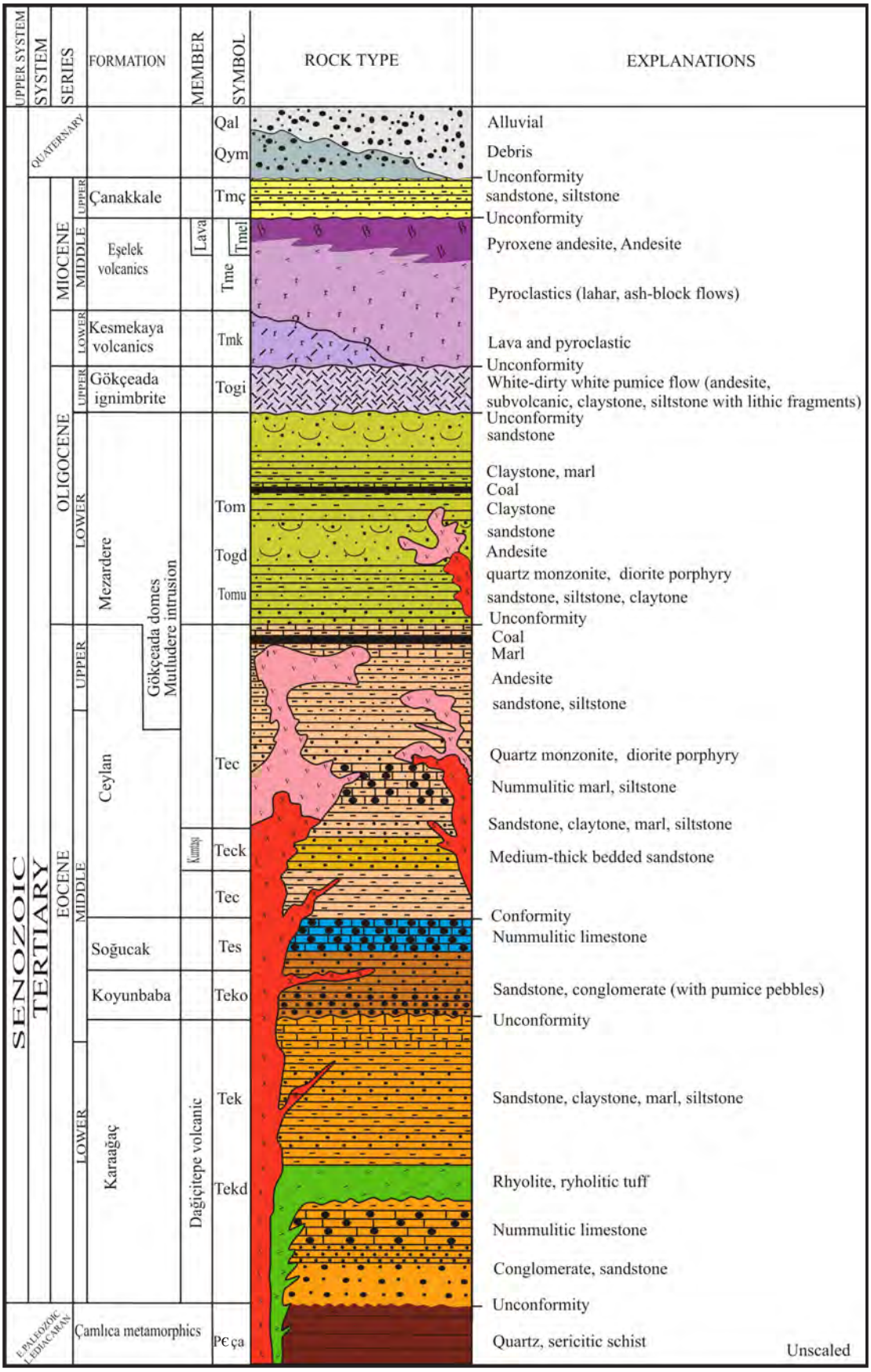

Figure 2- Generalized columnar section of Gökçeada.

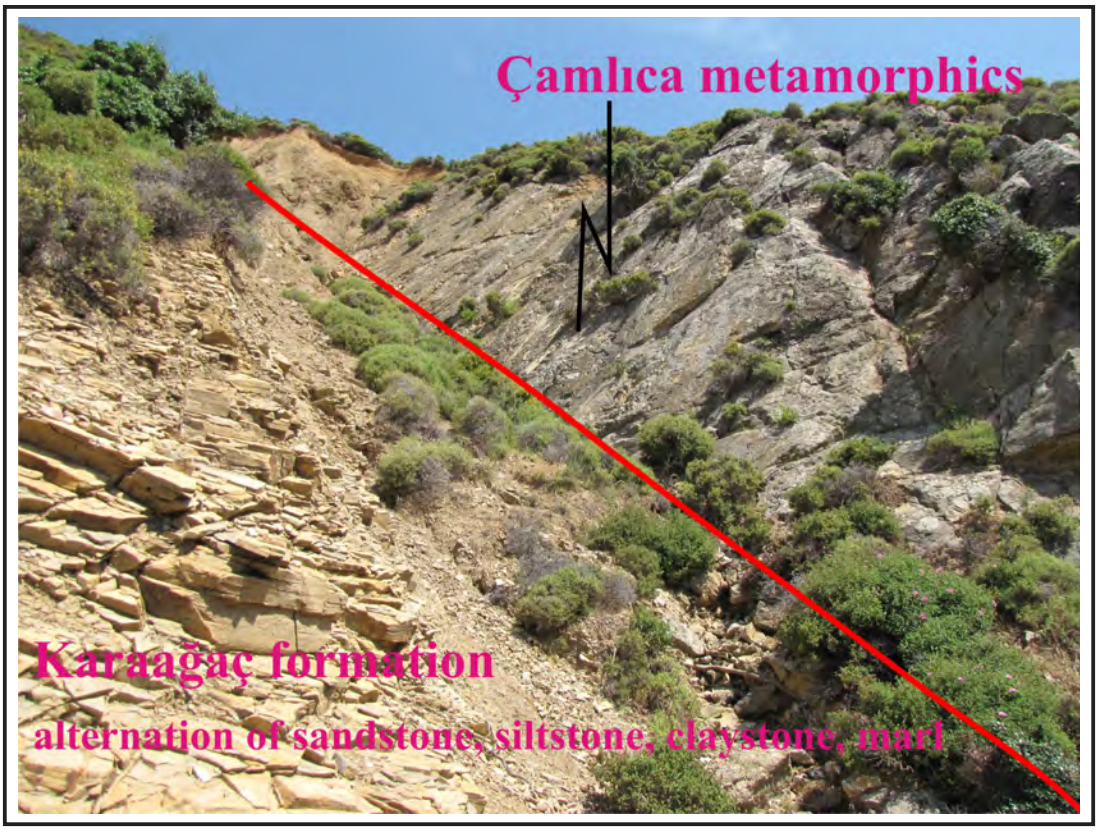

Figure 3- Tectonical contact between Çamlıca metamorphics and Karaağaç Formation (Dağiçi Hill)

Figure 4- Discordant contact between Çamlıca metamorphics and Karaağaç Formation (in the stream at west of Dağiçi Hill).

Assilina sp., *Nummulites* spp., *Discocylina* spp., Linderina? sp. fossils were found and described by Dr. Şükrü Acar. According to this fossil content, the depositional age of the unit should be latest Kuvizian-earliest Lutetian.

2.2.1. Dağiçitepe Volcanic Member (Tekd)

Much altered rhyolitic volcanics which crop out at coast and places close to coasts, northwest of Gökçeada, were first introduced within scope of this study and named as Dağiçitepe Volcanic Member. Unit crops out in Asar Hill, Taşlı Stream, Günbatan Hill, Oğlak Hill, Oğlak stream, Dağiçi Hill and Çatal Hill, and its type locality is Dağiçi Hill (Figure 1).

The unit is composed of lava and tuffs in rhyolitic composition. Lava outcrops are in the form of domes, much jointed and fractured. Especially, well developed columnar structures are observed on the coast. Lavas are white to gray colored and porhyritic in texture. Macroscopically; much quartz, biotite and hornblende phenocryts, and intense epidotization in feldspars are observed.

Lavas of Dağiçitepe volcanics cut Çamlıca metamorphics and are emplaced within Karaağaç Formation. The tuffites which are distinctive with their white color are observed as conformable in deposits. In the first phase of the volcanic activity first tuffs then lavas have erupted and emplaced in the environment, and were occasionally cut by Oligocene aged sub volcanic rocks (Figure 5).

Figure 5- Contact of Karaağaç Formation and Dağiçitepe volcanic (northwestern slope of the hill, elevation: 355 m).

It is considered that volcanic activities in question were effective between ranges of Kuvizian-Lutetian as tuffs intercalate with Karaağaç Formation and domes cut those deposits.

Similar type, whitish tuffs related to volcanics show 1 to 6 meters thickness as intercalated with Lower-Middle Eocene deposits in Limnos Island as well (Innocenti et al., 1994).

2.3. Koyunbaba Formation (Teko)

It crops out as clastics in red-brown, gray and greenish colors in Saklı Harbor at west-northwest of Gökçeada, northeast of Aktepe, south of Raşit Hill, northwest of Dereköy, north of Soğucak Hill, and on Kolbaşı Hill and around Kuş Foreland at north of the island. These clastics extend in SW-NE directions and were named as Koyunbaba Formation. The unit was first named by geologists of Esso Standard (1960) as the Koyunbaba member of Yeniköy Formation, then were upgraded into Formation level by Keskin /1974) and Kasar et al. (1983).

It begins with pebbles at the bottom and grades into conglomerate-sandstone-siltstone-marl intercalation in upper layers. Pebbles, thin to medium bedded formation, are mostly in the form of channel fill. The unit consists of schist, quartzite, limestone pebbles, and rhyolitic pebbles and pumice pieces which is considered as Early Eocene volcanism (Figure 6). Pebbles are well rounded and medium to well sorted. Dark brown, black colored nodules which formed with pyrite condensations are also observed in sandstones.

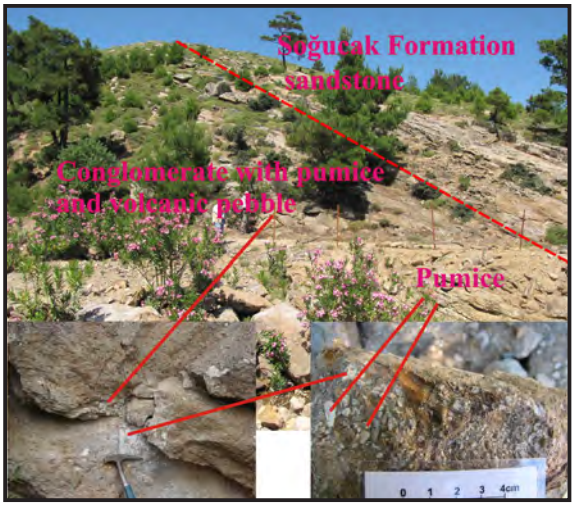

Figure 6- Koyunbaba Formation; volcanic conglomerate, sandstone with pumice (west – southwest of Yumurta Hill).

Koyunbaba Formation unconformably overlies Karaağaç Formation, however conformably underlies limestones of Soğucak Formation. Although there was not detected any fossil at outcrops of the formation

in Gökçeada, the age of it should be Middle Eocene according to regional correlation.

The unit was previously described as Fıçıtepe Formation by some investigators (Temel and Çiftçi, 2002; Ilgar et al., 2008; Varol and Baykal, 2008), but in the book of "Thrace Region Lithostratigraphical Units" (2006) of the Stratigraphy Committee it says that;

For Koyunbaba Formation: "Koyunbaba Formation is mainly formed by conglomerate and sandstones and sporadically consists of marl, clay, limestone and huge blocks of the basement. These lithologies represent bottom clastics which are the primary products of Middle-Late Eocene aged marine transgression. Koyunbaba Formation unconformably overlies older units and gradually transits into Soğucak Formation above".

For the Fıçıtepe Formation: "Fıçıtepe Formation is lithologically composed of conglomerate, sandstone and mudstone. It is gradually transitional with Karaburun member of the Karaağaç Formation below, however; there is angular unconformity with Middle Eocene Koyunbaba and Soğucak Formations above."

Considering stratigraphical and lithological characteristics of the unit mapped in Gökçeada, it was named as Koyunbaba Formation in this study.

2.4. Soğucak Formation (Tes)

Much nummulitic limestones and less amount sandy, pebbly limestones crop out in this formation. The unit that have similar characteristics were named as Soğucak Formation in Gökçeada (Sümengen and Terlemez, 1991) and the same name was also used for their outcrops in Gökçeada. It crops out extending in NW-NE directions, in west-northwest of Gökçeada among Saklı Harbor, Ak Hill, Yumurta Hill, Soğucak Hill, north of Soğucak Hill, Delik Hill and Karaçalı Hill, in northeast of Mutlu Hill and northwest of Ulukaya Hill (Figure 1).

The unit is generally composed of limestone and lesser amount of sandstone. Limestones are occasionally horizontally bedded, lensoidal, gray to pale gray, white colored, hard, porous and with dissolution spaces. It grades into clayey limestone in upper layers. Sandstones and thin pebbles are 1 to 2 meters thick at layers closer to bottom. Much gastropoda, coral and nummulite fossils were described in limestones belonging to Soğucak Formation. Varol and Baykal (2008) found Fabiania cassis (Oppenheim), *Spharegypsina* sp., *Alveolina* sp., *Gypsina* sp., *Nummulites* sp., *Discocylina* sp., *Gyroidinella* sp., *Rotalia* sp., *Asterocyclina* sp., *Globigerapsis* sp., *Asterigerina* sp., Rotalidae in the formation that display the characteristics of patch reef and aged the formation as Middle Eocene. Especially in Aktepe, nummulitic fossils with diameters exceeding 5 cm are available (Figure 7).

Figure 7- Soğucak Formation; nummulite fossils in limestones (South of Ak Hill).

While Soğucak Formation is transitional with Koyunbaba Formation in Gökçeada, it is unconformably overlain by Early Eocene aged Karaağaç Formation. This unit is transitional with the overlying Ceylan Formation and cut by Oligocene aged Gökçeada domes.

Soğucak Formation which is composed of sparitic, micritic limestones, pebble and sandy limestones reflect the deposition which occurred in shallow marine environment due to its sedimantological and structural characteristics and fossil assemblage (Ilgar et al., 2008).

Measured thicknesses of the unit are 60 and 120 meters around Ak Hill and Dereköy, respectively (Kesgin and Varol, 2003).

2.5. Ceylan Formation (Tec)

Ceylan Formation is formed by the alternation of claystone-sandstone-shale. The formation was first introduced by Ünal (1967) in Thrace and was first used in Gökçeada by Temel and Çiftçi (2002). The unit crops out in NE-SW directions and is observed in a large area of the island among Şirinköy, Dereköy, Şahinkaya, Tepeköy, Bademli Village, Kuzu Harbor and Gökçeada town center (Figure 1).

Ceylan Formation is formed by the alternation of shale-sandstone. Unit which is deposited in deep sea becomes shallower and grades into Mezardere Formation. Shales are greenish, bluish gray, hard and highly altered in places close to volcanics, metamorphosed in places, with splinted breaks, folded in places and are thin sandstone banded. Sandstones generally consist of quartz, yellowish gray colored, hard, with angular breaks, carbonate cemented, fine to medium grained. Plant residuals are occasionally observed. Sandstones which can be mapped in the study area were mapped as Sandstone Member (Figure 1). Non-economical, lensoidal lignite occurrences reaching up to 40-50 cm thicknesses were also encountered in the unit which graded into Mezardere Formation by getting shallower (Figure 8). Engraved tuff and very fine grained volcanic materials were also encountered within deposits of Ceylan Formation.

Figure 8- Lenses of lignite within upper layers of shallowing Ceylan Formation (eastern and northeastern slopes of Orta Hill).

Ceylan Formation which shows thicknesses of nearly 400–900 meters (Kesgin and Varol, 2003) conformably overlies Soğucak Formation and is conformably overlain by Mezardere Formation. The unit was also cut by Gökçeada domes.

Fossil assemblages which were obtained from Ceylan Formation deposited in turbiditic system, generally in deep sea, indicate that the unit is Middle-Late Eocene (Akartuna and Atan, 1978; Kesgin and Varol, 2003; Ilgar et al., 2008).

2.5.1. Sandstone Member (Teck)

Yellowish, pale brown, medium to thick bedded, well sorted mappable sections of sandstones containing top and bottom structures such as; cut, fill and flute etc. within Ceylan Formation were distinguished as the "Sandstone Member". The unit crops out in SE of Tepeköy, Dereköy, Doruk Hill and in vicinity of Kaleköy and Kuzu Harbor. Archeological excavations carried out in the region indicated that sandstones had been used as building stone since B.C. 3000 (Figure 9) (Hüryılmaz, H., 2011, oral communication).

Figure 9- Ceylan Formation; the use of Sandstone member as building stone in B.C. 3000 (Büyükdere valley, Yenibademli tumulus).

2.6. Mezardere Formation (Tom)

This unit which is formed by early Oligocene aged conglomerate and lesser amount of sandstone, siltstone and marl in Gökçeada was named as Mezardere Formation. The Formation was first introduced and named by Ünal (1967) in Thrace, and it was first used by Temel and Çiftçi (2002) in Gökçeada.

The unit extends as a strip in NE-SW directions between Kuzu Harbor and Aktaş Hill (SW of Gökçeada) in northeast of Gökçeada. Outcrops are observed in north of Dal Hill (NE of Gökçeada) and SE of Gökçeada town center, in east; between Dibek Hill and Gölyeri Hill, in Balıkçı locality, in southwest; north and east of Aktaş Hill (Figure 1).

The unit is generally formed by the alternation of conglomerate and by lesser amount of sandstone, siltstone and marl. Mezardere Formation begins to deposit with yellowish, mustard colored, fine to medium grained, medium to badly sorted, medium to thick bedded sandstones. These sandstones intercalate with blue-gray and white colored marls. Within marl bearing layers, bitumen and coal occurrences are encountered sporadically. In sandstones ripple marks and lamellibranch mollusks are observed in occasion.

The thickness of the unit is approximately 500 meters (Temel and Çiftçi, 2002).

Mezardere Formation conformably overlies Ceylan Formation. The unit is cut by Gökçeada domes, covered by Gökçeada ignimbrites and cut and covered by the products of Eşelek volcanism.

Based on nannofossil samples collected from outcrops of Mezardere Formation in Gökçeada, the age of the unit was determined as Early Oligocene (Ilgar et al., 2008).

The dominant lithology to be conglomerate and the occurrence of biostromal sandstone with lamellibranch and pebblestone layers, bituminuous marl and clayey lignite layers and frequent presence ripple marks from bottom to top show that the formation was deposited in littoral environment and the environment was sometimes subjected to low and high energy zones (Akartuna and Atan, 1978).

These rock assemblages were interpreted as delta front deposits by Sümengen et al. (1987).

2.7. Mutludere Intrusion (Tomu)

This unit was first introduced and mapped in this study and exhibits small outcrops in Kargalı stream, north of Mutlu Stream and Dereköy north (west of Tepeköy), and in Aksu Stream between Yenibademli and Kuzu Harbor on the island (Figure 1). The unit has intruded very close to surface and seated at very shallow depths.

The main body which is present with fewer dikes is in the composition of quartz monzonite and diorite porphyry (Figure 10).

Intrusion is generally altered-highly altered in places, and silica, silica veins-veinlets, sericite, chlorite, epidote, magnetite veins-veinlets in occasion, hydrothermal biotite veinlets, argillization and

Figure 10- Mutludere intrusion; diorite porphyry (Mutlu Stream).

carbonation are observed. In rock, coarse plagioclase and lesser amount of orthoclase and hornblende crystals are seen in crystalline groundmass in various sizes ranging from fine to coarse grain. Disseminated and pyrite vein-veinlets, chalcopyrite, magnetite, formations of malachite along fault and joint surfaces are observed in the rock. During microscopic studies, plagioclase, biotite and amphibole were described as diorite porphyry with phenocrysts. Plagioclases have polysynthetic twinning and zoning, with grain sizes ranging between 0.8-2 mm. Sericite, carbonate and clay alteration were detected in plagioclases in few amounts. Biotites have size range between 0.4-0.8 mm and few chloritization, opacification and hydrobiotitization were detected. Biotites are sometimes in the form of clusters, fine grained and widely chloritized. However, amphiboles observed in less amounts show transformation into carbonate, biotite, chlorite and opaque minerals. Groundmass material is silicified and was formed by microcrystalline quartz (secondary?), chloritized biotite, altered feldspar microcrystals and carbonates in trace amounts. Few apatite and zircon were detected as accessory minerals. Besides; anhedral opaque mineral is also observed as dispersed throughout the rock.

In mineralogical analysis of petrographical samples taken from surface and drill cores intrusion rock was described as diorite porphyry - monzodiorite porphyry. In zones where hydrothermal alteration is condensed the rock has almost lost its primary texture and preserved its minerals in few sections and is porphyritic in texture. As primary mineral, fully argillized and seritisized feldspar in few amounts were determined. In groundmass, argillized feldspars, dispersed silicification, carbonation, chloritization and formation of epidote were also observed.

In macroscopic and microscopic studies, the observation of coarse epidote minerals indicates that hydrothermal fluids that cause alteration are in mesothermal or hypothermal temperatures.

Due to the intrusion, in localities of Kargalı, Mutlu and Akarsu Streams, condensed, highly clayey, sericitic, chloritic, epidotic pyrite alteration with silica vein-veinlets, and hematitic-limonitic altered zones with malachite and azurite and magnetitic vein-veinlets are observed. Disseminated, pyritic vein-veinlets and mineralized zones with chalcopyrite are also observed in altered zones.

The unit has intruded into deposits of Karaağaç Formation and Ceylan Formation. The effects of the intrusion are observed in the vicinity of contact and host rocks have sporadically turned into hornfels as a result of low graded thermal metamorphism (Figure 11).

Figure 11- Fels-hornfels zone which developed at the contact of diorite-monzodiorite porphyry intruding into sedimentary rocks (Mutludere).

It was observed that the intrusion was emplaced cutting Late Eocene deposits, so it was deposited into the environment in post Eocene time. Furthermore; it is known that Fakos intrusion in Limnos Island is Early Miocene (Innocenti et al., 1994; Pe-Piper et al., 2009). The age of contact metamorphism created by the intruding granitoid in Semadirek (Samothrace) Island is 40,9±2,2 My (Seymour et al., 1996). Also, the age of Kestanbol granite emplaced in west Anatolia is 28 My (Fytikas et al., 1984). Gökçeada is the region of domes and several Oligocene aged domes and cryptodomes are observed in this area. When all these data are taken into consideration, it is considered that Mutludere intrusion was emplaced into the region in Oligocene time. However, looking in regional scale, it should not be ignored that these intrusions has begun to emplace into the region starting from Middle Eocene.

2.8. Gökçeada Domes (Togd)

Volcanic rocks cover very large areas in Gökçeada. All volcanics in the Island were collected under the name of "Ayvacık Formation" by Temel and Çiftçi (2002) and were defended that these had formed in early Middle Miocene. Nonetheless; these volcanics in the island show differences in terms of their structural shapes, products, compositions and their ages. Andesite and diorite porphyry type volcanic rocks which emplaced in the form of dome-cryptodome arranging in NE-SW directions were named as Gökçeada domes in this study. Domes have been emplaced into the region in shallow depths due to the intrusion which is considered to have begun in Middle Eocene and formed small lava flows cropping out in places (Figure 1).

Andesite and rocks in diorite porphyry composition are observed in the form of domes which intruded into shallow depths in 3 km diameters in occasion. In addition to lava domes, small lava flows and monogenetic breccias are also encountered with many sills and dikes. In lavas, both magmatic and sedimentary derived enclaves are observed.

Lavas are generally holocrystalline porphyritic in texture in thin section studies. Main mineral constituents are formed by plagioclase and amphibole minerals which are observed in the form of subhedral or euhedral prismatic phenocrysts or microphenocrysts, and clinopyroxene and biotite minerals in trace amounts. Euhedral apatite and opaque minerals are observed as accessory constituent. In some amphibole phenocrysts, inner zoning is available. Plagioclase phenocrysts sometimes gather and form glomerocrystal groups. Magma mixing textures are spread in plagioclase phenocrysts. In all amphibole minerals weak corrosions at circumferences and reaction belts formed by pyroxene+opaque mineral aggregates are observed.

The groundmass is generally microcrystalline in subvolcanic ones, and the degree of crystallinity is a bit higher compared to samples flowing at the surface and is formed by coarser size minerals. The textural feature of the groundmass implies that the cooling conditions could be close to subvolcanic conditions. Mineralogical composition of the groundmass is basically formed by plagioclase minerals,

clinopyroxene minerals which are observed as needlelike, opaque minerals and by chlorite minerals which are possibly to be the secondary origin.

Gökçeada domes have been emplaced into Eocene units cutting all those units between Mesozoic-Eocene time intervals and flown as small lava flows in occasion. Domes have baked and deformed deposits in places (Figure 12), and sometimes have formed sudden cooling walls as they contacted with aqueous surface.

Figure 12- Subvolcanics of Gökçeada domes cutting Ceylan Formation (Köklü Hill).

Gökçeada domes were emplaced into the island in Oligocene. According to radiometric dating made within scope of this study in Çal Hill (NW of Uğurlu village) the age was detected as 28,6±0,8 My using K/Ar method. However, Ercan et al. (1995) detected 30,4 My and 34,3 My according to radiometric dating carried out in domes in Ulukaya and Kapıkaya, respectively. All these data indicate that the magmatic activity which forms the domes of Gökçeada occurred in Early Oligocene.

2.9. Gökçeada Ignimbrite (Togi)

It crops out in east and south of Gökçeada, and was first introduced in this study and named as Gökçeada ignimbrite. Outcrops start from east of Gökçeada and extend until Aktaş Hill at southern coast (Figure 1). The center of eruption of the ignimbrite could not be detected and have been emplaced into east and south of the island, most probably generated from a caldera that remained in the sea. Similar ignimbrites are also available in Limnos Island located at south of Gökçeada (Innocenti et al., 1994).

Gökçeada ignimbrite is in white, dirty white and pink colors and observed as pumice flows.

Pumices, which is one of the components forming ignimbrite are generally white, dirty white in color and consist of biotite and amphibole minerals. Lithics are usually formed by andesitic subvolcanic rock fragments. Rock fragments such as claystone and shale were also encountered sometimes. Dense pumice bearing, white colored ignimbrites have occurred due to pumice flows. In general, lithics are denser in lower layers, pumices become denser towards upper layers and their diameters occasionally reach 20-25 cm. Pumices are generally rounded and acquire a view of flame structure in occasion. Taken and detached fragments of claystone and shale were also encountered. Their sizes may range from a few millimeters to few decimeters, and were subjected to changes in color and view by the effect of temperature. Particles of wood residuals are also encountered within the unit (Figure 13). Sizes of pink colored ignimbrite components are smaller (<2 cm) compared to white colored ones and rich in lithic. Pink colored ignimbrites are more coherent compared to white colored ignimbrites and were formed by pumice flows in the first phase of the eruption due to column depression. Pumice back falls are also present on flow occasionally.

Figure 13- Wood residuals within Gökçeada ignimbrite (northern-northeastern slopes of Aktaş Hill).

Gökçeada ignimbrite unconformably overlies Ceylan and Mezardere Formations and is unconformably overlain by Kesmekaya and Eşelek volcanics. Ash-block flow and lahar type forms which are considered to be the products Eşelek volcanics are present on ignimbrite.

As it overlies Mezardere Formation which is stratigraphically known as Early Oligocene and underlies Early-Middle Miocene Eşelek volcanics, it is considered that the volcanic activity that forms Gökçeada ignimbrites have become effective in Late Oligocene.

Ignimbrite formations of Gökçeada are most probably the products belonging to a volcano which remained in sea, the area where Gökçeada-Biga Peninsula and Limnos Island surrounds. Ignimbrites are also present in Biga Peninsula and Limnos Island, and it is highly probable that one part of Gökçeada ignimbrites is the equivalent of some ignimbrites in those areas.

2.10. Kesmekaya Volcanics (Tmk)

Nomenclature for ash-block flows and andesitic lavas located at south of Gökçeada were given as; tuff-agglomerate-andesite (Akartuna and Atan, 1978), Çan volcanics (Ercan et al., 1995), Hisarlıdağ volcanics (Kesgin and Varol, 2003) and Ayvacık formation (Temel and Çiftçi, 2002) in previous studies (names come from outside the island). This unit was first introduced and named as Kesmekaya volcanics in this study. Volcanics crop out between Sürmeli and Aktaş hills in southern coast of Gökçeada (Figure 1).

Kesmekaya volcanics are located on Gökçeada ignimbrites with formations of blocky ash flow, debris flow and lahar type pyroclastic flow which formed due to domal eruptions.

Lavas have been emplaced by flowing over blocky ash flows. They are gray to pink colored, generally andesitic in composition and porphyritic in texture. Flow structures are macroscopically observed and consist of plagioclase, biotite and hornblende as phenocryst.

In microscopic studies, hypocrystalline series is porphyritic in texture and is fine grained. Plagioclase and clinopyroxene minerals which are observed almost in the form of subhedral or euhedral phenocrysts form the main mineral constituents. Apart from these, fully opacified mineral pseudomorphs which are widely observed in sizes of microphenocryst or phenocryst and are highly probably to be the residual of amphibole and/or mica were also encountered.

Textures of magma mix such as; dusty zones, mesh texture, corroded edges etc. are widely observed in plagioclase phenocrysts.

Phenocryst components of the rock are located in a microcrystalline groundmass, and it is constituted by rodlike prismatic plagioclase minerals, needlelike mica minerals, rare clinopyroxene minerals and opaque minerals. Volcanic glass material can be distinguished under microscope. Phenocryst/groundmass ratio of the rock is high.

The unit overlies Gökçeada ignimbrite and is overlain by Eşelek volcanics though its contact cannot be clearly detected.

According to K/Ar radiometric dating performed in lavas of Kesmekaya volcanics, 37,2±1 My was detected in Sümeli Hill, but there are still some suspects as the age determination has been carried out in plagioclases. The unit overlies Gökçeada ignimbrite and has similar stratigraphical and lithological characteristics with Early Miocene volcanics in Biga Peninsula in regional correlation (Dönmez et al., 2005, 2008). Therefore; it is considered that the volcanism that forms Kesmekaya volcanics might have occurred in Early Miocene.

2.11. Eşelek Volcanics (Tme)

Volcanic products which are formed by lava and pyroclastics in basaltic andesite and andesitic compositions in east of Gökçeada were first mapped in this study and named as Eşelek volcanics. The unit spreads on a large area including Kocaçavuş and Esencik Hills at southwest of Eşelek starting from Eğrice Hill (north of Kuzu Harbor) and Dal Hill (southeast of Kuzu Harbor).

Eşelek volcanics are composed of lavas and pyroclastics in basaltic andesite and andesitic compositions. Debris flow and pyroclastics in the character of blocky ash flow located below are overlain by lava flows which are not very thick and widespread. Lavas related to the unit were distinguished and mapped as member.

Pyroclastics are formed by blocky ash flow and lahar type forms. Sizes of blocks in ash-block flows are quite variable and can occasionally reach up to 1 meter. Peat formations as in black stains and dark brown colored ironoxide nodules are present in tuffs.

2.11.1. Lava Member (Tmel)

Lavas have generally sheet jointed structure. Lavas that overlie pumice flows most probably have come to aqueous environment and been subjected to quench fragmentation due to sudden cooling. Therefore; there is observed a brecciated structure especially at the bottom. Lavas which are named as pyroxene andesite are gray colored, porphyritic in texture and have thin phenocrysts.

In thin section studies, they have holocrystalline porphyritic texture and are fine to medium grained. Main mineral constituents are plagioclase minerals which are observed as subhedral or euhedral prismatic phenocrysts, and few biotite minerals accompanying those plagioclases. Opague minerals are widely present as an accessory component. Thin opacification belts around amphibole and biotite phenocrysts are abundant. In the body of plagioclase phenocrysts, textural features indicating magma mixture has widely developed. Besides; it was observed that mantling was quite abundant in the outer edges of many plagioclase phenocrysts and of some were surrounded by spheluritic texture K-feldspar mantles. K-feldspar occurrences in spheluritic texture are occasionally observed also in the form of patches in groundmass of rock. The character of groundmass is microcrystalline and is fully crystallized. Groundmass mineralogy is formed by rodlike prismatic plagioclase minerals, needlelike mica minerals and opaque minerals. Groundmass texture has become complicated because of probable metasomatic substitution processes. To describe rodlike prismatic plagioclase minerals is often difficult. Phenocryst/groundmass ratio of the rock is high. Additionally; magmatic enclaves that are visible by naked eye in hand specimens and which are possibly to have generated from monzodiorite or diorite were also observed. As these are holocrystalline in texture, they can easily be noticed within groundmass of rock. The mineral composition is constituted by plagioclase, clinopyroxene and biotite minerals.

Eşelek volcanics overlie Mezardere Formation and Gökçeada ignimbrite but is unconformably overlain by Çanakkale Formation. Lavas have cut, baked and deformed Gökçeada ignimbrite in their contacts (Figure 14). Besides; lavas have been disintegrated due to sudden cooling when flowing over ignimbrites probably in aqueous environment and caused orientation in pumices as well within ignimbrite.

It is considered that the unit was emplaced into the medium in Early-Middle Miocene period as the unit overlies Kesmekaya volcanics and unconformably underlies Late Miocene Çanakkale Formation.

2.12. Çanakkale Formation (Tmç)

The unit which is composed of conglomerate, sandstone siltstone and marl was named as "Çanakkale Formation" and was first described by Şentürk and Karaköse (1987). It outcrops in narrow areas at east, southeast and south of Gökçeada (Figure 1). The outcrop in east and southeast is present in the peninsula at east–northeast of Tuzgölü (Salt Lake). The outcrops in south on the other hand are observed in small areas along the coast between Tuzgölü and Kapıkaya.

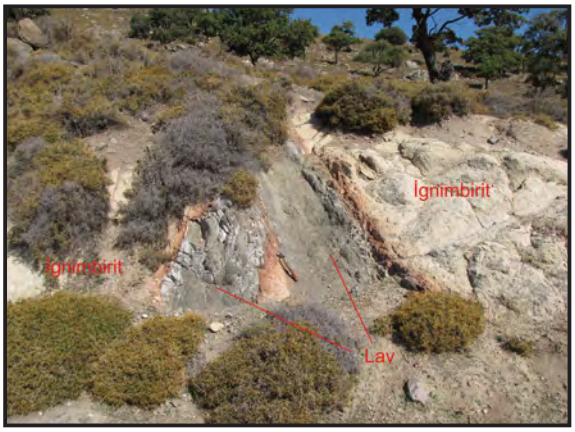

Figure 14- Dikes of Eşelek volcanics cutting Gökçeada ignimbrite (along the road in south-southwest of Kocabaş Hill)

It is generally composed of less consolidated conglomerate, sandstone, siltstone and marl intercalations. The formation is made up of carbonates of laterally and vertically transitional shoreface, beach, tidal flat, falling tide delta and tidal environment (Ilgar et al., 2008). The dominant lithology of the unit is sandstone. Sandstones are pale yellow-yellowish gray, loose cemented, dispersive, fine to medium grained, very well sorted, and cross bedded in occasions. Very fine grained shale, conglomerate, bioclastic conglomerate layers take place between sandstones.

Çanakkale Formation of which its thickness was determined as approximately 15 meters in the island (Temel and Çiftçi, 2002) transgressively overlies Eşelek volcanics. The upper part of the formation is covered by recent beach deposits.

The unit was aged as Pontian by Akartuna and Atan, (1978) in the island. However, it was aged as Late Miocene (Middle-Late Panonian) by Atabey et al. (2004) in Biga Peninsula.

Çanakkale Formation is the only unit representing Late Miocene Sea in the region and reflects rocky shore environment.

2.13. Debris (Qym)

It is observed as in the form of free debris flows on the slopes of exposed domes on the island.

2.14. Alluvials (Qal)

It is composed of Quaternary aged conglomerate, sandstone, siltstone and mudstones which developed in stream beds, on ancient depressions and on shore belt plains. The unit is observed in east-northeast of Uğurlu village, south of Şirinköy, south of Yerkaya Hill and Kapıkaya locality, between the town center of Gökçeada and Kaleköy and along the stream beds and plains around Eşelek village (Figure 1).

3. Tectonics

Gökçeada is the island which has a high risk of earthquake in Aegean seismological region. During archeological excavations carried out on the island, it was revealed that settlements located on the island had been affected from earthquake and remnants of people subjected to natural disaster in Yenibademli, Höyük were detected (Hüryılmaz, 2011).

Gökçeada is generally under the control of northeast–southwest extending fault sequences. The northern part of the island has been uplifted relative to southern part and the inclination of beds varies between 20°-40° towards southeast. Units get younger starting from west to east (Figure 15). The strongest data of tectonical uplift are metamorphic rocks cropping out in a very narrow area at north of the island.

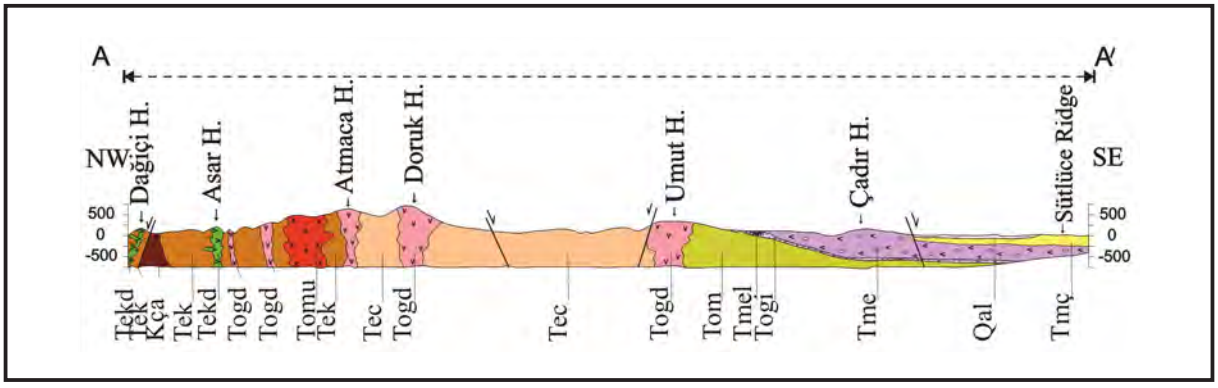

Figure 15- Schematic geological section (unscaled) of Gökçeada in NW-SE direction (Kça; Çamlıca metamorphics, Tek; Karaağaç Formation, Tekd; Dağiçitepe volcanic, Tec; Ceylan Formation, Tom; Mezardere Formation, Tomu; Mutludere intrusion, Togd; Gökçeada domes, Togi; Gökçeada ignimbrite, Tme; Eşelek volcanics, Tmel; Eşelek volcanics lava member, Tmç; Çanakkale Formation, Qal; Alluvial).

Gökçeada was tectonically studied by Koral et al. (2008). According to the authors, the fault system in which it was considered to be in North Anatolian Fault System had a great effect in acquiring the recent morphology of the island. This system extends as linear along the northern coast at westernmost side of the island. Another fault segment however extends along the long axis of the island. The fault called "Kefalos Fault" in southeastern part of the island restricts Tuzla Lake depression. These faults are generally right stepped and almost dip slip oblique faults (Figure 16). The authors detected that these oblique faults had also their northwest directing antithetic and northeast directing synthetic faults.

Lineaments specified as antithetic and synthetic faults by Koral et al. (2008) have definite contact which formed by the intrusion of Gökçeada domes into sedimentary units according to us. During studies performed by us, locations of tectonical zones detected along the long axis of Gökçeada were changed in certain amounts, and additionally; İnceburun, Aktepe, Zeytinli, Kuzu Limanı and Koç Dere Faults were determined (Figure 16).

İnceburun Fault: It is a tectonical zone with a strike of N30W and dip amount of 45SE in Karaağaç Formation that has the alternation of siltstone, sandstone, claystone and marl in stream at southwest of İnceburun location.

Aktepe Fault: It extends along valley at east of Uğurlu village, Aktepe, Kolbaşı Hill and Oğlak Hill and is a right lateral oblique fault with a strike of N60E and dip amount of 50SE.

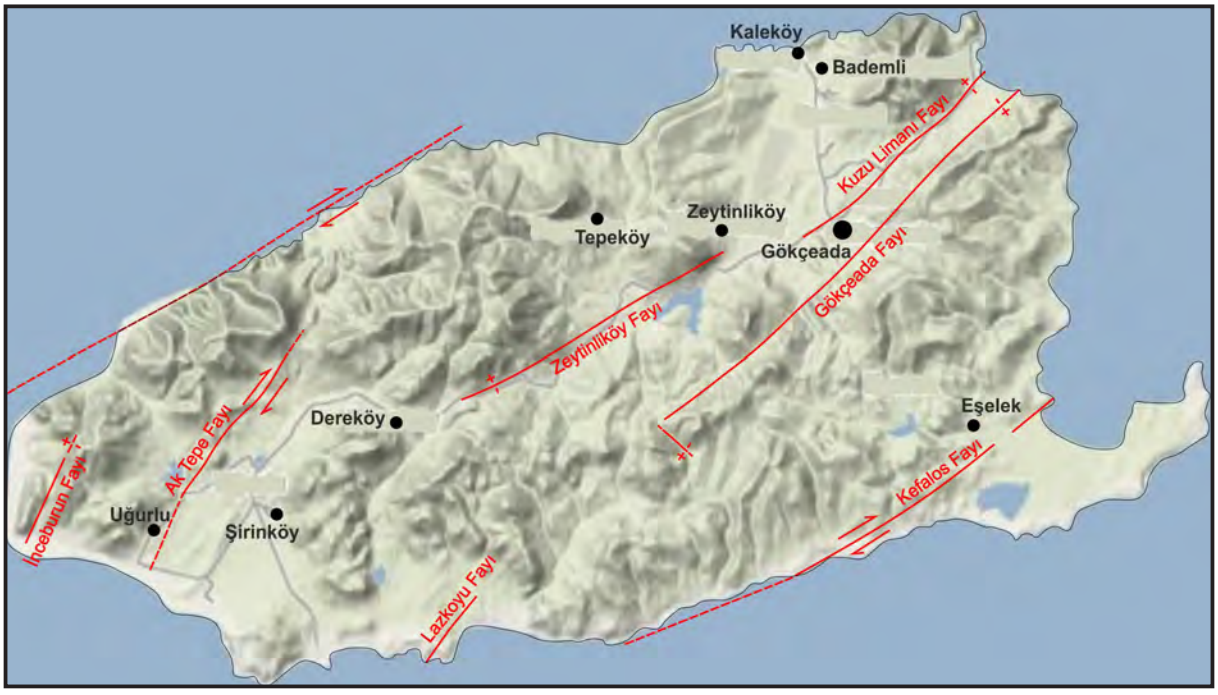

Figure 16- Significant faults of Gökçeada transferred on Googleearth image.

Zeytinliköy Fault: This zone is observed until Zeytinliköy along the Gökçeada-Dereköy auto road in south-southeastern parts of Doruk Hill and has developed within Ceylan Formation.

Kuzu Harbor: This tectonical zone has a strike of N40E and dip amount of 55SE between Kuzu Harbor and Gökçeada and developed within Ceylan formation.

Koç Dere Fault: It is observed as NW-SE directing dip slip normal fault zone at the contact of Middle-Upper Eocene Ceylan Formation and Oligocene aged Gökçeada domes in Koç Stream.

4. Results

In this investigation, 1/25.000 detailed geological and 1/100.000 scaled revision studies were performed throughout the island and significant contributions were made for the geology of the island by new findings obtained. Within this scope;

It was detected that the primary depositional age of Çamlıca metamorphics, which had been dated as Paleozoic by previous investigators (Akartuna and Atan, 1978), was Late Ediacaran and/or Early Paleozoic (Tunç et al., 2002) as a result of studies carried out in their equivalences in Biga Peninsula. So the age of Çamlıca metamorphics in the island was assessed as the Late Ediacaran and/or Early Paleozoic.

The unit which had been defined as the Fıçıtepe Formation in the island by some previous investigators (Temel and Çiftçi, 2002; Ilgar et al., 2008; Varol and Baykal, 2008) was described as Koyunbaba Formation because of contact relationships and lithological characteristics, and it can be correlated with Koyunbaba Formation which was introduced in MTA (2006) and display a spread in Thrace.

In this study, the presence of deep/semi deep seated rocks in Gökçeada were detected and mapped the first time. Due to the intrusion, highly clayey, serisitic pyrite alteration with chlorite and epidote and silica vein-veinlet in occasion; and altered zones with malachite and azurite in occasion with hematite and limonite, and magnetite vein-veinlets are observed. Within altered zones disseminated and pyritic vein-veinlet, and chalcopyritic mineralized zones are also present.

Volcanics have been formerly grouped under Oligocene (Ercan et al., 1995, Kesgin and Varol, 2003) or in one formation at the age of Early-Middle Miocene (Temel and Çiftçi, 2002) in previous studies. However, in this study these volcanics were separated into six different formations according to their stratigraphical and lithological characteristics

at different ages. Also, the products of Eocene aged acidic volcanism were first time detected in the island.

While Oligocene volcanics are observed in central and northern parts of the island in the form of domes, the products of Miocene aged volcanism are located in southern and eastern parts of the island in the form of lavas and pyroclastics. Island volcanics which crop out in the island which are called as Çan volcanics (Ercan et al., 1995), Hisarlıdağ volcanics (Kesgin and Varol, 2003) and Ayvacık Formation (Temel and Çiftçi, 2002) in previous studies were defined in detail and named considering their lithological characteristics. Again, the presence of ignimbrites most probably originating from a center which remained in the sea was detected the first time on the island.

Gökçeada was tectonically studied in detail by Koral et al. (2008). As a result of studies carried out by us, the locations of tectonical zones which had been detected along the long axis of Gökçeada were changed in certain amounts, and additionally; İnceburun, Ak Tepe, Zeytinli, Kuzu Harbor and Koçdere Faults were investigated.

Acknowledgement

This study was made within scope of "Batı Anadolu Polimetal Maden Aramaları Projesi" (Project of West Anatolian Polymetal Mineral Explorations) of MTA between the years 2008-2011. We would like to thank to Dr. Evren Yazgan and Dr. Evren Atakay Gündoğdu for petrographical descriptions, to Dr. Şükrü Acar and Ayşegül Aydin for paleontological descriptions, and to Prof. Erdinç Yiğitbaş who revised this article and made invaluable criticisms.

Received: 18.01.2014
Accepted: 12.11.2014
Published: June 2015

References

Akartuna, M. 1950. İmroz Adasında bazı jeolojik müşahadeler. *Türkiye Jeoloji Kurumu Bülteni* 2/2, pp.8-17.

Akartuna, M. Atan, O.R. 1978. Gökçeada'nın (Çanakkale) jeoloji ve sedimantaloji hakkında ön rapor. *Maden Tetkik ve Arama Genel Müdürlüğü Jeoloji Dairesi Rapor Arşivi Rapor No: 105.* Ankara. (unpublished).

Atabey, E., Ilgar, A., Saltık, A. 2004. Çanakkale havzasının Orta-Üst Miyosen stratigrafisi, Çanakkale, KB Türkiye. *Maden Tetkik ve Arama Dergisi* 128, pp.79-97.

Barr, S.R., Temprley, J., Tarney, J. 1999. Lateral growth of the continental crust through deep level subduction-accretion: Are-evaluation of central Greek Rhodope. *Lithos* 46, pp.69-94.

Dönmez, M., Akçay, A. E., Genç, C.Ş., Acar, Ş. 2005. Biga Yarımadasında Orta-Üst Eosen volkanizması ve denizel ignimbiritler. *Maden Tetkik ve Arama Dergisi* 131, pp.49-61.

Dönmez, M., Akçay, A. E., Duru, M., Ilgar A., Pehlivan, Ş. 2008. 1/100.000 Ölçekli Türkiye Jeoloji Haritaları Çanakkale H17 Paftası. No: 101. *Maden Tetkik ve Arama Genel Müdürlüğü.* Ankara.

Duru, M., Pehlivan, Ş., Ilgar A., Dönmez, M., Akçay, A. E. 2008. 1/100.000 Ölçekli Türkiye Jeoloji Haritaları Ayvalık İ17 Paftası. No: 98. *Maden Tetkik ve Arama Genel Müdürlüğü,* Ankara.

Ercan, T., Satır, M., Dora, A., Sarıkoğlu, E., Yıldırım, T., Adis, C., Walter, H.J., Özbayrak, İ.H. 1995. Biga Yarımadası, Gökçeada, Bozcaada ve Tavşan Adaları'ndaki Tersiyer yaşlı volkanitlerin petrolojisi ve bölgesel yayılımı. *Maden Tetkik ve Arama Dergisi* 117, pp.55-86.

Esso Standard, 1960. I sayılı Marmara petrol bölgesi AR/EST/105, 106, 108 ve 109 hak sıra numaralı sahalara ait terk raporu. *TPAO Arama Grubu Arşivi. Rapor No: 131.* Ankara, (unpublished).

Fytikas, M., Innocenti, F., Manetti, P., Mazzuoli, R., Peccerillo, A., Villari, L. 1984. Tertiary to Ouaternary evolution of volcanism in the Aegean region: The Geological Evolution the Eastern Medditrranean. J. E. Dixon, A. H. F. Robertson (Ed.). *Geological Society of London.* Special Publication. 17, pp.687- 699.

Hüryılmaz, H. 2011. Gökçeada-Yenibademli Höyük 2010 Yılı Kazıları. 33. Kazı sonuçları toplantısı, 23-28 Mayıs *2011. Malatya. Kültür Varlıkları ve Müzeler Genel Müdürlüğü Yayın No: 155-1. pp.1-18.*

Ilgar A., Demirci, E.S., Duru, M., Pehlivan, Ş., Dönmez, M., Akçay, A. E. 2008. 1/100.000 ölçekli Türkiye Jeoloji Haritaları Çanakkale H15 ve H16 Paftaları. No: 100. *Maden Tetkik ve Arama Genel Müdürlüğü,* Ankara.

Innocenti, F., Manetti, P., Mazzuoli, R., Pertusati, P., Fytikas, M., Kolios, N. 1994. The geology and geodynamic significance of the island of Limnos, North Aegean Sea, Greece. Neues jahrbuch für Geologie und Palaontolgie-Monatshefte. H.11,661-691

Kasar, S., Bürkan, K., Siyako, M., Demir, O. 1983. Tekirdağ-Şarköy- Keşan – Enez bölgesinin jeolojisi ve hidrokarbon olanakları. *Türkiye Petrolleri Anonim Ortaklığı Arama Grubu Rapor No. 1771.* Ankara, (unpublished).

Keskin, C. 1974. Ergene Havzası ve kuzeyinin stratigrafisi. *Türkiye İkinci Petrol Kongresi Bildiriler Kitabı* 131-163.

Kesgin, Y., Varol, B. 2003. Gökçeada ve Bozcaada'nın Tersiyer jeolojisi (Çanakkale). *Türkiye. Maden Tetkik ve Arama Dergisi*. 126, pp.49-67.

Koral, H., Öztürk, H., Hanilçi, N. 2008. Tectonically induced coastal uplift mechanism of Gökçeada Island, Northern Aegean Sea, Turkey. *Quaternary International* 197 (2009) pp.43–54.

MTA. 2006. Trakya Litostratigrafi Birimleri Kitabı. Stratigrafi Komitesi. *Maden Tetkik ve Arama Genel Müdürlüğü*. Ankara.

Okay, A.İ., Siyako, M., Bürkan K. A. 1990. Biga Yarımadası'nın jeolojisi ve tektonik evrimi. *Türkiye Petrol Jeologları Derneği Bülteni* 2/1, pp.83-121

Okay, A.İ., Satır, M. 2000. Coeval plutonism and metamorrphism in a Latest Oligocene metamorphic core complex in Northwest Turkey. *Geological Magazine* 137/5, pp.495-516.

Okut, M. 1975. Çanakkale ili, Gökçeada ilçesi hammadde prospeksiyon raporu. *Maden Tetkik ve Arama Genel Müdürlüğü Kuzeybatı Anadolu Bölge Müdürlüğü Rapor No: 297.* Balıkesir. (unpublished)

Papanikolaou, D., Panagopoulos, A. 1981. On the structural style of Southern Rhodope, Greece. *Geologica Balcanica* 11, pp.12-22.

Pe-Piper, G., Piper, J. W., Koukouvelas, I., Dolansky, L. M., Kokkalas S. 2009. Postorogenic shoshonitic rocks and their origin by melting underplated basalts. The Miocene of Limnos, Greece. *Geological Society of America Bulletin* 1-2, pp.39-54.

Seymour, K. S., Tsikouras, V., Kotopouli, K., Hatzipanayiotou, K., Pe-Piper, G. 1996. A window to the operation of microplate tectonics in The Tethys Ocean: the geochemistry of the Samothrace granite. Aegean Sea. *Mineralogy and Petrology* 1, pp.251–272.

Sfondrini, G. 1961. Surface geological report on Ar/ TPAO/1/538 and 537. *Türkiye Petrolleri Anonim Ortaklığı Arama Grubu Rapor No: 1429.* Ankara. (unpublished).

Sümengen, M., Terlemez, l.,Şentürk, K., Karaköse, C. 1987. Gelibolu Yarımadası ve güneybatı Trakya havzasının stratigrafisi, sedimentolojisi ve tektoniği. *Maden Tetkik ve Arama Genel Müdürlüğü Rapor No: 8128.* Ankara. (unpublished).

Sümengen, M., Terlemez, İ. 1991. Güneybatı Trakya yöresi Eosen çökellerinin stratigrafisi. *Maden Tetkik ve Arama Dergisi* 113, pp.17-30.

Şentürk, K. Karaköse, C. 1987. Çanakkale Boğazı ve dolayının jeolojisi. *Maden Tetkik ve Arama Genel Müdürlüğü Rapor No: 9333*. Ankara. (unpublished)

Temel, R. Ö., Çiftçi, N. B. 2002. Gelibolu Yarımadası, Gökçeada ve Bozcaada Tersiyer çökellerinin stratigrafisi ve ortamsal özellikleri. *Türkiye Petrol Jeologları Derneği Bülteni* 14, pp.17-40.

Tunç, İ. O., Yiğitbaş, E., Şengün, F., Wazeck, J., Hofmann, M., Linnemann, U. 2002. U-Pb zircon geochronology of northern metamorphic massifs in the Biga Peninsula (NW Anatolia-Turkey): new data and a new approach to understand the tectonostratigraphy of the region. *Geodinamica Acta.* 25, 3-4, Special Issue: Tectonics of the Eastern Mediterranean - Black Sea Region: Part A Dedicated in honor of Aral Okay's 60th birthday. doi:10.1080/09853111.2013.87724

Ünal, O. 1967. Trakya jeolojisi ve petrol imkanları. *Türkiye Petrolleri Anonim Ortaklığı Arama Grubu Rapor No: 391*, 103p. Ankara (unpublished).

Varol, B., Baykal, M. 2008. Trakya Tersiyer karbonatlarının sedimantolojik ve kronostratigrafik özellikleri. *Türkiye Petrolleri Anonim Ortaklığı Araştırma Merkezi.* 104p. Ankara. (unpublished).

BULLETION OF THE MINERAL RESEARCH AND EXPLORATION

Foreign Edition 2015 150

CONTENTS

Bull. Min. Res. Exp. (2015) 150: 19-50

Bulletin of the
Mineral Research and Exploration

http://bulletin.mta.gov.tr

BENTHIC FORAMINIFERAL BIOSTRATIGRAPHY OF MALATYA OLIGO-MIOCENE SUCCESSION (EASTERN TAURIDS, EASTERN TURKEY)

Fatma GEDİK[a*]

[a] *Maden Tetkik ve Arama Genel Müdürlüğü, Jeoloji Etütleri Dairesi, 06800, Ankara-Turkey.*

Keywords:
Benthic Foraminifera,
Oligocene, Miocene,
Biostratigraphy, Malatya.

ABSTRACT

The benthic foraminiferal biostratigraphy of Oligo-Miocene aged Muratlı and Petekkaya formations which crop out over wide regions around Akçadağ town, west of Malatya province in Eastern Taurids were revealed in this study. Systematical sampling was carried out in measured stratigraphical sections in four locations in order to perform stratigraphical and paleontological investigations. Benthic foraminifera taken from 182 hard rock samples were defined and three biozones were determined as; SBZ 21-22, belonging to Oligocene (Rupelian - Early Chattian), SBZ 23 (Late Chattian) and SBZ 25 belonging to Lower Miocene in shallow marine deposits in the region. It was stated that the assemblage of planktic foraminifer and nannoplankton which stratigraphically detected within Chattian - Burdigalian units in the succession most probably indicated Aquitanian age. Besides; Oligo-Miocene transition in the region was approved with this study based on biostratigraphical locations of benthic foraminiferal taxa.

1. Introduction

Malatya Oligo-Miocene basin is located in west of Malatya province around Akçadağ district at the junction of Tauride - Anatolide platform, East Anatolian Region and surrounded by districts of Doğanşehir in south, Hekimhan in north, Darende in northwest, Yazıhan in northeast and Yeşilyurt in southeast (Figure 1). Marine sediments observed in and around the study area have been deposited between Jurassic – Middle Miocene times, and Oligocene and Lower Miocene aged units in this study were investigated in detail. However, pre Eocene-Eocene rock units and post Miocene young units were not studied to the contrary of these aforementioned units. Basement units in the region are constituted by Middle Triassic – Cretaceous, Jurassic – Cretaceous and Upper Senonian neritic limestones, Late Cretaceous – Paleocene clastic and carbonate rocks, Early – Middle Eocene terrigenous clastic rocks, Middle – Late Eocene neritic limestones and sedimentary deposits formed by clastic and carbonate rocks and by Mesozoic ophiolites (Figure 2). As for the younger deposits cropping out near the study area are composed of Late Miocene – Pliocene terrigenous clastics, pyroclastic rocks and Pliocene - Plio Quaternary terrigenous deposits, alluvial fan, debris and young alluvial deposits (Figure 3). As geological units at the basement and young deposits are out of the scope of study, detailed information can be obtained from the articles of Ayan (1961), Akkuş (1971), Yoldaş (1972), Kurtman (1978), Örçen (1986), Karaman et al. (1993) and Alkan (1997).

Oligocene aged Muratlı formation and Lower Miocene aged Petekkaya formation investigated in eastern Taurus were studied in detail and four stratigraphical sections were measured within this purpose. Total of 28 taxa were defined in 182 rock samples which were taken from these sections (Gedik; 2010, 2014), and 3 biozones were detected as SBZ 21-22, SBZ 23 belonging to Oligocene and SBZ 25 belonging to Lower Miocene in shallow marine deposits in the region. With the help of stratigraphical horizons in which foraminiferal taxa are present all stratigraphical sections were correlated both by

* *Corresponding author: Fatma Gedik, gedik@mta.gov.tr*

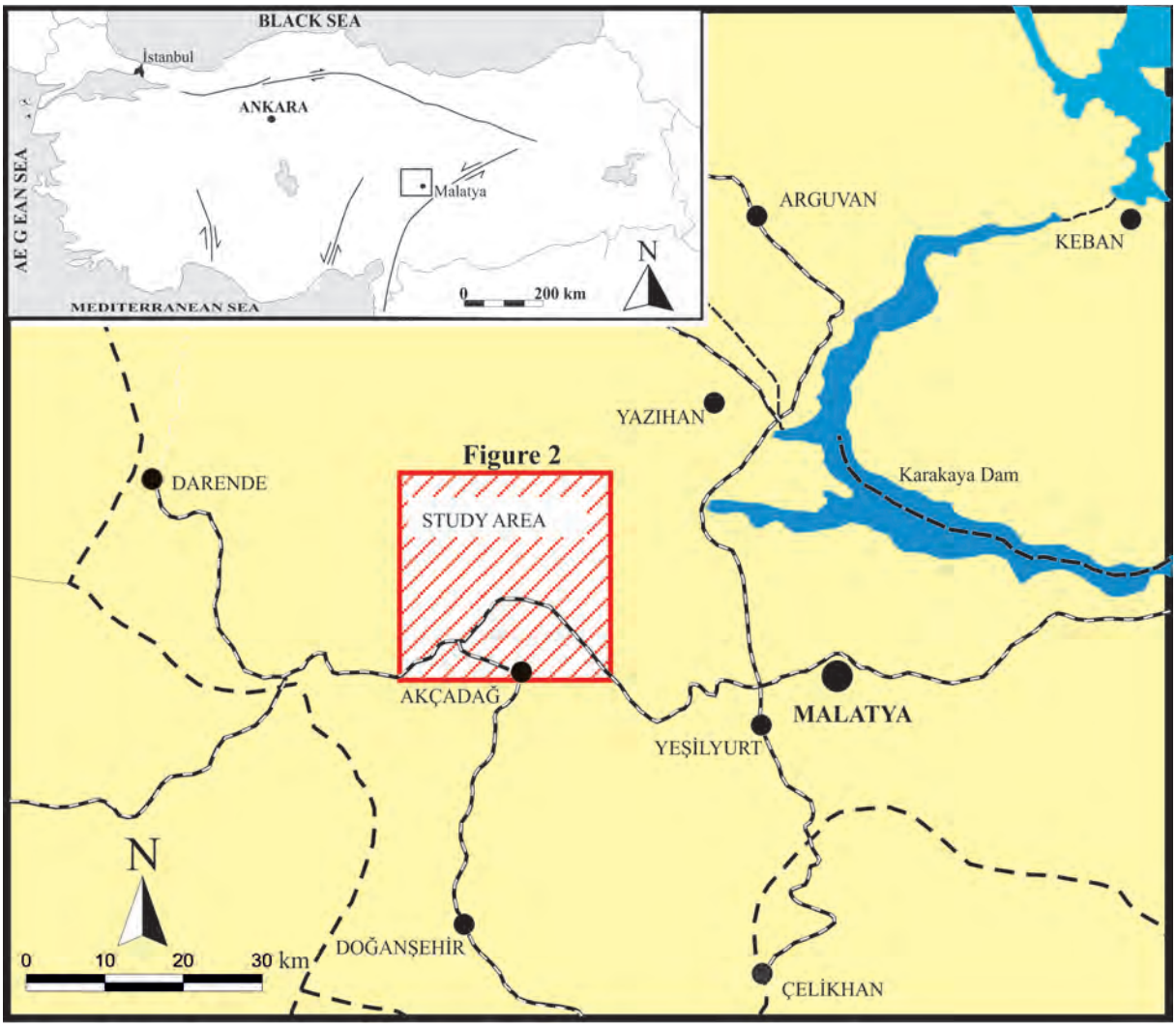

Figure 1- Location map.

lithologically and biostratigraphically (Gedik, 2014; Figure 4).

Thin sections of photographed foraminiferal taxa in this study are kept in the archive of the General Directorate of Mineral Research and Exploration.

Abbreviations: SBZ (Shallow benthic foraminiferal zone), HYM (Karamağara measured stratigraphical section), FGM (Edilme measured stratigraphical section), FGK (Kuzkaya measured stratigraphical section), FGD (Develi measured stratigraphical section).

2. Material and Method

Total of 182 hard rock samples taken from four measured stratigraphical sections form the material of this study. In hard rock samples, random and oriented thin sectioning method was applied. Besides; clayey limestone-marl samples and macrofossils collected for the determination of fauna and flora belonging to planktic foraminifera, nannoplanktons and ostracodes were used in the determination of biostratigraphy for correlation.

3. Measured Stratigraphical Sections

3.1. Kuzkaya Measured Stratigraphical Section (FGK)

Kuzkaya measured stratigraphical section starts at coordinates of X1: 02 869; Y1: 53 721 and finishes at coordinates of X2: 02 588; Y2: 54 505 (Figure 2). The length of the section which is composed of Early Miocene sediments was measured as 69 meters and total of 40 samples were collected. Samples collected from bottom to top were lithologically defined by giving their fossil contents and coded as FGK 1-26 (Figure 5). The succession of which its bottom contact relationship cannot be observed starts with

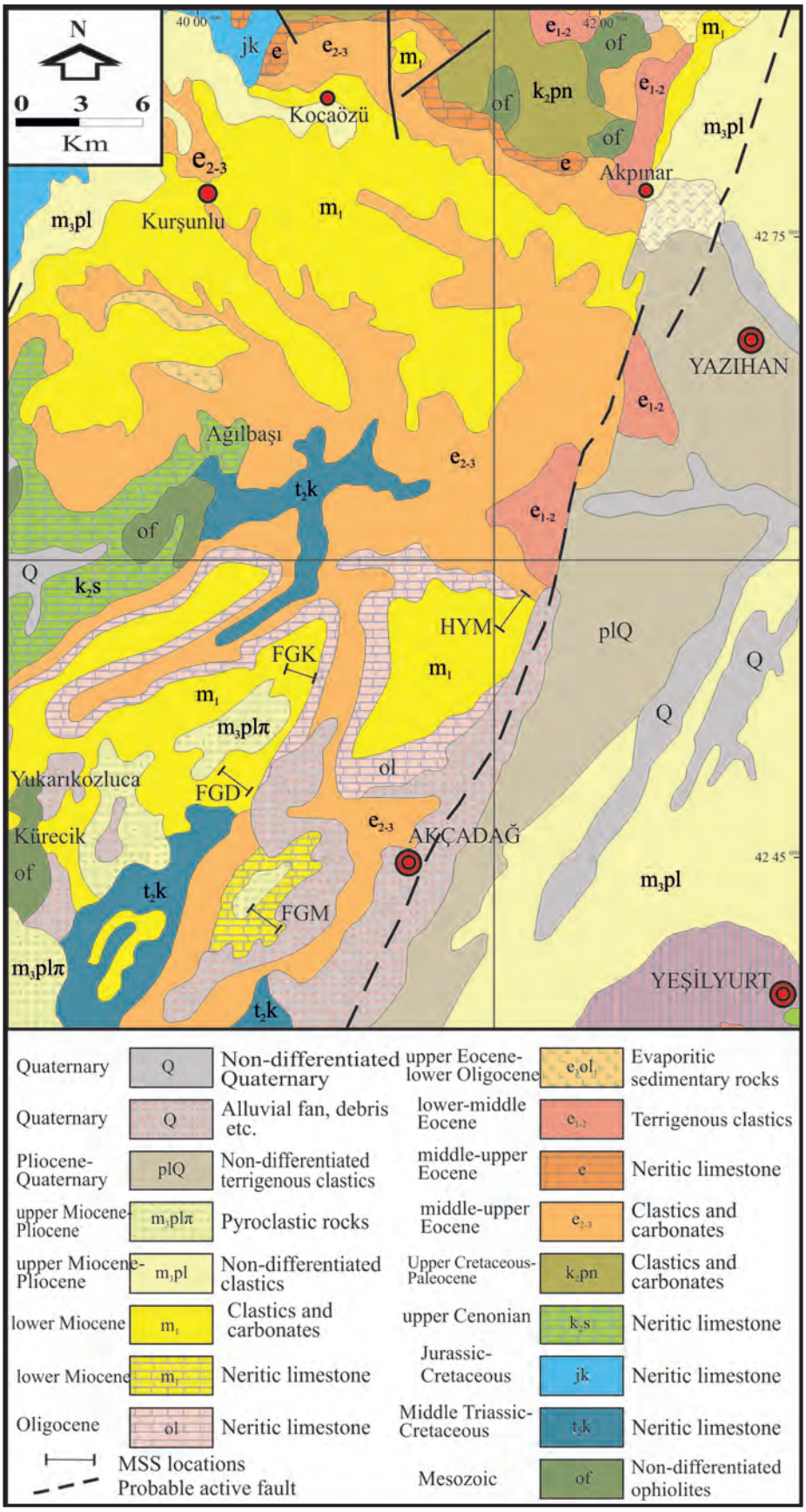

Figure 2- Geological map of the study area (from 1/500 000 scaled map of MTA).

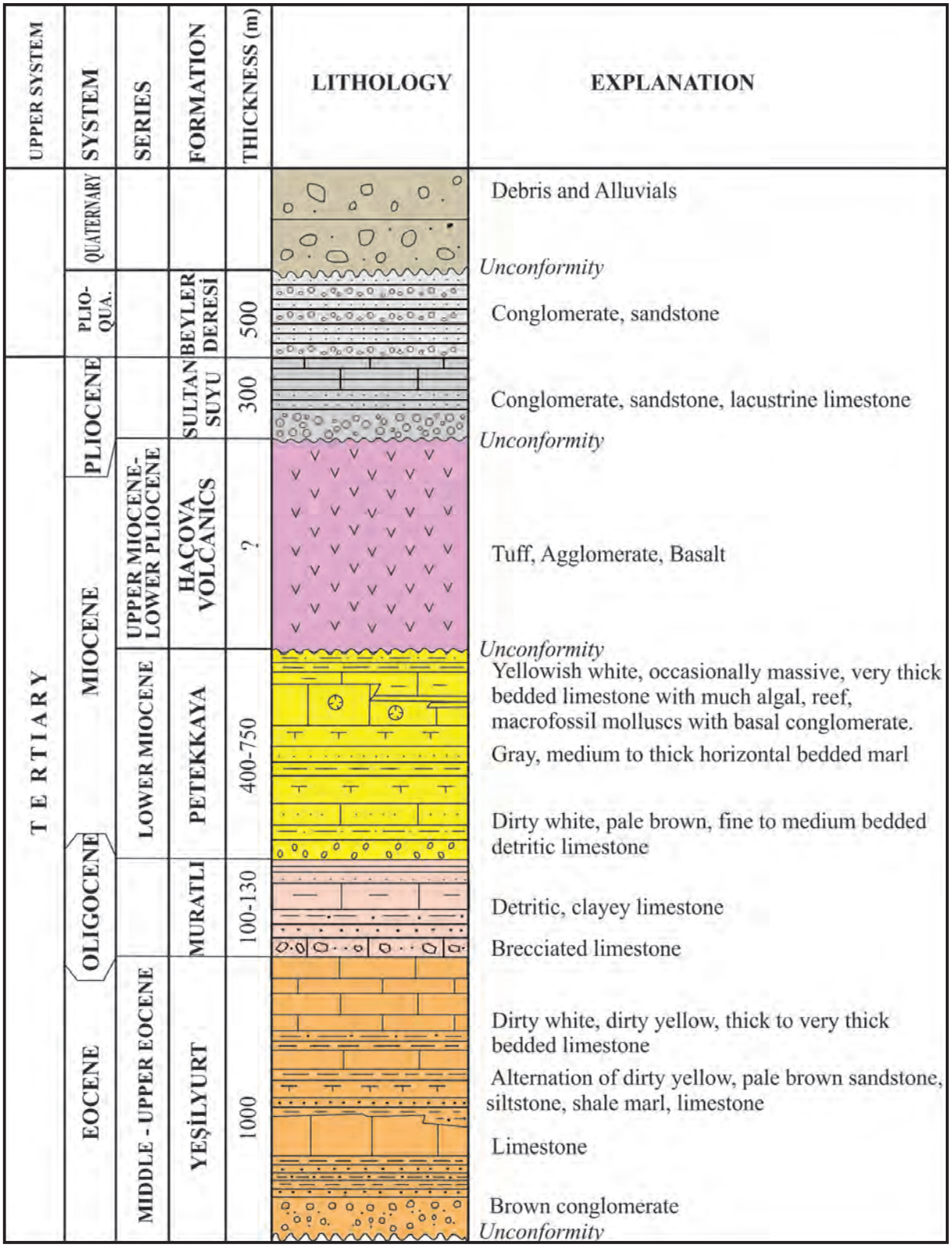

Figure 3- Generalized stratigraphical section of the study area (from Karaman et al., 1993).

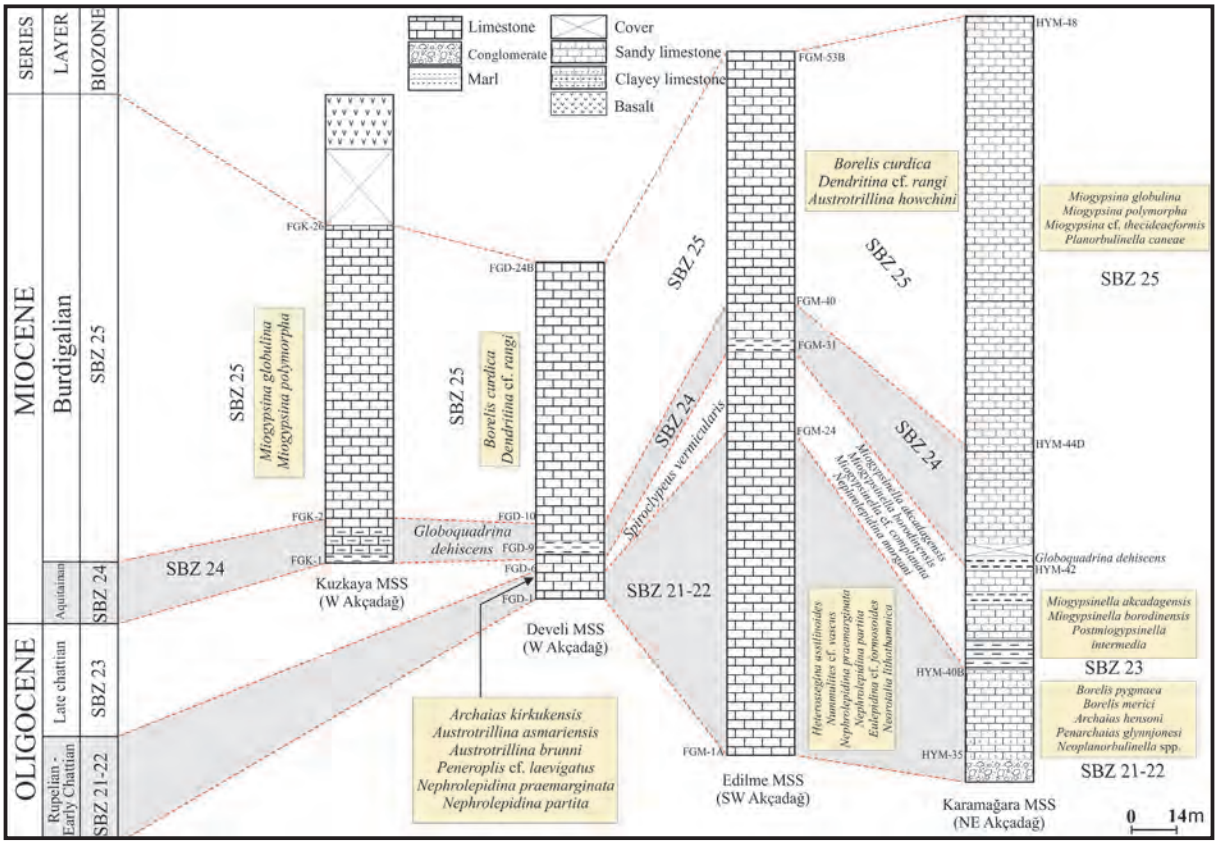

Figure 4- Lithological and biostratigraphical correlation table of the measured stratigraphical sections in the study area (Gedik, 2014; Figure 4).

approximately 3 meters thick, gray to beige colored, medium to thick bedded, fully horizontal, much macro shell imprint bearing, highly disintegrated marl and clayey limestones. The unit is highly rich in planktic foraminifer, nannoplankton and ostracode contents (FGK-1). Described planktic foraminifera are; *Globigerinoides primordius* Blow and Banner, *Globigerina ciperoensis* Bolli, *G. praebulloides occlusa* Blow and Banner, *G. praebulloides leroyi* Blow and Banner, *G. praebulloides* s.s. Blow, *G. ouachitaensis gnaucki* Blow and Banner, *G. ouachitaensis* s.s Howe and Wallace, *G.* cf. *angulisuturalis* Bolli, *Globigerinella* cf. *obesa* (Bolli), and nannoplanktons are; *Cyclicargolithus abisectus* (Müller), *C. floridanus* (Roth and Hay), *Coccolithus eopelagicus* (Bramlette and Riedel), *Dictyococcites bisectus* (Hay, Mohler and Wade), *Sphenolithus moriformis* (Brönnimann and Stradner). Ostracodes decribed within same samples are *Krithe papillosa* (Bosquet), *Ruggeria dorukae* (Bassiouni), *Xestoleberis* cf. *ventricosa* Müller, *Cytheropteron* sp., *Bairdia* sp., *Quadracythere* sp. Furthermore; small benthic foraminifera such as *Pararotalia* sp. and *Nonion* sp. were also described. The age of the unit is dated as Late Oligocene – Early Miocene according to planktic foraminifers and as Late Aquitanian - Burdigalian according to ostracodes. However; nannoplankton assemblage gives Oligocene age. The first occurance of *M. polymorpha* observed in limestones just above the unit indicates Burdigalian age. Taking the age intervals of planktic foraminifers and ostracode fauna in marls and the first occurance of *M. polymorpha* into consideration the unit was most probably thought to be in Aquitanian age, as *M. polymorpha* has not been reported in Aquitanian age in studies carried out so far (Drooger, 1993). The assemblage which constitutes the unit does not contain benthic foraminifer and is the equivalent of M1 of planktic foraminifera and NN1-NN2 zones of nannoplanktons according to Berggren (1995). However, its equivalence in shallow benthic zonation corresponds to SBZ 24 zone of Cahuzac and Poignant (1997). In beige to white colored, fine grained, medium to thick bedded clayey limestone layer Burdigalian aged *Miogypsina polymorpha* (Rutten) was described at 4th meter of the succession (FGK-2). The first occurance of *M. polymorpha* draws the lower boundary of SBZ-25 zone. Just

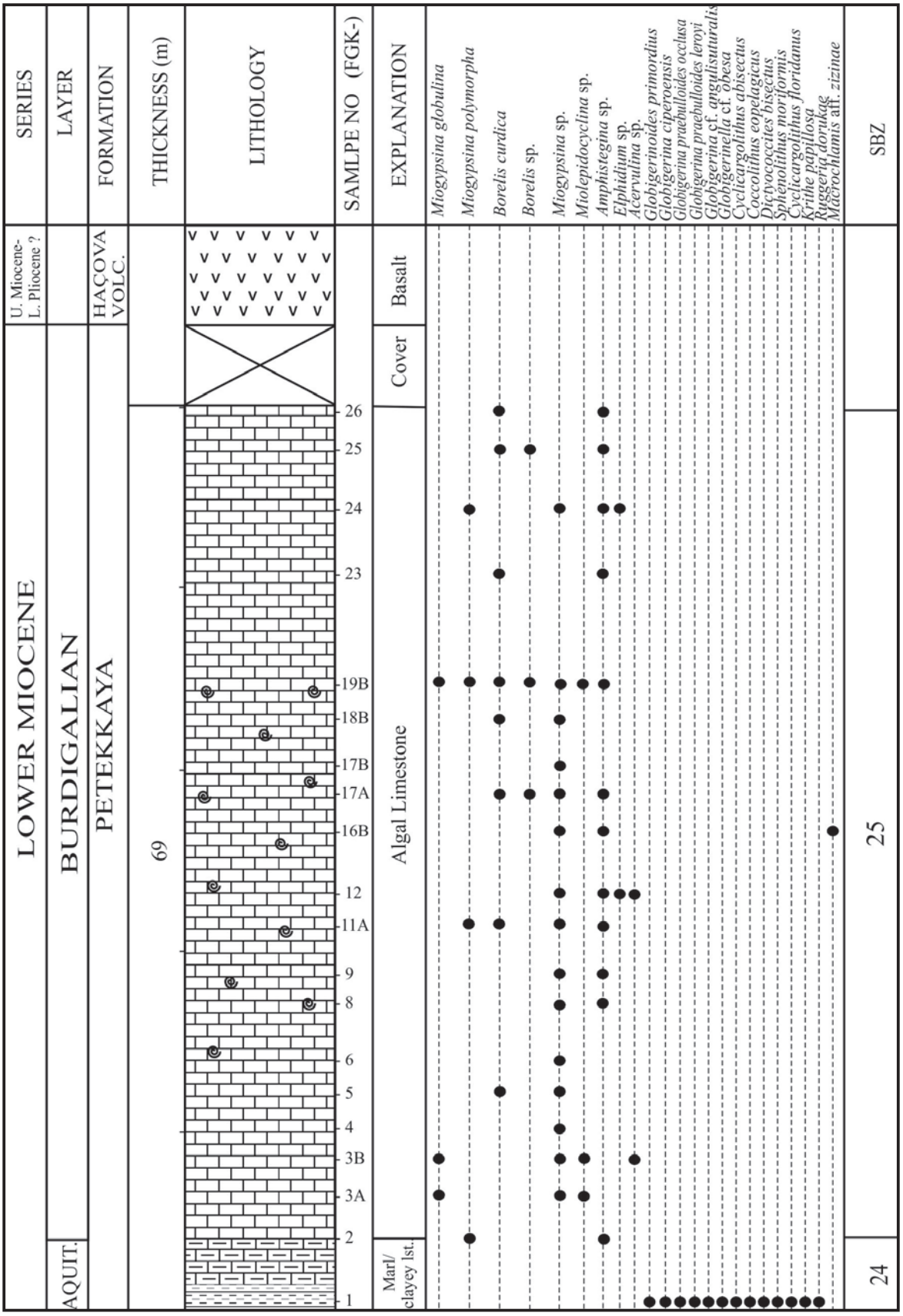

Figure 5- Stratigraphical distributions of larger benthic and planktonic foraminifera, nannoplankton, ostracode and macro fossils (NW Akçadağ, W Malatya).

in the following layers, *Miogypsina globulina* (Michelotti) was detected which is the characteristic of Burdigalian age (FGK-3A, 3B). The succession continues almost in the same characteristics until 69th meter starting from this level. Beige-white colored, medium to thick bedded, occasionally massive, with solution openings, chalky, with much macro shell limestones exhibit a reefal characteristic throughout the succession. Alga, bryozoa, coral and bivalves accompany with much large benthic foraminiferal fauna in almost all layers. Macro hand specimens were collected from the intermediate levels of reefal limestones (FGK-16B), and Burdigalian aged *Macrochlamis* aff. *zizinae* (Blanckenhorn) was described. It was determined that the life span of genus *Miogypsina* started approximately from the 4th meter of the succession and continued until 68th meter (i.e. the end of the succession). It was observed that Burdigalian aged *Borelis curdica* (Reichel), *Borelis* sp., *Miolepidocyclina* sp., *Amphistegina* sp., *Elphidium* sp., *Acervulina* sp. taxa accompany with genus *Miogypsina* in layers of reefal limestones. However; the last occurance of *B. curdica* draws the upper boundary of SBZ 25 zone. Approximately; 70 meters thick, covered area was passed after 69th meter, and it was seen that dense arenitized basalts had cut and covered Burdigalian aged reefal limestones in places where topography was high (1594th meter).

3.2. Develi Measured Stratigraphical Section (FGD)

Develi measured stratigraphical section starts at coordinates of X1: 04 156; Y1: 48 465 and finishes at coordinates of X2: 03 601; Y2: 46 141 (Figure 2). The length of the section which consists of Oligocene and Early Miocene sediments was measured as 103.6 meters and total of 41 samples were collected. 22 hard rock samples are much fossilliferous and were selected for oriented thin section study. Collected samples were lithologically described from bottom to top by giving their fossil contents and coded as FGD 1-24B (Figure 6). Taxa of *Archaias kirkukensis* Henson, *Austrotrillina asmariensis* Adams, *A. brunni* Marie, *Nephrolepidina praemarginata* Douvillé, *N. partita* Douvillé, *Neorotalia lithothamnica* Uhlig and *Peneroplis* cf. *laevigatus* d'Orbigny were described in yellowish, beige to white colored, medium bedded limestones at the bottom of succession (FGD-2A, 2B, 3). According to shallow benthic foraminiferal zones which were prepared by Cahuzac and Poignant (1997) for whole Tethys Oligo-Miocene, these levels correspond with Rupelian – Early Chattian (i.e. SBZ 21-22). *Nephrolepidina* sp., *Eulepidina* sp. and *Austrotrillina* sp. were detected in beige-white colored limestones just above those levels (FGD-4, 5). *Pelecyora* (*Cordiopsis*) *islandicoides* (Lamarck) which can live in lower saline lagoonal environments and represent Burdigalian – Pliocene age interval was described though representing the shallow marine environment from bivalves in the same levels. Approximately; at 10th meter of the succession it was seen that beige to white colored limestone layers consisted taxa of *Planorbulina brönnimanni* Bignot and Decrouez, *Spiroclypeus vermicularis* Tan, *Spiroclypeus* sp., *Archaias* sp., *Nephrolepidina* sp., *Eulepidina* sp., *Miogypsinella* sp., *Austrotrillina* sp., *Amphistegina* sp. and of highly developed Rotaliid individuals (FGD-6, 7). These levels of the succession were dated as Late Chattian (SBZ-23) considering both the benthic foraminiferal fauna detected and the underlying Rupelian – Early Chattian aged limestone layers and in overlying Early Miocene (Aquitanian) aged marls in which planktic foraminiferal fauna is observed. The overlying, beige to white colored marls which are approximately 3 meters thick is rich in planktic foraminifer and nannoplankton content. From planktic foraminifers; *Globigerinoides primordius* Blow and Banner, *Globigerina ciperoensis* Bolli, *G. praebulloides occlusa* Blow and Banner, *G. praebulloides leroyi* Blow and Banner, *G. ouachitaensis* s.s. Howe and Wallace, *G. praebulloides* s.s. Blow, *G.* cf. *angulisuturalis* Bolli, *Globigerinella obesa* (Bolli), *Globoquadrina dehiscens* (Chapman, Parr and Collins), *G. venezuelana* (Hedberg), *Neogloboquadrina continuosa* (Blow), *Globoturborotalia euapertura* (Jenkins), ? *Globigerinoides sacculifer* (Brady), ? *G. quadrilobatus* (d'Orbigny), ? *G. altiaperturus* Bolli; and from nannoplanktons; *Cyclicargolithus abisectus* (Müller), *Coccolithus eopelagicus* (Bramlette and Riedel), *Dictyococcites bisectus* (Hay, Mohler and Wade), *Sphenolithus moriformis* (Brönnimann and Stradner), *Discoaster deflandrei* Bramlette and Riedel, *Pontosphaera plana* (Bramlette and Sullivan) and *Helicosphaera* sp. were described. *Siphonina* sp., *Elphidium* sp., *Ammonia* sp. and *Uvigerina* sp. were described among small benthic foraminifera at the same level (FGD-9). The age of this lithological unit according to planktic foraminifers are Early Miocene and Late Rupelian-Chattian according to nannoplanktons. The first occurance of *Globoquadrina dehiscens* from foraminiferal species described within unit shows Aquitanian age (zone M1b). So, the age of this unit which is in different lithology was accepted as Aquitanian. Beige to white, thick bedded, micritic limestone layers with solution

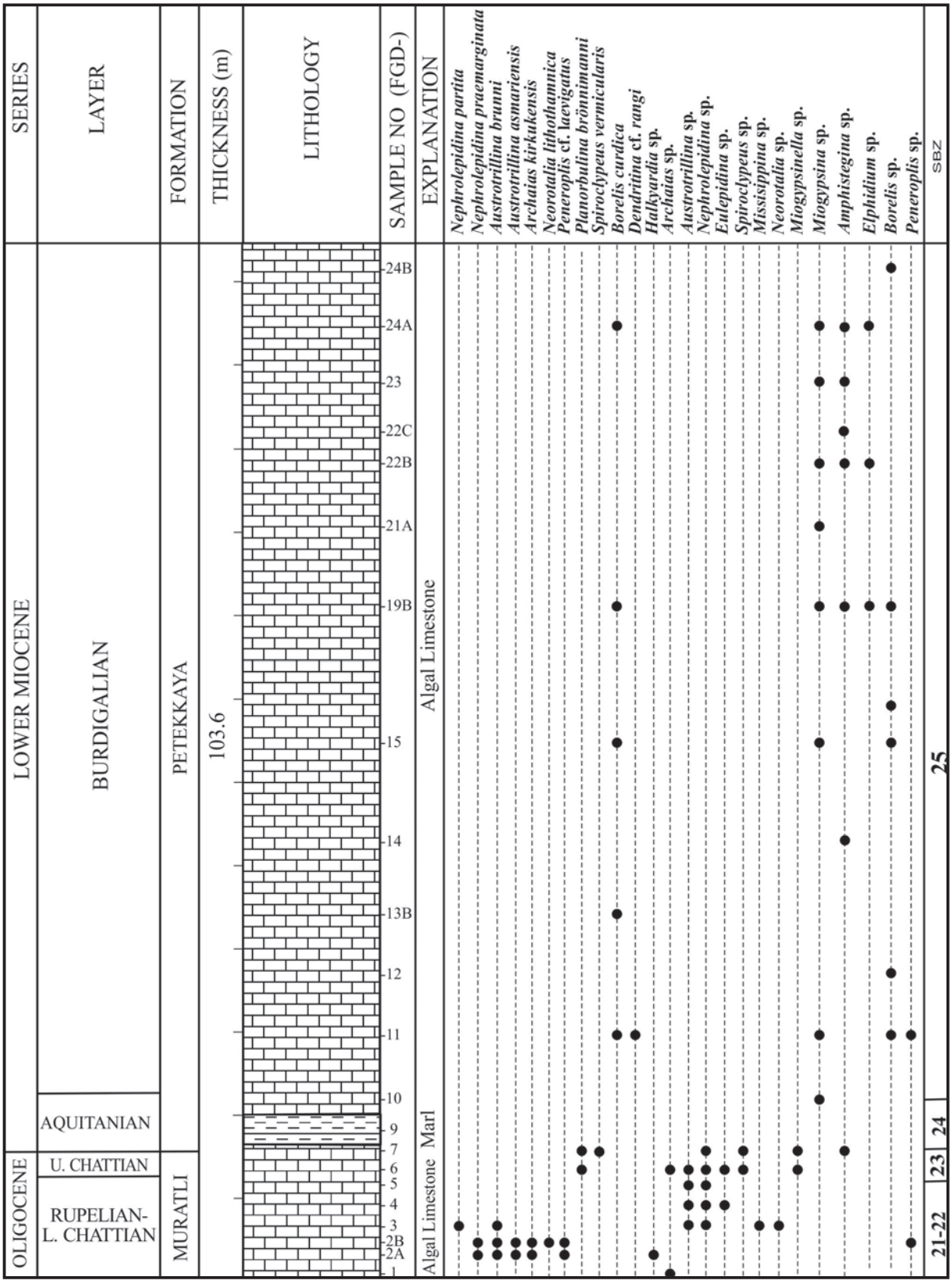

Figure 6- Stratigraphical distributions of larger benthic foraminifera detected in Develi measured stratigraphical section (W Akçadağ, W Malatya).

openings which have an approximate thickness of 10 meters and transitionally overlie the marl deposit (17th meter of the succession) are the levels in which genus *Miogypsina* was first observed. Starting from this level (FGD-11) to the uppermost level of the succession in shallow marine limestones which is characterized with similar features, it was seen that genus *Miogypsina* was sometimes accompanied by Burdigalian aged benthic foraminifers such as *Borelis curdica* (Reichel), *Dendritina* cf. *rangi* d'Orbigny, *Amphistegina* sp., *Elphidium* sp. and *Peneroplis* sp., and algae, bryozoas, corals and bivalves. Oligocene-Early Miocene aged (most probably Burdigalian according to its level structure) *Hyotissa hyotis* (Linné) which represents very shallow marine environment with average salinity in bivalves was described at 50th meter of the succession. However, at 93rd meter of the succession Burdigalian aged *Pecten* aff. *burdigalensis* Lamarck was described. Besides, it was also seen that *Clypeaster* sp. from echinides was abundant in identical levels (FGD-22B).

3.3. Edilme Measured Stratigraphical Section

Edilme measured stratigraphical section starts at coordinates of X1: 06 627; Y1: 43 539 and finishes at coordinates of X2: 05 020; Y2: 44 990 (Figure 2). The length of section which consists of Oligocene and Early Miocene sediments was measured as 218.4 meters and total of 94 samples were collected. 27 hard rock samples are much fossilliferous and oriented thin section study was carried out for these specimens. Collected samples were lithologically described from bottom to top by giving their fossil contents and coded as FGM 1A-53 B (Figure 7). At the bottom of the succession *Pelecyora* (*Cordiopsis*) *islandicoides* (Lamarck) and *Glycymeris bimaculatus* (Poli) from bivalves were described which represent Burdigalian – Pliocene age interval. The succession is represented by limestones in which similar features are observed up to 126th meter. Limestones are beige to white colored, thick to very thick bedded and much fossilliferous. From benthic foraminifers, taxa of *Nephrolepidina praemarginata* Douvillé, *N. partita* Douvillé, *Planorbulina brönnimanni* Bignot and Decrouez, *Austrotrillina asmariensis* Adams, *Heterostegina assilinoides* Blanckenhorn, 1890 emend. Henson, *Eulepidina* sp., *Nephrolepidina* sp., *Miogypsinella* sp., *Austrotrillina* sp., *Operculina* sp., *Asterigerina* sp., *Spiroclypeus* sp. and *Amphistegina* sp. were described in beige to white colored limestones until 103rd meter. Furthermore; alga, coral, bryozoa and bivalves accompany with foraminiferal fauna at almost all levels. It was seen that at 103rd meter Lepidocyclinid foraminifers formed peak zone in yellowish to beige colored, medium to thick bedded limestone layers (FGM -19). At this level, taxa of *Nephrolepidina praemarginata* Douvillé, *N. partita* Douvillé, *Eulepidina* cf. *formosoides* Douvillé, *Heterostegina assilinoides* Blanckenhorn, 1890 emend. Henson, *Neorotalia lithothamnica* Uhlig, *Spiroclypeus* sp., *Eulepidina* sp., *Nephrolepidina* sp., *Amphistegina* sp. were described. The location of these species in the zonation prepared for all Tethys Oligocene is Rupelian – Early Chattian (SBZ 21-22) (Cahuzac and Poignant, 1997). *Nephrolepidina morgani* (Lemoine and Douvillé) was described in limestones just above this level (FGM-24). The first occurance of this species draws the lower boundary of zone SBZ 23. In identical levels, *N. morgani* species is also accompanied by taxa of *Austrotrillina asmariensis* Adams, *A. brunni* Marie, *Miogypsinella* sp. ve *Amphistegina* sp. (FGM-29). In beige to white colored, thick bedded limestones at 155th meter, taxa of *Miogypsinella akcadagensis* (Gedik and Sirel), *M. borodinensis* Hanzawa, *M.* cf. *complanata* (Schlumberger), *Postmiogypsinella* sp., *Miogypsina* sp., *Amphistegina* sp., *Nephrolepidina* sp. were described (FGM-30A). Considering the interpretations made for the stratigraphical distributions of taxa described, it was determined that the age of these levels were Late Chattian (SBZ 23). In these limestones layers, the last occurance of *M.* cf. *complanata* species specifies the upper boundary of the zone SBZ 23 (FGM 30B). In identical levels *Spondylus* aff. *podopsideus* Lamarck was described which represents Eocene – Early Miocene age interval from bivalves. Following these layers, white colored, 4 meters thick marls were observed nearly at 127th meter. *Cyclicargolithus floridanus* (Roth and Hay), *Coccolithus eopelagicus* (Bramlette and Riedel), *Ericsonia robusta* (Kamptner) and *Cyclicargolithus abisectus* (Müller) were described from nannoplanktons in marly layers. Nannoplankton species decribed within unit give the age of Oligocene. However, the unit was correlated with Aquitanian aged marls (SBZ 24) which was characterized by the first occurance of *G. dehiscens* located over Late Chattian in Develi and Karamağara sections and was considered that these units were isochronous. Limestones of which their thicknesses were estimated as 87.6 meters and continue up to 219th meter on marls constitute the uppermost levels of the succession. Limestones are

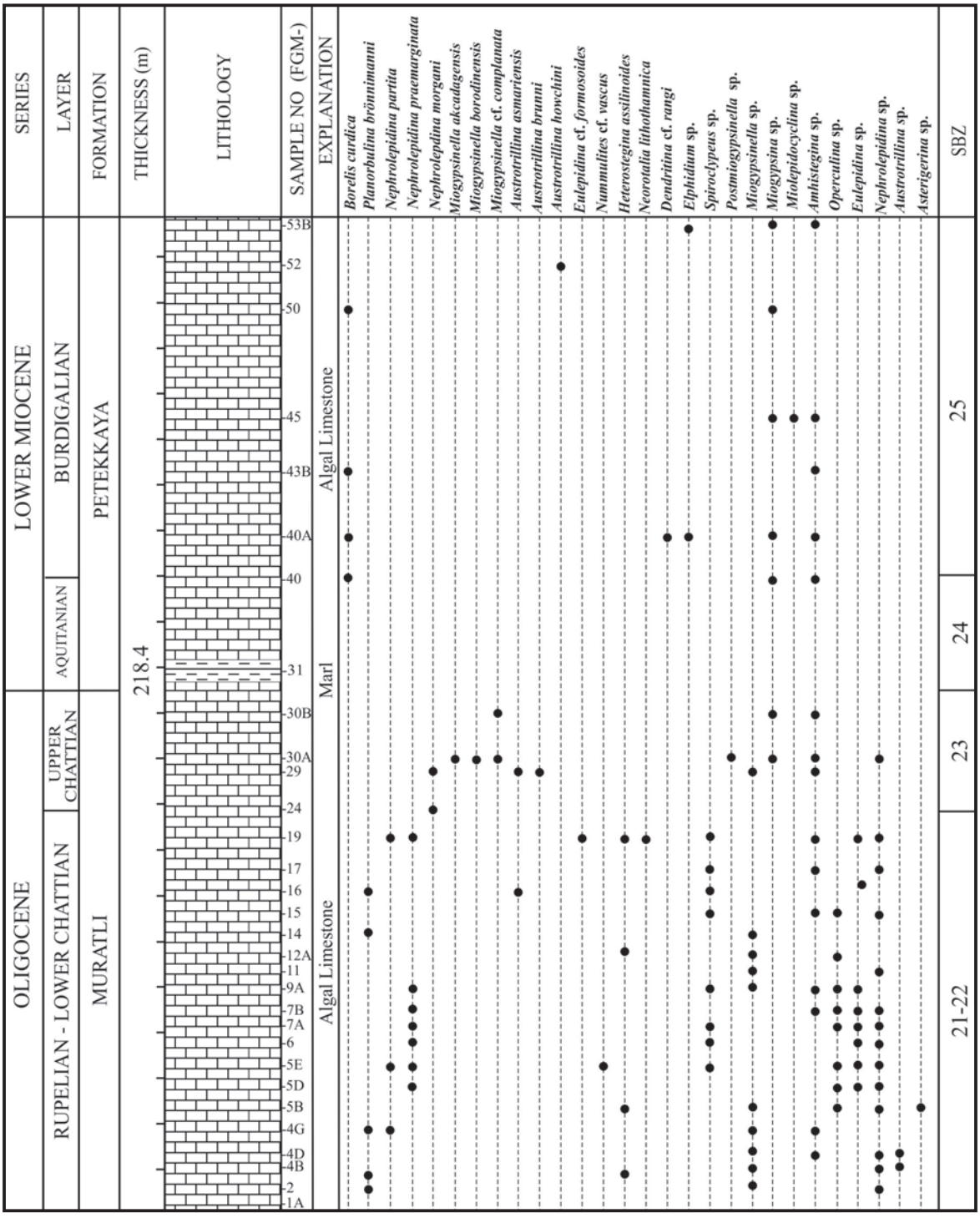

Figure 7- Stratigraphical distributions of larger benthic foraminifera detected in Edilme measured stratigraphical section (SW Akçadağ, W Malatya).

beige to white colored, medium, thick to very thick bedded, occasionally massive and have solution openings. The taxa of Burdigalian aged (SBZ 25) *Borelis curdica* (Reichel), *Austrotrillina howchini* (Schlumberger), *Dendritina* cf. *rangi* d'Orbigny, *Miolepidocyclina* sp., *Amphistegina* sp., *Elphidium* sp. were described, and *Miogypsina* species in these levels which have rich foraminiferal fauna are accompanied with alga, bryozoa, coral and bivalves. *B. curdica* starts from the bottom of Burdigalian and continues its presence almost until the uppermost levels of the succession.

3.4. Karamağara Measured Stratigraphical Section (HYM)

Karamağara measured stratigraphical section starts at coordinates of X1: 16 599; Y1: 57 032 and finishes at coordinates of X2: 12 705; Y2: 58 026 (Figure 2). The length of the section which consists of Oligocene and Early Miocene sediments was measured as 237.6 meters and total of 25 samples were collected. 9 hard rock samples are much fossilliferous and oriented thin section study was carried out for these specimens. Collected samples were lithologically described from bottom to top by giving their fossil contents and coded as HYM 35-48 (Figure 8). At the bottom of the succession 6 meters thick, gray-white-beige colored, fine to medium bedded monogenic pebble, and beige to yellow colored, fragile-brecciated limestone layers with rounded carbonate pebbles-sands were observed. Then, 1 meter thick, cream to pale brown colored, thick bedded, massive, fine textured, much fossilliferous sandy limestone layer was observed over the succession. *Austrotrillina brunni* Marie, *Miogypsinella* sp., *Archaias* sp., *Penarchaias* sp., *Asterigerina* sp. and much Miliolidae (HYM-35) was observed in these levels. The succession continues primarily with pebbly-sandy limestones then with yellow-beige-white colored, medium to thick bedded, fractured, sandy-chalky limestones until 32nd meters. In these limestones which continue up to marls, taxa of *Borelis pygmaea* Hanzawa, *Borelis merici* Sirel, *Penarchaias glynnjonesi* (Henson), *Austrotrillina brunni* Marie, *Archaias hensoni* Smout and Eames, *Neoplanorbulinella* spp., *Asterigerina* sp., *Operculina* sp. and *Amphistegina* sp. were determined. Based on this fossil assemblage, the age of the bottom for the succession was determined as Rupelian - Lower Chattian (SBZ 21-22). In hand specimens collected from sandy limestone levels at 35th meter of the succession *Pecten burdigalensis* Lamarck (HYM-40A) from bivalves was described. One to two meters ahead of these layers are the first levels in which species belonging to genus *Miogypsina* is observed (HYM-40B). In these partly clastic limestones, it was observed that genus *Miogypsina* was accompanied by taxa of *Miogypsinella* sp., *Amphistegina* sp., *Heterostegina* sp., *Operculina* sp., *Asterigerina* sp. and *Elphidium* sp. Just above these elevations, it was seen that 10 meters thick, white-greenish colored marls were deposited. Nevertheless; the age data in marls could not be found. Yellow to beige colored, 15 meters thick, fine to medium bedded, jointed, much fossilliferous sandy limestone and sandstone, and 8 meters thick, white to green colored marl and beige colored, fine to medium bedded limestone deposition was observed on marls (HYM-41). In marls, Chattian - Aquitanian aged *Globigerinoides primordius* Blow and Banner, *Tenuitellinata juvenilis* (Bolli), *Globigerinita incrusta* Akers, *Globigerina praebulloides leroyi* Blow and Banner, *G. praebulloides occlusa* Blow and Banner, *G. praebulloides praebulloides* Blow, *G. ouachitaensis gnaucki* Blow and Banner, *G. ouachitaensis ouachitaensis* Howe and Wallace, *G.* cf. *angulisuturalis* Bolli, *Globorotaloides* cf. *suteri* Bolli, *Paragloborotalia* spp., *Globoguadrina* sp. and *Globigerinoides* sp. were described. In clayey limestones over marls, *Miogypsinella akcadagensis* (Gedik and Sirel), *M. borodinensis* Hanzawa, *Postmiogypsinella intermedia* Sirel and Gedik and *Miogypsina* spp. were described. This limestone layer which consists of rich benthic foraminiferal taxa (HYM-42) was aged as Upper Chattian (SBZ 23) as the lower boundary of the underlying marls had been drawn based on the first occurance of *G. dehiscens*. Marly layers which remain just below the covered area and correspond with 70th meter of the succession are rich in terms of planktic foraminifer and nannoplankton content (HYM-42A). Planktic foraminifera described in the unit are *Globoturborotalia euapertura* (Jenkins), *Globigerina ouachitaensis* s.s. Howe and Wallace, *G. ouachitaensis gnaucki* Blow and Banner, *G. praebulloides occlusa* Blow and Banner, *G. praebulloides leroyi* Blow ve Banner, *G. praebulloides* s.s. Blow, *G.* cf. *angulisuturalis* Bolli, *G. ciperoensis* Bolli, *Globoquadrina dehiscens* (Chapman, Parr ve Collins), *G. venezuelana* (Hedberg), *G. praedehiscens* Blow and Banner, *G. selli* Borsetti and *Globigerinoides primordius* Blow and Banner. Nannoplanktons described in the unit are on the other hand; *Discoaster deflandrei* Bramlette and Riedel, *Coccolithus eopelagicus* (Bramlette and Riedel), *Cyclicargolithus abisectus* (Müller), *C. floridanus* (Roth and Hay), *Reticulofenestra hampdenensis* Edwards, *R. umbilica* (Levin), *R. reticulata* (Gartner and Smith), *R. hillae* Burky and Percival, *Zygrhablithus bijugatus* (Deflandre), *Lanternithus minutus* Stradner, *Ericsonia formosa* (Kamptner), *E. subdisticha* (Roth and Hay), *Cruciplacolithus tenuis* (Stradner), *Braarudosphaera bigelowi* (Gran and Braarud), *Helicosphaera perch-nielseniae* Haq, *H. euphratis* Haq, *H. obligua* Bramlette and Wilcoxon, *H. kamptneri* Hay and Mohler, *H. recta* Haq, *Coronocyclus nitescens* (Kamptner), *Dictyococcites bisectus* (Hay, Mohler and Wade), *Pontosphaera multipora* (Kamptner), *P. plana* (Bramlette and Sullivan), *Micrantholithus crenulatus* Bramlette and Sullivan, *Sphenolithus moriformis* (Brönnimann and Stradner), *S. predistentus* Bramlette

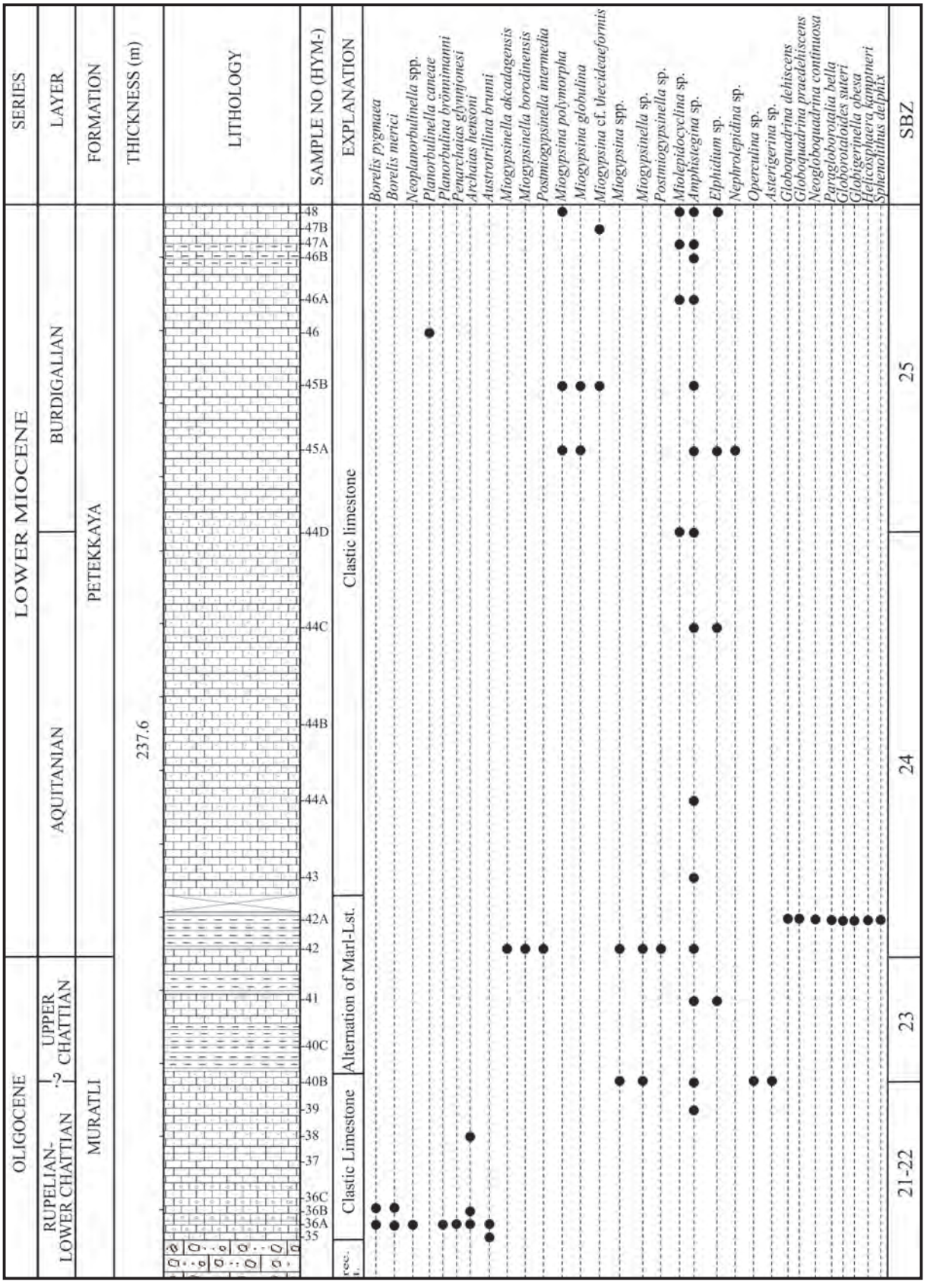

Figure 8- Stratigraphical distributions of larger benthic foraminifera, planktonic foraminifera and nannoplanktons detected in Karamağara measured stratigraphical section (NE Akçadağ, W Malatya).

and Wilcoxon, *S. distentus* (Martini), *S. delphix* Burky and *Sphenolithus* sp. The age of the unit according to planktic foraminifera and nannoplanktons are Early Miocene. The presence of typical planktic foraminiferal species *G. dehiscens* and nannoplankton species *S. delphix* indicate M1b and NN1-NN2 (Aquitanian) zones (Berggren et al., 1995). Then, thick covered area was passed and it was considered that marl-claystone deposition could occur in this area as well. The succession, starting from covered area to uppermost levels, is white colored, medium to thick bedded, much macro fossilliferous, chalky, with solution openings, sandy and clayey in places, and continues with the characteristic of reefal limestone and ends at 237.6th meter. Reefal limestones were fully traced in terms of benthic foraminifers such as; *Miogypsina globulina* (Michelotti), *M. polymorpha* (Rutten), *M.* cf. *thecideaeformis* (Rutten), *Planorbulinella caneae* Freudenthal, *Miogypsina* sp., *Miolepidocyclina* sp., *Heterostegina* sp., *Amphistegina* sp., *Asterigerina* sp., *Operculina* sp. and *Elphidium* sp. and of alga, bryozoa, coral and bivalves in all layers which is the characteristics for Burdigalian (HYM 43-48). These reefal limestones based on benthic foraminiferal taxa detected were accepted as the Burdigalian age and its equivalence is SBZ 25 in larger foraminiferal zonation.

4. Biostratigraphy

In order to carry out biostratigraphical study, first all paleontological data in sections were revealed and their stratigraphical distributions were traced as much as possible. All collected fossils were studied again considering their lithological and stratigraphical sequence and age intervals of sections were determined. While determining the age of sections stratigraphical sequence and characteristics of similar facies were used in cases when fossil data are insufficient or missing. Total of three larger benthic foraminiferal zones were detected in measured sections (Figure 9). The study of Cahuzac and Poignant (1997) was taken as a basis in the zonation of larger benthic foraminifer. Besides, it was benefited from the geological time table in which biozones of planktic foraminifera and nannoplanktons, and Mediterranean layers were explained ranging from Late Eocene to Late Miocene (Hardenbol et al., 1998).

Detected biozones are given below as;

4.1. SBZ 21-22 (Rupelian-Early Chattian)

The lower boundary of this biozone was drawn by the last occurance of Discocyclinides and a couple of *Nummulites* species (*N. retiatus*); whereas, the upper boundary was drawn by the first occurance of Lepidocyclinides (Cahuzac and Poignant, 1997). Investigators have divided this biozone into two parts as; SBZ-21 which corresponds to Early-Middle Rupelian which its lower boundary was drawn by the first occurance of *Nummulites vascus* and *Nummulites fichteli*, and SBZ-22 (22a, 22b) which corresponds to Late Rupelian-Early Chattian which its lower boundary was drawn by the first occurance of Lepidocyclinides. However; in this study *Nephrolepidina praemarginata* and *N. partita* which are the first representatives of Lepidocyclinid foraminifera, and *Nummulites* cf. *vascus* which draw the lower boundary of Rupelian with its first occurance were observed together in the Edilme measured stratigraphical section. And, in the Develi measured stratigraphical section, Lepidocyclinid foraminifera were observed at the bottom of Oligocene lithostratigraphical units. Similar finding was also observed in another comprehensive study carried out in east and southeast of Turkey (Sirel 2003; Hatay-Arabil Section; Elazığ-Karaman and Sarıbuğday Sections; Muş-Kelereşdere Section). As the first and last occurances of species mentioned in measured stratigraphical sections in the study region could not be traced sufficiently considering these findings, this biozone was described as SBZ 21-22.

SBZ 21-22 biozone is formed by the representatives of families of Soritid, Peneroplid, Miliolid and Austrotrillinid, and was determined by taxa of *Archaias kirkukensis*, *Austrotrillina asmariensis*, *A.brunni* and *Peneroplis* cf. *laevigatus*. Sirel (2003) defined similar foraminiferal assemblage in west of Malatya province between Priabonian with *Nummulites fabianii* and Late Chattian with *Miogypsinoides complanatus,* and dated as Rupelian-Early Chattian. Oligocene aged this foraminiferal assemblage with porcelain test was described in several previous studies carried out in regions belonging to Mediterranean Tethys (Iran, Iraq, Spain, Italy, Turkey) (Henson 1950, Grimsdale 1952, Hottinger 1963, Bignot 1972, Barbin and Bignot 1986, Sartorio and Ventruni 1988, Sirel 1996, Sirel et al., 2013).

SBZ 21-22 is characterized by *Nephrolepidina partita* and *N. praemarginata* species in shallow marine limestones of the Edilme measured stratigraphical section. Besides; these index species are accompanied by taxa of *Eulepidina* cf.

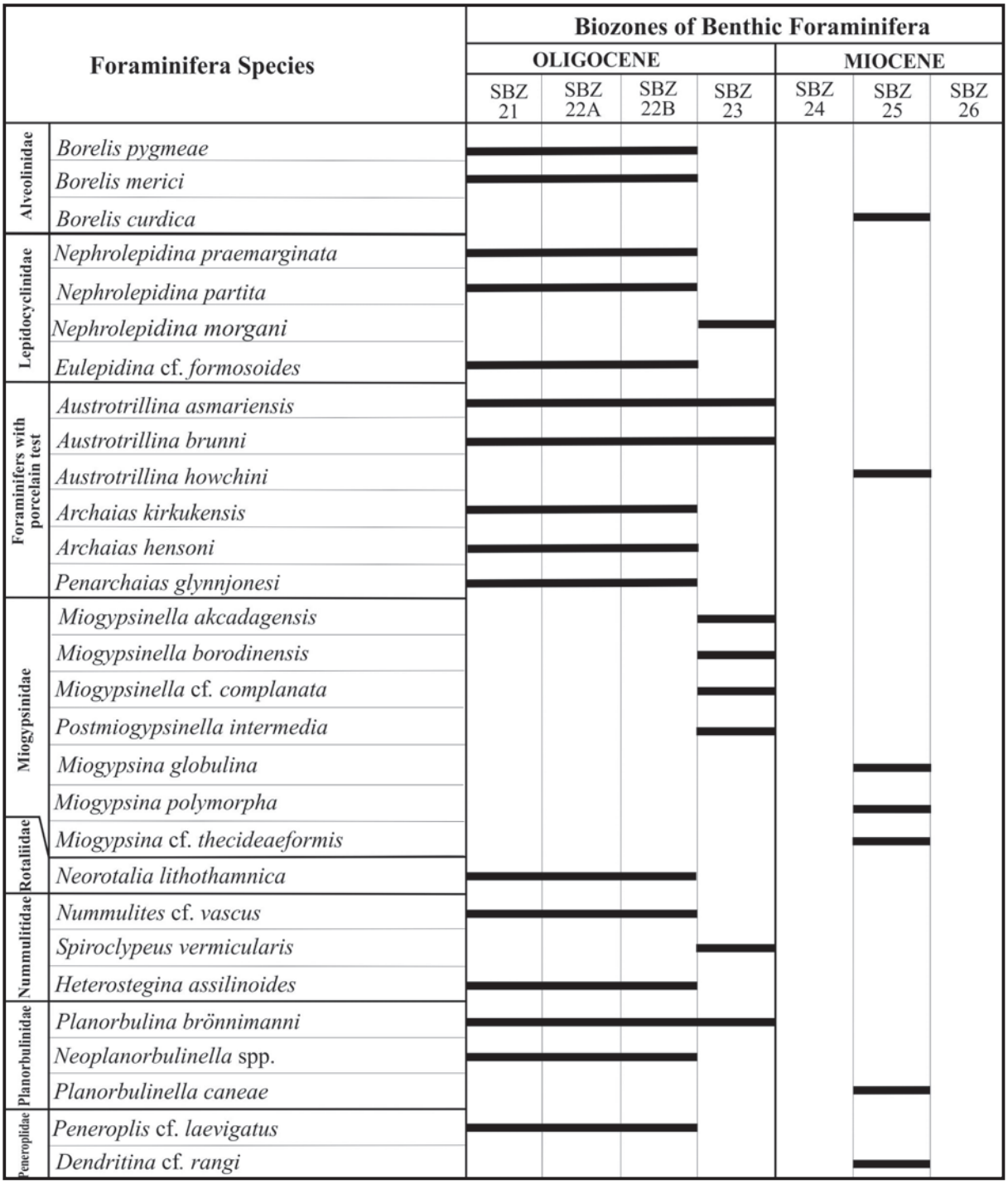

Figure 9- Stratigraphical distributions of larger benthic foraminiferal species in biozones of Oligocene-Lower Miocene.

formosoides, *Nummulites* cf. *vascus*, *Heterostegina assilinoides* and *Neorotalia lithothamnica*.

This biozone was discriminated by the presence of *Borelis pygmaea* and *Borelis merici* species in clastic limestones of the Karamağara measured stratigraphical section. These species are accompanied by taxa of *Archaias hensoni*, *Penarchaias glynnjonesi* and *Neoplanorbulinella* spp.

4.2. SBZ 23 (Late Chattian)

The lower and upper boundaries of this biozone were drawn by the first occurance of *Miogypsinoides* species and the first occurance of *Miogypsina*

gr. *gunteri*, respectively (Cahuzac and Poignant, 1997). Investigators have made the description of this biozone especially by taking the developments of *Miogypsinoides* species (*M. complanatus*, *M. borodinensis*, *M. formosoides* and *M. lateralis*) as basis. The development of Miogypsinid species were clearly seen in this study too.

Late Chattian SBZ 23 zone is characterized with the finding of *Miogypsinella akcadagensis*, *M. borodinensis* and *M.* cf. *complanata* together with *Nephrolepidina morgani* in shallow marine carbonates of the Edilme stratigraphical section and with the presence of *Miogypsinella akcadagensis* and *M. borodinensis* in Karamağara section. Moreover; accompany of *Postmiogypsinella intermedia* to index species is significant in the Karamağara measured stratigraphical section. SBZ 23 was also determined by the coexistence of miogypsinids (*Miogypsina basraensis*, *Miogypsinoides formosensis* and *M. sivasensis*) which occur in shallow marine carbonates and clastic rocks in Muş Kelereşdere section in eastern Turkey and *Nephrolepidina morgani* (Özcan et al., 2009).

4.3. SBZ 25 (Burdigalian)

The lower and upper boundaries of this biozone were drawn by the first occurance of *Miogypsina* gr. *globulina* and by the extinction of species belonging to genus *Miogypsina*, respectively (Cahuzac and Poignant, 1997).

In the study area, marls rich in planktic foraminifera and nannoplankton assemblages take place among layers of shallow marine limestone where larger benthic biozones of SBZ 23 (Late Chattian) and SBZ 25 (Burdigalian) are defined. This unit which is in different lithology does not contain any benthic foraminifer. However, considering both the presence of index planktic foraminifer species *G. dehiscens and S. delphix* in nannoplanktons which are defined in Develi and Karamağara Measured Stratigraphical Sections, and the presence of marls which are stratigraphically defined in the succession between the zones of SBZ-23 and SBZ-25 indicate that this marly unit indicates Aquitanian age.

5. Results

• Four stratigraphical sections were measured in the study area which covers Oligo-Miocene successions and; systematically, 182 hard rock samples were taken from these sections. As a result of paleontological studies, total of 28 taxa were defined belonging to Soritidae, Planorbulinidae, Peneroplidae, Austrotrillinidae, Alveolinidae, Lepidocyclinidae, Miogypsinidae and Nummulitidae families.

• In Oligocene shallow marine deposits, SBZ 21-22 biozone with species of *Archaias kirkukensis*, *A. hensoni*, *Penarchaias glynnjonesi*, *Borelis merici*, *B. pygmaea*, *Austrotrillina asmariensis*, *A. brunni*, *Peneroplis* cf. *laevigatus*, *Nephrolepidina praemarginata*, *N. partita*, *Eulepidina* cf. *formosoides*, *Nummulites* cf. *vascus*, *Heterostegina assilinoides*, *Neorotalia lithothamnica* and SBZ 23 biozone with speices of *Miogypsinella borodinensis*, *M.* cf. *complanata*, *Nephrolepidina morgani* and *Spiroclypeus vermicularis* were detected.

• As a result of biostratigraphical study of Miocene aged marine units, zone SBZ 25 was described, and limestones characterized by very shallow and shallow marine environments were characterized by the presence of *Borelis curdica*, *Dendritina* cf. *rangi, Austrotrillina howchini* and *Miogypsina globulina*, *M. polymorpha*, *M.* cf. *thecideaformis*, *Planorbulinella caneae* species, respectively.

• Biozones determined in the study area were correlated by Cahuzac and Poignant (1997) with larger benthic foraminifer zonation which was prepared for European Oligocene - Miocene. It was also seen that, biozones defined in the region had been in mainly compatible with European zonation.

• Based on biostratigraphical locations of benthic foraminiferal taxa defined in Develi, Edilme, Kuzkaya and Karamağara measured stratigraphical sections, Oligo – Miocene transition was observed in the region. Marine units ranging from Oligocene to Miocene exhibit the characteristic of uninterrupted succession in lithostratigraphically and biostratigraphically correlated sections. Paleontological findings also support this observation.

• Stratigraphically, Chattian - Burdigalian aged marls in the region consist assemblages of rich planktic foraminifer and nannoplankton assemblages. Considering both the presence of index planktic foraminifer species *G. dehiscens and S. delphix* in nannoplanktons which are defined in Develi and Karamağara measured stratigraphical sections, and the presence of marls which are stratigraphically defined within Late Chattian - Burdigalian aged shallow marine carbonate succession indicate that this

unit which is in different lithology indicates Aquitanian age.

• Cosmopolitan species *M. globulina* was observed in Burdigalian aged shallow marine carbonates in Kuzkaya and Karamağara measured stratigraphical sections, and was described over wide geographical regions ranging from Central America to Indo-Pacific and West (Mediterranean) Tethys. The co-existence of this species with *M. polymorpha* which is seen in stratigraphical records (only from Indo-Pacific) highly support the assumption of a probable marine connection between Indo-Pacific and Mediterranean Tethys in Burdigalian time in the region (Harzhauser et al., 2002; Reuter et al., 2009, Qom formation, Iran).

Acknowledgements

This investigation has been supported within the scope of MTA project number 2005-14J3 and covers one part of the study which had been prepared as a PhD thesis in Geological Engineering Department of the Institute of Sciences in Ankara University, Ankara, Turkey. The author fully thanks to Dr. Ercüment Sirel (AU) for his supports and contributions in making of this PhD thesis, to Dr. Aynur Hakyemez (MTA) for description of planktonic foraminifera, to Ayşegül Aydın (MTA) for the determinations of nannoplanktons, to Assoc. Prof. Yeşim Büyükmeriç (İslamoğlu) for description of macrofossils (BEU) and to Dr. Gönül Çulha (MTA) for description of ostracods.

Received: 22.04.2014
Accepted: 14.10.2014
Published: June 2015

References

Akkuş, M.F. 1971. Darende-Balaban Havzasının (Malatya, ESE Anadolu) jeolojik ve stratigrafik incelenmesi: *Maden Tetkik Arama Dergisi*, 76: 1-60, Ankara.

Alkan, H. 1997. Malatya Baseninin Jeolojisi ve Petrol Olanakları. *Türkiye Petrolleri Anonim Ortaklığı Report*, 3766, Ankara.

Ayan, T. 1961. Malatya Kuzeyindeki Hekimhan-Ebreme köyü bölgesinin (K39-c3) detay jeolojisi ve petrol imkanları. *Maden Tetkik ve Arama Genel Müdürlüğü Report No*, 4186 (unpublished), Ankara.

Berggren, W. A., Kent, D. V., Swisher, C. C., Aubry, M. P. 1995. A revised Cenozoic geochronology and chronostratigraphy. In: W. A. Berggen, D. V. Kent, M. P. Aubry& J. Hardenbol, Eds., Geochronology, time scale and global correlations an unified temporal framework for an historical geology. *Soc. Econ. Pal. Miner. Spec. Public., 54*: 129-212.

Barbin V., Bignot, G. 1986. New proposal for an Eocene-Oligocene boundary according to microfacies from the Priabonian type-section. In: Pomerol Ch., & Premoli Silva I. (eds.), Terminal Eocene Events. *Developments in Paleontology and Stratigraphy,* 9: 49-52, 3 figs. Elsevier, Amsterdam.

Bignot, G. 1972. Les microfaciès et leur utilisation stratigraphique. *Mém. Bur. Rech. Géol. Min*., 77: 93-107, 3 pls. Paris.

Cahuzac, B., Poignant, A. 1997. Essai de biozonation dans les bassins européens à I'aide des grands foraminifères néritiques. *Bulletin Society Géological de France,* 168 (2): pp. 155 - 169.

Drooger, C. W. 1993. Radial foraminifera; morphometrics and evolution. North Holland, Amsterdam, 242 p.

Gedik, F. 2010. Malatya Havzasındaki Sığ Denizel Sedimanların Oligo-Miyosen Bentik Foraminifer Tanımlaması ve Biyostratigrafisi, Doktora Tezi, Ankara Üniversitesi, 185 p., 25 plates, Ankara.

Gedik, F. 2014. Malatya Oligo-Miyosen Havzasının Bentik Foraminifer Faunası, (Doğu Toroslar, D Türkiye), *Maden Tetkik ve Arama Dergisi*, 149: 93-136 (in print).

Grimsdale, T.F. 1952. Cretaceous and Tertiary Foraminifera from the Middle East. *Bulletin of the British Museum (Natural History)*, (Geology), 1 (8): 223-247, 1 fig., pls. 20-25. London.

Hardenbol, J., Thierry, J., Farley, M. B., Jacquin, T., de Graciansky, P. C., Vail, P. R. 1998. Mesozoic and Cenozoic Sequence Stratigraphy of European Basins, *SEPM Special Publication* 60.

Harzhauser, M., Piller, W.E., Steininger, F.F. 2002. Circum-Mediterranean Oligo-Miocene biogeographic evolution the gastropods point of view, *Palaeogeography, Palaeoclimatology, Palaeoecology,* 183: pp.103-133.

Henson, F. R. S. 1950. Middle eastern Tertiary Peneroplidae (Foraminifera) with remarks on the phylogeny and taxonomy of the family. Ph.D. thesis, Leiden University, West Yorkshire Printing Co., Wakefield, 70 p., 10 pls.

Hottinger, L. 1963. Quelques Foraminifères porcelanés oligocènes dans la série sédimentaire prébétique de Moratalla (Espagne méridionale). *Eclogae geologicae Helvetiae*, Basel, 56 (2): pp.963-972.

Karaman, T., Poyraz, N., Bakırhan, B., Alan, İ., Kadınkız, G., Yılmaz, H., Kılınç, F. 1993. Malatya-Doğanşehir-Çelikhan dolayının jeolojisi. *Maden Tetkik ve Arama Genel Müdürlüğü Report No*, 9587 (unpublished), Ankara.

Kurtman, F. 1978. Gürün Bölgesinin jeolojisi ve tektonik özellikleri: *Maden Tetkik ve Arama Dergisi*, 91: 1-12.

Örçen, S. 1986. Medik-Ebreme (KB Malatya) dolayının biyostratigrafisi ve paleontolojisi: *Maden Tetkik ve Arama Dergisi,* 105/106: 39-68, Ankara.

Özcan, E., Less, G. 2009. First record of the co-occurrence of western Tethyan and Indo-Pacific larger foraminifera in the Burdigalian of the Mediterranean province, *Journal of Foraminiferal Research*, 39 (1): 23-39.

Reuter, M., Piller, W.E., Harzhauser, M., Mandic, O., Berning, B., Rögl, F., Kroh, A., Aubry, M.P., Wielandt-Schuster, U., Hamedani, A. 2009. The Oligo-Miocene Quom Formation (Iran): evidence for an early Burdigalian restriction of the Tethyan Seaway and closure of its Iranian gateways, International *Journal of Asian Earth Sciences*, 98: pp.627-650.

Sartorio, D., Ventruni, S. 1988. Southern Tethys Biofacies. Agip S.P.A., *Donato Milanese*: 166 p.

Sirel, E. 1996. Praearchaias, a new soritid genus (Foraminiferida) and its Oligocene shallow - water foraminiferal assemblage from the Diyarbakır region (SE Turkey). *Geologica Romana*, 32: pp. 167 - 181.

Sirel, E. 2003. Foraminiferal description and biostratigraphy of the Bartonian, Priabonian and Oligocene shallow-water sediments of the southern and eastern Turkey, *Revue de Paléobiologie*, Genève, 22 (1): pp. 269-339.

Sirel, E., Gedik, F. 2011. *Postmiogypsinella*, a new Miogypsinidae (Foraminifera) from the Late Oligocene in Malatya Basin, Turkey, *Revue de Paléobiologie*, Genève, 30 (2): pp. 591-603.

Sirel, E., Özgen-Erdem, N., Kangal, Ö. 2013. Systematics and biostratigraphy of Oligocene (Rupelian-Early Chattian) foraminifera from lagoonal-very shallow water limestone in the eastern Sivas Basin (central Turkey). *Geologia Croatica*, Zagreb, 66/2: pp. 83-109.

Yoldaş, R. 1972. Malatya kuzeyinin jeolojisi ve petrol olanakları: *Maden Tetkik ve Arama Genel Müdürlüğü Rapor No,* 4936 (unpublished), Ankara.

PLATES

PLATE - 1

Figures 1-7: *Archaias kirkukensis* Henson

Rupelian- Early Chattian, Develi measured stratigraphical section, W Malatya, Eastern Turkey, X20

1: Equatorial section, A form (FGD-2A/11/1; Gedik 2014, plate 1, figure 3); 2: Equatorial section, A form, (FGD-2B/5/2; Gedik 2014, plate 1, figure 13); 3: Slightly tangential equatorial section, (FGD-2A/11/3; Gedik 2014, plate 1, figure 12); 4: Axial section, A form, (FGD-2A/4/5; Gedik 2014, plate 1, figure 14); 5: Axial section, A form,(FGD-2B/12/7; Gedik 2014, plate 1, figure 4); 6: Equatorial section, A form, (FGD-2A/7/2; Gedik 2014, plate 1, figure 6); 7: Equatorial section, A form, (FGD-2A/11/4; Gedik 2014, plate 1, figure 7).

Figures 8-9: ***Archaias hensoni*** Smout and Eames

Rupelian-Early Chattian, Karamağara measured stratigraphical section, NE Akçadağ, W Malatya, Eastern Turkey, X20.

8: Axial section, A form, (HYM-38/1; Gedik 2014, plate 2, figure 1); 9: Equatorial section, A form, (HYM-38/2/1; Gedik 2014, plate 2, figure 5).

Figures 10, 11: *Penarchaias glynnjonesi* (Henson)

Rupelian-Early Chattian, Karamağara measured stratigraphical section, NE Akçadağ, W Malatya, Eastern Turkey, X 40.

Axial section, A form, planispiral septa following the first septum and septa belonging to uniserial stage are seen, (HYM-36A; Gedik 2014, plate 2, figure 9), (HYM-36A/3; Gedik 2014, plate 2, figure 7).

Figures 12-16, 24, 29: *Austrotrillina asmariensis* Adams

Rupelian-Early Chattian, Develi measured stratigraphical section, W Malatya, Eastern Turkey, X 36.

12: Equatorial section, A form, (FGD-2B/8/1; Gedik 2014, plate 4, figure 3); 13: Slightly tilted equatorial section, (FGD-2A/3/13; Gedik 2014, plate 4, figure 7); 14: Equatorial section, B form, (FGD-2A/7/1; Gedik 2014, plate 4, figure 1); 15: Equatorial section, A form, (FGD-2A/3/8; Gedik 2014, plate 4, figure 12); 24: Equatorial section, A form, (FGD-2A/3/12; Gedik 2014, plate 4, figure 10); 29: Tilted equatorial section, A form, (FGD-2A/4/3).

16: Late Chattian, Edilme measured stratigraphical section, W Malatya, Eastern Turkey, X 36.

Equatorial section, (FGM-29/1/6; Gedik 2014, plate 3, figure 25).

Figures 17, 18: Miliolid forms with agglutinated shells X 30, (FGD-6; FGD-7; Gedik 2014, plate 3, figure 6, 7).

Figure 19-23, 26, 27: *Austrotrillina brunni* Marie

Rupelian-Early Chattian, Develi and Karamağara measured stratigraphical sections, W Malatya, Eastern Turkey, X 36.

19, 20, 21, 23, 27: Equatorial section, (FGD-2B/7/1; Gedik 2014, plate 3, figure 14); (FGD-2B/13/3; Gedik 2014, plate 3, figure 15); (FGD-2B/12/1; Gedik 2014, plate 3, figure 20); (HYM-35/1/1; Gedik 2014, plate 3, figure 19); (FGD-2A/9/7; Gedik 2014, plate 3, figure 13).

Figure 22: Late Chattian, Edilme measured stratigraphical section, W Malatya, Eastern Turkey, X 36.

Equatorial section, (FGM-29/7/2; Gedik 2014, plate 3, figure 5); 26: Tilted equatorial section, (HYM-36A/3/1; Gedik 2014, plate 3, figure 18).

Figure 25, 28: *Austrotrillina howchini* (Schlumberger)

Burdigalian, Edilme measured stratigraphical section, W Malatya, Eastern Turkey, X 36.

25: Non centered equatorial section, (FGM-52/2; Gedik 2014, plate 3, figure 24); 28: Tangential section showing subepidermal thick alveolarine structure, (FGM-52/1; Gedik 2014, plate 3, figure 17).

PLATE - 1

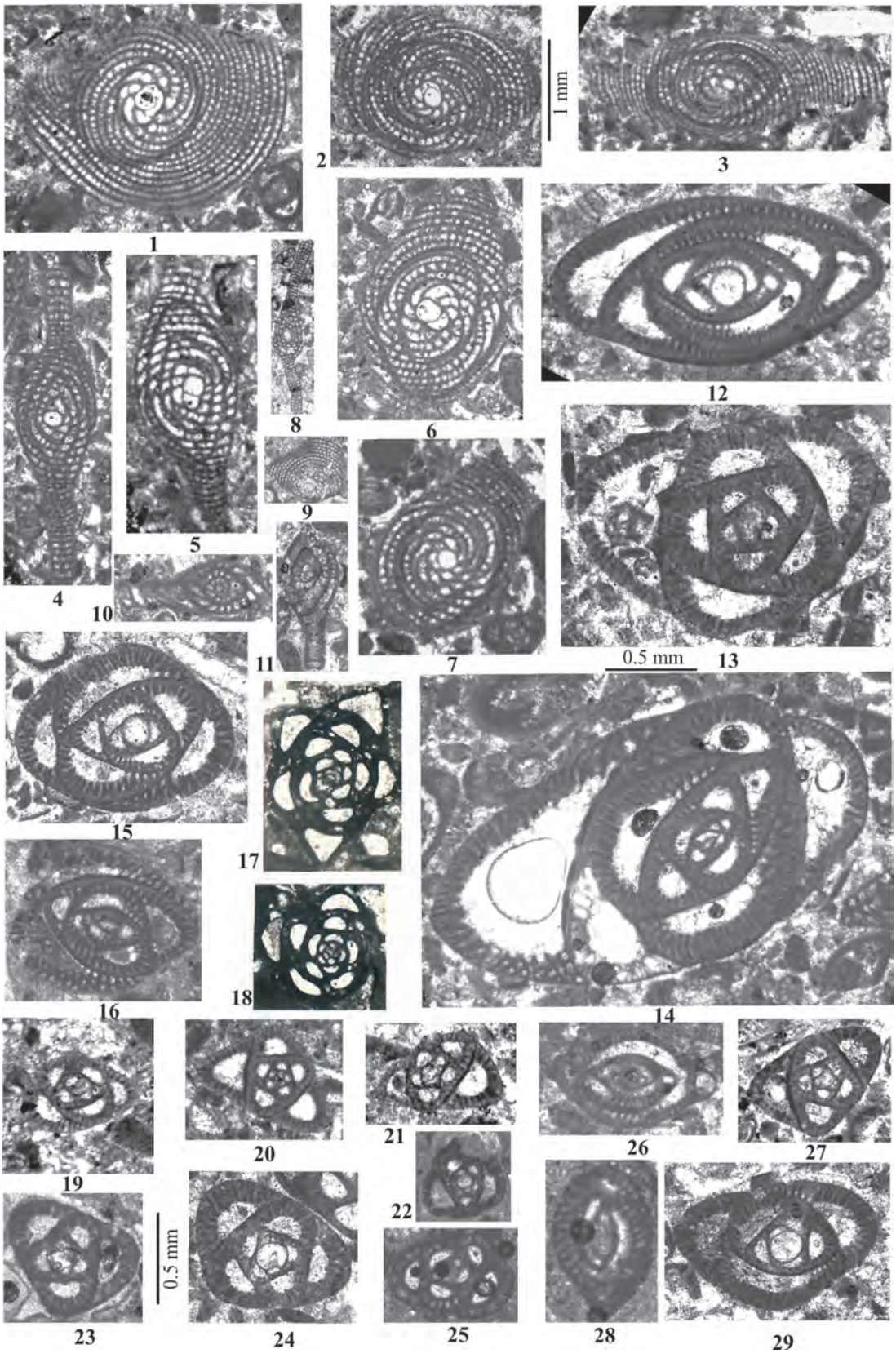
1 mm
0.5 mm
0.5 mm
1
2
3
4
5
6
7
8
9
10
11
12
13
14
15
16
17
18
19
20
21
22
23
24
25
26
27
28
29

PLATE - 2

Figure 1-8: *Borelis curdica* (Reichel)

Burdigalian, Develi, Edilme and Kuzkaya measured stratigraphical sections, W Malatya, Eastern Turkey, X 40.

1, 5: Equatorial section, (FGD-11/7/1; Gedik 2014, plate 5, figure 1); (FGK-25/3); 2, 3, 6, 7, 8: Axial section, (FGD-11/6/1; plate 5, figure 4); FGM-40A/1; FGK-23/1; FGK-25/11; FGM-43B/1); 4: Mature individual, axial section showing the aperture especially in the last whorl, (FGD-13B/1/1; Gedik 2014, plate 5, figure 5).

Figures 9, 10: *Borelis merici* Sirel

Rupelian-Early Chattian, Karamağara measured stratigraphical section, W Malatya, Eastern Turkey, X 60.

9: Non centered axial section, (HYM-36A/5/4; Gedik 2014, plate 3, figure 10); 10: Axial section, young individual, (HYM-36W/2; Gedik 2014, plate 3, figure 8).

Figure 19: *Borelis pygmaea* Hanzawa

Rupelian-Early Chattian, Karamağara measured stratigraphical section, W Malatya, Eastern Turkey, X 60.

Axial section, A form, (HYM-36A/1/1; Gedik 2014, plate 3, figure 11).

Figures 11, 13-15, 17, 21-23: *Planorbulina brönnimanni* Bignot and Decrouez

Oligosen, Develi, Karamağara and Edilme measured stratigraphical sections, W Malatya, Eastern Turkey, X35.

11, 15, 22: Oblique equatorial section, (MA-91; Gedik 2014, plate 2, figure 10); (MA-89; Gedik 2014, plate 2, figure 12); (MA-92; Gedik 2014, plate 2, figure 14); 13, 14, 17, 21: Sub axial section, (FGM-12D/1, FGM-2/1, FGM-4G/3, MA-90); 23: Oblique section, (MA-69; Gedik 2014, plate 2, figure 15).

Figures 12, 16, 18, 20: *Neoplanorbulinella* spp.

Rupelian-Early Chattian, Karamağara measured stratigraphical section, NE Akçadağ, W Malatya, Eastern Turkey, X 72.

12, 18, 20: Axial section, A form, (HYM-36A/11/1, HYM-36A/5/2, HYM-36A/3/2); 16: Axial section, B form, (HYM-36A/2/1; Gedik 2014, plate 2, figure 30).

PLATE - 2

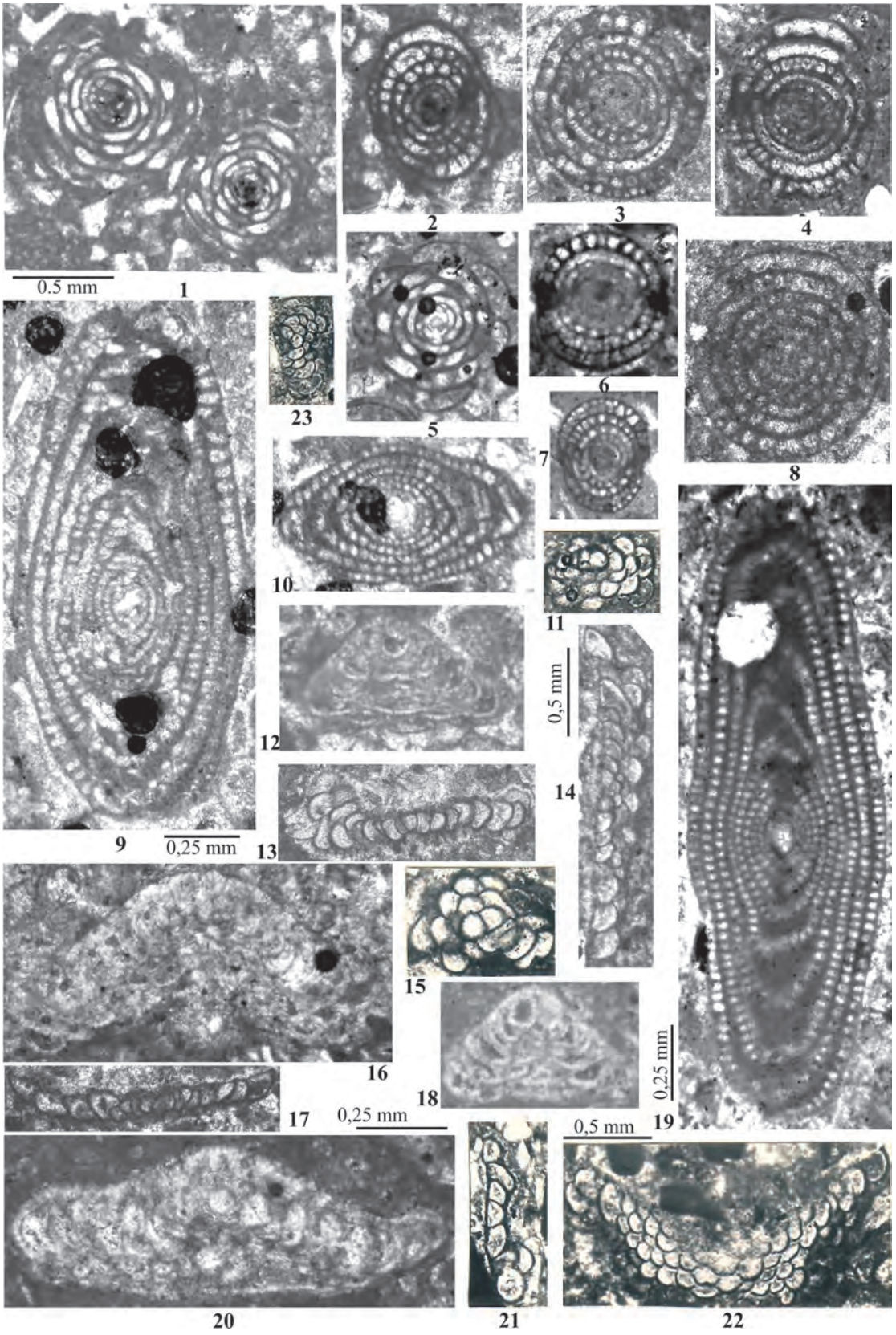
0.5 mm
1
2
3
4
23
5
6
8
7
10
11
12
0,5 mm
14
9
0,25 mm
13
15
16
18
0,25 mm
19
17
0,25 mm
0,5 mm
20
21
22

PLATE - 3

Figures 1-5: *Nephrolepidina praemarginata* Douvillé

Rupelian-Early Chattian, Edilme and Develi measured stratigraphical sections, W Malatya, Eastern Turkey, all figures, X 30.

1, 3: Equatorial section, (FGM-19/3, FGD-2B); 2: Oblique equatorial section, (FGD-2B; Gedik 2014, plate 6, figure 4); 4: Axial section, (MA-88; Gedik 2014, plate 6, figure 10); 5: Oblique equatorial section, (FGM-19/4/1; Gedik 2014, plate 6, figure 2).

Figures 6, 7: *Nephrolepidina morgani* (Lemoine and Douvillé)

Late Chattian, Edilme measured stratigraphical section, W Malatya, Eastern Turkey, X 30.

6: Equatorial section, (FGM-29/7/5; Sirel and Gedik 2011, plate 3, figure 8); 7: Axial section, (FGM-29/1/4; Sirel and Gedik 2011, plate 3, figure 9).

Figure 9: *Eulepidina cf. formosoides* Douvillé

Equatorial section, (FGM-19/11/1; Gedik 2014, plate 7, figure 10).

Figure 8: *Eulepidina sp.*

Axial section, (FGM-19/11/3; Gedik 2014, plate 7, figure 11).

Figure 10, 11: *Nephrolepidina partita* Douvillé

Rupelian-Early Chattian, Edilme measured stratigraphical section, W Malatya, Eastern Turkey, X 30.

10: Equatorial section, tiny sphere like first septum and half-moon shaped second septum are seen, (FGM-19/27/4; Gedik 2014, plate 7, figure 9); 11: Axial section, large umbo at the center of the test is very clearly seen, (FGM-5E/6/1; Gedik 2014, plate 7, figure 2).

Figures 12-14: *Neorotalia lithothamnica* Uhlig

Rupelian-Early Chattian, Edilme measured stratigraphical section, W Malatya, Eastern Turkey, X 50.

12: Equatorial section, (FGM-19/3/1; Gedik 2014, plate 12, figure 5); 13: Non centered equatorial section, (FGM-19/24/2; Gedik 2014, plate 12, figure 4); 14: Axial section, (FGM-19/25/1; Gedik 2014, plate 12, figure 7).

PLATE - 3

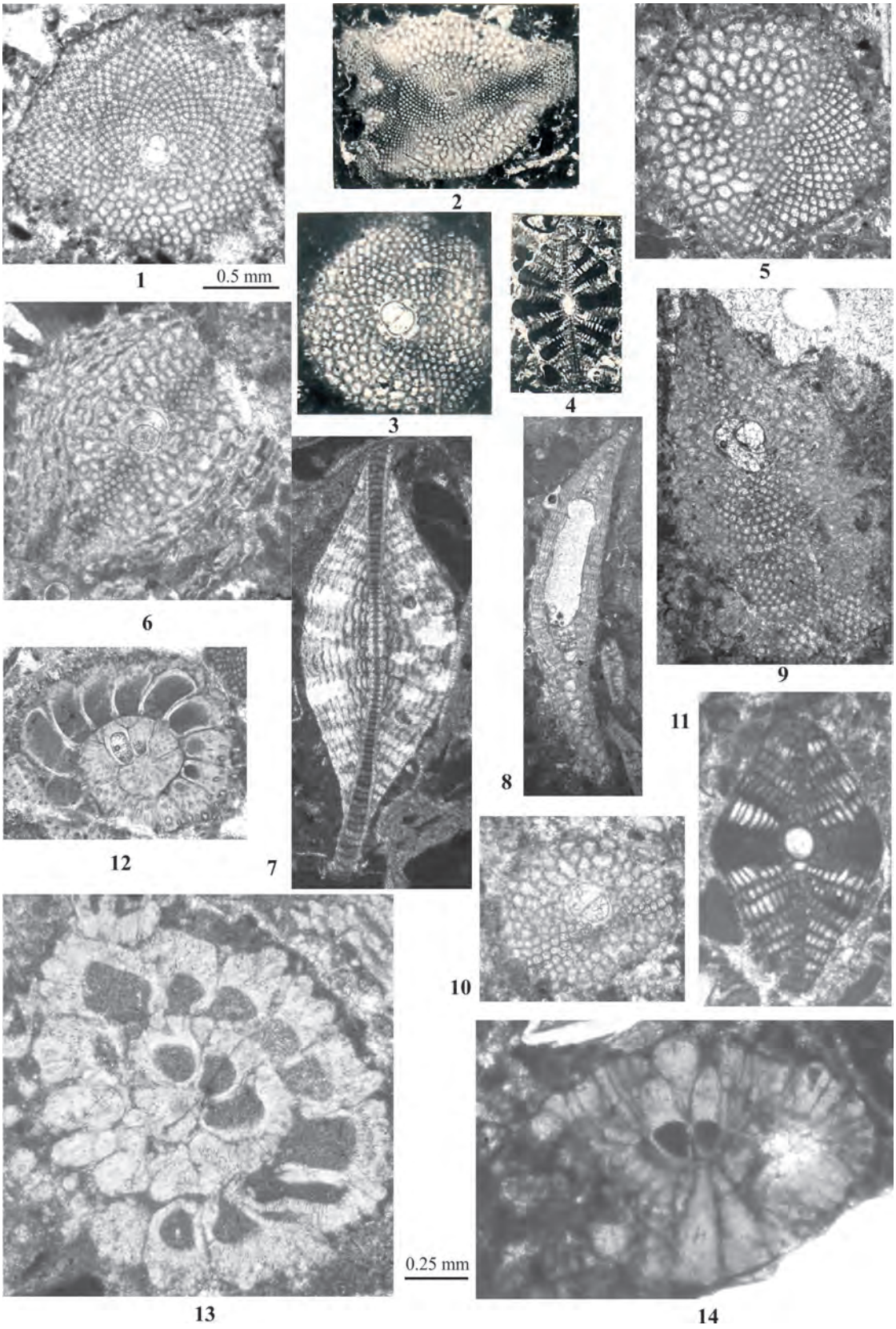

PLATE - 4

Late Chattian, Edilme and Karamağara measured stratigraphical sections, W Malatya, Eastern Turkey, X 60.

Figures 1, 2: *Miogypsinella borodinensis* Hanzawa

1: Equatorial section, showing embryonic chambers and spiral chambers (X=13) and miogypsinid equatorial chambers with basal stolons, (FGM-30A/6/3; Sirel and Gedik 2011, plate 2, figure 7); 2: Axial section, (FGM-30A/11/1; Sirel and Gedik 2011, plate 2, figure 6).

Figures 3, 4: *Miogypsinella akcadagensis* (Gedik and Sirel)

3: Equatorial section, (FGM-30A/3/1; Sirel and Gedik 2011, plate 2, figure 1), showing embryonic, spiral chambers of the rotaloid stage with X=9 (number of spiral chambers) and miogypsinid equatorial chambers, megalospheric form; 4: Axial section, (FGM-30A/5/2; Sirel and Gedik 2011, plate 2, figure 5).

Figures 5-9: *Postmiogypsinella intermedia* Sirel and Gedik

5, 7-9: Axial section, A form, (HYM-42/3/1; Sirel and Gedik 2011, plate 1, figure 5); (FGM-30A/3/2; Sirel and Gedik 2011, plate 1, figure 9); (FGM-30A/2/3; Sirel and Gedik 2011, plate 1, figure 6); (HYM-42/1/4; Sirel and Gedik 2011, plate 1, figure 7); 6: Equatorial section, (HYM-42/7/4; Sirel and Gedik 2011, plate 1, figure 12).

Figure 10: *Miogypsinella cf. complanata* (Schlumberger)

Axial section, A form, (FGM-30A/2/2; Sirel and Gedik 2011, plate 3, figure 1).

PLATE - 4

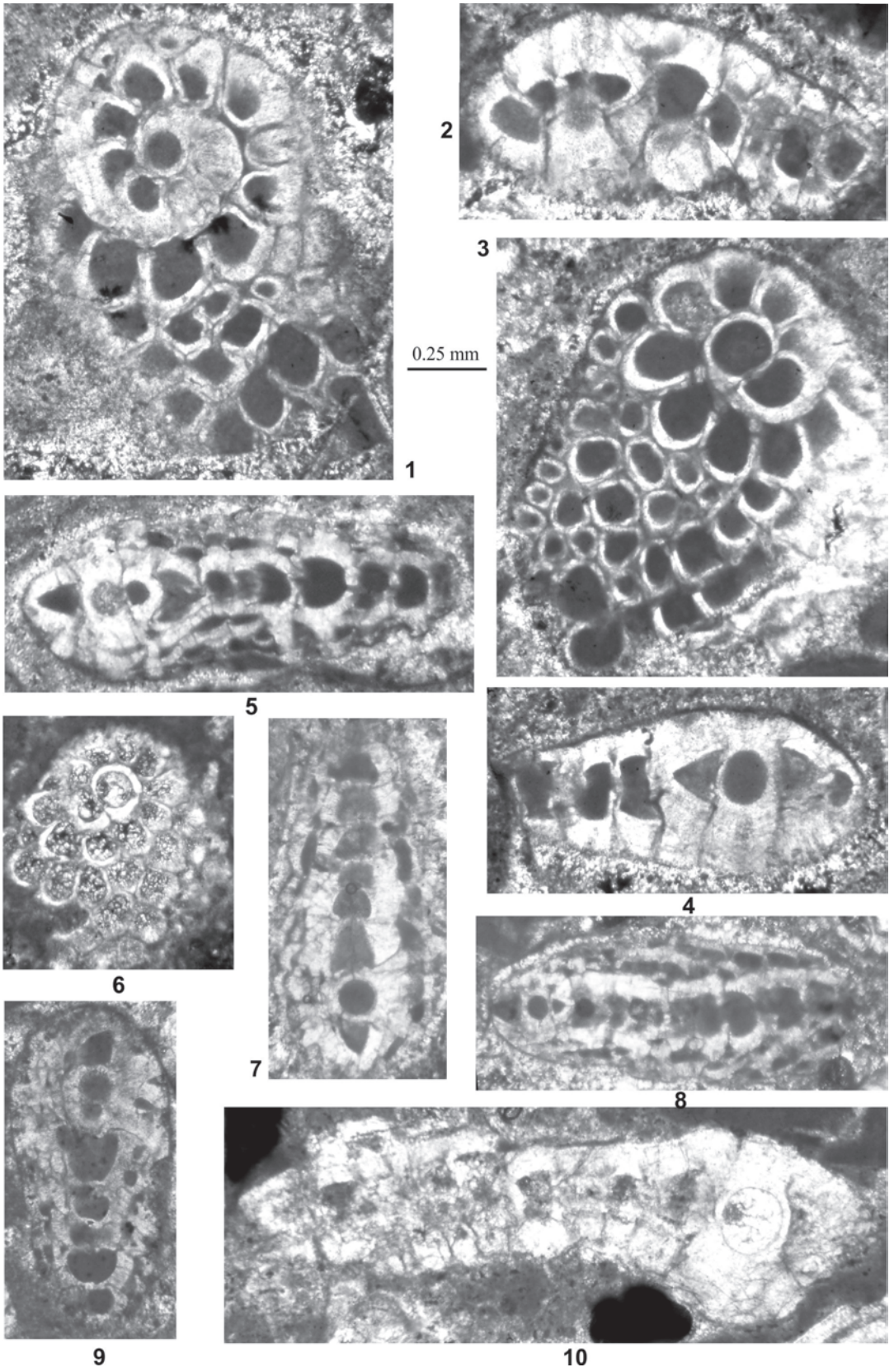

PLATE - 5

Burdigalian, Karamağara measured stratigraphical section, W Malatya, Eastern Turkey, X 60.

Figures 1, 2: *Miogypsina globulina* (Michelotti)

1: Equatorial section, (HYM-45A; Gedik 2014, plate 10, figure 1); 2: Axial section, (HYM-45A; Gedik 2014, plate 10, figure 2).

Figure 3, 4: *Miogypsina polymorpha* (Rutten)

3: Equatorial section, (HYM-48/1/1; Gedik 2014, plate 11, figure 3); 4: Axial section, (HYM-45A/1/2).

Figure 5: *Miogypsina cf. thecideaeformis* (Rutten)

Axial section, (HYM-45W; Gedik 2014, plate 9, figure 1).

PLATE - 5

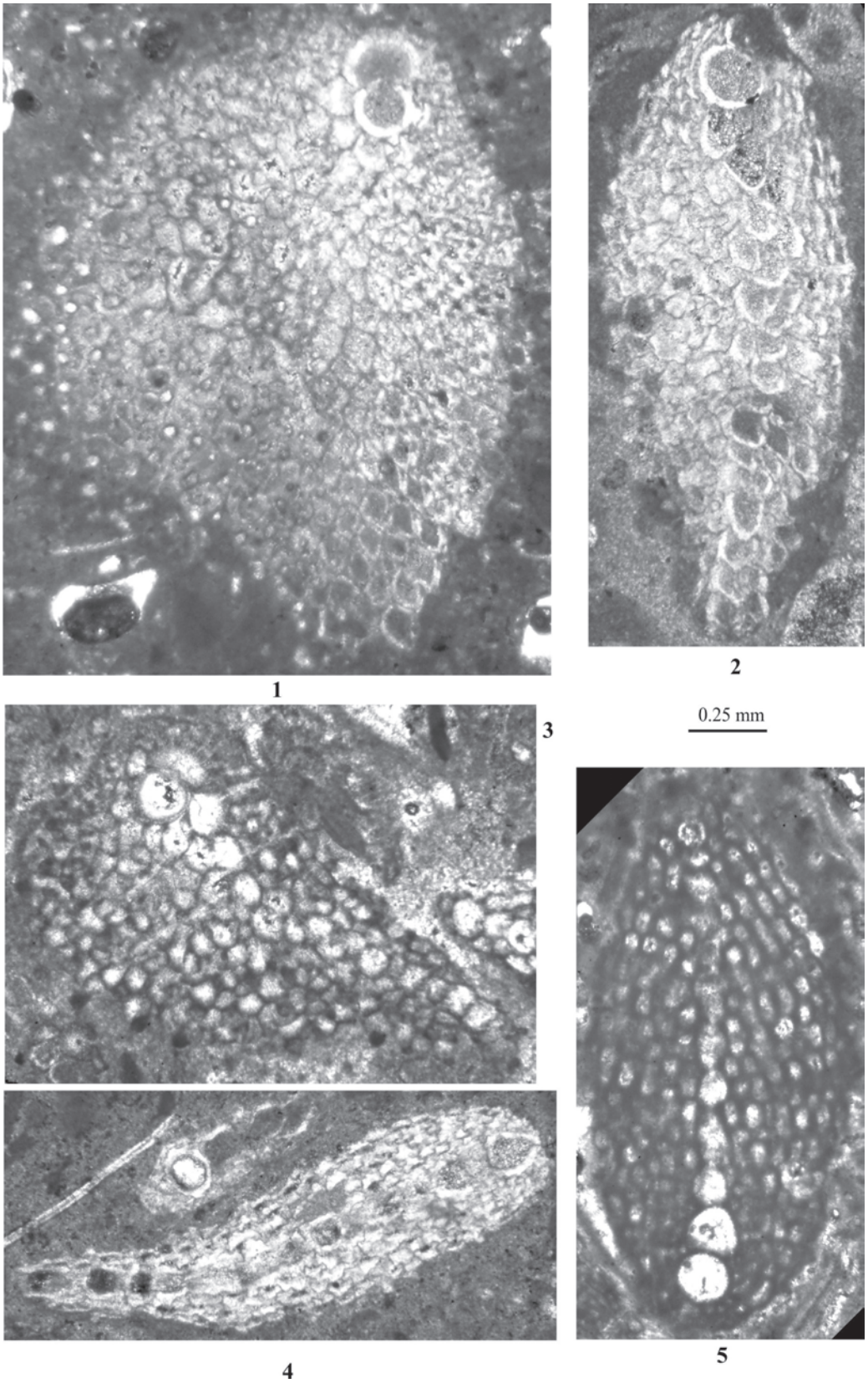

PLATE - 6

Figures 1, 2, 4: *Spiroclypeus vermicularis* Tan, 1937

Late Chattian, Develi measured stratigraphical section, W Malatya, Eastern Turkey, X 15.

1, 2: Equatorial section, A form, (FGD-7; Gedik 2014, plate 13, figure 1, figure 2).

4: Axial section, A form, (FGD-7; Gedik 2014, plate 13, figure 5).

Figures 3, 5: *Spiroclypeus* sp.

Oligocene, Develi and Edilme measured stratigraphical sections, W Malatya, Eastern Turkey, X 15.

Equatorial section, (FGD-6, FGM-18; Gedik 2014, plate 13, figure 3, figure 4).

Figure 6: *Planorbulinella caneae* Freudenthal

Burdigalian, Karamağara measured stratigraphical section, W Malatya, Eastern Turkey.

Equatorial section, (HYM-46; Gedik 2014, plate 9, figure 9).

Figures 7-10, 20: *Heterostegina assilinoides* Blanckenhorn, 1890 emend. Henson, 1937

Rupelian-Early Chattian, Edilme measured stratigraphical section, W Malatya, Eastern Turkey, X 20.

7: Equatorial section, A form, (FGM-19/2); 8, 9, 10: Axial section, A form, (FGM-5W, FGM-4A, FGM-19); 20: Uncompleted equatorial section, A form, (FGM-19/8; Gedik 2014, plate 13, figure 10).

Figures 11, 12: *Peneroplis cf. laevigatus* d'Orbigny

Rupelian-Early Chattian, Develi measured stratigraphical section, W Malatya, Eastern Turkey, X 20.

Equatorial section, (FGD-2A, FGD-2B; Gedik 2014, plate 3, figure 3, figure 2).

Figure 13: *Peneroplis sp***.**

Equatorial section, X20, (FGD-2B; Gedik 2014, plate 3, figure 4).

Figures 14-16: *Nummulites cf. vascus* Joly and Leymerie

Rupelian-Early Chattian, Edilme measured stratigraphical section, W Malatya, Eastern Turkey, X 20.

14-16: Axial section, (FGM-5E/2/3, FGM-5E/5/5, FGM-5E/3/1; Gedik 2014, plate 13, figure 16, figure 19, figure 17).

Figures 17, 18: *Dendritina cf. rangi* d'Orbigny

Burdigalian, Develi measured stratigraphical sections, W Malatya, Eastern Turkey, X 40.

Equatorial section, (FGD-11/5/1, FGD-11/6/7; Gedik 2014, plate 9, figure 7, figure 8).

Figure 19: *Operculina sp.*

Equatorial section, (FGM-9B; Gedik 2014, plate 13, figure 20).

Figure 21: Nummulitidae (*Spiroclypeus ?/ Heterostegina ?* sp.)

Tilted equatorial section, (FGM-5W; Gedik 2014, plate 13, figure 11).

Figure 22: *Amphistegina sp.*

Equatorial section, (FGM-7A; Gedik 2014, plate 13, figure 21).

PLATE - 6

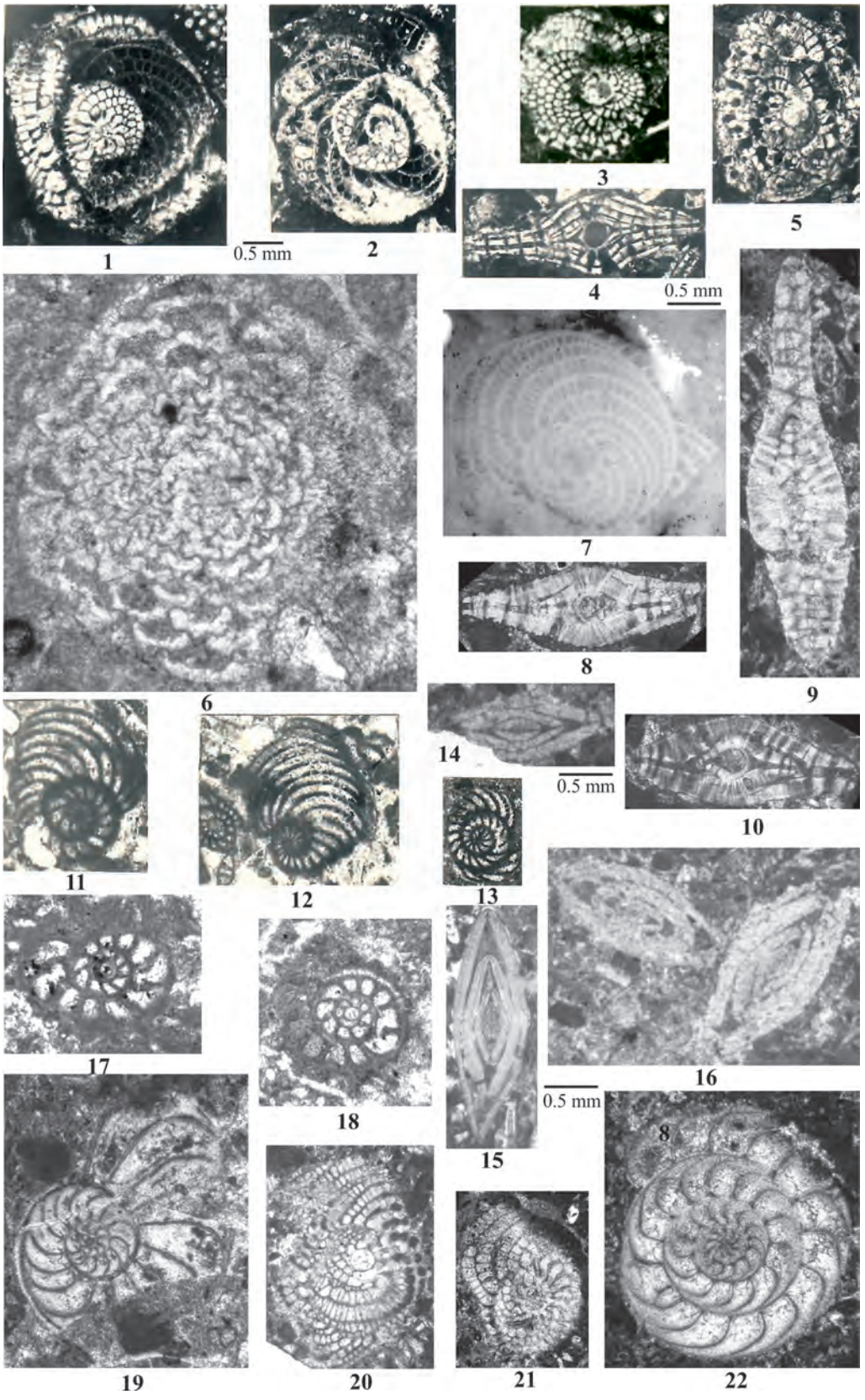
1
0.5 mm
2
3
4
0.5 mm
5
6
7
8
9
11
12
14
0.5 mm
13
10
17
18
15
16
0.5 mm
19
20
21
22

BULLETION OF THE MINERAL RESEARCH AND EXPLORATION

Foreign Edition 2015 150

CONTENTS

Bull. Min. Res. Exp. (2015) 150: 51-64

Bulletin of the
Mineral Research and Exploration

http://bulletin.mta.gov.tr

THE SECRETS OF MASSIVE SULFIDE DEPOSITS ON MID-OCEAN RIDGES AND KÜRE-MAĞARADORUK COPPER DEPOSIT

Yılmaz ALTUN[a]*, Hüseyin YILMAZ[a], İlyas ŞİNER[a] and Fatih YAZAR[a]

[a] *Eti Bakır A. Ş. Maden Arama Grubu, Samsun.*

Keywords:
Cyprus Type, Massive Sulfide Deposits, Küre Mağaradoruk, Hydrothermal Vent, Lineiite.

ABSTRACT

Küre region is located in western part of the Pontide tectonic belt. The oldest rocks around Küre are Paleozoic metamorphic rocks constituting "Rhodope-Pontide" continent. Liassic-pre Liassic ophiolites and basaltic volcanics, which form Paleotethys Ocean Floor are situated on "Rhodope-Pontide" continent as Paleotethys Ocean Floor residuals. Massive sulfide deposits in Küre Region are closely associated with pre Liassic – Liassic basaltic volcanics and intercalating black shale. These deposits are considered to have formed during hydrothermal mineralization processes when basaltic volcanism had stopped and defined as "Black Smoker" today. Massive sulfide bodies in Mağaradoruk copper deposits are lens shaped. Although ore lenses take place sometimes in basalts and black shales, they are generally located on basalts and are covered by black shales. In Küre region, fold structures are intensely observed, and Mağaradoruk deposit is located on western flank of an overturned anticline. Mağaradoruk deposit is formed by several small and a big ore body and by less developed, underlying stockwork disseminated ore. The big ore body is 600 m long, 250 m wide and nearly 40 m thick. As main ore minerals; pyrite and chalcopyrite are observed. In few amounts; marcasite, magnetite, hematite, sphalerite, covelline, neo-digenite, malachite, azurite, fahlers are seen. In fewer amounts; bravoite, lineiite (karolite), limonite, and in trace amounts; chromite, rutile anatase, chalcosine, cuprite, tenorite, pyrrhotite, valleriite, bornite, galenite, native copper and native gold are observed. Main gangue minerals are; quartz, siderite-ankerite calcite, dolomite and chlorite. Mağaradoruk massive sulfide deposit rocks resembles to Siirt Madenköy, Ergani massive sulfide deposits, to "Cyprus" type massive sulfide deposits and modern Cyprus type massive sulfide deposits in terms of mineral contents; and to Ergani Mihrapdağı, Papuke, Pakotai and Parakoa deposits in terms of cover rocks, which are Cyprus type massive sulfide deposits, in New Zealand.

1. Introduction

The purpose of this study is to investigate geological environments, wall rock relationships and ore minerals of the Mağaradoruk deposit, and to compare these deposits with other "Cyprus" type massive sulfide deposits considering their like and unlike characteristics. This deposit was revealed by studies carried out around Aşıköy, Kızılsu, Toykondu and Bakibaba deposits which are located within the boundaries of Küre Town, Kastamonu. Within this scope, the geological research of deposits was performed, structural relationships were asserted, and the ore and gangue minerals were detected analyzing drill cores. The obtained data were then compared with "Cyprus type massive sulfide deposits" and the newly forming "modern Cyprus massive sulfide deposits".

Küre copper deposits have been the subject of Mining Sector for many years. However; mineral exploration and development studies in scientific manner began with the foundation of Republic of Turkey.

Nikitin (1926) studied the geology of Küre vicinity, the ore mineralogy of Bakibaba and cinders.

* *Corresponding author: Yılmaz Altun, yilmazaltun@etibakir.com.tr*

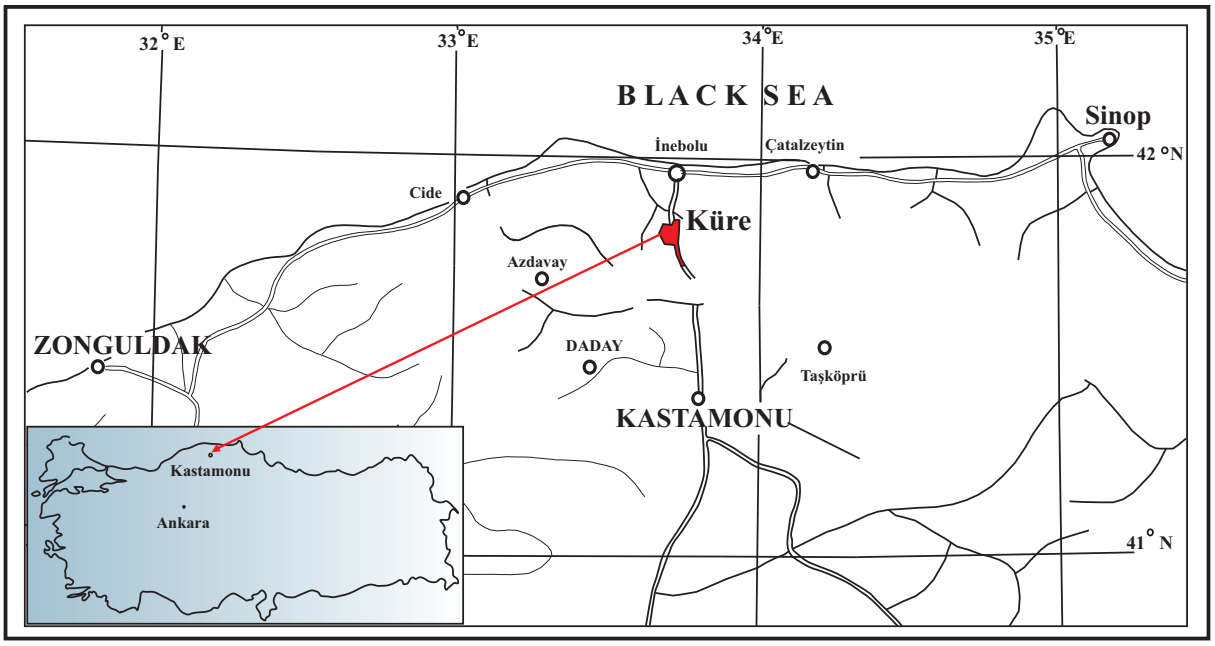

Figure 1- Location map of the study area.

Kovenko (1944) studied the geology of close vicinity of Küre deposits in 1938 for MTA Institute.

Pieniazek (1945) asserted that Küre deposits were derived from hydrothermal metasomatic origin.

Pollack (1964), in his short study, mentioned about the relationship of mineralization with tectonics. He also pointed out that, faults determined the geometry of ore bodies and ore boundaries occurred passing through faults.

Sarıcan (1968) performed a reserve estimation based on data obtained by MTA and Etibank between 1963 and 1965.

Çağatay et al. (1980) carried out a detailed mineralogical study in Küre surround and mentioned about the importance of cobalt and gold in these deposits in terms of economics in addition to copper.

Pehlivanoğlu (1985) carried out a geological investigation in Küre copper deposits and its vicinity. He also pointed that, copper deposits were in stockwork disseminated within upper layers of volcanic sequence, and these deposits were formed in the form of massive ore between the overlying sedimentary sequence and those volcanic sequence.

The Metal Mining Agency of Japan (MMAJ), (1985) studied the geology and geophysics of the region among Taşköprü-Devrekani-Küre-Ağlı towns for Etibank Co. The agency has also performed drilled investigations around Küre, but there have not been detected any mineral reserves.

Kuşçu and Erler (2002), based on data obtained by studies carried out on the mineral deposits of Küre region, stated that pyrites in this region had been subjected to deformational effects and accordingly; the series of deformation and late deformation texture had been formed.

Altun et al. (2009) have obtained results in studies performed between 2005 and 2008 in Küre copper deposits, and suggested that northern and western continuity of the new ore body detected in Mağaradoruk should have been investigated.

2. Geology

2.1. Regional Geology

The study area is located on the western part of "Pontide" tectonic belt. Investigators such as; Şengör and Yılmaz (1983) and Yılmaz (1980) claimed that metamorphic massifs in "Western Pontides" belongs to "Rhodope-Pontide" continent, "Paleotethys" ocean crust in North in Permo-Triassic had become an active continental margin by southward subduction. They also stated that thick flyschoidal deposit had been formed on "Paleotethys" ocean crust in Early Jurassic, and Küre ophiolites, which represents "Paleotethys" ocean curst, had been placed on "Rhodope-Pontide" continental margin due to the closure of "Paleotethys" in Dogger. Şengün (2006) said that, associating Küre basin with the beginning of detachment of Eastern and Western

Pontides in Early Mesozoic would be more acceptable, rather than being a European marginal basin. He also claimed that Küre ophiolite should have been emplaced within rotational processes as it had been in Antalya basin or in Western Pontides, and as a reason to this, he showed the Küre ophiolite to be cut off by granites.

The oldest units, in this part of Western Pontides, are gneiss, schist, marble, quartzite in greenschist facies which form metamorphic massifs like Daday-Ballıdağ and Ilgaz-Kargı, and metaophiolites intercalating with them (Ketin, 1962; Pehlivanoğlu, 1985). Most of the rocks forming these massifs are Paleozoic (Ketin and Gümüş, 1963). The age of ophiolites, which are transitional with metamorphic rocks, is Cretaceous (Ketin and Gümüş, 1963). Fossiliferous Upper Paleozoic rocks are encountered in most the region and represented by Carboniferous coals. It has large and small outcrops as slices of allochthonous thrust on Cretaceous flysch. Permian is represented by clastic rocks such as; conglomerate, sandstone and sandy shales in places where they overlie coaly units, and by greywacke and limestone in other places. Triassic is observed as massive limestone below Liassic flysch between Devrekani and Abana, only in east of Küre. Liassic, which shows a wide distribution between the southern part of Küre and İnebolu, is represented by ophiolitic rocks consisting of oceanic sediments, serpentines, gabbros, diabase dikes and mafic volcanic rocks (Güner, 1980; Pehlivanoğlu, 1985). This unit grades into gray greywacke in upper layers. Minor fossil findings in deposits mainly indicate Liassic-Lower Dogger (Ketin and Gümüş, 1963). Liassic deposits in Küre overlie mafic pillow lavas of the ophiolitic sequence (Bailey et al., 1967), and are overlain by Malm-Lower Cretaceous reefal massive limestones which begin to deposit with red basal conglomerate. In the region between Kastomonu-İnebolu, Liassic-Malm aged intrusives composed of granodiorite-adamellite are observed which cut Liassic flysch (Pehlivanoğlu, 1985). Malm - Lower Cretaceous limestones are transgressively overlain by a Lower Cretaceous flysch in northern parts of the region which starts with Lower Cretaceous conglomerate and continues with the alternation of sandstone–sandy limestone–marl (Pehlivanoğlu, 1985). The Upper Cretaceous flysch is composed of sandstone, clayey limestone and marl alternation. It consists of intercalations of Pontide island arc volcanism, which is composed of calc alkaline andesite and dacites towards south, along the coastline in west (Pehlivanoğlu, 1985). The Upper Cretaceous flysch around Küre has developed more as marl and limestone intercalation and conformably grades into Paleocene limestones. Eocene in flysch facies is composed of marl–shale–sandstone alternation which occasionally consists of intercalations of lava, tuff and agglomerate, but Oligocene is only in flysch facies. Neogene basins consist of terrigenous and lagoonal deposits.

2.2. Geology of the Study Area

Ultrabasic rocks at the bottom, the overlying Küre formation, which is formed by basaltic rocks and black shales, and cross cutting gabbro-diorite and dacites are located around Küre massive sulfide deposits

Ultrabasic rocks, located at the bottom of the study area, are composed of serpentinized peridotite, dunite and pyroxinites, and outcrop in NW of Küre, Elmakütüğü hill, around Ömer Yılmaz locality and in east of Karacakaya hill (Figure 2). The lower boundary of ophiolites in Küre region is not observed, and chromite and chrome spinal are observed in rare amounts (Bailey, et al., 1967). Boundaries of the unit with other units are faulted.

Küre formation, which is abundantly observed in Küre and its vicinity, is mainly composed of basaltic rocks and black shales. Basaltic rocks are widely observed in the form of pillow lavas. The unit was defined by Kovenko (1944) and Ketin (1962) as diabase, by Bailey et al. (1967) as mafic volcanic rocks (pillow lava, breccia, tuff), by Güner (1980) as basaltic sequence, by Çağatay and Arda (1984) as spilite, by Pehlivanoğlu (1985) as basic volcanic sequence and by MMAJ (1995) as Küre volcanics.

Basaltic volcanic rocks are formed by basalt, hyaloclastic and pillow lavas (Figure 2). They mostly consist of plagioclase, clinopyroxene and/or phenocrysts of iron-titanium. Feldspar microliths, calcite veins and amygdales are locally observed. Massive basalt lavas in lower layers grade into pillow lavas and breccias towards upper layers (Güner, 1980; Çağatay and Arda, 1984; Pehlivanoğlu, 1985). Pillow structures are well developed (Figure 3).

Massive basalt flows are green to blackish green, very fine grained, ophitic to sub-ophitic in texture, and they contain albitized, carbonated plagioclases and chloritized, carbonated augites (Çağatay and Arda, 1984; Pehlivanoğlu, 1985). Carbonation and silicification is widespread in mineralized parts. The diameter of pillows in lavas is in between 25-200 cm. The material between pillows is made up of pelagic sediments or chloritized mafic glass. Pillow lavas are ophitic to intersertal in texture. They also consist of albitized plagioclases, chloritized augites, very rare

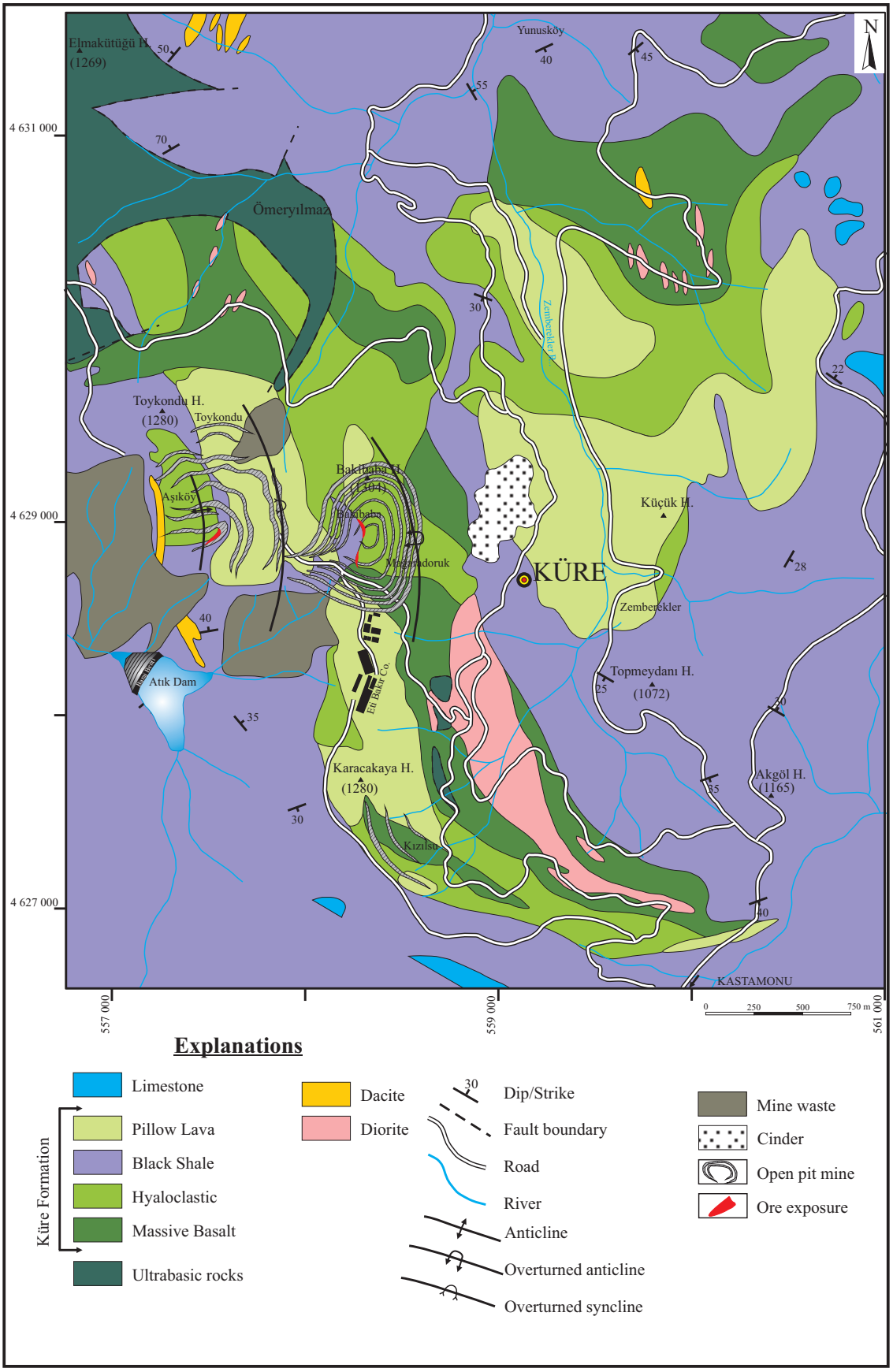

Figure 2- Geological map of the study area (modified from Metal Mining Agency of Japan (MMAJ), 1995).

Figure 3- Basalts in pillow structure.

opaque minerals and secondary quartz (Pehlivanoğlu, 1985). Koç et al (1995) claim that Küre basalts are in tholeiitic character and derived from a SiAl and SiMa type magma (Figure 4). Güner (1980) has studied the geochemical characteristics of these lavas and concluded that these were tholeiitic in character and were the product of oceanic ridge volcanism (Figures 5 and 6).

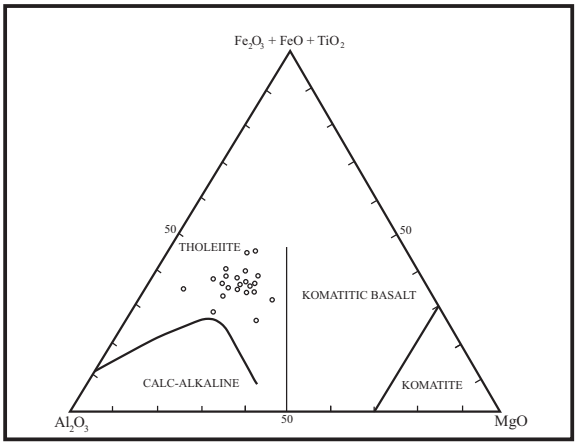

Figure 4- Jensen (1976) diagram of volcanics (from Koç et al., 1995).

Basalts cover very wide areas around Küre, in Kızılsu, Bakibaba, Aşıköy and Mağaradoruk deposits and their vicinities (Figure 2). Total thicknesses of these basalts are more than 2000 meters. Basalts are formed by several lava flows, and their physical characteristics, and mineralogical contents mostly resemble to each other. However; it is understood from black shale and massive sulfide bodies that this body was a lava accumulation heaped on each other which generated at different stages.

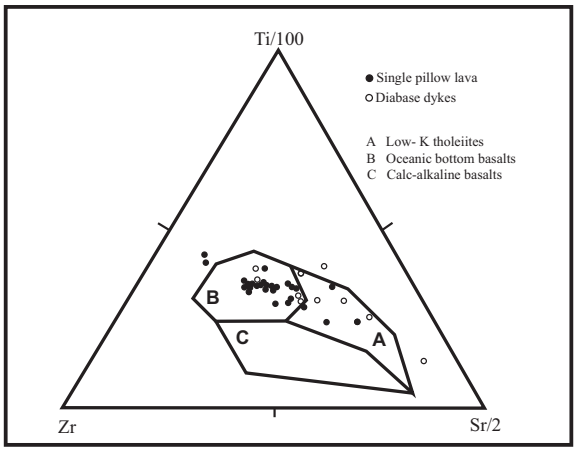

Figure 5- The plot of basaltoids around Küre on Pearce and Can discrimination diagram (1973) (Güner, 1980).

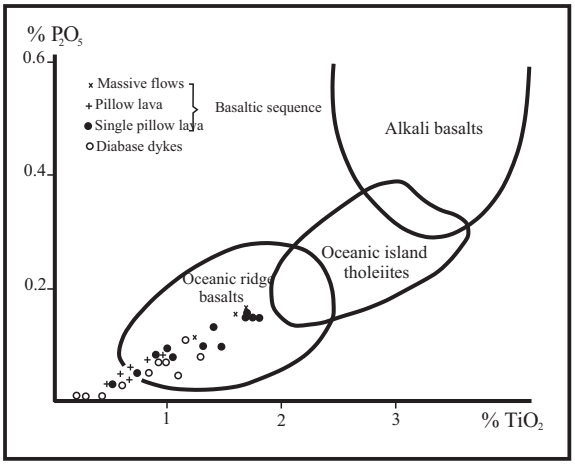

Figure 6- The variation of P_2O_5 among basaltoids around Küre with respect to TiO_2 according to Ridley et al. (1974) (Güner, 1980).

Black shales were named as “argillite” in several previous studies (Bailey et al., 1967; Çağatay and Arda, 1984). The “black shale” definition was first used by Güner (1980). Although it is accepted that black shales overlie basaltic sequence of Küre ophiolite (Pehlivanoğlu, 1985), several black shales are encountered within basalts around Küre deposits. Some of them are closely associated with mineralization, but the others are observed between basalts and/or as lenses in basalts as they were in Mağaradoruk deposit (Figure 7, 8 and 9).

Black shales are cut by Dogger aged granitic intrusions, dacite dyke and sills. Although these shales are considered as roof rock of the massive ore, they are located both as roof and basement rock of the massive ore in Mağaradoruk deposit (Figure 9).

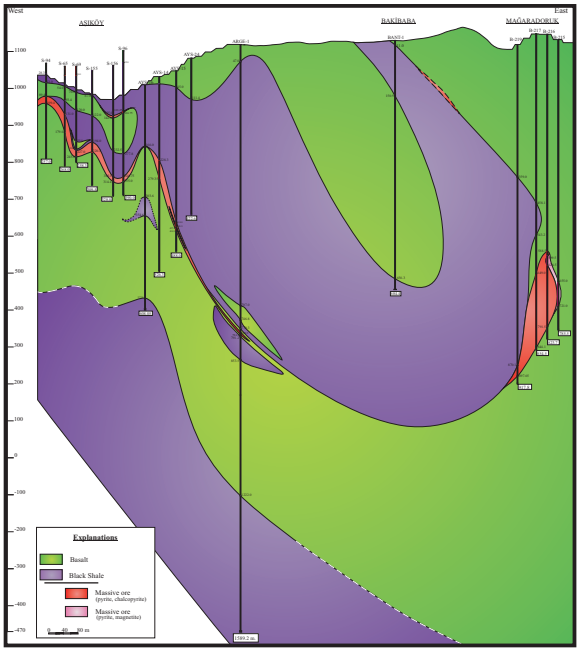

Figure 7- Geological section crossing Aşıköy, Bakibaba and Mağaradoruk deposits.

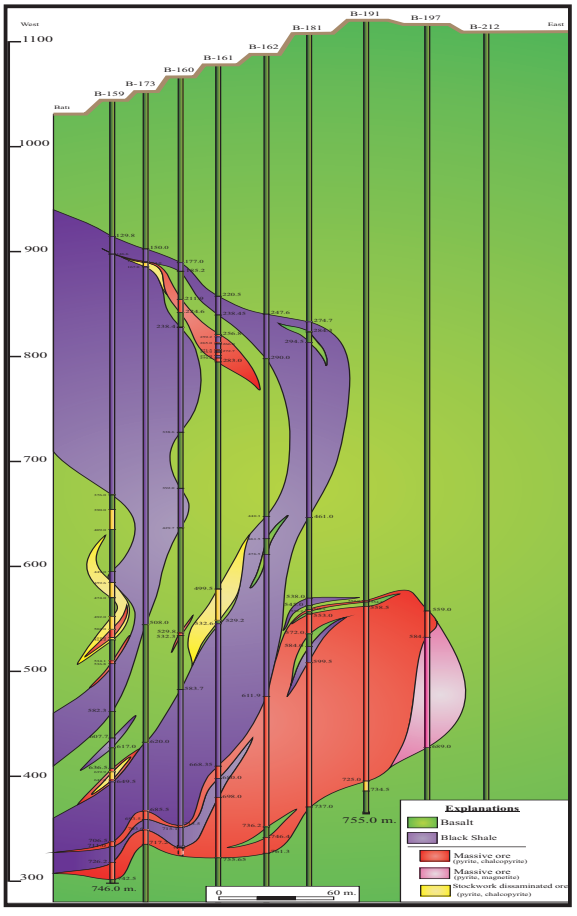

Figure 8- Vertical cross section (to the axis of north-south directing overturned anticline) in Mağaradoruk deposit.

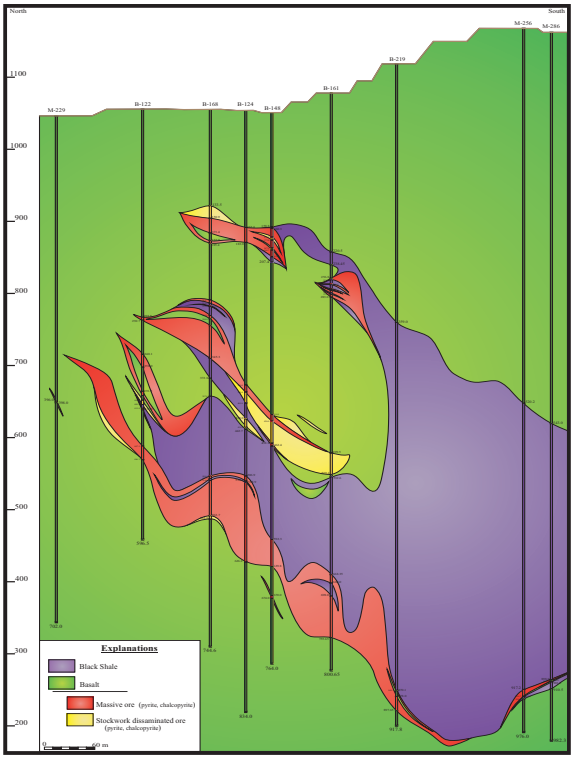

Figure 9- Parallel cross section (to the axis of north-south directing overturned anticline) in Mağaradoruk deposit.

Black shales are nearly 150 m thick in Aşıköy village (Çağatay and Arda, 1984). The true thickness of these shales in Mağaradoruk is more than 200 meters.

It is dark gray to black, very fine grained and thin bedded, and consists of basaltic pebble and blocks on the boundary with basaltic lavas. Upper layers show transition into graded sandstone (Çağatay and Arda, 1984). Petrographic and X-ray diffraction and ore microscopy studies show that this rock is formed by illite, quartz, chlorite, siderite and muscovite, and secondarily consists of coal-like material, graphite, pyrite, chalcopyrite, chrome spinal, ilmenite and hematite (Güner, 1980; Çağatay and Arda, 1984).

Gabbros and diorites are observed around Küre, on Dikmen mountain at west, in the vicinity of İkiçay bridge along İnebolu road at north of Küre, around Dibekköy at east and at south of Küre in the form of big and small intrusions; and as restricted bodies in lower parts of the basaltic sequence (Pehlivanoğlu, 1985). Gabbros are dark green and gray to green colored. Labrodorites consist of augite and olivine; however, diorites consist of amphibole, biotite and albite.

Dacites in the west of Aşıköy and Toykondu open pit mining area contain corroded quartz and phenocrysts of partly seriticized plagioclase (Pehlivanoğlu, 1985). When relationships of dacites with black shales are taken into consideration, it was concluded that these dacites could most probably be sill – dyke (Figure 2).

3. Structural Geology

Liassic volcanic rocks and black shales around Küre have been effectively folded, and their fold axes are roughly in N-S direction (Figure 2). The dome, which its long axis is in N-S direction in Aşıköy, has a quite high inter-limb angle (Bailey et al., 1967; Pehlivanoğlu, 1985). Basalts between Aşıköy and Mağaradoruk, which overlie black shales in east of this anticline, are mostly in the form of pillow lava. There is also observed N-S extending overturned anticline between Aşıköy and Bakibaba-Mağaradoruk, and a nearly N-S extending overturned anticline towards east of Bakibaba-Mağaradoruk deposits (Figure 2). This overturned anticline also plunges towards south in Mağaradoruk deposit.

4. Ore Deposits

Massive and stockwork disseminated sulfide deposits, which are known as Küre copper deposits and mainly composed of pyrite and chalcopyrite, are located at west of Küre town center, and they align in the order of Toykondu, Aşıköy, Bakibaba, Mağaradoruk and as Kızılsu from north to south (Figure 2).

Küre copper deposits have been the subject of mine operations since ancient times. Mining activities in the region dates back to Greek and Roman times and have also continued during Seljuk, Genoa and Ottoman times. The mining activities of Ottomans in Bakibaba deposit ended in 1845. Mineral exploration and development studies in scientific manner began in 1935 with the foundation of the General Directorate of Mineral Research and Exploration (MTA), and Aşıköy deposits was explored in 1944. Exploration studies, which began in 1963 in Bakibaba deposit, were revealed in two ore bodies as north and south sections (Sarıcan, 1968). It is understood that the deposit, which has been known and operated since ancient times, is the southern ore body in Bakibaba copper deposit from historical documents, operational traces and from cinder heaps around Bakibaba. The northern ore body here has been operated by Black Sea Copper Co. (K.B.İ.) for many years since 1968, but the site was abandoned due to pyrite fire in galleries in 1990 (Ildız and Dağcı, 1990).

The whole ore deposits in Toykondu, Kızılsu, Bakibaba and Aşıköy, which were taken over by Cengiz Holding from Etibank Co. in 2004 and produced by open pit mining method, has been depleted until 2009 (Altun et al., 2009). The ore, which was explored by studies carried out in Aşıköy deposit between the years 2005-2008, still continues its production by open pit mining method.

Mağaradoruk massive sulfide deposits were explored as a result of exploration studies, which began in 2008 and intensified around Mağaradoruk hill, on the eastern steps of Bakibaba open pit mining.

4.1. Mineralization

Kovenko (1944), Pollack (1964) and Bailey at al. (1967) claimed that the mineralization in Küre copper deposits were hydrothermal in origin and formed by metasomatic processes. Çağatay (1981) interpreted deposits as being based on basaltic volcanism and sea floor product. Koç et al. (1995) state that these deposits resemble genetically to "Kieslager type" deposits which form in forearc rather than "Cyprus type" deposits. Üşümezsoy (1988) says that these deposits are associated with the opening of Kimmeridgian basins, and they are products of bimodal rift volcanism and oceanic spread volcanism.

The mineralization in Küre deposits is closely associated with basalt-black shale units. As a result of studies, Küre basalts are mid ocean ridge basalts (Güner, 1980). Massive sulfide bodies like black shales, which are located with Küre basalts, are in the position of basement and roof rock. Some of the ore bodies here are located within basalts, of some are in black shales or on basalts, and are overlain by black shales (Figure 7 and 8). The black shale overlying the massive sulfide ore (Figure 10) consists of ore bands, which are mainly composed of occasionally well sorted pyrite and chalcopyrite in places where the mineralization thins out (Figure 11).

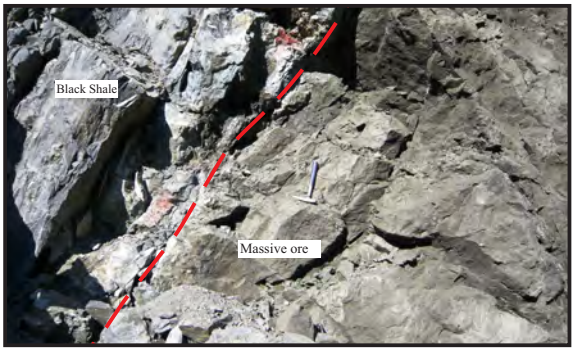

Figure 10- Black shale covering the massive ores.

Figure 11- Traces of sorting in massive ore bands which are formed by pyrite and chalcopyrite in black shale.

Total of 30 samples taken from drill cores in main ore body of the Mağaradoruk deposit were analyzed in terms of Cu, Zn, Pb, Au, Ag, Co, Ni, As, Mo, Sb, Se and Ti contents (Table 1). Analyses were performed in ALS Mineral Laboratory. Samples were dissolved by quadruple acid solution method and analyzed by Inductively Coupled Plasma Atomic Emission Spectrometry (ICP-AES) method. Au element was analyzed by Atomic Absorption Spectroscopy (AAS) method. One sample, which has Au concentration higher than 10 ppm, was dissolved by Fire Assay Fusion technique and analyzed by Gravimetric method.

Küre deposits resemble to "Cyprus" type massive sulfide deposits of which have ophiolitic wall rocks, defined by Galley and Koski (1999), because of the environment where Mağaradoruk deposit is located. This resemblance is also supported by Cu, Pb, Zn discrimination diagram (Figure 12), which was prepared by using analyses of samples taken from major sulfide body in Mağaradoruk deposit (Table 1).

On the other hand, Zaccarini and Garuti (2008) emphasize that Co/Ni ratio in massive sulfide deposits, of which their main rock is serpentine, varies between 0.29 and 1.97. However; the ratio of massive sulfide deposits of which the main rock is basalt varies between 1.09 and 8.

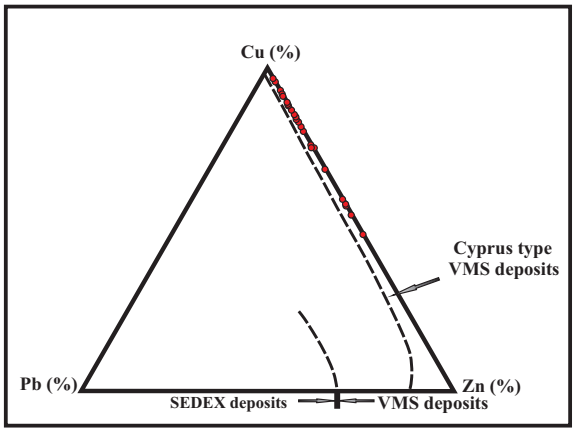

Figure 12- Cu, Pb, Zn discrimination diagram (from Galley and Koski, 1999).

Table 1- Results of analysis of samples taken from drill cores cutting main ore body in Mağaradoruk deposit.

Sample	Cu	Zn	Pb	Au	Ag	Co	Ni	As	Mo	Sb	Se	Ti	Co/Ni
	%	ppm	ppm	ppm	ppm	ppm	ppm	ppm	ppm	ppm	ppm	%	
M-1	5.86	18700	282	1.58	8.17	5580	31.2	461	39.4	26.7	70	<0.005	178.85
M-2	4.51	20400	209	2.1	11.7	3770	16.4	597	37.6	31.1	37	<0.005	229.88
M-3	5.26	7650	114.5	2.82	7.9	9080	101.5	471	56.6	28	156	0.009	89.46
M-4	4.66	11200	112	1.725	8.34	6710	32.2	356	43.5	21.6	56	<0.005	208.39
M-5	8.01	9660	146.5	1.805	8.61	5960	52.5	431	57.4	26.2	102	<0.005	113.52
M-6	4.8	8980	137	1.615	7.7	4280	62.4	363	58.1	17.85	50	0.052	68.59
M-7	7.35	12900	131	1.8	9.95	6240	47.3	458	59.9	24.9	118	<0.005	131.92
M-8	4.49	7780	83.9	1.685	8.07	6490	43.6	323	47.4	16.1	66	<0.005	148.85
M-9	4.75	1760	179	2.5	12.65	4810	34.3	456	32.1	15.1	73	0.043	140.23
M-10	6.14	2070	206	3.1	14.6	2930	29.5	463	43	16	45	0.042	99.32
M-11	6.05	4680	133	1.39	5.68	5180	13.6	295	50.3	12.9	25	<0.005	380.88

Table 1- (continued)

M-12	6	12050	133	1.29	5.59	6600	19.6	359	49.8	14.1	33	0.007	336.73
M-13	1.575	1440	47.2	0.392	1.23	13000	48.5	199	43.6	6.92	198	<0.005	268.04
M-14	2.36	1790	57.4	0.633	2.25	7940	37.8	193.5	47.8	7.33	114	<0.005	210.05
M-15	4.44	5560	145.5	1.495	5.03	9700	38.3	412	52.8	15.5	69	<0.005	253.26
M-16	4.62	2100	80.2	0.875	1.77	8650	36.1	291	48.5	8.19	89	<0.005	239.61
M-17	7.15	9460	160	1.76	9.13	5490	52.1	278	58.5	14.6	59	<0.005	105.37
M-18	5.09	8510	104	2.09	9.83	4930	22.5	472	46.1	16.05	61	0.031	219.11
M-19	3.15	23000	119.5	2.65	12.9	3850	21.2	390	43.4	17.8	38	0.017	181.60
M-20	1.01	8370	89.3	0.652	9.37	1000	67.6	184	18	9.1	31	0.394	14.79
M-21	11.85	38800	199.5	8.35	38.4	2840	17	375	67.7	23.3	18	<0.005	167.06
M-22	8.27	18350	138	10.7	30	3950	17.2	266	62.7	18.05	20	<0.005	229.65
M-23	3.24	4710	96.6	3.37	5.46	4520	17.1	416	42.5	15.85	35	<0.005	264.33
M-24	6.47	2730	140.5	1.845	5.92	5150	21.2	332	55.1	13.55	27	<0.005	242.92
M-25	5.28	4540	140	1.145	3.93	7810	33.2	332	61.6	11.35	66	<0.005	235.24
M-26	4.07	5300	196	2.43	13.05	3730	18.5	556	42.1	30.8	22	<0.005	201.62
M-27	4.41	13550	302	2.67	18.3	3150	25.3	890	35.8	35.6	26	<0.005	124.51
M-28	3.14	21200	120.5	1.985	9.46	4470	24.5	327	36.9	20.2	29	<0.005	182.45
M-29	3.6	38100	169.5	2.25	13.55	5090	32.9	448	39.8	22.8	44	<0.005	154.71
M-30	3.53	26100	159	2.95	12.85	4950	36.6	618	41.5	26.9	40	0.008	135.25

Co/Ni ratio in Mağaradoruk deposit (Table 1) is; however, much higher than values in massive sulfide deposits of which their wall rock is basalt.

Küre massive sulfide deposits should have formed either by the occurrence of basalts that had occurred by Liassic-pre Liassic submarine volcanism or as a result of hydrothermal processes which occurred when the volcanism had ended. Constantinou (1980) states that Cyprus type deposits have been shaped on Mid Ocean Ridges and formed by hydrothermal circulation when there was a gap in magmatic activity.

Brathwaite and Pirajno (1993) assert that Papuke, Pakotai and Parakoa massive sulfide deposits in New Zealand are "Cyprus" type massive sulfide deposits and were formed due to basaltic volcanism in mid ocean ridges in "Black Smoker" environment. Irregular ore lenses in Papuke deposit are surrounded by claystones and sandstones. Ore lenses in Pakotai deposit are located in mudstones. In Parakoa deposit, small sulfide lenses are in volcanic rocks and shales. (Brathwaite and Pirajno, 1993). Ergani Mihrapdağı mineralization is located between Eocene mudstones and chloritized basalt, and Ergani Anayatak mineralization occurs between bedded diabases (Bamba, 1976; Wijkerlooth, 1944). Siirt Madenköy massive sulfide deposit is, on the other hand, located in porphyritic spilites (Çalgın, 1987; Yıldırım and Alyamaç, 1976; Ulutürk, 1999). Mineralizations observed in Koçali ophiolitic complex in Southeast Anatolian Orogenic Belt are located in highly altered oceanic crust origin spilitized basic volcanics and mudstone-radiolarites (Yıldırım et al., 2012; Yıldırım, 2013; Yıldırım et al., 2014). The occurrence of massive sulfide lenses in Mağaradoruk deposit in basalts and black shales, and being overlain by back shales show big resemblance with formation of environments of deposits mentioned above (Figure 13).

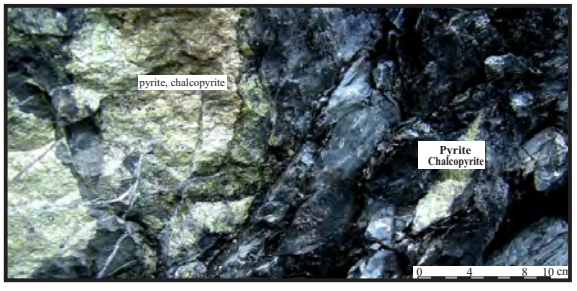

Figure 13- Small massive sulfide lenses observed in black shales.

The occurrence of massive sulfide lenses in Mağaradoruk deposit in more than one level (Figures 7, 8 and 9) supports the opinion of Harper (1999). He suggests that "Cyprus" type massive sulfide deposits could form in several levels starting from the top of magma chamber to sedimentary cover rocks.

There is a very special hydrothermal field on Juan de Fuca ridge in Pacific Ocean, 300 km away from Washington. There is observed a graben there which is 1 km wide and 100-200 m deep. In this graben, there are four sulfide formations, which are formed by several hydrothermal vents (black smoker) that cover wide areas with lengths reaching 400-500 meters. Massive sulfide deposits in Küre occur in a limited area and close to each other (Figure 2). This situation highly resemble to massive sulfide deposits in mid ocean ridges and Troodos today (Stos-Gale et al., 1997), and to locations of Ergani copper deposits (Wijkerlooth, 1944). Stockwork disseminated ore consisting of sulfidic dissemination, veins and veinlets with quartz and carbonate veins in basalts have better developed mostly below massive ore bodies as it is in Ergani copper deposits (Wijkerlooth, 1944).

The maximum thickness of stockwork disseminated ore is 50 meters. In Mağaradoruk deposit towards bottom and margins, silicified, seriticized magnetite, hematite and disseminated pyrite, chalcopyrite bearing basalt show a gradual transition into chloritized basalt. Stockwork disseminated ore, which is observed in Trans-Atlantic Geotraverse (TAG), is formed by quartz-pyrite-chalcopyrite, and continues down to 95 meters below sub sea floor Besides; silicified wall rock breccia gradually grades into chloritized basalt at the bottom of stockwork disseminated ore zone (Hannington et al., 1998).

On the eastern margin of the massive ore body in Mağaradoruk deposit, magnetite and hematite accompany with other sulfides like pyrite and chalcopyrite (Figure 8, 14). Similar characteristics are also observed in Siirt Madenköy (Çalgın, 1978) and Ergani copper deposits (Çağatay, 1978; Bamba, 1976).

Although; the reserve of deposits in some of "Cyprus" type massive sulfide deposits reaches 30 million tones, the approximate size of them are 5 million tones (Galley and Koski, 1999). Mağaradoruk massive sulfide deposit is among the biggest ones with its 29 million tones in reserve.

4.2. Mineralization and Structural Relationships

Basalts in Mağaradoruk and Bakibaba were formed most probably in the same phase with basalts at the bottom of Aşıköy, and they form an overturned anticline which is pushed westward which its long axis is in N-S direction (Figure 2).

Massive ore bodies are observed both inside these basalts and along the contacts with black shales. These bodies, which are above 780 m height of Mağaradoruk deposit, are seen as overturned position. Big ore body in Mağaradoruk deposit is located in non-overturned lower part of the western flank of this overturned anticline (Figure 10).

Ore bodies are in the form of highly tilted lenses (60°-85°) in most parts of Aşıköy, Bakibaba and Mağaradoruk deposits. However; these structures were acquired after the formation of rocks in which ore and ore bodies are kept. It is significant to know in which environment these ore bodies have occurred. When basalts located at the bottom of massive ore bodies especially in Mağaradoruk and Aşıköy deposits and in other deposits were studied, it was seen that these basalts possessed an irregular topography with depressions and hills. Massive ore bodies are thicker in depression zones whereas; they are less or not developed at all on hills (Figures 7, 8 and 9).

This topographical difference has a close relationship with mineralization. However; whether this mineralization had occurred as a result of volcanic activity or due to a pre mineralization movement in post volcanism cannot be understood, because of deformations they had been subjected to after formations. Looking at contemporaneously forming hydrothermal vents (black smokers) in TAG massive sulfide deposits in detail, fractures parallel to axis, faults in east-northeast directions and a couple of graben like depressions (Kleinrock and Humphris, 1996), the presence of four hydrothermal vents (black smokers) in 2-3 km intervals in a 1 km wide, 100-200 m deep graben in Juan de Fuca Ridge and still the occurrence of sulfide deposition in these vents are the answers to this question.

4.3. Ore and Gangue Minerals

In Küre Mağaradoruk massive sulfide deposit, mainly; pyrite, chalcopyrite (Figures 14 and 16), in few amounts; marcasite, sphalerite (Figures 14c, 14d and 14h), covelline, neo-digenite, malachite, azurite, fahlers, in very few amounts; bravoiite (Figure 14g), lineiite, karolite (Figures 14e, 14f), limonite, hematite, magnetite and in trace amount; chalcosine (Figure 17), cuprite, tenorite, pyrrhotine, valleriite, bornite, galenite, native copper, native gold (Figure 14h), chromite, rutile and anatase are observed. Main gangue minerals are quartz, siderite-ankerite, calcite, dolomite and chlorite. Bravoiite, lineiite, magnetite (Figure 15), hematite and native copper (Figure 18) in Mağaradoruk deposit are observed more than they are in Aşıköy and Bakibaba deposits (Çağatay et al., 1980, 1982). Similar mineral assemblages are also observed in Ergani (Wijkerlooth, 1944; Göymen- Aslaner, 1963; Çağatay, 1978) and Siirt Madenköy copper deposits (Çağatay, 1978; Çalgın, 1978; Ulutürk, 1999).

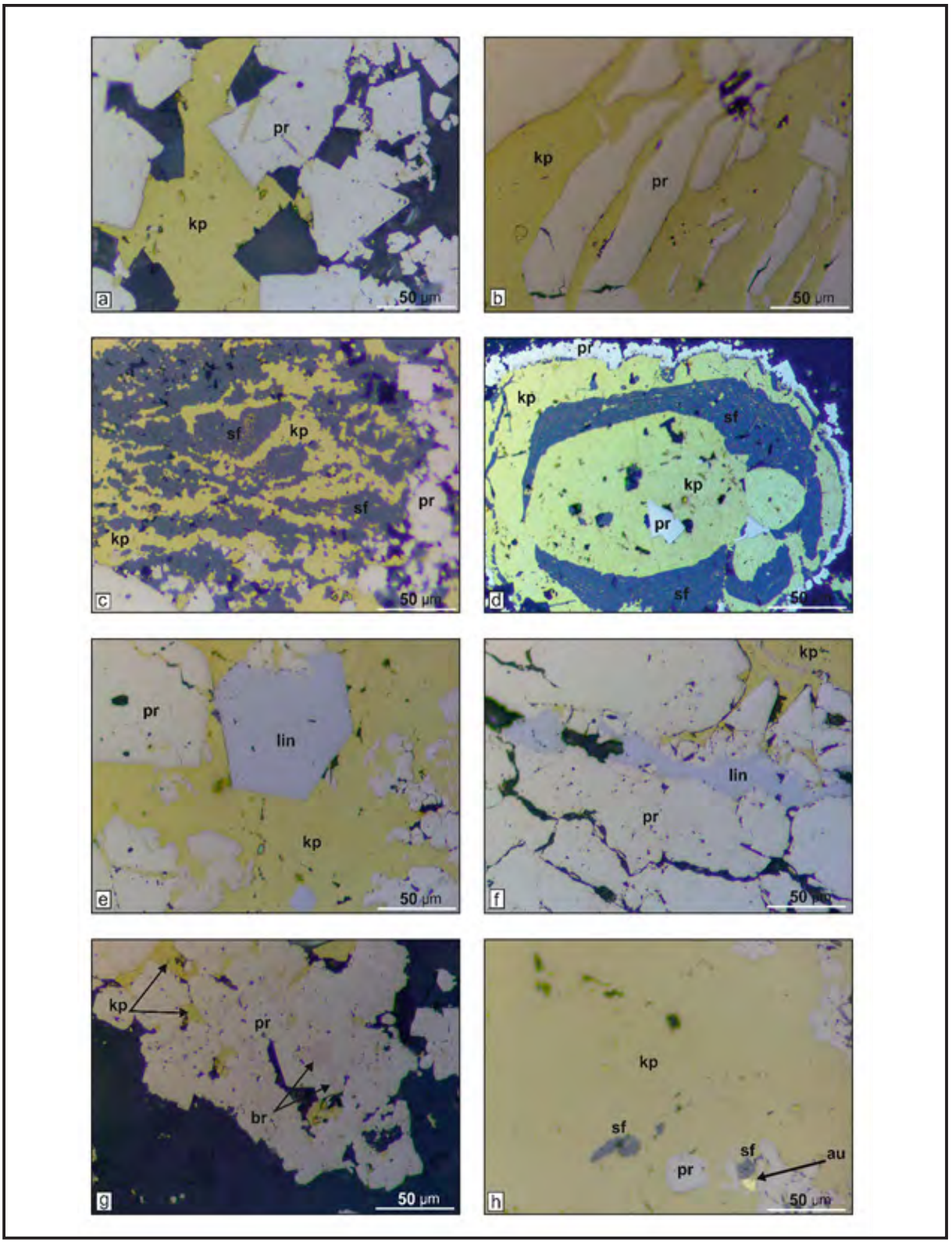

Figure 14- a) Chalcopyrite (Ccp) and gangue minerals (black) infilling grain voids of euhedral pyrites (py), b) chalcopyrite infilling cataclastic fractures of pyrites, c) chalcopyrite and sphalerite (sp) showing intergrowth which surround euhedral, subhedral pyrites, d) sphere with concentric crust which was formed by pyrite, chalcopyrite and sphalerite, e) euhedral lineiite (lin) in chalcopyrite which surrounds pyrite, f) lineiite accumulations and gangue minerals which fulfill cataclastic fractures of pyrite, g) bravoite (br) accumulations (as banded and worm like) which reveal the zoning structure of pyrite in pyrite, h) native gold which is observed among pyrite, chalcopyrite and sphalerite.

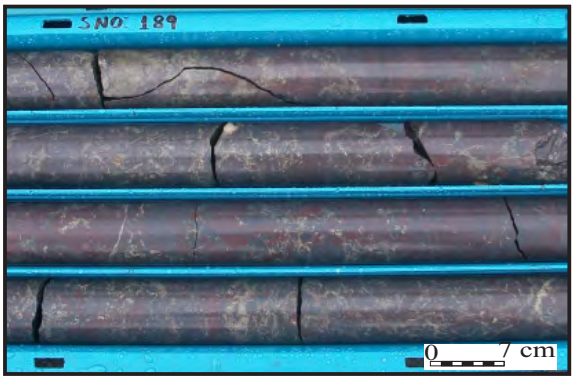

Figure 15- Massive ore which is formed by pyrite, chalcopyrite and magnetite in east of Mağaradoruk deposit.

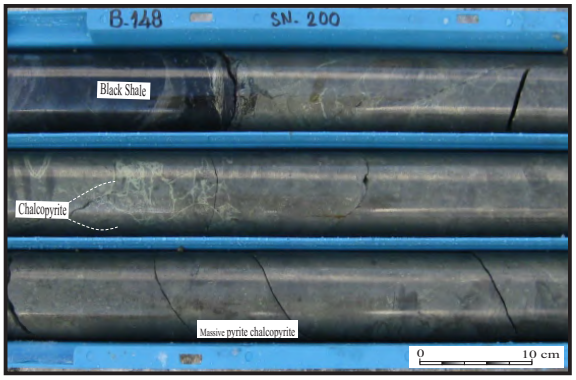

Figure 16- Chalcopyrite veins within massive pyrite, chalcopyrite in Mağaradoruk deposit.

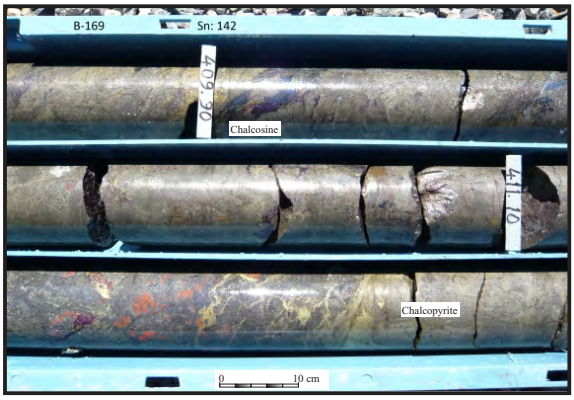

Figure 17- Chalcopyrite and chalcosine veins in massive pyrite and chalcopyrite in Mağaradoruk deposit.

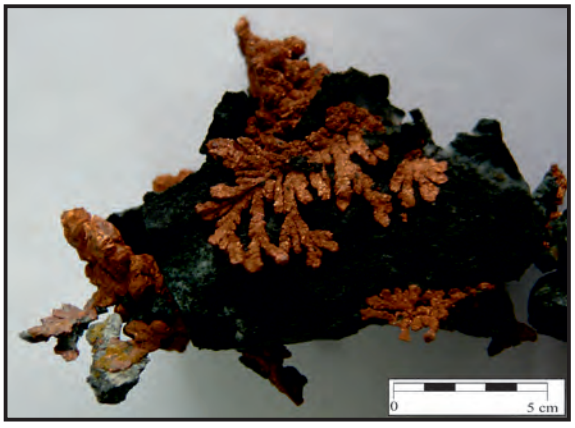

Figure 18- Native copper in basalt.

Main ore minerals in "Cyprus" type deposits are pyrite, chalcopyrite, sphalerite, pyrrhotine and magnetite (Constantinou and Govett, 1972). These are accompanied by lineiite and valeriite in few amounts.

Main ore minerals in TAG massive sulfide deposit are pyrite, chalcopyrite, sphalerite and bornite. Most observed gangue mineral is anhydrite (Thompson et al., 1988; Rona et al., 1993; Brown and Mc Clay, 1998).

4.4. Alteration

Main rocks in Mağaradoruk deposit are basalts, pillow lavas, hyaloclastics and black shales. The ones, which have traces of hydrothermal differentiation, are basaltic rocks. Basaltic rocks are formed by several lava flows which were formed in different times though they have similar mineralogical characters. They are partly more fresh, but mostly chloritized and carbonated away from ore bodies. They do not show any significant change until a distance very close to ore bodies. Epidotization is quite often observed in upper parts of ore bodies. In basalts, which consist of massive ore bodies, the primary textures of the rock have completely disappeared just above the massive ore.

As going away from massive ore bodies, the sericitization gives way to chloritization. Stockwork disseminated ore, which is formed by sulfide vein, veinlet and disseminations below massive sulfide bodies, grade into chloritized basalt with continuously weakening ore as it was in Ergani Anayatak deposit (Wijkerlooth, 1944). This zone becomes narrow towards deeper levels but do never develop under the whole massive ore body. Here; pyrite, chalcopyrite disseminations and veinlets are accompanied by magnetite and hematite dissemination, vein and veinlets.

5. Results

Küre - Mağaradoruk copper deposit should be a massive sulfide deposit, which developed based on hydrothermal processes when volcanism has ended in the environment in which Liassic- pre Liassic mid ocean ridge basalts had been formed.

This deposit is formed by a couple of small and a big massive ore deposit, and consists of less developed, stockwork disseminated ore below massive ore body.

In Mağaradoruk massive sulfide deposit, the abundance of magnetite-hematite-pyrite-bravoite at the bottom, chalcopyrite in middle parts and sphalerite in uppermost layers indicate a mineral zonation.

The presence of several massive sulfide deposits in Troodos massive, which are very close to each other, the observation of massive sulfide deposits within narrow area such as; Şahgeltepe, Mihrapdağ, Arpameydanı and Anayatak in Ergani, several hydrothermal vents that are arranged in short distances in Atlantic and Pacific mid ocean ridges to form contemporaneous sulfide deposits indicate that massive sulfide deposits in Küre (Mağaradoruk, Toykondu, Aşıköy, Bakibaba ve Kızılsu) might have also been formed in similar environments.

Massive sulfide lenses, in Mağaradoruk massive sulfide deposit, are mostly located on basaltic rocks within basaltic rocks and black shales, and are covered by black shales. This deposit resembles to Siirt Madenköy, Ergani massive sulfide deposits, to "Cyprus" type massive sulfide deposits and "modern Cyprus type massive sulfide deposits" in terms of mineral contents; and to Ergani Mihrapdağı, Papuke, Pakotai and Parakoa deposits in terms of cover rocks, which are Cyprus type massive sulfide deposits, in New Zealand.

Received: 14.01.2014
Accepted: 05.01.2015
Published: June 2015

References

Altun, Y., Yılmaz, H., Hatko, C., Yılmaz, B. 2009. Kastamonu- Küre Bakır yatakları ve bu yataklar da 2005- 2008 yılları arasında yapılan arama çalışmaları ile elde edilen sonuçlar. Eti Bakır A.Ş. Genel Müdürlüğü, Kastamonu (unpublished).

Bailey, H., Barnes, J. W., Kupfer, D. H. 1967. Türkiye Kastamonu ile Küre Bölgesi cevher yatakları ve jeolojisi. *Etibank Genel Müdürlüğü raporu* (unpublished).

Bamba, T. 1976. Ophiolite and related copper deposits of the Ergani mining district, Southeastern Turkey. *Bulletin of the Mineral Research and Exploration 86, pp.36-50*

Brathwaite , R.L., and Pirajno, F. 1993. Metallogenic map of New Zealand. *Institue of Geological and Nuclear Sciences Monograph* 3.

Brown, D., McClay, K. R. 1998. Sulfide Textures in the Active TAG massive sulfide deposit 26° N, Mid– Atlantic Ridge. Herzig, P.M., Humphris, S.E., Miller, D.J., and Zierenberg, R.A. (Eds.). Proceeding of the Ocean Drilling Program, Scientific Results, 158p.

Constantinou, G. 1980. Metallogenesis associated with the Troodos ophiolite. A. Panayiotu (Ed.). *Ophiolites Proceeding İnternational Ophiolite Symposiu,* 1980 Nicosia-Cyprus, pp.663-674.

Constantinou, G., Govett, G.J.S. 1972. Genesis of sulphide deposits, ochre and umber of Cyprus. *Institute Mining Metallurgy* 8(b), pp.33-46.

Çağatay, A. 1978. Güneydoğu Anadolu bakır yatak ve zuhurlarının jeolojik-mineralojik etüdü sonunda elde edilen jenetik bulgular. *Maden Tetkik ve Arama Dergisi* 89, pp.46- 69.

Çağatay, N. 1981. Yeni gelişmelerin ışığında Türkiye'nin volkanik kökenli masif sülfid yatakları. *1.Türkiye Jeoloji Mühendisliği Bilim ve Teknoloji Kongresi. Jeoloji Mühendisleri Odası Yayını* 6, pp.35-36.

Çağatay, A., Pehlivanoğlu, H., Altun, Y., 1980. Küre piritli bakır yataklarının kobalt-altın mineralleri ve yatakların bu metaller açısından ekonomik değeri. *Maden Tetkik ve Arama Dergisi,* 93/94 (1979-1980), pp.110-117.

Çağatay, A, Arman, B., Altun, Y., Pehlivanoğlu, H. 1982. Küre (Kastamonu) Yataklarında izlenen ve lineyit grubundan olan kobalt mineralinin elektron mikroprob analizi. *Karadeniz Teknik Üniversitesi Yer Bilimleri Dergisi* 2 (1-2), pp.131-134.

Çağatay, A., Arda, O. 1984. Küre Bölgesindeki kayaçların mineralojik incelenmesi. Kastamonu (unpublished).

Çalgın, R. 1978. Siirt-Madenköy bakır yatağının jeolojisi ve mineralizasyonu. *Maden Tetkik ve Arama Genel Müdürlüğü Rapor No: 5651, Ankara* (unpublished)

Galley, A.G., Koski, R.A. 1999. Setting and Caracteristics of ophiolite hosted volcanogenic massive sulphide deposits. *United States, Society of Economic Geologists* 8, pp.221-246.

Göymen- Aslaner, G. 1963. Doğu Anadolu'da bulunan Ergani maden bakır yatağının ve bilhassa yantaşlarının maden mikroskopik incelenmesi. *Maden Tetkik ve Arama Dergisi* 72, pp.177-187.

Güner, M. 1980. Küre civarının masif sülfid yatakları ve jeolojisi pontidler (Kuzey Türkiye). *Maden Tetkik ve Arama Dergisi* 93/94, pp.65-109.

Hannigton, M.D., Galley, A.G., Herzig, P.M., Petersen, S. 1998. A comparison of the TAG Mound and stockwork complex with Cyprus- type massive sulfide deposits: Proceedings Ocean Drilling Program, Scientific Results 158, pp.389- 415.

Harper, G.D. 1999. Structural Styles of hydrotermal discharge in ophiolite/seafloor systems. pp.53-73 (chap.3) in Barrie , C.T., and Hannington, M.D. (eds.). Volcanic Associated massive sulfide deposits. *Reviews in Economic Geology Society of Economic Geologists* 8, Chap- 3, pp.53- 73.

Ildız, T. , Dağcı, Z. 1990. Bakibaba rezerv hesapları raporu. Karadeniz Bakır İşletmesi Genel Müdürlüğü Ankara.

Jensen, L.S. 1976, A new cation plot for classifying subalkalic Volcanic rocks: *Ontorio Dep. Mines., Mise Paper*, 66, pp.1-22.

Ketin, İ. 1962. 1/500 000 ölçekli jeolojik haritası Sinop paftası ve izahnamesi. *Maden Tetkik ve Arama Enstitüsü Yayınları*, Ankara.

Ketin, İ., Gümüş, A. 1963. Sinop-Ayancık arasında 3. bölgeye dahil sahaların jeolojisi. *Türkiye Petrolleri Anonim Ortaklığı Rapor No: 288.*

Kleinrock, M. C., Humphris, S. E. 1996. Structural control on seafloor hydrothermal activity at the TAG active mound. *Nature* 382, pp.149-153.

Koç, Ş., Unsal, A., Kadıoğlu, Y.K. 1995. Küre (Kastamonu) cevherleşmelerini içeren volkanitlerin jeolojisi, jeokimyası ve jeotektonik konumu. *Maden Tetkik ve Arama Dergisi* 117, pp.41-54.

Kovenko, V. 1944. Küre'deki eski bakır yatağı ile yeni keşfedilen Aşıköy yatağının ve Karadeniz orta ve doğu kesimleri sahil bölgesinin metallojenisi. *Maden Tetkik ve Arama Dergisi* 2/3, pp.180-211.

Kuşçu, İ., Erler, A. 2002. Pyrite deformation textures in the deposits of the Küre Mining District (Kastamonu-Turkey). *Turkish Journal of Earth Sciences* 11, pp.205-215.

Metal Mining Agency of Japan 1995. The Republic of Turkey Report on The Mineral Exploration of Küre Area.

Nikitin, V. 1926. Küre bakır madeni. *Maden Tetkik ve Arama Derleme Rapor No: 850,* Ankara (unpublished).

Pearce J.A., Cann, J.R., 1973, Tectonic setting of basic volcanic rocks determined using trace element analysis: *Earth Planet. Sci. Lett.,* 19, pp.290-300.

Pehlivanoğlu, H. 1985. Kastamonu- Küre piritli bakır yatakları (Bakibaba, Aşıköy) ve çevresinin jeoloji raporu. *Maden Tetkik ve Arama Rapor No: 1744*, Ankara (unpublished).

Pieniazek, J. 1945. Küre araştırmaları kati raporu. Etibank Küre Bakırlı Pirit İşletmesi Müessesesi, (unpublished).

Pollak, A. 1964. Küre pirit- bakır yatağı hakkında rapor. *Maden Tetkik ve Arama Genel Müdürlüğü Rapor No: 3693*, Ankara (unpublished).

Ridley, W.L., Rhodes, J.M., Reid, A.M., Jakes, P.; Shih. C., Bass, M. 1974, Basalts from Leg 6 of the Deep-Sea Drilling Project: *Journal of Petrology,* 15.

Rona, P.A., Hannington, M.D., Raman, C.V., Thompson, G., Tivey, M.K., Humphris, S.E., Lalou, C., and Petersen, S. 1993. Active and relict sea floor hydrothermal mineralization at the TAG hydrothermal field, MidAtlantic Ridge. *Economic Geology* 88, pp.1987−2013.

Sarıcan, K. 1968. Bakibaba cevher yatağı arama ve değerlendirme çalışmaları raporu. Küre Etibank, Karadeniz Bakır İşletmeleri Raporu (unpublished).

Stos- Gale, Z.A., Maliotis, G., Gale, N.H., Annetts, N. 1997. Lead isotope characteristics of the Cyprus copper ore deposits applied to provenance studies of Copper axhide in gots Archaeometry 39, pp.107-109.

Şengör, A. M. C., Yılmaz, Y. 1983. Türkiye'de Tetis'in Evrimi: Levha Tektoniği Açısından Bir Yaklaşım. *Türkiye Jeoloji Kurumu Yerbilimleri Özel Dizisi* No. 1, Ankara

Şengün, M. 2006. Anadolu'nun Kenet Kuşakları ve Jeolojik Evrimine İrdelemeli ve Eleştirel Bir Bakış. *Maden Tetkik ve Arama Dergisi* 133, pp.1-26.

Thompson, G., Humphris , S.E., Schroeder, B., Sulanowska, M., and Rona, P.A. 1988. Active vents and massive sulfides at 26°N (Snakepit) on the Mid-Atlantic Ridge. *Canada Mineral* 26, pp.697-711.

Ulutürk, Y. 1999. Siirt Madenköy bakır yatağı. *Maden Tetkik Arama Genel Müdürlüğü Rapor No:* 7562. Ankara (unpublished).

Üşümezsoy, Ş. 1989. Istranca Metamorfik Kuşağı Rift Volkanitlerinin Petrolojisi, Karadeniz Kimmeriyen Çanağının Açılımı ve Masif Sülfidlerin Kökeni. 42. Türkiye Jeoloji Kurultayı Bildiri Kitabı, 20p.

Wijkerslooth, P. 1944. Elazığ ili (Ergani-Maden) bakır yatakları hakkındaki bilgiye yeni bir ilave. *Maden Tetkik ve Arama Dergisi* 33, pp.76-104.

Yildirim, N., Ilhan, S., Yildirim, E., Dönmez, C. 2012.The Geology, Geochemistry and Genetical Features of the Ormanbaşı Hill (Sincik, Adiyaman) Copper Mineralization. Bulletin Mineral Research and Exploration., 144, pp.75-104.

Yıldırım, N. 2013. Havza-Kuşak Madenciliği Kapsaminda Keşfedilen "GD Anadolu Kıbrıs Tipi VMS Metalojenik Kuşağı": Koçali Karmaşığı, Adiyaman Bölgesi, Türkiye. *MTA Doğal Kaynaklar ve Ekonomi Bülteni,* 14, pp.47-55

Yıldırım, N., Dönmez, C., Kang, J., Lee, I., Yıldırım, E., Özkümüş, S., Çiftçi, Y., Günay, K., İlhan, S. 2014. Manyetit'çe zengin Kıbrıs tipi VMS yataklarına GD Türkiye'den bir örnek: Ortaklar (Gaziantep) VMS yatağı. *67.Türkiye Jeoloji Kurultayı 14-18 Nisan/April 2014*

Yıldırım, R., Alyamaç, F. 1976. Siirt ili Madenköy-Hürmüz yöresi jeoloji etüdü. *Maden Tetkik ve Arama Genel Müdürlüğü Rapor No: 5851, Ankara*

Yılmaz, O. 1980. Daday- Devrekani masifi kuzeydoğu kesimi litostratigrafi birimleri ve tektoniği. *Hacettepe Üniversitesi Yerbilimleri Dergisi* 5- 6, pp.101-131.

Zaccarani, F., Garuti, G. 2008. Mineralogy and chemical composition of VMS deposits of northern Apennine ophiolites, İtaly evidence for the influence of country rock type on ore composition. *Mineralogy and Petrology* 94, pp.61-83.

BULLETION OF THE MINERAL RESEARCH AND EXPLORATION

Foreign Edition 2015 150

CONTENTS

Bull. Min. Res. Exp. (2015) 150: 65-76

Bulletin of the
Mineral Research and Exploration

http://bulletin.mta.gov.tr

OROGENIC GOLD PROSPECTIVITY MAPPING USING GEOSPATIAL DATA INTEGRATION, REGION OF SAQEZ, NW OF IRAN

Alireza Almasi[a]*, Alireza Jafarirad[a], Peyman Afzal[b] and Mana Rahimi[c]

[a] *Department of Geology, Science and Research branch, Islamic Azad University, Tehran, 1477893855, Iran,*
[b] *Department of Mining Engineering, Faculty of Engineering, Islamic Azad University, South Tehran branch, Tehran, 1777613651, Iran*
[c] *Department of Geomatics, Geological Survey of Iran (GSI) Tehran, 1387835841, Iran*

Keywords:
Mineral Prospectivity Mapping, Index Overlay, Fuzzy Logic, Orogenic Gold, Sanandaj-Sirjan, Saqez, GIS

ABSTRACT

The aim of this study is to map orogenic gold prospecting areas in the region of Saqez, NW of Iran. In order to achieve this task geological, geochemical and airborne geophysical data are analyzed and integrated using index overlay and fuzzy logic methods. Geological map of Saqez (1:100000 scale) is used to assign lithological weights based on their favorability for hosting orogenic Au mineralization. Also a fault density map is produced and assigned based on the structural map which is included in the geological map. For preparing geochemical evidence maps, data from 535 stream sediment samples are examined using Number-Size multifractal method for Au, As, Bi and Hg. The detected thresholds are used to assign the catchment basins of the stream sediment samples. Aeromagnetic data is employed to detect the edges of magnetic anomalies based on an enhanced edge detection method. Extracted lineaments are then converted to a density map and assigned properly. Airborne radiometric data is also used to produce two evidence maps. Potassium count grid independently and K/Th ratio map are employed to distinguish locations with hydrothermal activity. Finally after integrating evidence maps, new locations with high potentials of Au mineralization are identified considering that the gold indications of the study area (Qolqoleh, Kervian and Ghabaghloujeh) are placed in the first priority of the fuzzy logic prospectivity map.

1. Introduction

The amount of digital geoscientific data available in mineral exploration is increasing rapidly, and the technologies for storing, maintaining and analyzing these data have been developing equally fast during recent years. The spatially referenced geosciences data such as airborne geophysical data, geochemical data, geological and structural data are especially suitable for quantitative analysis using a Geographic Information System (GIS), in order to derive information that is useful in mineral exploration (Jafarirad, 2009; Jafarirad and Busch, 2011; Magalhaes and Souza Filho, 2012; Nykanen et al., 2008). As stated by Luo and Dimitrakopoulos (2003), these quantitative methods are often used to: (1) extract the maximum amount of information from the data; (2) effectively combine data from diverse information sources; (3) rank potential targets (mineral sites); and (4) reduce data processing and evaluation time. In this paper, a reconnaissance scale mineral prospectivity map is presented for orogenic gold mineralization in Saqez area, northern part of Sanandaj-Sirjan metamorphic zone, NW of Iran (Figure 1).

The region under study with area of about 1800 km^2 comprises Sardasht-Saqez orogenic gold zone with Qolqoleh, Kervian and Ghabaghloujeh indications in the SW (Figure 1). Former studies revealed that these gold occurrences are hosted by upper cretaceous meta-volcanosedimentary rocks and

* *Corresponding author: Alireza Almasi, alirezaalmassi@gmail.com*

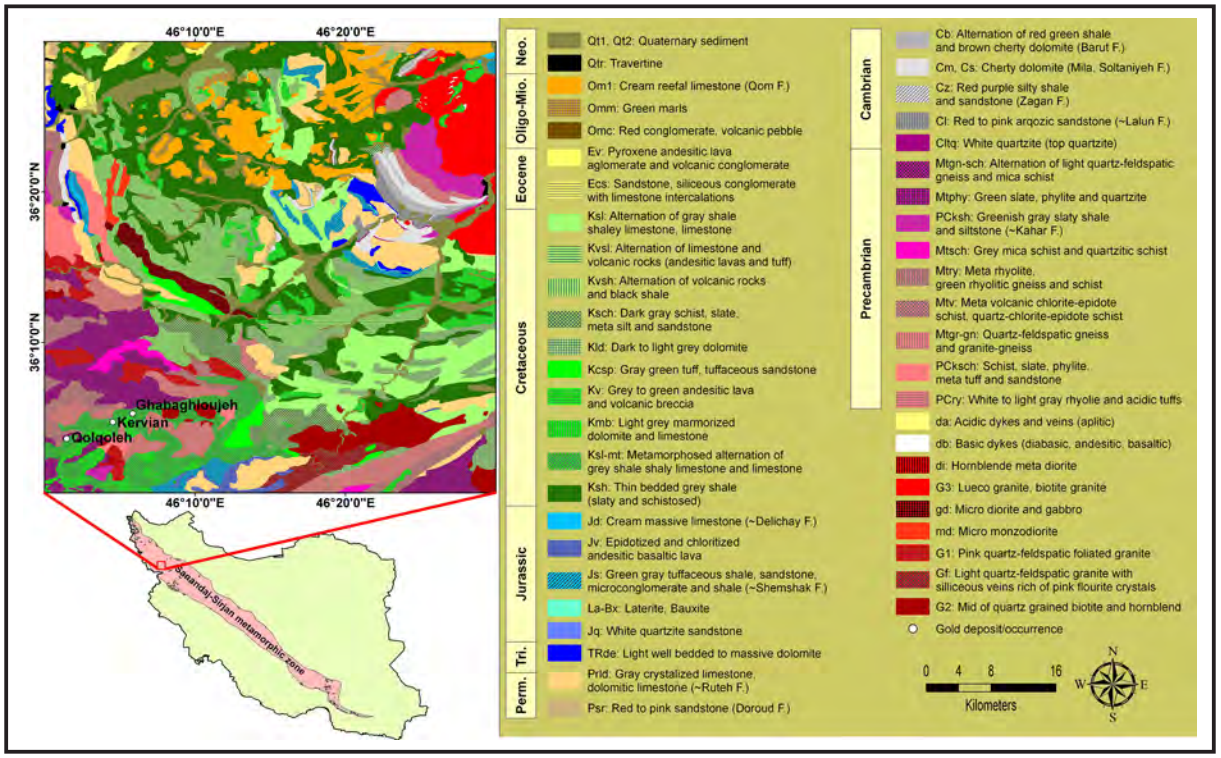

Figure 1- Saqez geological map (1:100000 scale: after Babakhani et al., 2003).

are placed over ductile to brittle shear zones and are located within or adjacent to the major deep Saqez-Sardasht thrust fault and other confining normal faults across this structural zone. The secondary host rock in these indications (especially in Qolqoleh) is altered mylonitic granite. Due to metamorphic genesis of Au mineralization in this region, felsic units are only important as heat sources for percolating hydrothermal fluids. Moreover endowment of As, Bi and Hg have been recorded in these indications (Aliyari et al., 2007, 2009, 2012; Tajeddin, 2011).

Information about the genesis model and effective factors in Au mineralization derived from the former studies was summarized in table 1, and was used to comprehend the genetic model for gold prospectivity mapping. Due to few known Au deposits/indications in the study area, knowledge-driven index overlay and fuzzy logic approaches were chosen for preparing information layers and integration (Bonham Carter, 1994; Carranza, 2008; Magalhaes and Souza Filho, 2012; Nykanen et al., 2008).

Table 1- Characteristics of Qolqoleh, Kervian and Ghabaghloujeh deposits/indications.

Deposit/ indication	Host rocks	Genetic type	Age of mineralization	Enriched element(s) / structural features	Resource (t) grade (g/t)	Data source
Qolqoleh	Meta-sedimentary, mafic to interamediate (andesite to andesitic basalt) meta-volcanic rocks, sericite schist	Orogenic (ductile to brittle shear zone)	Upper Cretaceous-Tertiary	As and Hg / intersecting faults and fractures	Up to 0.37 Moz @ 3.5 g/t	Aliyari *et al.*, (2007, 2009); Tajeddin, (2011)
Kervian	Meta-sedimentary and felsic to mafic meta-volcanic rocks	Orogenic (ductile shear zone)	Upper Cretaceous-Tertiary	As, Bi and Hg / intersecting faults and fractures	Unknown	Heidari, (2004); Heidari *et al.*, (2006); Tajeddin, (2011)
Qabaqloujeh	Phyllite, schist meta-volcanic, and mylonitic rocks	Orogenic (ductile to brittle shear zone)	Upper Cretaceous-Tertiary	As and Bi / intersecting faults and fractures	0.035 (Moz) @ 1 g/t	Tajeddin, (2011)

2. Materials

Saqez region because of its high potential for diverse kinds of mineralization was the subject of different surveys in recent years. Hence, geochemical data used in this research comes from 535 stream sediment samples which were gathered and analyzed by Geological Survey of Iran (GSI) in 2005. The samples were chemically analyzed using fire assay method for Au and ICP-MS method for Au pathfinders As, Bi and Hg. Detection limit for analyzing Au was 1 ppb and detection limits for analyzing As, Bi and Hg were 0.5, 0.1 and 0.1 ppm respectively. In order to produce geochemical anomaly maps and considering the fact that stream sediment samples represent upstream lithologies, elemental concentrations were assigned to the catchment basins of the samples.

Meanwhile, aeromagnetic and aeroradiometric data are from two separate airborne geophysical surveys. In northern part of the study area with area of about 1546 Km^2, aeromagnetic and aeroradiometric data were achieved from a helicopter-borne geophysical survey that was carried out by Prakla and Austirex for Atomic Energy Organization of Iran (AEOI) in 1976. Line spacing and flight elevation of this survey were 500 and 120 meters respectively. In the south-western part (polygonal shape zone) with area of about 283 km^2, aeromagnetic and aeroradiometric data are from a geophysical survey which was conducted by Fugro Airborne Surveys Corporation and GSI in 2006 with line spacing and flight elevation of 200 and 60 meters respectively.

In order to include all the information layers in final integrations the study area was limited to the extension of the airborne geophysical surveys (the rectangular shape in the north and the polygonal shape in the southwest). Microsoft office excel 7 and Oasis Montaj (6.4.1 CN) software were used for analyzing geochemical and airborne geophysical data respectively, and ArcGIS 9.3 was employed for producing and integrating evidence maps.

3. Preparing information layers

In order to produce raster information layers (evidence or factor maps) with assigned crisp numbers between 1-10, or fuzzy memberships (0-1) using fuzzy functions such as linear, large and near (Bonham Carter, 1994; Carranza, 2008; Nykanen *et al*., 2008; Tsoukalas & Uhrig, 1997), geological, geochemical, aeromagnetic and airborne radiometric data had to be analyzed and interpreted using a range of different methods. In order to prevent missing data in the places where one information layer among overlapping layers does not have a value (nodata), crisp value 1 or a ~0 fuzzy value were assigned to such areas. Coordinate system for all the maps is UTM (Universal Transfer Mercator) zone 38N. The steps of preparing each layer are presented in following sections.

3.1. Geochemical data

Number-Size (N-S) multifractal model (Mandelbrot, 1983; Deng et al., 2010; Hashemi and Afzal, 2013) was applied on the geochemical data from stream sediment samples in order to delineate anomaly thresholds for Au, As, Bi and Hg. Thereafter for producing geochemical anomaly maps, the detected thresholds were used to classify the catchment basins of the samples (Figure 2). Afterwards for preparing factor maps, crisp values 1-10 were assigned to each geochemical map based on the thresholds resulted from N-S multifractal analysis (Table 2). Meanwhile fuzzy memberships for Au, As, Bi and Hg were produced using fuzzy large function with midpoint and spread of 7 and 5 for Au and 7 and 3 for elemental paragenesis respectively (Table 2).

3.2. Airborne geophysical data

Airborne geophysical data including aeromagnetic and aeroradiometric data resulted in producing three separate evidence maps. Aeromagnetic data is known as an important source of information for studying lineaments and structures (Bierlein et al., 2006; Henson et al., 2010; Li, 2013). Many edge detection filters such as analytic signal, vertical derivative, total horizontal derivative (THD) and tilt derivative (TDR) are available to accomplish this task (Ferreira et al., 2011; Verduzco et al., 2004). However in this research, after removing IGRF from northern and southern Total Magnetic Intensity (TMI) maps, in order to place the magnetic anomalies over their causative bodies and to minimize the effects of shallow magnetic sources, Reduction to The Pole (RTP) and Upward Continuation (UC) filters were applied on TMIs respectively. Thereafter for detecting the magnetic edges THD and TDR were applied on RTP UCs respectively (Almasi et al., 2014). For rasterizing the edges and converting them into an evidence map, a density map which calculates the density of linear features in the neighborhood of each output grid cell (Silverman, 1986) was produced and

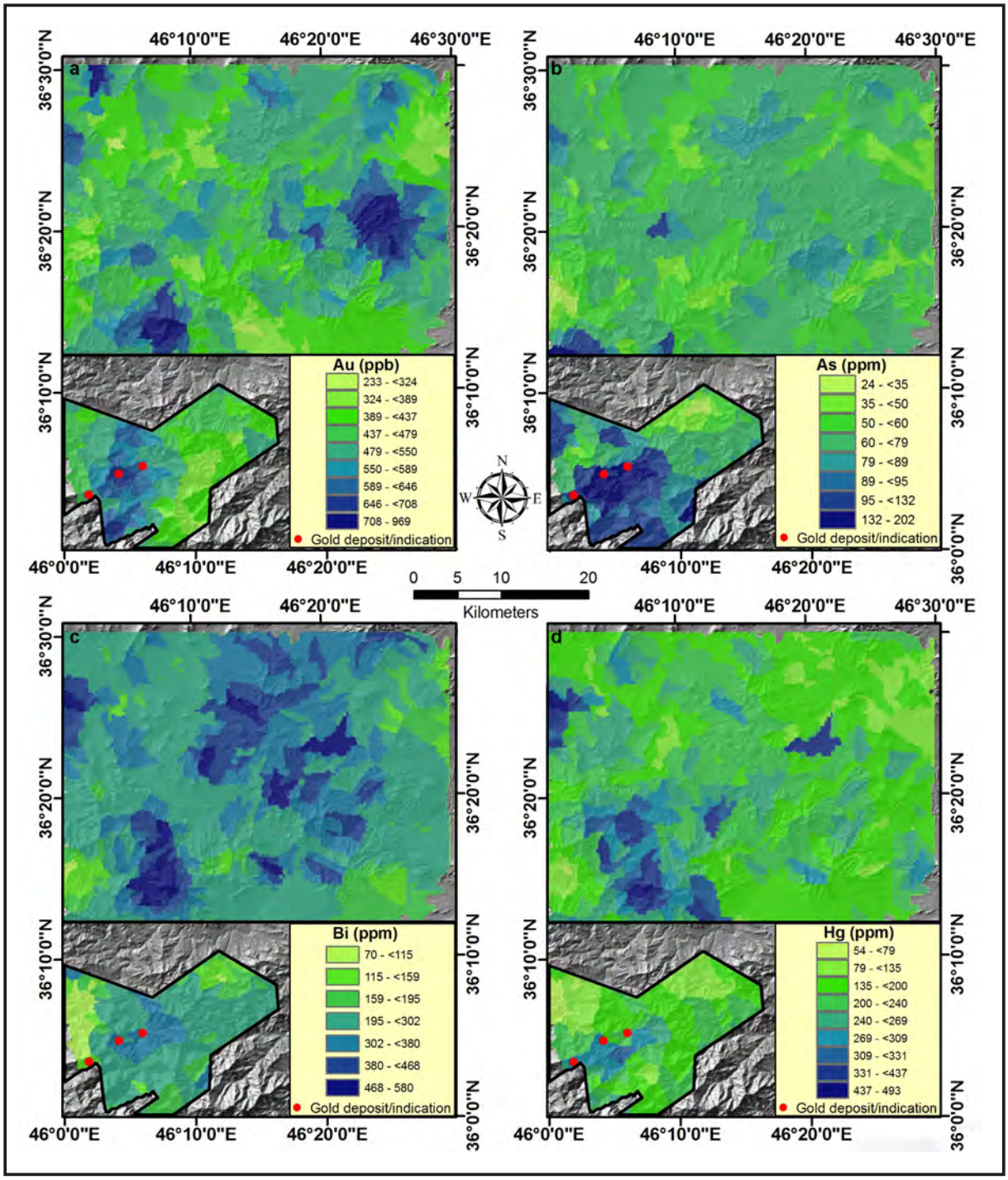

Figure 2- Geochemical maps for a) Au, b) As, c) Bi and d) Hg using N-S multifractal model.

assigned 1-10 (Figure 3). Fuzzy membership of the lineaments' density map was produced using fuzzy large function with midpoint and spread of 7 and 5 respectively (Figure 3).

Airborne radiometric data is capable of mapping felsic igneous rocks which contain high amounts of radioactive elements (Th, K and U), and also is able for mapping places with hydrothermal activities (de Souza Filho et al., 2007; Magalhães and Souza Filho 2012; Silva et al. 2003). Potassium count data and the ratio of K/Th (after Airo, 2001, 2007) are used to distinguish these locations. K/Th ratio anomalies for north and south of the study area were mapped and assigned appropriately. Converting K count into an information layer was based on the

Table 2- Crisp (C) and fuzzy (F) values based on N-S thresholds for Au, As, Bi and Hg

Au thresholds (ppb)	Value		As thresholds (ppm)	Value		Bi thresholds (ppm)	Value		Hg thresholds (ppm)	Value	
	C	F		C	F		C	F		C	F
Nodata	1	~ 0	Nodata	1	0.003	Nodata	1	0.003	Nodata	1	0.003
233 - <324	2	0.002	24 - <35	3	0.07	70 - <115	4	0.16	54 - <79	2	0.02
324 - <389	3	0.014	35 - <50	4	0.16	115 - <159	5	0.27	79 - <135	3	0.07
389 - <437	4	0.06	50 - <60	5	0.27	159 - <195	6	0.39	135 - <200	4	0.16
437 - <479	5	0.16	60 - <79	6	0.39	195 - <302	7	0.5	200 - <240	5	0.27
479 - <550	6	0.32	79 - <89	7	0.5	302 - <380	8	0.6	240 - <269	6	0.39
550 - <589	7	0.5	89 - <95	8	0.6	380 - <468	9	0.68	269 - <309	7	0.5
589 - <646	8	0.66	95 - <132	9	0.68	468 - 580	10	0.74	309 - <331	8	0.6
646 - <708	9	0.78	132 - 202	10	0.74				331 - <437	9	0.68
708 - 969	10	0.86							437 - <493	10	0.74

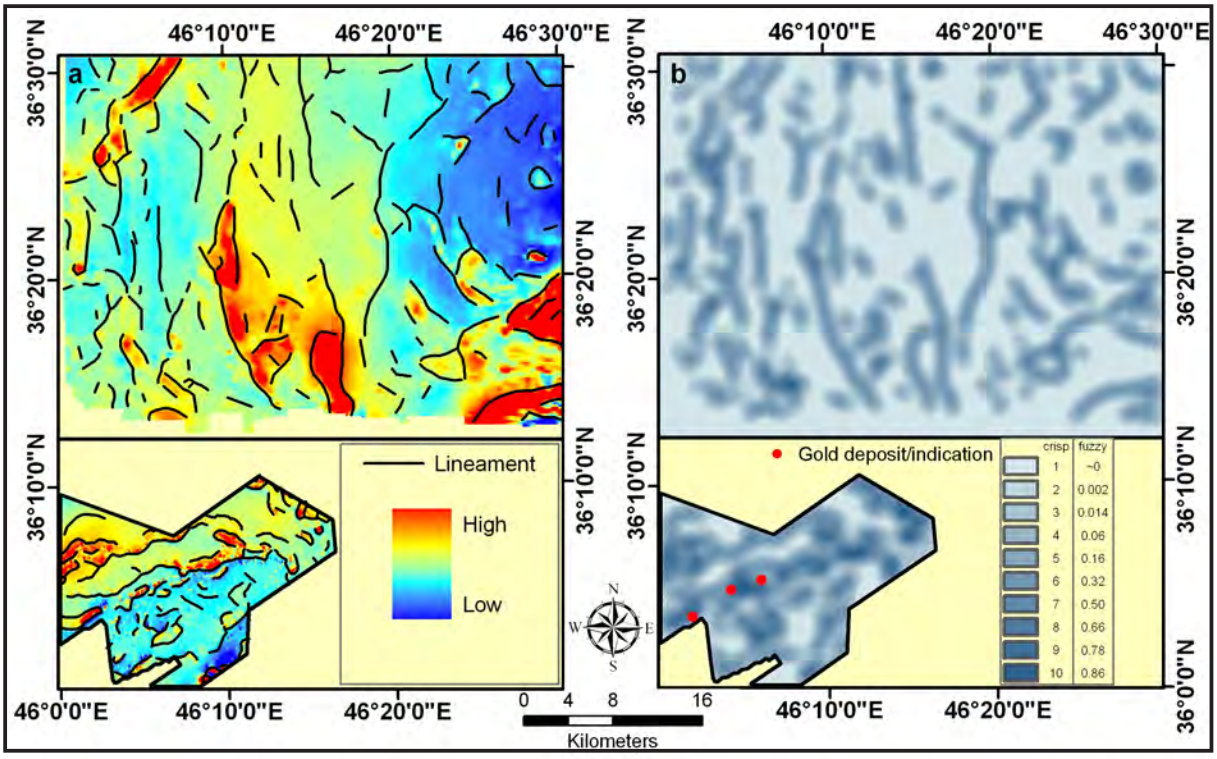

Figure 3- a) extracted lineaments using enhanced edge detection method with RTP in the background, b) lineaments' density map and its assigned crisp and fuzzy values.

correlation of high amounts of potassium count with felsic intrusions and its median value over hydrothermal activities and the edges of felsic units (after Airo, 2001, 2007) where the gold indications and Au anomalies of the study area are placed. Thus for enhancing median amount in potassium count grids, near function with midpoint and spread of 5 and 0.003 respectively was applied on the K grid, thereafter this layer was assigned 1-10.

Near fuzzy function is used for enhancing an intermediate crisp value in a fuzzy set. The spread and mid parameters are subjectively defined to reflect the expert opinion. An example of the near algorithm is given in figure 4. The near function is also known as a sinusoidal membership function (Burrough and McDonnell, 1998; Tsoukalas and Uhrig, 1997).

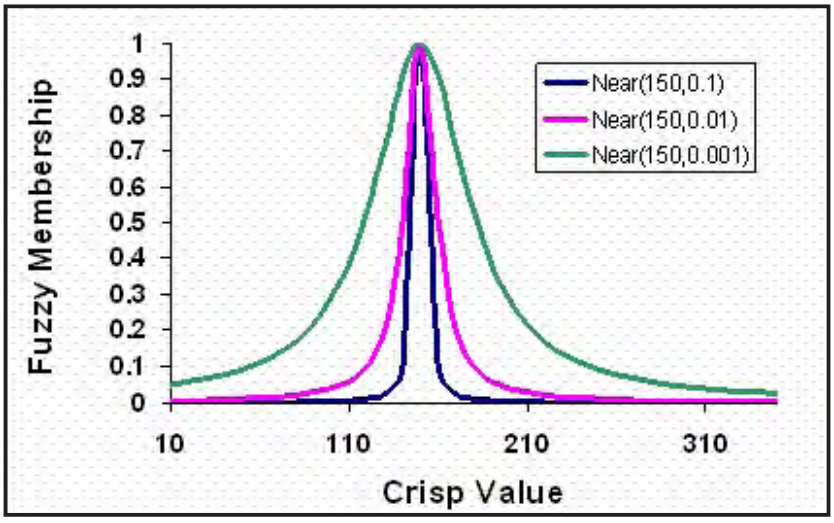

Figure 4- Example of near fuzzification using different midpoint and spread values.

Fuzzy membership of K layer was generated by applying fuzzy large function with midpoint and spread of 7 and 5 respectively on the median enhanced K map (Figure 5).

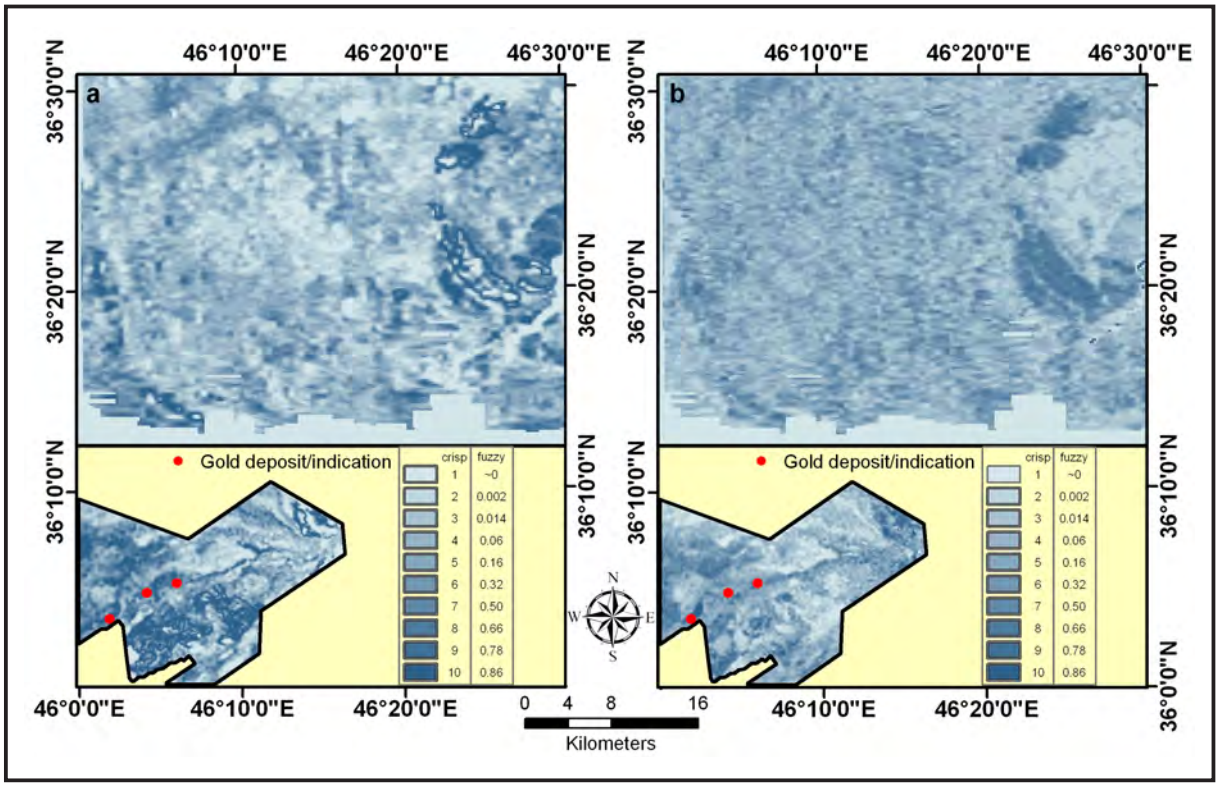

Figure 5-a) K evidence map and fuzzy membership, b) K/Th evidence map and fuzzy membership.

3.3. Geological data

For weighing the geological map, host rocks of the gold indications (Qolqoleh, Kervian and Ghabaghloujeh) were considered as highest values and lithological units were assigned based on their favorability for Au mineralization (Table 1). For instance geological units Ksl-mt and Mtgr-gn which represent meta-volcanosedimentary and mylonitic granites of the geological map (Figure 1) were assigned with the weights 10 and 9 respectively. Other units were weighed based on their similarity to

the host lithologies and their properness for hosting Au mineralization. For example units Mtgn-sch, Ksh, Mtgn-sch and Ksh were given weights of 8 and 7 were other meta-volcanosedimentary units of the study area. In order to produce geological evidence map, the rest of the lithologies were assigned using the values presented in table 3 (Figure 6). In addition, fuzzy membership of the geological units was produced with multiplying 8/100 by the crisp values of the table 3.

Table 3- Crisp and fuzzy values assigned to the lithological units of the geological map

Units	Crisp	Fuzzy
Ksl-mt	10	0.8
Mtgr-gn	9	0.72
Mtgn-sch, Ksh	8	0.64
PCry, Ksl	7	0.56
Gd, Kcsp,	6	0.48
G1,Kvsh, PCksh	5	0.4
di, G3, Kmb, Mtphy,	4	0.32
Cb, Cl, Cs, Cz, Js, Mtry, Mtsch, Mtv, Om1, PCksch, Prld, Psr, Qtr, TRde	3	0.24
Other units or Nodata	1	0.08

Another information layer was also produced using fault lines of the Saqez geological map (1:100000 scale: Babakhani et al., 2003). These structures were used for building a density map and then assigned 1-10. Its fuzzy membership was constructed using fuzzy large function with midpoint and spread of 7 and 5 respectively (Figure 6).

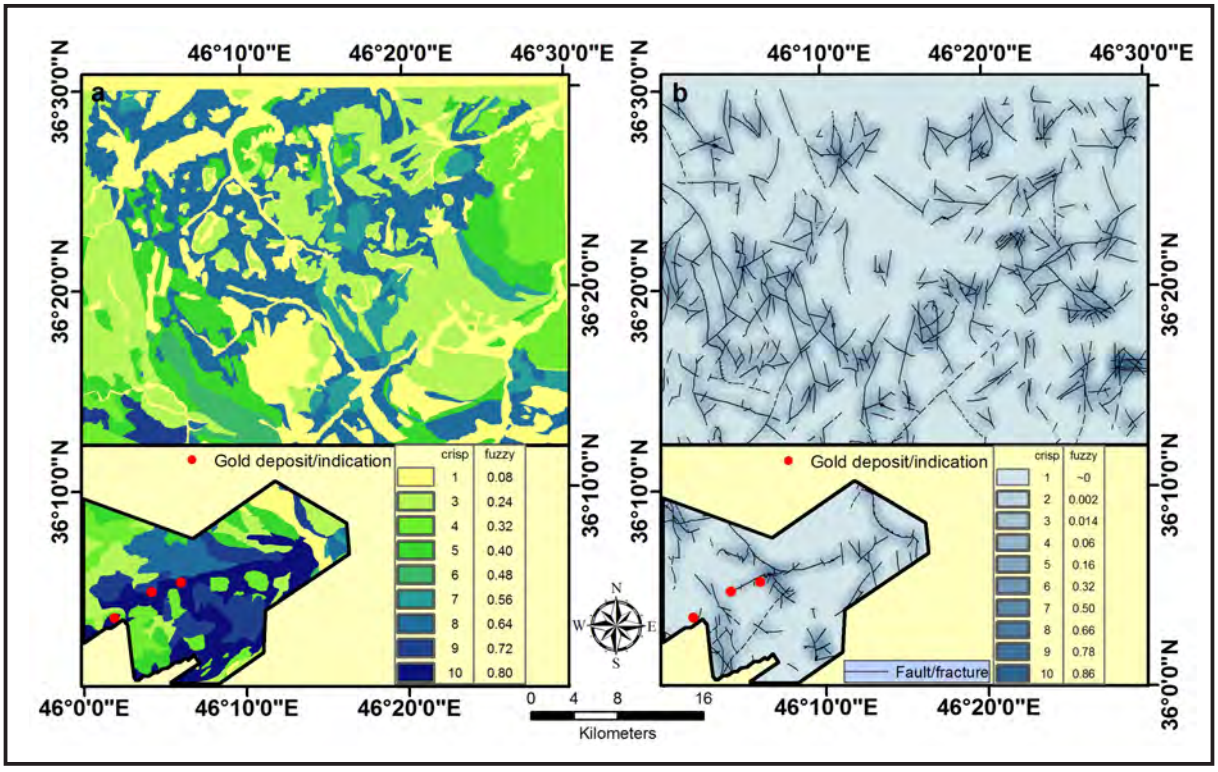

Figure 6- a) geological unit information layer and its fuzzy membership, b) structures (faults and fractures) of the geological map and its assigned crisp and fuzzy values using density map.

4. Index overlay and fuzzy logic methods

Mineral prospectivity maps were generated with integrating factor maps using knowledge-driven index overlay and fuzzy logic methods (Bonham Carter, 1994, Nykanen et al., 2008). Index overlay integration is based on following equation:

$$S = \sum W_i S_{ij} / \sum W_i \quad \text{(equation 1)}$$

Where:

Wi = the weight of ith factor map (which is 1 in simple overlay)

Sij = the ith spatial class weight of jth factor map

S = the spatial unit value in output map

Different weights were multiplied in each layer based on their relativity and correlation with orogenic gold type mineralization of the study area. Some examples of multi-class index overlay modeling applied to mineral prospectivity mapping can be found in Harris et al. (2001), Chico-Olmo et al. (2002) and Billa et al. (2004).

The fuzzy set theory which was established by Zadeh (1965) is the cornerstone of fuzzy logic modeling. Demicco and Klir (2004) discuss the rationale and illustrate the applications of fuzzy logic modeling to geological studies but they do not provide examples of fuzzy logic applications to mineral prospectivity mapping. Recent examples of applications of fuzzy logic modeling to mineral prospectivity mapping are found in Carranza and Hale (2001), Carranza (2002), Tangestani and Moore (2003), Ranjbar and Honarmand (2004), Rogge et al. (2006) and Nykänen et al. (2008). Typically, application of fuzzy logic modeling to knowledge-driven mineral prospectivity mapping involves three main feed-forward stages: (1) fuzzification of evidential data; (2) logical integration of fuzzy evidential maps with the aid of an inference network and appropriate fuzzy set operations; and (3) defuzzification of fuzzy mineral prospectivity output in order to aid its interpretation. Each of these stages in fuzzy logic modeling of mineral prospectivity is employed in this study in order to orogenic gold prospectivity mapping in the case study area.

5. Results and discussion

The biggest challenge in orogenic gold prospectivity mapping in GIS was defining a unified and clear exploration model based on the genesis of the gold occurrences in the study area. Presences of different overlapping signs of mineralization were needed for converting a place to a high potential prospect. The other challenge was having only three known Au occurrences in the study area (Qolqoleh, Kervian and Ghabaghloujeh gold occurrences) which was a limitation for using an empirical (data-driven) integration method such as weight of evidence. On the other hand, the strength was having a variety of datasets especially high resolution airborne geophysical data. Nine evidence maps namely Au, As, Bi, Hg (Figure 2 and table 2), aeromagnetic lineaments (Figure 3b), K (Figure 5a), K/Th (figue 5b), lithologies (Figure 6a) and faults of the geological map (Figure 6b) were generated and assigned with crisp values. In this stage each on these layers were given a value based on their importance for orogenic gold exploration in the study area. Weight 10 was selected for geological structures, lineaments extracted from aeromagnetic data and Au factor maps, 9 was considered for K map, 8 was chosen for K/Th and geology factor maps and 7 was multiplied in the layers of As, Bi and Hg. After integration with index overlay, values 7 and 8 were considered as the first priority for orogenic Au mineralization in the prospectivity maps and values 6 and 5 were selected as second and third priorities respectively (Figure 7a and b). Area of the first, second and third priorities are 9.33, 68.82 and 271.48 km^2.

Au, As, Bi, Hg (Figure 2 and table 2), aeromagnetic lineaments (Figure 3b), K (Figure 5a), K/Th (Figure 5b), lithologies (Figure 6a) and faults of the geological map (Figure 6b) fuzzy memberships were produced using fuzzification techniques. For fuzzy modeling, fuzzy or operator was employed in order to combine similar fuzzy members: 1) elemental paragenesis As, Bi and Hg, 2) structures (Figure 6b) and lineaments (Figure 3b) and 3) K and K/Th ratio (Figure 5). Secondly, these layers were integrated with other fuzzy memberships which were produced in former stages such as geology and Au layers using gamma operator with gamma value of 0.8. Finally for defuzzification and prioritizing fuzzy logic mineral prospectivity map, Concentration-Area (C-A) multifractal model (after Cheng et al., 1994; Afzal et al., 2012) was applied on the pixel values of the generated map (Figure 8). Values greater than 0.6 were considered as the first priority, values 0.46 to 0.6 was considered as second priority and values 0.28 to 0.46 was regarded as the third priority (Figure 9). Area of the first, second and third priorities are 11.82, 52.13 and 227.62 km^2.

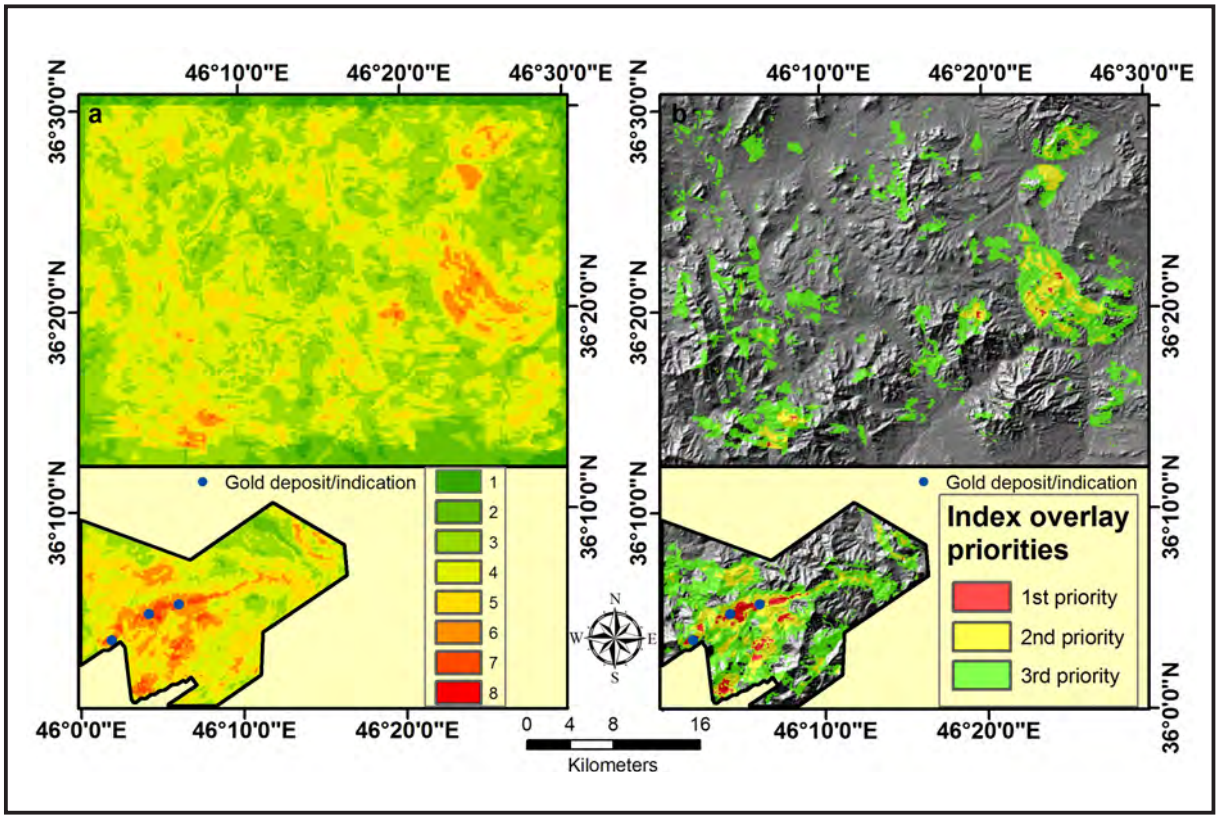

Figure 7- a) orogenic gold prospectivity map using index overlay, b) indicated priorities.

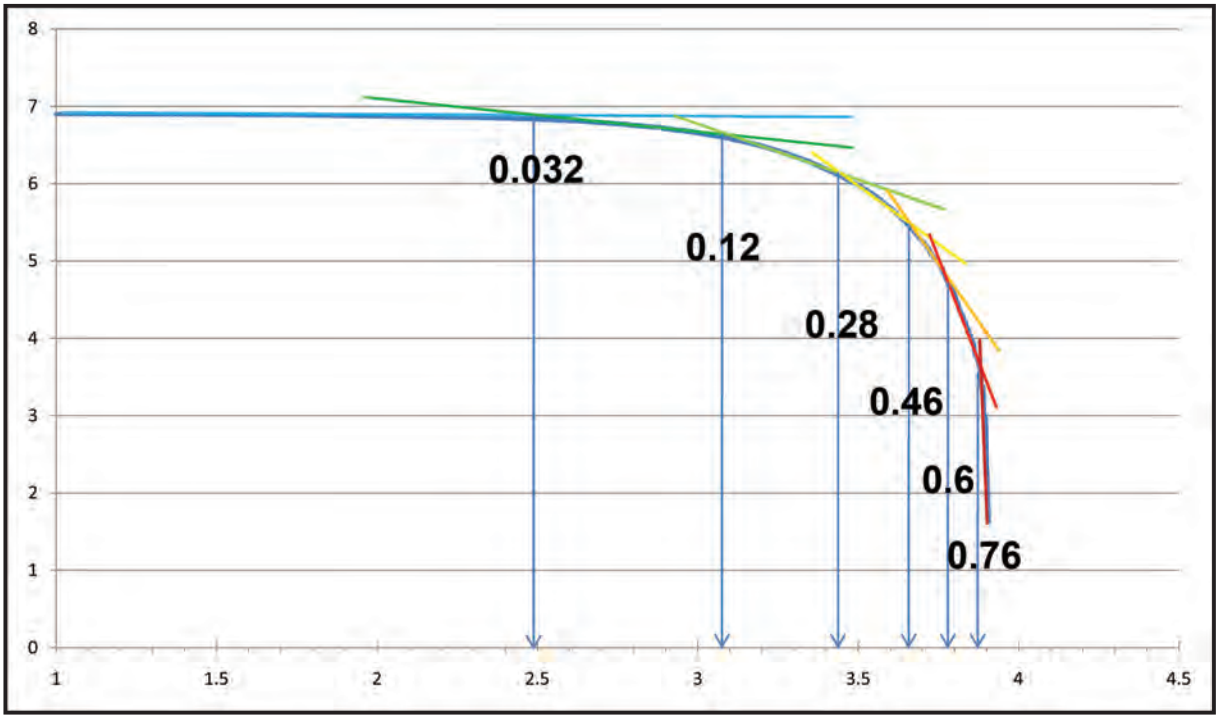

Figure 8- C-A log-log plot and the delineated thresholds for prioritizing fuzzy logic integration.

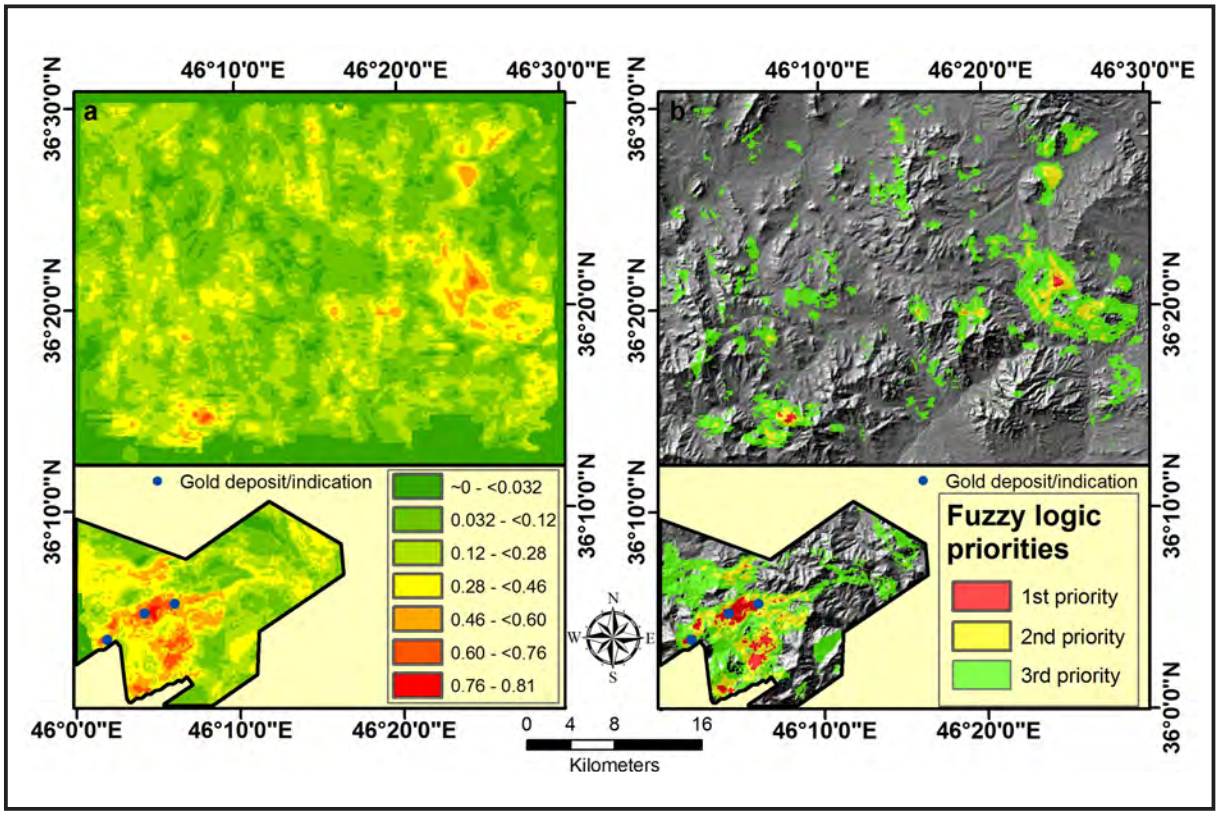

Figure 9- a) orogenic gold prospectivity map using fuzzy logic, b) indicated priorities.

6. Conclusion

Data integration using GIS resulted in the following main conclusions:

1) Comparing the areas of the first priorities in fuzzy logic and index overlay modeling (fuzzy: 11.82 km^2 > index overlay: 9.33 km^2) revealed that fuzzy logic model is more powerful for orogenic gold prospectivity mapping and it is less likely for fuzzy modeling to lose a high potential location.

2) In the mineral prospectivity map resulted from index overlay integration model (Figure 7), Qolqoleh and Kervian gold occurrences are located in the first priority but Ghabaghloujeh occurrence is placed in the second priority area, however in the prioritized orogenic gold prospectivity map of the fuzzy logic model (figure 9) all the three gold indications are located in the first priority zone, which is another score for fuzzy modeling.

3) Concentration-Area (C-A) multifractal model is an effective technique for defuzzification of the mineral prospectivity map resulted from fuzzy logic modeling.

4) Other first priority locations have been specified in the south and north of the Sardasht-Saqez zone and also in the east of the study area (Figure 9). These locations are suggested for more exploration and field checking.

5) Most important evidences for orogenic gold prospectivity mapping are faults and fractures and hydrothermal activity which can be exposed using airborne magnetic and radiometric data.

6) Au anomalies in the NW of the study area (Figure 2) and their absence in final potential maps can be construed as a sign for having other types of Au mineralization in the region.

Acknowledgement

Authors would like to acknowledge the guidance of Dr. Hassan Kheyrollahi in interpreting airborne geophysical data.

Received: 04.05.2014
Accepted: 28.08.2014
Published: June 2015

References

Afzal P., Zarifi A. Z., Khankandi S. F., Wetherelt A., Yasrebi A. B. 2012. Separation of uranium anomalies based on geophysical airborne analysis by using Concentration-Area (C-A) Fractal Model, Mahneshan 1:50000 Sheet, NW IRAN. *Journal of Mining and Metallurgy* 48 A (1), 1-11.

Airo M. L. 2001. Aeromagnetic and aeroradiometric response to hydrothermal alteration. *Surveys in Geophysics* 23, 273-302.

Airo M. L. 2007. Application of aerogeophysical data for gold exploration: implications for the central lapland greenstone belt. *Geological Survey of Finland, Special Paper* 44, 187-208.

Aliyari F., Rastad E., Zengqian H. 2007. Orogenic Gold Mineralization in the Qolqoleh Deposit, Northwestern Iran. *Resource Geology* 57(3), 269-282.

Aliyari F., Rastad E., Arehart G. B. 2009. Geology and geochemistry of D-O-C isotope systematics of the Qolqoleh Gold Deposit, Northwestern Iran; implications for ore genesis. *Ore Geology Reviews* 36, 306-314.

Aliyari F., Rastad E., Mohajjel M. 2012. Gold Deposits in the Sanandaj-Sirjan Zone: Orogenic Gold Deposits or Intrusion-Related Gold systems? *Resource Geology* 62(3), 296-315.

Almasi A., Jafarirad A., Kheyrollahi H., Rahimi M., Afzal P., 2014. Evaluation of structural and geological factors in orogenic gold type mineralisation in the Kervian area, north-west Iran, using airborne geophysical data. *Exploration Geophysics,* http://dx.doi.org/10.1071/EG13053.

Babakhani A. R., Hariri A., Farjandi F. 2003. Geological map of Saqez (1:100000 scale). *Geological Survey of Iran* (GSI).

Bierlein F. P., Murphy F. C., Weinberg R. F., Lees T. 2006. Distribution of orogenic gold deposits in relation to fault zones and gravity gradients: targeting tools applied to the Eastern Goldfields, Yilgarn Craton, Western Australia. *Mineralium Deposita* 41, 107-126.

Billa M., Cassard D., Lips A.L.W., Bouchot V., Tourliére B., Stein G., Guillou-Frottier L. 2004. Predicting gold-rich epithermal and porphyry systems in the central Andes with a continental-scale metallogenic GIS. *Ore Geology Reviews* 25(1-2), 39-67.

Bonham Carter G. F. 1994. Geographic Information Systems for Geoscientists – Modelling with GIS (Computer Methods in the Geosciences 13). Pergamon Press, New York.

Burrough P.A.,McDonnell R.A. 1998. Principles of geographical information systems. New York, *Oxford University Press*, 333 pp.

Carranza E.J.M. 2002. Geologically-constrained mineral potential mapping (examples from the Philippines), Ph.D. Thesis, Delft University of Technology, The Netherlands, ITC (International Institute for Geo-Information Science and Earth Observation) Publication No. 86, Enschede, 480 pp.

Carranza E. J. M. 2008. Geochemical anomaly and mineral prospectivity mapping in GIS. Handbook of Exploration and Environmental Geochemistry, Vol. 11. Elsevier, Amsterdam.

Carranza E. J. M., Hale M. 2001. Geologically-constrained fuzzy mapping of gold mineralization potential, Baguio district, Philippines. *Natural Resources Research* 10(2), 125-136.

Cheng Q. M., Agterberg F. P., Ballantyne S. B. 1994. The separation of geochemical anomalies from background by fractal methods. Journal of *Geochemical Exploration* 51, 109-130.

Chica-Olmo M., Abarca F., Rigol J.P. 2002. Development of a decision support system based on remote sensing and GIS techniques for gold-rich area identification in SE Spain. *International Journal of Remote Sensing* 23(22), 4801-4814.

De Souza Filho C. R., Nunes A. R., Leite E. P., Monteiro L. V. S., Xavier R. B. 2007. Spatial analysis of airborne geophysical data applied to geological mapping and mineral prospecting in the Serra Leste region, Caraja´s Mineral Province, Brazil. *Surveys in Geophysics* 28, 377-405.

Demicco R., Klir G. (Eds.) 2004. Fuzzy Logic in Geology, Elsevier, Amsterdam.

Deng J., Wang Q., Yang L., Wang Y., Gong Q., Liu H. 2010. Delineation and explanation of geochemical anomalies using fractal models in the Heqing area, Yunnan Province, China. *Journal of Geochemical Exploration* 105, 95-105.

Ferreira F., de Castro L., Bongiolo A., de Souza J., Romeiro M. 2011. Enhancement of the total horizontal gradient of magnetic anomalies using tilt derivatives: Part II — Application to real data. *SEG Technical Program Expanded Abstracts* 2011, 887-891.

Harris J.R., Wilkinson L., Heather K., Fumerton S., Bernier M.A., Ayer J., Dahn R. 2001. Application of GIS processing techniques for producing mineral prospectivity maps – a case study: mesothermal Au in the Swayze Greenstone Belt, Ontario, Canada. *Natural Resources Research* 10(2), 91-124.

Hashemi M., Afzal P. 2013. Identification of geochemical anomalies by using of number–size (N–S) fractal model in Bardaskan area, NE Iran. *Journal of Arabian Geosciences* 6, 4785-4794.

Henson P. A., Blewett R. S., Roy I. G., Miller J. McL., Czarnota K. 2010. 4D architecture and tectonic evolution of the Laverton region, eastern Yilgarn Craton, Western Australia. *Precambrian Research* 183, 338-355.

Heidari S. M. 2004. Mineralogy, geochemistry and fabrics of gold mineralization in the Kervian ductile shear

zone (southwest of Saqez). University of Tarbiat Modares, Tehran, Iran, M.Sc. thesis, 245 pp.

Heidari S. M., Rastad E., Mohajjel M., Shamsa M. J. 2006. Gold mineralization in ductile shear zone of Kervian (southwest of Saqez). Geosciences 58, 18-37.

Jafarirad A. R. 2009. Modeling of conceptual and Empirical Geospatial Datasets for Mineral Prospecting Mapping. TUC, Germany, PhD dissertation, 190 pp.

Jafarirad A. R., Busch W. 2011. Porphyry copper mineral prospectivity mapping using interval valued fuzzy sets topsis method in central Iran. *Journal of Geographic Information System* 3, 312-317.

Li L. 2013. Improved edge detection tools in the interpretation of potential field data. *Exploration Geophysics* 44, 128-132.

Luo X., Dimitrakopoulos R. 2003. Data-driven fuzzy analysis in quantitative mineral resource assessment. *Computers and Geosciences* 29, 3-13.

Magalhães L. A., Souza Filho C. R. 2012. Targeting of Gold Deposits in Amazonian Exploration Frontiers using Knowledge- and Data-Driven Spatial Modeling of Geophysical, Geochemical, and Geological Data. *Survey in Geophysics* 33, 211-241.

Mandelbrot B. B. 1983. The Fractal Geometry of Nature. Freeman, San Francisco.

Nykänen V., Groves D. I., Ojala V. J., Eilu P., Gardoll S. J. 2008. Reconnaissance-scale conceptual fuzzy-logic prospectivity modelling for iron oxide copper – gold deposits in the northern Fennoscandian Shield, Finland. *Australian Journal of Earth Sciences* 55(1), 25-38.

Ranjbar H., Honarmand M. 2004. Integration and analysis of airborne geophysical and ETM+ data for exploration of porphyry type deposits in the Central Iranian Volcanic Belt using fuzzy classification. *International Journal of Remote Sensing* 25(21), 4729-4741.

Rogge D.M., Halden N.M., Beaumont-Smith C. 2006. Application of data integration for shearhosted Au potential modelling: Lynn Lake Greenstone Belt, Northwestern Manitoba, Canada. In: J.R. Harris (Ed.), GIS for the Earth Sciences, *Geological Association of Canada Special Publication* 44, Geological Association of Canada, St. John's, pp. 191-210.

Silva A. M., Pires A. C. B., Mccafferty A., Moraes R. A. V., Xia H. 2003. Application of airborne geophysical data to mineral exploration in the uneven exposed terrains of the Rio Das Velhas greenstone belt. *Revista Brasileira de Geociências* 33, 17-28.

Silverman B. W. 1986. Density Estimation for Statistics and Data Analysis. Chapman and Hall, New York, 177 pp.

Tangestani M.H., Moore F. 2003. Mapping porphyry copper potential with a fuzzy model, northern Shahr-e-Babak, Iran. *Australian Journal of Earth Sciences* 50(3), 311-317.

Tajeddin H. 2011. Gold ore controlling factors in metamorphic rocks of Saqez-Sardasht, NW of Sananda-Sirjan metamorphic zone. Tarbiat Modarres University, Tehran, Iran, PhD dissertation, 436 pp.

Tsoukala L. H., Uhrig R. E. 1997. Fuzzy and Neural Approaches in Engineering. Wiley, New York.

Verduzco B., Fairhead J. D., Green C. M., MacKenzie C. 2004. New insights into magnetic derivatives for structural mapping. *The Leading Edge* 23(2), 116-119.

Zadeh L.A. 1965. Fuzzy sets. *IEEE Information and Control* 8(3), 338-353.

BULLETION OF THE MINERAL RESEARCH AND EXPLORATION

Foreign Edition 2015 150

CONTENTS

Bull. Min. Res. Exp. (2015) 150: 77-108

Bulletin of the
Mineral Research and Exploration

http://bulletin.mta.gov.tr

GEOLOGICAL FACTORS CONTROLLING POTENTIAL OF LIGNITE BEDS WITHIN THE DANIŞMEN FORMATION IN THE THRACE BASIN

Doğan PERİNÇEK[a*], Nurdan ATAŞ[a], Şeyma KARATUT[a] and Esra ERENSOY[a]

[a] *Çanakkale Onsekiz Mart Üniversitesi, Mühendislik Fakültesi, Jeoloji Mühendisliği Bölümü, Çanakkale*

Keywords:
Thrace Basin, Lignite,
Thrace Fault System

ABSTRACT

This project has been conducted for the General Directorate of Turkish Coal Enterprise. The aim of this study is to understand lignite potential of the basin. Subsurface data (including numerous wells and several seismic lines) provided by TPAO, MTA and TKİ were used. Structure and thickness maps of Oligocene-Miocene-Pliocene units prepared for the basin. Purpose of this work is to understand economical values of lignite seam beds interbedding in the Danişmen Formation (Oligocene-Early Miocene). For this purpose, from bottom to top following maps were prepared: Structural map of the top Osmancık (Oligocene) Formation, thickness map of the Danişmen Formation, paleo-topographic map of unconformity surface which is at the top of the Danişmen Formation, total thickness map of Ergene-Kırcasalih formations (Late Miocene-Pliocene). Finally total thickness map of the lignite layers was prepared. It was the main purpose of the work. Lignite seam layers are located in middle of the Danişmen Formation. Also several stratigraphic correlations were conducted to understand lateral continuation of lignite layers. The first obstacle to reach lignite is thickness of the Ergene and Kırcasalih formations which overlie lignite bearing Danişmen Formation. Main structural event controlling the thickness variation of the Danişmen Formation is Thrace Fault System (Perinçek, 1991); it was active during Middle Miocene. Danişmen Formation extensively or partially was eroded along the fault zone and on the en-echelon folds of the fault system. Amount of erosion is variable and in some areas Danişmen Formation completely was eroded. As a result Ergene Formation lies directly on Osmancık Formation. Lignite layers are also eroded at these localities. Elevated areas related the Thrace Fault System partially was eroded; however these areas were still paleo-elevated areas during the accumulation of Ergene Formation. Onlapping sequence of Ergene Formation is thinner on these areas. At the end of this project, thicker lignite areas were delineated. Addition to this, thin overburden areas on lignite are located. Considering these results, new permit areas were selected. In order to refine this work, a suggested facies map of Danişmen Formation is advise to be prepared.

1. Introduction

According to the agreement between Çanakkale Onsekiz Mart University and Turkish Coal Enterprise (TKİ) lignite potential of Thrace Basin was investigated. The project which lasted 1.5 years was started in mid 2009 and ended in December 2010. Underground geology data set necessary for the implementation of this project was provided by TKİ, TPAO and MTA. The data set includes shallow and deep well data, seismic sections and core samples from some wells. Permission to access the data was taken from TKİ at the beginning of study.

In the second half of the project, in order to reliably determine the locations of the wells to be drilled in the license area, seismic lines of Turkish Petroleum Corporation (TPAO) that were provided by TKİ were evaluated. Total lignite thickness map was compared to other thickness and structure maps that were produced in the first stage of project and thus data synergy and consistency were maintained

* *Corresponding author: Doğan Perinçek, perincek@yahoo.com*

and considering seismic assessment new license areas were proposed in the Thrace basin.

The Thrace basin is surrounded by Istranca at north, Rhodope at west and Menderes massif to the south. The Istranca massif is represented by gneissic rocks at the bottom and overlying Paleozoic and Mesozoic sedimentary rocks that were metamorphosed in greenschist facies (Üşümezsoy, 1982; Taner and Çağatay, 1983). The sedimentary rocks are cut by Late Cretaceous granodioritic rocks and locally covered by a volcano-sedimentary unit (Taner and Çağatay, 1983). Granitic rocks are exposed at southern flank of the Istranca massif (Öztunalı and Üşümezsoy 1979).

Intense geological research has been carried out in the Thrace basin to exploit oil and gas potential of the region. Studies of Kopp et al. (1969), Turgut et al. (1983, 1991), Saner (1985) and Siyako (2006 *a, b*) discuss the geology of basin. Geology maps prepared by the General Directorate of Mineral Research and Exploration are the most important sources for stratigraphical nomenclature of the Thrace basin (İmik, 1988; Umut, 1988a, Çağlayan and Yurtsever, 1998, Şentürk et al., 1998 *a, b*).

In central and northern Thrace, Miocene and post-Miocene units cover the Eocene-Oligocene sequence. Therefore, lithostratigraphic framework of the Thrace basin is established based on information from rock units exposing in southern Thrace, Gallipoli Peninsula, Bozcaada and Gökçeada and also seismic lines oil exploration wells. Eocene-Oligocene sequences of the Thrace basin crop out at south of the Sea of Marmara and Biga Peninsula (Siyako et al., 1989), in the area between Mudanya and Tirilye and Armutlu Peninsula (Akartuna, 1968) and therefore the southern border of the basin is not definite (Siyako, 2006 *b*).

The Thrace basin is a triangular shaped intermountain Tertiary basin in which Middle Eocene-Pliocene units are exposed (Keskin, 1974). In the basin sedimentation was probably started in the Early Eocene with a transgressive sequence (Keskin, 1974, Doust and Arıkan, 1974, Turgut et al., 1983, Saner, 1985). Ignoring discontinuities and erosion, sedimentation as continued until very recently. The basement of basin is comprised by a metamorphic complex. The Tertiary sequence that almost comprises the whole Thrace region exposing from southern flanks of the Istranca Mountains (Figure 1) has a thickness of more than 9000 m (Kopp et al., 1969; Turgut et al., 1983; Turgut et al., 1991; Perinçek, 1987; Görür and Okay, 1996; Turgut and Eseller, 2000; Siyako, 2005; 2006*a*; 2006*b*). Tertiary units in Thrace are composed mostly of clastics but contain carbonates in shelf areas and ridges and hills in the central basin. These units were deposited in seven different time intervals in basins characterized by significant uplift and erosion stages (Figures 1 and 2). In central parts of the basin, sedimentation is partly continuous whilst some parts come up with discontinuity and erosion stages. The

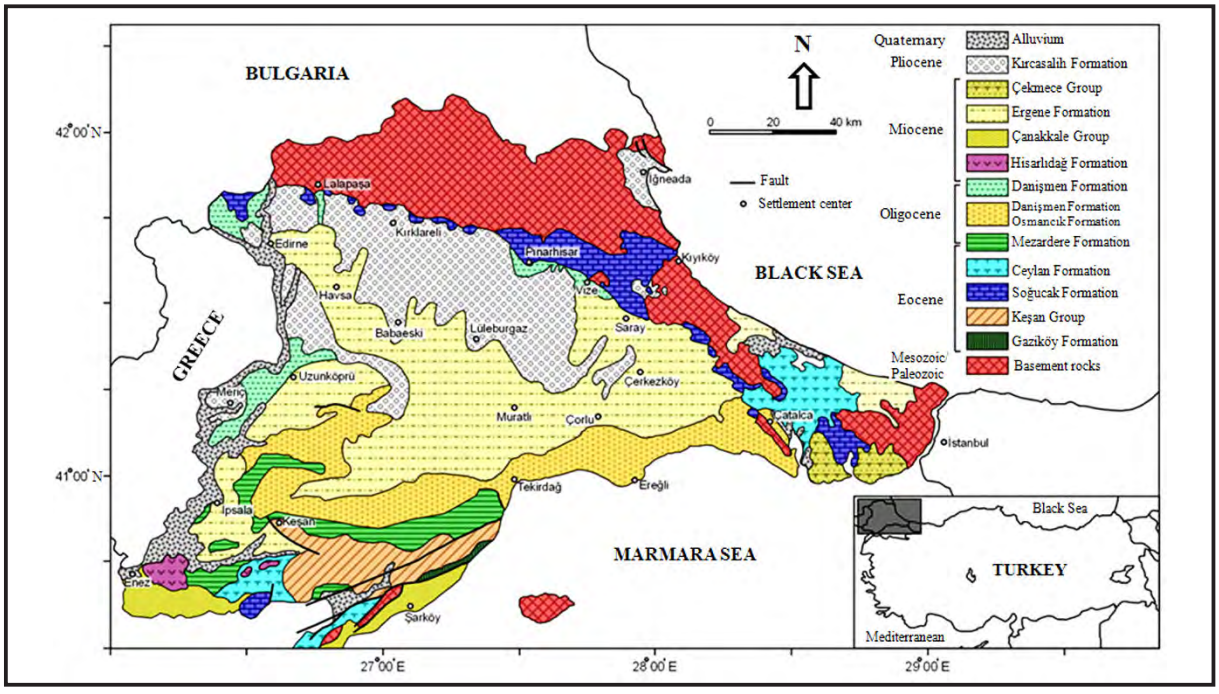

Figure 1- Geology map of Thrace basin (Kasar et al., 1983; Türkecan and Yurtsever, 2002; Siyako, 2006*b*).

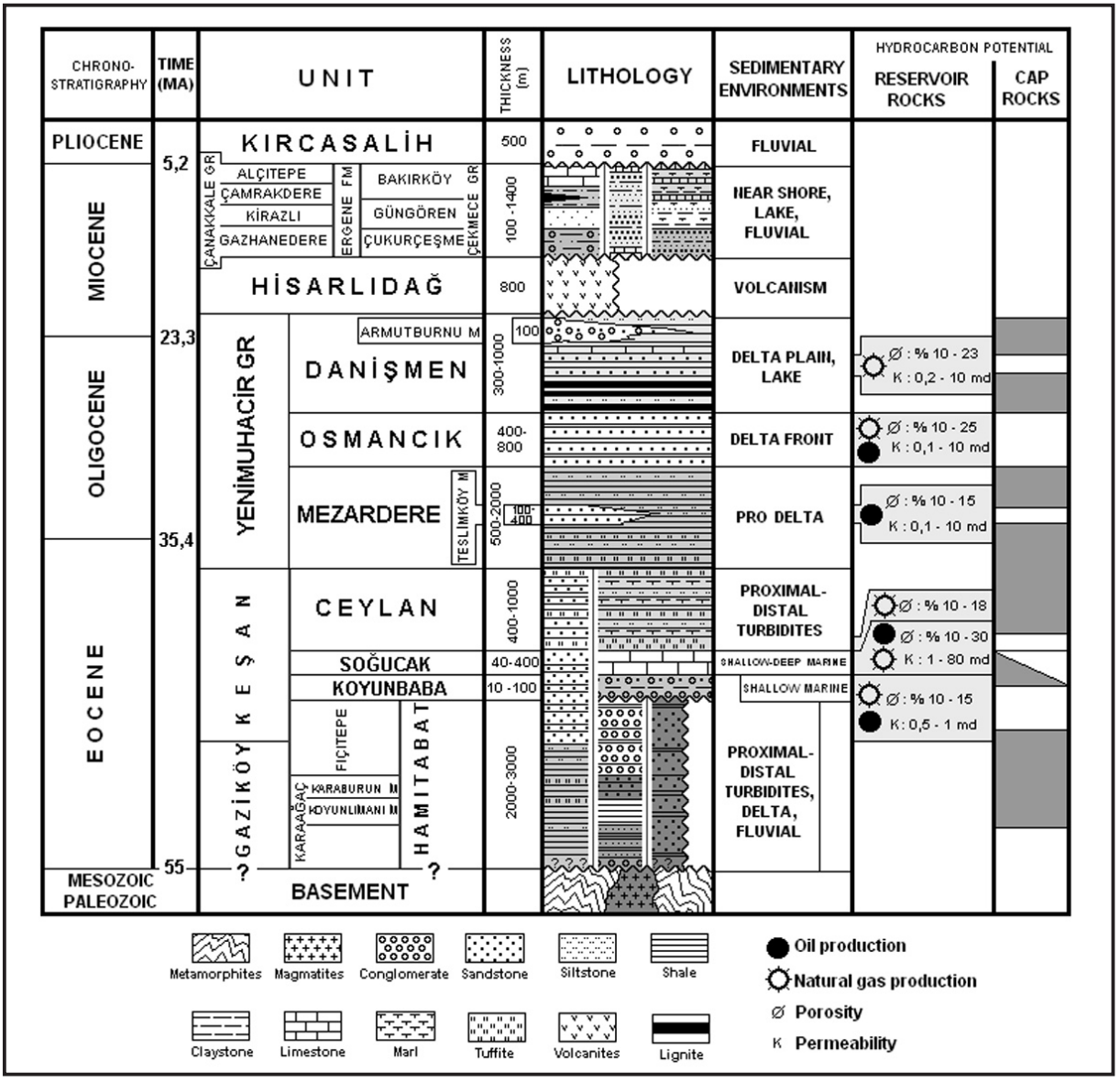

Figure 2- Generalized stratigraphic section of the Tertiary sequence in the Thrace basin (Siyako 2006*a*).

basin is a fast-depositing type and has a syntectonic character. As revealed from several seismic lines, the sequence which at the beginning filled pits of an irregular topography has transgressive onlaps above the basement toward the land (Burke and Uğurtaş, 1974; Perinçek, 1987).

The Eocene transgression attained maxima in the Early Oligocene. In the Middle Eocene-Early Oligocene, deep parts of the basin were filled by turbiditic currents that were carried by density flows whilst carbonates were deposited in shelf and Kuleli – Babaeski paleo-height at the north (Turgut et al., 1983; Keskin, 1974). In the meantime, the Thrace basin was controlled by a deltaic system of a large river and submarine fans were formed (Turgut et al., 1983). In the Late Eocene-Early Oligocene aged dacitic and andesitic ashes formed interlayers within the sediments (Doust and Arıkan, 1974; Turgut et al., 1983). Eocene transgression was followed by Middle Oligocene-Lower Miocene regression (Keskin, 1974; Ediger, 1982; 1988; Turgut et al., 1983; Saner, 1985). After a pause in sedimentation during the Middle Miocene, terrestrial palinofasies of the Ergene and Kırcasalih formations of Late Miocene ? – Early Pliocene age were deposited (Ediger, 1982). The pause in sedimentation was in the Middle Miocene and Late Miocene, Early Pliocene-Pleistocene aged fine grained terrestrial unit was the first product of new deposition period. There was also a less significant unconformity between Late Miocene and Pliocene.

Due to its lignite potential the basin has been the subject of intense geologic research (e.g. Lebküchner, 1974; Kara et al., 1996; Şengüler et al., 2000; Şengüler et al., 2003; Sütçü et al., 2009, Şengüler, 2008, 2013). Lignite fields in north of Thrace basin are generally found on flanks of the Istranca massif – İstanbul-Silivri-Sinekli; Tekirdağ-Saray-Küçük Yoncalı; Tekirdağ - Saray - Safaalan; Tekirdağ - Saray – Edirköy fields. Coal occurrences in south of the Thrace basin include Keşan, Malkara, Uzunköprü and Meriç fields. Lignites at north and south of the basin gradually deepen to the center of basin and attain a depth of 600 m within the 10.000 m-thickened sequence (Şengüler, 2013). Lebküchner (1974) studied regional geology and fossil assemblage and chronology of the formation so called ligniferous sandstone. Kara et al. (1996) studied general geology of the basin and provided information on important coal fields in the Thrace basin. Şengüler et al. (2000) studied coal samples collected from Keşan, Malkara and Uzunköprü coal fields. In these studies, they particularly investigated the operated veins and evaluated the deposition environment of coal. In a report prepared as 2 volumes by Şengüler (2008), distribution, properties and deposition model of Thrace coals and known field and enterprises are explained. Thrace basin coals were deposited in delta swamps of lacustrine environments. High deposition rate resulted in deposit thickness to be high which complicated the correlation of coal veins (Şengüler, 2013). During the formation of Danişmen Formation fluvial conditions were effective which hampered lignite deposition.

The North Anatolian Fault Zone (NAFZ), which is one of the important structural components comprising the general tectonic frame of Anatolia and Balkans has been active since Miocene and studied in detail by several earth scientists (Ketin, 1957; Fourquin, 1979; Barka, 1981; Barka and Hancock, 1984). The North Anatolian Fault Zone extends along the Cretaceous suture belt or cuts this belt a few times. The Thrace fault system which is the oldest branch of NAFZ in Thrace shows similar features to NAFZ. The Thrace fault system is composed of three fault members (Perinçek, 1987; 1991). The structural lines forming this fault system extends from Silivri to Edirne through the basin (Figure 1). The aim of this work is to 1) to determine the geometry of fault system, 2) evaluate the tectonic interrelations and origin, 3) to determine its age and 4) discuss slip rate of Thrace fault system. With the exception of last item, Perinçek (1987, 1991) has accomplished the objectives of all others.

Within the scope of project, following studies were implemented which are summarized below. These studies are composed of regional maps that are required to determine the lignite potential of Thrace basin. Information obtained by the virtue of these maps is useful not only for TKİ but also for TPAO and MTA. Results from this project are intended to contribute to studies of all relevant governmental organizations

As a result these studies, the maps produced are Osmancık Formation structure map, Danişmen Formation discordance plane paleo-topography map, thickness map for Danişmen and Ergene Formations and total thickness map of lignite levels within the Danişmen Formation. The reason for construction of thickness and structure maps mentioned above is to determine the economic depth of lignite levels and the areas where lignite has the maximum thickness. One of the obstacles encountered in lignite explorations in Thrace basin is that lignite occurs at a considerable depth under a thick cover.

In addition to maps, another important study is the correlations among the wells. These might significantly contribute to determining the lateral facies changes of Danişmen Formation and lateral thickness change of lignite layers. It is possible to see the vertical and horizontal facies changes in correlations. Even different lithology descriptions were made by different geologists in wells that are opened in close distances by TKİ and MTA which complicated the correlation. Therefore, it took a long time for data coupling.

Lignite exploration in Thrace was carried out in northeastern and south of basin where lignite levels are widely exposed. Using the outcomes of this study that was conducted for TKI a new exploration strategy was established. In this respect, new licenses are proposed for paleo-heights of the Thrace Fault System. The areas where the Danişmen Formation exposing around the paleo-height areas were partly eroded and where the overlying Ergene Formation is thinner are selected as target areas. This new strategy is one of the most important results of present study and no other exploration study was conducted using the proposed approach.

2. Stratigraphy

The simplified geology map and generalized stratigraphic columnar section of the Thrace basin are given figures 1 and 2, respectively. The relations of

Danişmen Formation to Osmancık Formation and to its members are shown in figure 3.

In the Thrace basin Paleocene-Pleistocene deposits are separated from each other with an angular unconformity (Siyako, 2006*b*). Paleocene-Lower Eocene deposits are exposed in a limited area in southwest Thrace and Gallipoli Peninsula and overlain by Middle Eocene limestone (Siyako, 2006*a, b*).

Early-Middle Eocene aged various terrestrial and marine units are in vertical and lateral transition (Figure 3) (Siyako, 2005; 2006*a*). In the Late Eocene Keşan Formation and overlying Ceylan Formation were deposited and both units, although there are some lithological differences, are composed of marine turbidites. Getting shallow depth of environment during Late Eocene-Early Oligocene the sequence so called Yenimuhacir Group (Figure 3) was deposited (Kasar et al., 1983; Saner, 1985; Sümengen and Terlemez, 1991; Atalık, 1992; Siyako, 2005, 2006*b*). In association with this system, the Mezardere, Osmancık and Danişmen formations were deposited until Early Miocene (Ünal, 1967; Kasar et al., 1983; Siyako, 2005; 2006*b*). At the end of this stage, the region was completely filled and uplifted and became a land and following an erosion stage deposition of Late Miocene-Pliocene units was started.

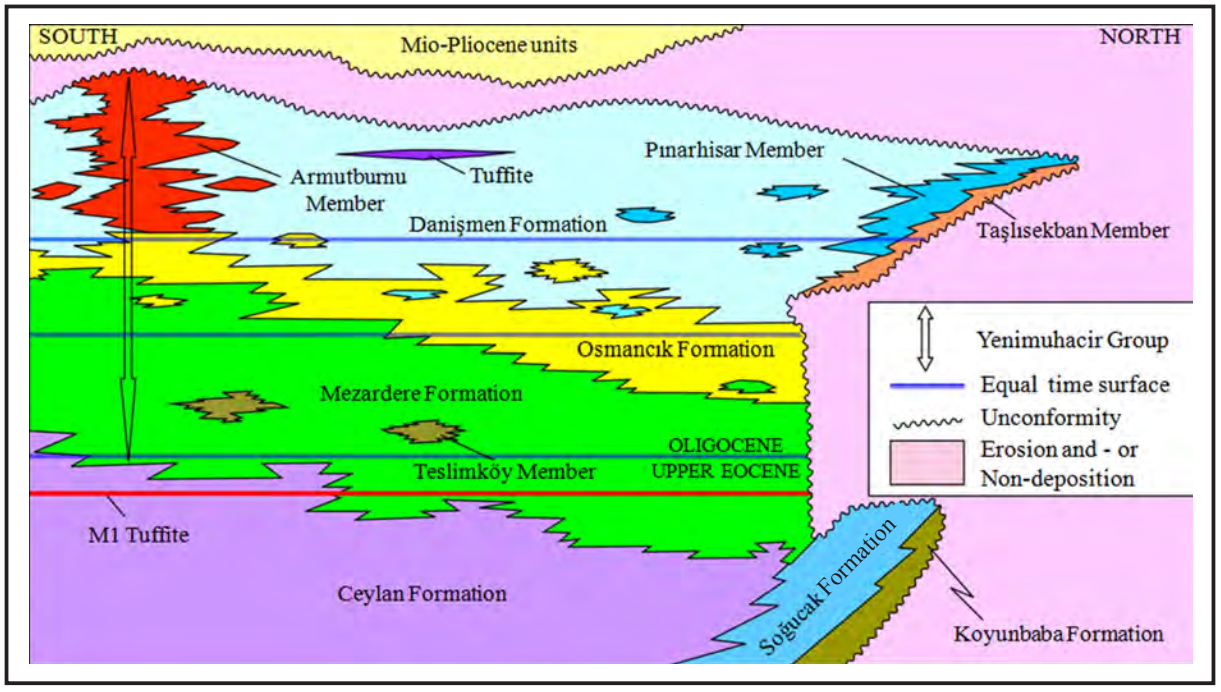

Figure 3- Correlation of Ceylan Formation and Yenimuhacir Group units. Taşlısekban, Pınarhisar and Armutburnu members were differentiated from bottom to top within the Danişmen formation (Siyako, 2006*b*).

During the Early-Middle Miocene, the volcanics of Hisarlıdağ formation with scarce sediment interlayers were formed in southwestern Thrace.

The Upper Miocene units are known as Çanakkale and Çekmece groups and Ergene Formation (Siyako, 2006*b*). The Karatepe Basalt is also of Miocene age. Pliocene is represented by the Kırcasalih Formation which is widely exposed particularly in northern Thrace (Siyako, 2006*b*). The Pleistocene units are investigated as Marmara Formation which is composed of marine terrace deposits around the Sea of Marmara.

2.1. Yenimuhacir Group

The name of Yenimuhacir was first used as a formation name. Later, Ünal (1967) studied the unit as a group in which four different formations were differentiated. In first studies conducted in the region the unit which was referred as "ligniferous sandstones" represents delta front and delta flat environments of the Yenimuhacir group (Siyako, 2006*b*). The Yenimuhacir group, from bottom to top, is composed of Mezardere, Osmancık and Danişmen formations (Figures 1 and 3). In its type section the thickness of Mezardere formation is 1540 m (Kasar et al., 1983). According to palynological studies, the age of formation is Late

Eocene-Early Oligocene which may be up to Late Oligocene within the basin fill (Ediger and Alişan, 1989; Batı et al., 1993; Batı et al., 2002).

The unit gradually passes to underlying Ceylan and Keşan formations. In paleohighs where underlying Ceylan formation is absent it is transitional to Soğucak Formation. In areas where Mezardere and Osmancık formations are absent, the Yenimuhacir group unconformably overlies the older lithologies (Figure 3). The unit is eroded and unconformably overlain by young units.

Formations comprising the Yenimuhacir group are formed in delta front, delta plain and prodelta of a classical delta system and interfinger to each other in lateral and vertical directions and therefore should be mapped separately. The Yenimuhacir group is composed of clastic rocks such as shale, siltstone, sandstone and conglomerate lithologies with coarser grain-size to the top. These clastics contain tuff, limestone and lignite interlayers. Tuffs can be differentiated as marker and traced in a long distance. Sandstone levels are also found within the unit and they can be mapped separately as the Teslimköy member (Figures 2 and 3) (Kasar et al., 1983).

Total thickness of the Yenimuhacir group is 3500 m. Based on palynomorph assemblage, it is of Late Eocene-Early Miocene age (Alişan, 1985; Gerhard and Alişan, 1987; Ediger and Alişan, 1989; Batı et al., 1993; Batı et al., 2002).

2.2. Stratigraphy of units below and above the Danişmen Formation

2.2.1. Osmancık Formation

The Osmancık formation is generally transitional to underlying Mezardere and overlying Danişmen formations. In many parts of the region the Osmancık and overlying Danişmen formations are unconformably overlain by Ergene and Kırcasalih formations. The Osmancık formation is a regressive unit that was deposited in a prograding delta front environment with grain size distribution getting coarser to the top. It is mostly composed of sandstone, shale and less amount of conglomerate, limestone and tuff levels. In the type section the Osmancık formation has a thickness of 810 m. Similar thicknesses were also observed in wells drilled in the Thrace region (Temel and Çiftçi, 2002). In palynological studies conducted on Osmancık formation yielded terrestrial and marine palynomorphs of Early-Late Oligocene age (Ediger and Alişan, 1989; Batı et al., 1993; Batı et al., 2002; Siyako, 2006*b*).

2.2.2. Danişmen Formation

Danişmen shale was first described in formation stage by Ünal (1967). Kasar et al. (1983) changed the name to Danişmen Formation since the lithology is not homogeneous. Taşlısekban and Pınarhisar members were differentiated at the base of unit whilst Armutburnu member occurs in lateral and vertical transition. The Danişmen Formation gradually changes to underlying Osmancık formation. In some areas the Danişmen Formation is significantly eroded and unconformably overlain by young units. The unit unconformably sets above the older units on the flanks of Istranca where Osmancık and Mezardere formations are absent. The Danişmen Formation is the upmost unit of regressive delta system and represents for delta flat facies. It is composed of lacustrine, swamp, flood plain and fluvial deposits. The unit consists of claystone, sandstone, conglomerate and coal layers (Figure 4). Fish fossils on exposures in northern Thrace and silicified woods in southern Thrace are very common. Tuff-tuffite and limestone levels are rarely observed. The underground thickness of Danişmen Formation is nearly 1000 m. Since units is eroded from the top, its original thickness might be more than that (Siyako, 2005; 2006*b*). Thickness decreases to the margins of basin. The unit was aged as Late Oligocene by Kasar and Eren (1986) and Batı et al. (2002) and Early Oligocene by Saraç (1987). In some other works it is suggested to be Late Oligocene-Early Miocene in age (Alişan, 1985; Gerhard and Alişan, 1987; Batı et al., 1993). Vertebrate faunas are very common in lignite veins of the Danişmen Formation. According to descriptions on vertebrate fossil, the age of formation corresponds to Middle Oligocene (Umut et al., 1983; 1984).

The base of lignite levels in lower part of the Danişmen Formation observed in drilling works is explained as the contact between Danişmen and Osmancık Formations (Siyako, 2005; 2006*b*). In unpublished geology maps of TPAO that cover only a small area, Osmancık and Danişmen formations were partly differentiated on lignite-bearing sandstones (Bürkan, 1992).

Taşlısekban, Pınarhisar and Aramutburnu members were differentiated within the Danişmen formation. In areas where Danişmen formation is exposed lignite layers in this formation are exploited as open and underground pits.

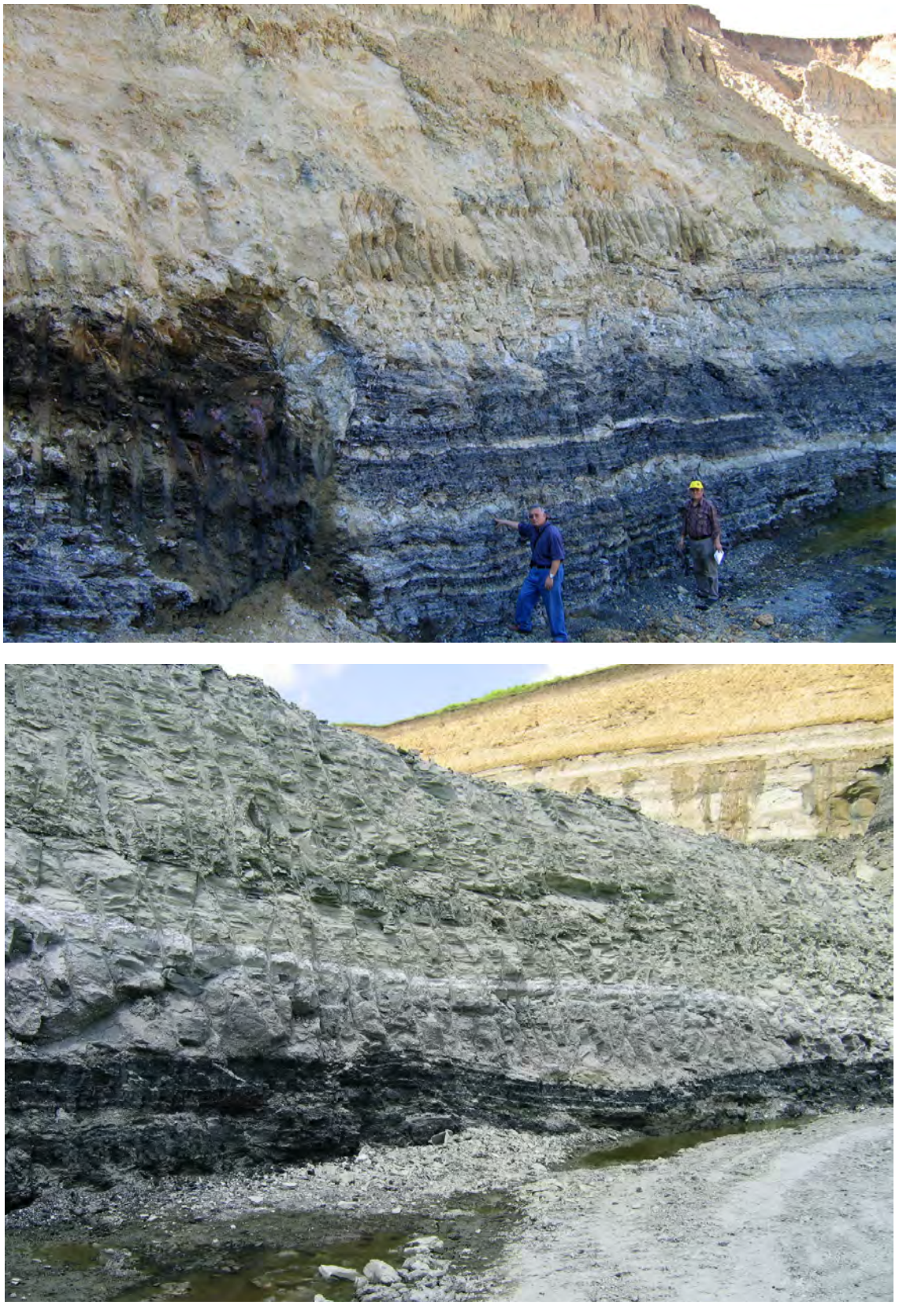

Figure 4a and b- Lignite layers within the Danişmen Formation are alternated with marls and locally covered with sandstone layers.

Taşlısekban Member: The unit was first named by Kasar (1987). The unit unconformably overlies the older units. It is transitional to overlying Pınarhisar member. The Taşlısekban member is composed of conglomerate, sandstone and marl. Claystone and lamellibranchia agglomerations are rare. Exposures in Çatalca start with a coarse grained slope wash facies derived from the basement and Soğucak Formation (Çağlayan and Yurtsever, 1998). The Taşlısekban member comprises the basal conglomerates of Pınarhisar member limestones. Thickness of Taşlısekban member is maximum 30 m. According to its stratigraphic setting the age of unit might be Oligocene.

Pınarhisar Member: It is gradually transitional to Taşlısekban member at the bottom and claystone and shale levels of the Danişmen formation to the top. The Pınarhisar member is represented by partly clayey shallow-marine, lagoon limestones with manganeferous levels at the upper parts (Siyako and Kasar, 1985). Limestones also contain sandstone and conglomerate interlayers together with oolite, abundant lamellibranches, gastropod and ostracode. In the type section, thickness was measured as 70-80 m and average thickness ranges from 5 to 20 m. The age of unit is reported as Early Oligocene (Gökçen, 1971; Kasar and Eren, 1986) and Oligocene (Umut et al., 1983; 1984).

Armutburnu Member: On its type section, the Armutburnu member is in lateral and vertical transition to both Osmancık and Danişmen Formations (Figure 3). It is overlain by young deposits with an angular unconformity. The member is represented by red colored, thick bedded-massif channel fill conglomerate and sandstone that were deposited in a delta flat. It is composed rarely of flood plain mudstone and sparsely of coal levels. Its thickness is about 100 m (Temel and Çiftçi, 2002). The age of Armutburnu member is reported as Late Oligocene in Gallipoli (Temel and Çiftçi, 2002) and Oligocene in western Thrace (Umut et al., 1984). Considering the Miocene age suggested by N.V.Turkse Shell (1969), Oligo-Miocene age is accepted for the unit (Siyako, 2006*b*).

2.2.3. Ergene Formation

Miocene deposits at north of Ganosdağ-Korudağ-Hisarlıdağ paleo-height are included to Ergene Formation. Çelebi and Sinanlı members were differentiated within the unit. Kasar et al. (1983), Turgut et al. (1983) and Perinçek (1991) examined the Ergene and Kırcasalih Formations under Ergene Group.

The unit is unconformable with older units and overlying Kırcasalih Formation. The unit is composed of cross bedded conglomerates and sandstones of fluvial and lacustrine environment and sandstone and claystone lithologies with abundant plant and vertebrate fossils (Duman et al., 2004; Siyako, 2006*b*). Thickness of formation is 0-60 m in basin margins and 800-1200 m at the center of basin (Siyako, 2006*b*; Perinçek 2010*a, b, c*). According to Perinçek (1987) the Ergene Group (together with Ergene and Kırcasalih Formations) is of Late Miocene-Pliocene age. The age of Ergene Formation is given as Middle-Late Miocene by Umut et al. (1983), Çağlayan and Yurtsever (1998) and Duman et al. (2004) and Late Miocene by Umut (1988*b*) and İmik (1988). The unit is exposed in a large area in central part of Thrace.

Çelebi Member: The Çelebi member has an angular unconformity with Armutburnu member of underlying Danişmen Formation (Umut et al., 1984). The clastics of Çelebi member comprising the basement of Ergene Formation are in vertical and lateral transition to this formation (İmik, 1988). At south of Uzunköprü the unit is composed of white, gray, greenish lacustrine limestones. Horizontal, thin-medium bedded limestone layers are interbedded with rare clay and sandstone (Umut et al., 1984; Umut, 1988*a*; İmik, 1988). Thickness of unit is about 40 m. The age of Çelebi member is accepted Middle-Late Miocene like Ergene Formation which is in vertical and lateral transition to this member (Siyako, 2006b).

Sinanlı Member: The unit conformably covers the Ergene Formation and is also in lateral transition to this formation. It is unconformably overlain by Kırcasalih Formation (Umut et al., 1983). The Sinanlı member was deposited in a fluvial-lacustrine environment. It starts with nodular limestone level and continues to the top with massive, partly clayey sandstone and claystone interlayered limestone level (Umut et al., 1983; Çağlayan and Yurtsever, 1998). Thickness of Sinanlı member is 10-40 m. The age of Sinanlı member is Middle-Late Miocene like Ergene Formation which is in vertical and lateral transition to this member.

2.2.4. Karatepe Basalt

It was first named as a formation by Umut et al. (1983). It is found in lower levels of the Ergene Formation and within the clastics of the Ergene Formation (Siyako, 2006*b*). The Karatepe Basalt is composed of black olivine basalts. Basalts are generally as lava flow and show columnar structure. According to Siyako (2006*b*) they are Late Miocene in age. Volcanic activity of Karatepe Basalt is suggested to be associated with Thrace Fault System (Perinçek 2010*b, c*).

2.2.5. Kırcasalih (Thrace) Formation

The name of Kırcasalih Formation was first used by Ünal (1967). Umut et al. (1984), Umut (1988*a, b*), İmik (1988) and Çağlayan and Yurtsever (1998) described the unit as Thrace Formation.

The Kırcasalih Formation unconformably sets above almost all older units in Thrace (İmik, 1988; Siyako 2006*b*). It is overlain by Quaternary deposits. The formation is composed of uncompacted pebble, coarse grained conglomerate, sandstone and rare claystone. Pebbles generally consist of quartz, quartzite, rarely schist, metagranite and volcanite rock fragments. The unit was deposited in a fluvial environment. Based on seismic sections and well data, thickness of unit is 500 m (Siyako, 2006*b*). Considering its stratigraphic setting, the age of Kırcasalih Formation is Late Miocene-Pliocene (Çağlayan and Yurtsever, 1998) however, Pliocene age is more appropriate.

3. Structural Geology

It is known that structural lines that are described as Thrace fault system by Perinçek (1987, 1991) are right-lateral strike slip fault which were formed before the deposition of Ergene Formation. According to seismic data evaluation by Perinçek (1991), North Anatolian Fault in the Thrace basin was active before the Late Miocene. This fault was called from southeast to northwest as Kırklareli, Babaeski and Lüleburgaz Fault Zone (Figure 5). This fault system was active at the beginning of Late Miocene following the deposition of Danişmen Formation but before the deposition of Ergene Formation and en echelon structures were formed in association with this strike-slip fault system. Significant erosion was occurred along axes of these structures and particularly in the fault zones. Due to this erosion, in some parts of the basin Danişmen Formation was partly or completely eroded (Perinçek, 2010*a, b, c*; Perinçek et al., 2011). Ergene Formation that was

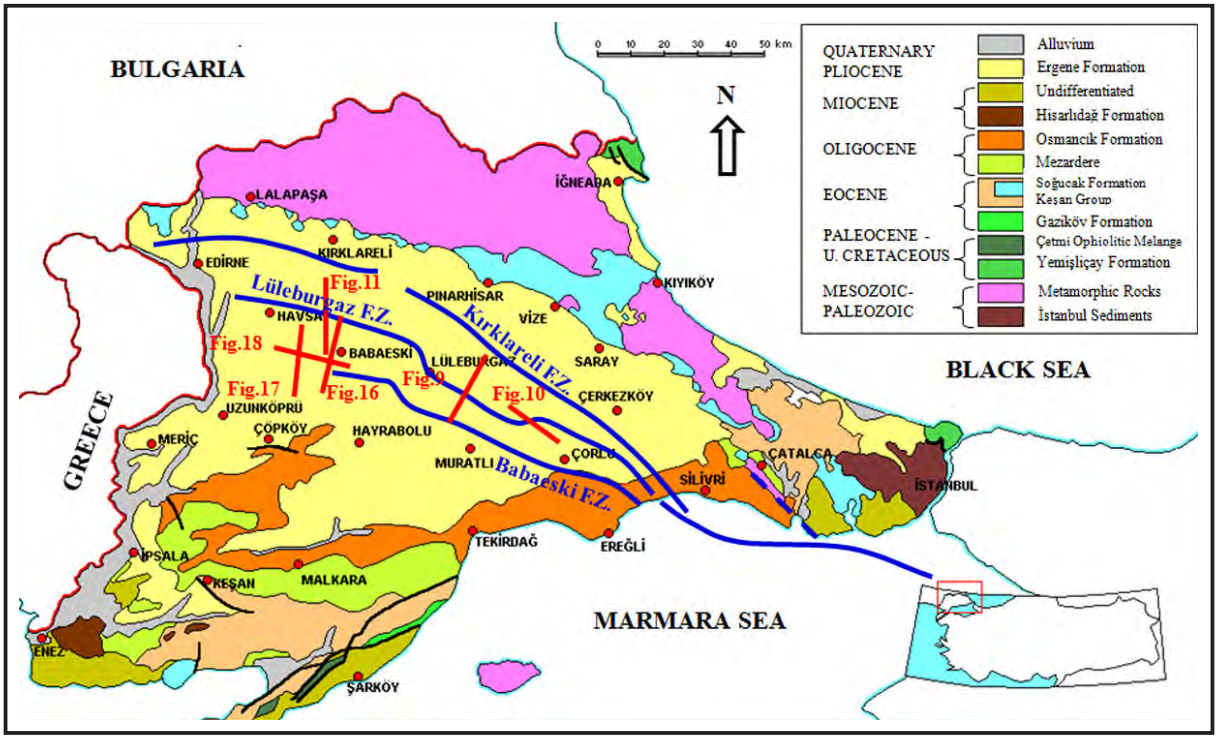

Figure 5 – Geology map of Thrace basin and Thrace fault zones (geology map: Kasar et al. (1983), fault lines: Perinçek, 1991; Perinçek, 2006). The Thrace fault system is buried under Late Miocene-Pliocene sequence (yellow colored in the map).

deposited following the erosion (Hamitabat field) directly sets above the Osmancık Formation in some areas. In addition to erosion of Danişmen Formation in paleo-heights that were developed as a result of faulting, the Ergene Formation was deposited as thinner since these areas preserved their structural heights. The Ergene Formation is thick in synclines in depression areas. The activity of such faults was continued after the deposition of Ergene Formation (Perinçek, 1991 and 2006; Perinçek and Karslıoğlu, 2007) and in some areas at east of basin discordance plane at the base of Ergene Formation was folded as a result of compression caused by the fault activity (Perinçek, 1987 and 1991).

4. The purpose and assessment of structure and thickness maps and their contribution to the project

To understand the lignite potential of Danişmen Formation thickness and structure maps were formed. These maps are Osmancık Formation structure map (Figure 6), elevation map (paleo-topography) of discordance plane above the Danişmen Formation (Figure 7), thickness map of Danişmen Formation (Figure 8), total thickness map of lignite levels within the Danişmen Formation and thickness map of Ergene Formation. Each of these maps was considered regarding lignite potential under investigation.

4.1. Structure map of the Osmancık Formation

Structure map of the Osmancık Formation is important to show the proximity of upper contact of unit to the surface. Just above this unit is Danişmen Formation and therefore the extent of lower contact of this formation could only be known from this map. Using well data from TPAO structure map of the Osmancık Formation was prepared (Perinçek, 2010*b, c*) (Figure 6). Red, orange and yellow colors on the map represent high lands, green and blue colors represent low-elevated areas and purple and pinkish colors stand for structural depressions (Figure 6). The most striking feature in the structure map of the Osmancık Formation is a SE extending paleo-height from Edirne to Akbaş, Haznedar, Mesutlua and Bayırtarla direction (Figure 6). This paleo-height partially disappears in SE direction but reappears around the Vakıflar well and continues ambiguously toward SE. Among the fault zones that are mapped as a continuation of NAFZ in Thrace region, the Lüleburgaz fault zone at the center has strike of WNW-ESE (Figures 5, 9, 10 and 11). It is shown in the structure map of the Osmancık Formation that (Figure 6) the long axis strike of this structural height matches with the orientation of Lüleburgaz fault zone (Perinçek, 2010*a, b, c*).

As a result, structural height is closely associated with fault system that cuts throughout the region. This map of regional scale clearly shows the relation between fault system and structural height. It is suggested that structural heights of Osmancık Formation should be considered for the lignite exploration. The Osmancık Formation is just below the Danişmen Formation and these two units are concordant. Therefore in high-elevated parts of the structure map of Osmancık Formation, lignite levels within the Danişmen Formation are expected to be encountered at shallow depths. Such structural heights are possibly achieved at 0 to 700 m whilst structural depressions are found at depths of 2000-2700 m. Lignite exploration works can be conducted in areas represented by yellow, orange, brown and red colors in figure 6. In other areas (green, blue, violet, and purple) the exploring of lignite layers at economic depths is quite limited.

4.2. Map of discordance surface (paleotopography) above the Danişmen Formation

Discordance plane above the Danişmen Formation was also mapped. This map may also be regarded as a paleotopography map. In the paleotopography map since discordance plane indicates areas of high elevation this map could also be useful tool for lignite exploration. Osmancık and Danişmen Formations are concordant and gradually transitional. Upper contact of Danişmen Formation is discordant and in some areas it is significantly eroded. Therefore structural maps of Osmancık (Figure 6) and Danişmen (Figure 7) formations are not the same **(**Perinçek, 2010*a, b, c*) because following the deposition of Danişmen Formation some parts of the basin are uplifted as a result of faulting and Danişmen Formation was eroded in these paleo-heights. As the amount of erosion increased in the Danişmen Formation the difference between the two structure maps becomes more distinct. In areas of limited erosion, for example at southeast of Edirne, the strike of anticline axis in structure map of Osmancık Formation is similar to that of Danişmen Formation. This similarity is also shown not in shapes but in strikes of synclines on both maps. In the area where erosion is intense and Havsa-1 and Minnetler-1 wells drilled by TPAO (Figure 7) are located, there is a significant difference between the two maps.

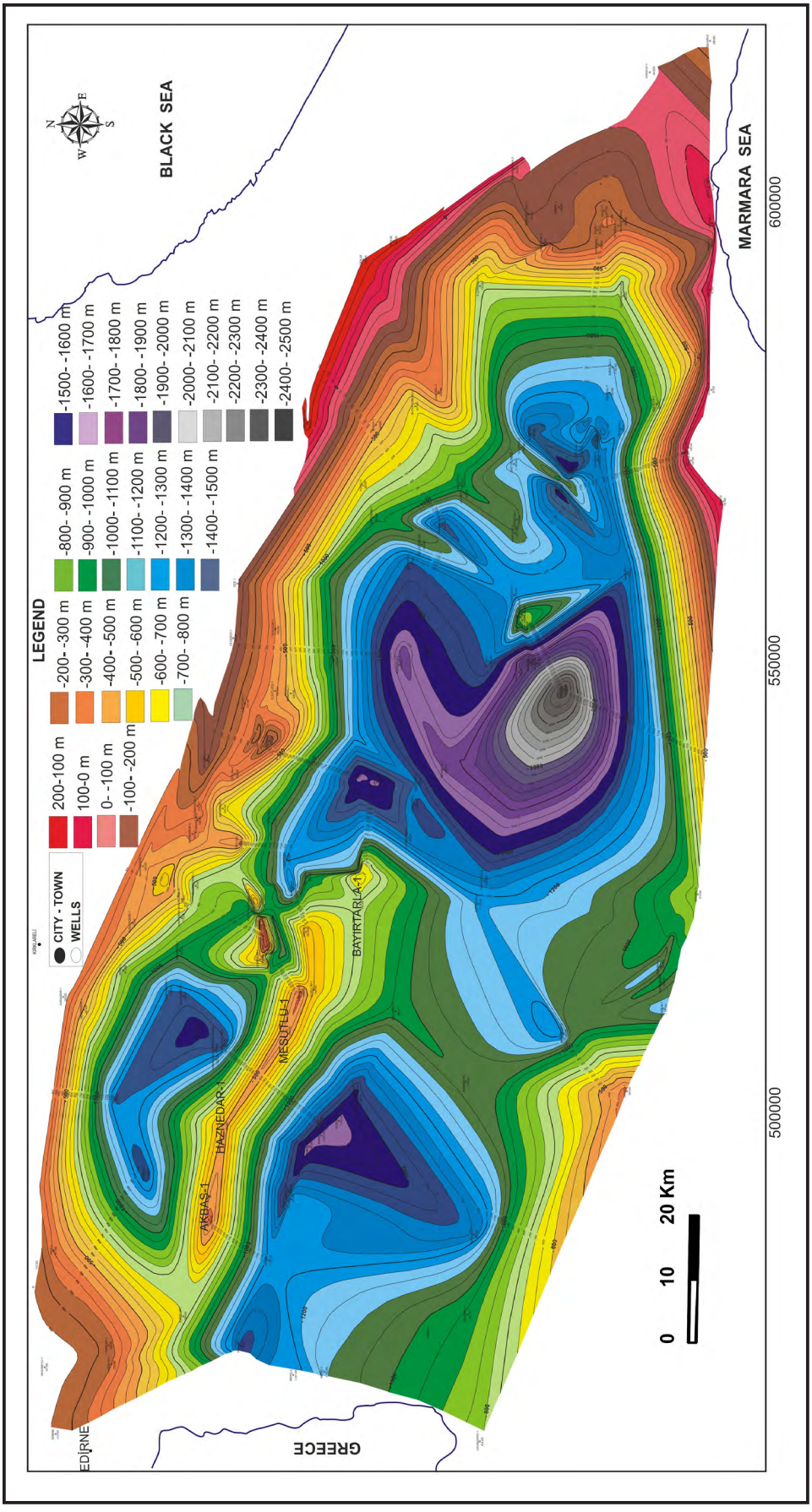

Figure 6- Structure map of the Osmancık Formation (Perinçek, 2010*b*, *c*).

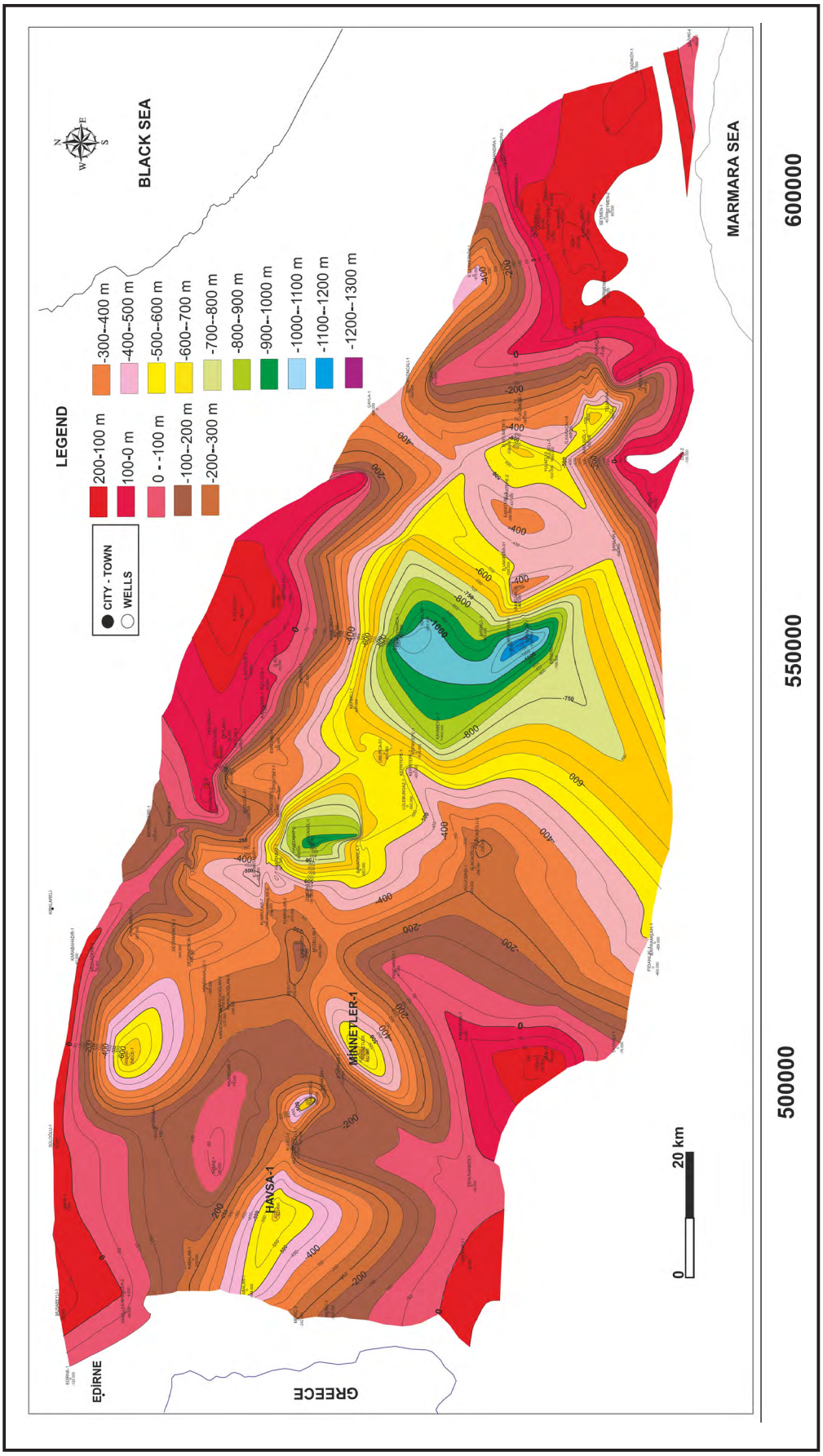

Figure 7– Discordance plane paleotopography map of Danişmen Formation (Perinçek, 2010*b*, *c*).

4.3. Thickness map of Danişmen Formation

Thickness distribution of Danişmen Formation in the basin is very important for lignite exploration. From this viewpoint, using the well data of TPAO thickness distribution of Danişmen Formation was made for the whole basin (Perinçek, 2010a, b, c) (Figure 8). This map shows the importance of erosion after the formation of Thrace fault system. Along the fault zone and in areas uplifted by the fault thickness of Danişmen Formation is lowered to 0 meter and in some areas it ranges from 0 to 300 m. Maximum thickness of Danişmen Formation is 1600 m. Purple, violet and blue fields in Figure 8 show areas where the formation is very thin or thin. Yellow and green areas stand for moderate thickness. Brown and red areas indicate the areas where the formation is the thickest. On this map the area where the unit extends from Edirne towards SE is quite distinct. The long axis strike of this area coincides with that of Lüleburgaz fault zone. Moreover, another area where Danişmen Formation is thin at south of Pınarhisar in northern margin of the basin, overlaps with Kırklareli fault zone (Figure 8). Uplift along the fault zone and subsequent erosion are the main reasons for thinning of Danişmen Formation. This erosion partly or completely removed the Danişmen Formation. Since lignite levels in this formation are also eroded lignite exploration should not be made in such erosional eras. In Kocagöl 1, İncibayır 1, Kumrular fields and in some parts of the Hamitabat field (Figure 8) thickness of Danişmen Formation is lowered to 0-100 m as a result of erosion activity. In figure 8, a small area is apparent at the center of region where the unit at southern and northern parts of the basin is very thick. The other thick section at north is between Kırklareli and Lüleburgaz fault zones. Danişmen Formation is also thick at south of Lüleburgaz fault zone. Its thickness at south is believed to be controlled by other factors rather than the fault zone. In this area Thrace basin is the deepest.

Thickness map of Danişmen Formation ends up with following results for the lignite exploration policy:

1. In paleo-heights of Thrace fault system, the Danişmen Formation was uplifted following the formation of fault system and then eroded. The NW-SE extending study area (green, blue, dark blue areas) at the center of map in figure 8 is related to abovementioned erosion. The area where Danişmen Formation along the northeast side of the map has a less thickness represents northeast margin of the Thrace basin. At present uplift formed by the Istranca Mountains on northeast of Thrace basin was land during the Eocene-Oligocene time. Just southwest of this land Osmancık fault separates a shallow shelf from deeper part of the basin. While Eocene-Oligocene units were deposited in the basin, the Osmancık fault was active, at the and of middle Miocene as a result of activation of NAFZ. Osmancık fault reactivated again. Osmancık fault significantly overlaps with Kırklareli fault zone. The reason for the absence or thinning of Danişmen Formation at northeast of Thrace basin (Figure 8) is that when this unit was depositing the area was a part of basin margin or it was a shore. In southern part of map in figure 8 Danişmen Formation gets thinner due to a structural reason. Although this area between Silivri and Tekirdağ along the coast of Sea of Marmara corresponds to deeper part of Thrace basin, Danişmen Formation gets thinner southward. This can be attributed to structural paleo-height caused by NAFZ during Late Miocene-Pliocene. As a result of this uplift, the area between Silivri and Tekirdağ was uplifted where Danişmen Formation was completely and Osmancık Formation was partly eroded. Seismic sections for this area clearly show uplift and associated erosion.

2. As a result of uplift caused by the Thrace fault system upper and middle parts or the whole Danişmen Formation were eroded. While NAFZ was active during Middle Miocene in Thrace basin, en echelon structures were formed oblique to the fault zone. The Hamitabat gas field is the best example for this (Figure 8). In some wells in this field Danişmen Formation was completely eroded, and therefore lignite layers are absent in this area. Structural factors associated with NAFZ are responsible for this erosion. Lignite layers within the formation are found in middle part of the sequence and just above this part. Therefore the degree of erosion should be evaluated carefully. Particularly at the center and southern margin of Thrace basin erosion is very intense. In these areas if thickness of Danişmen Formation is 0 to 400 m, lignite levels may have been completely eroded. Along the NE margin of Thrace basin the unit is quite thin but thinning is not related to erosion. In this area, although Danişmen Formation is thin economic lignite levels may be found in suitable facies.

3. In figure 8 in yellow, orange, red, brown and maroon colored areas Danişmen Formation has thickness of 700 to 1700 m. If thickness of Ergene Formation above the Danişmen Formation and thickness of lignite-free level in upper part of Danişmen Formation are added to each other, it becomes difficult to find lignite levels at economic depths. For this reason, thickness distribution of

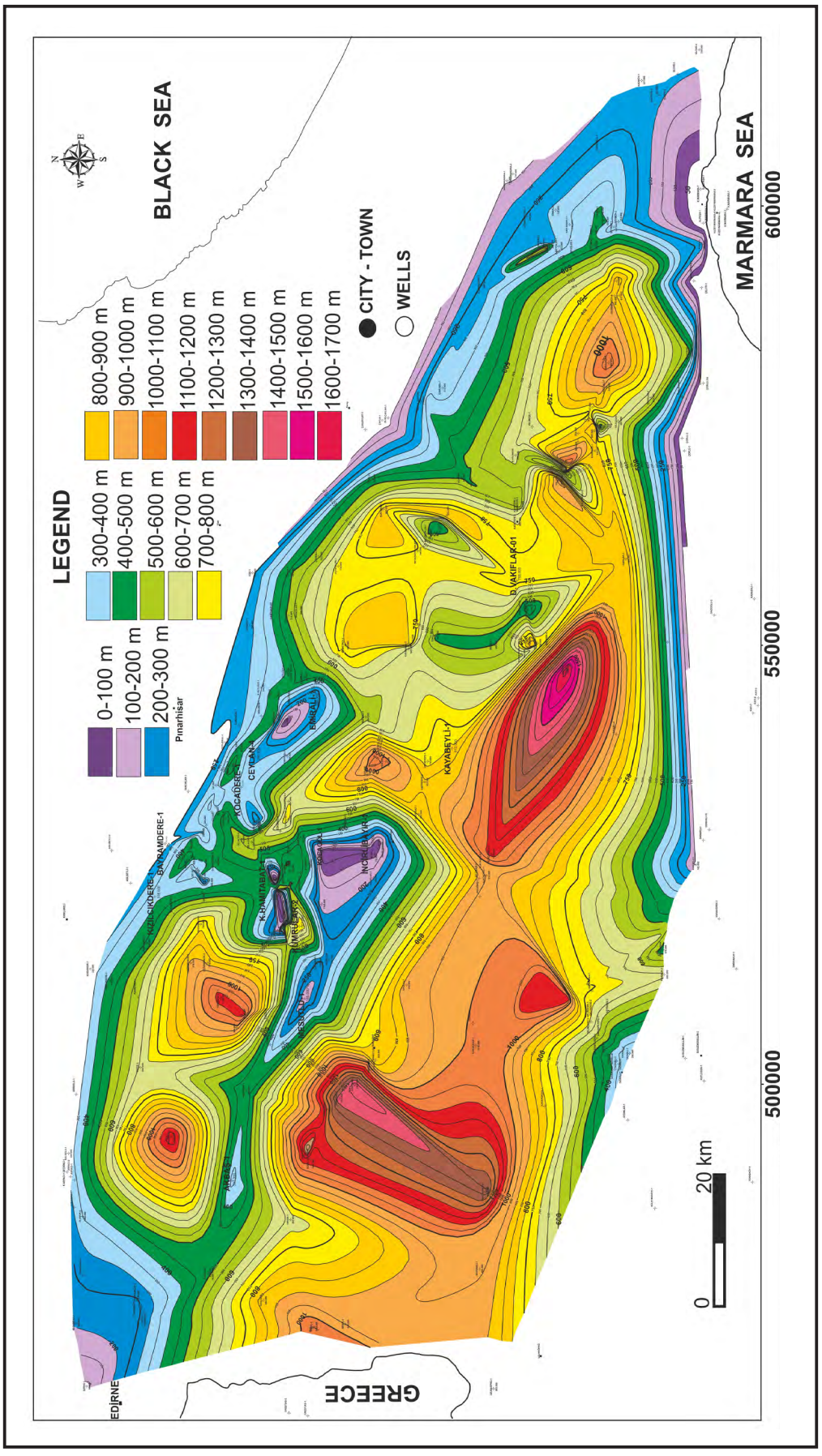

Figure 8– Thickness map of Danişmen Formation (Perinçek, 2010*b*, *c*).

Danişmen Formation should be carefully reviewed. In central and southern part of the basin, it must be stayed away from areas where unit is thinner than 400 m and thicker than 1000 m. This finding should be considered for lignite explorations works to be conducted in the coming years.

4. In thickness of map of Danişmen Formation in figure 8, this formation is thinner along the Akbaş 1-Mesutlu 1-İncilibayır 1 line due to Lüleburgaz fault zone traversing this area (Figure 5). In structure map of Osmancık formation around the same line (Figure 6) it is also observed as paleo-height. Continuation of the same fault zone extends around the Kayabeyli-1 and Vakıflar wells in eastern half of the map (Figure 8) and erosion effect arising from paleo-height by the fault system is apparent. Around Vakıflar Danişmen Formation is thin and as a result of erosion in this area lignite layers are completely removed. In this area NW-SE extending linearity was formed by the Lüleburgaz fault zone and its orientation is nearly the same as this fault zone. Along this fault zone a number of 3 seismic lines (Figures 9, 10 and 11) were reviewed which showed the importance of erosion. Considering the results of these seismic sections, it is favorable to have a lignite exploration license around

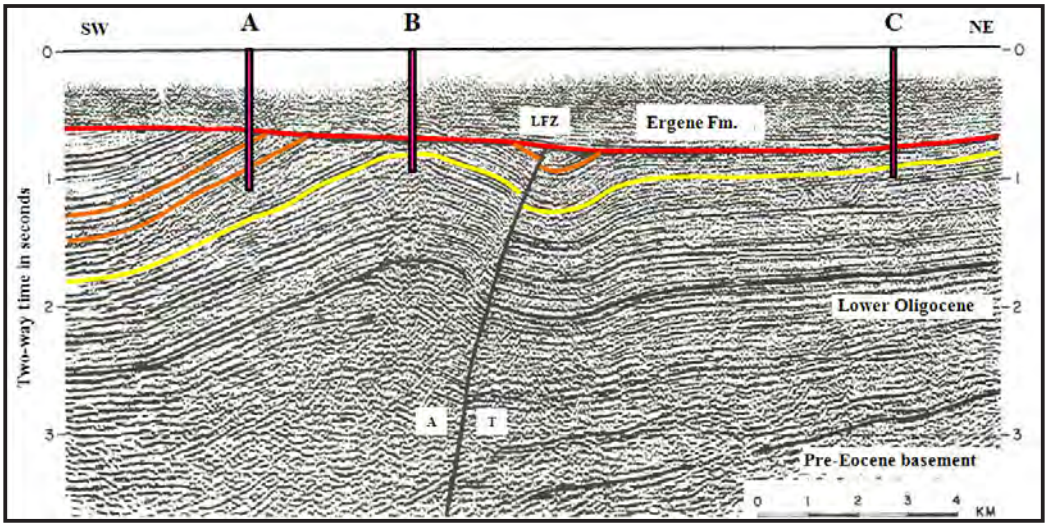

Figure 9 –Lüleburgaz Fault Zone (LFZ) is shown in seismic line (see Figure 5 for location). Right (T) and left (A) parts of the fault move towards the reader and from the reader, respectively (compiled from Perinçek, 1991; 2006).

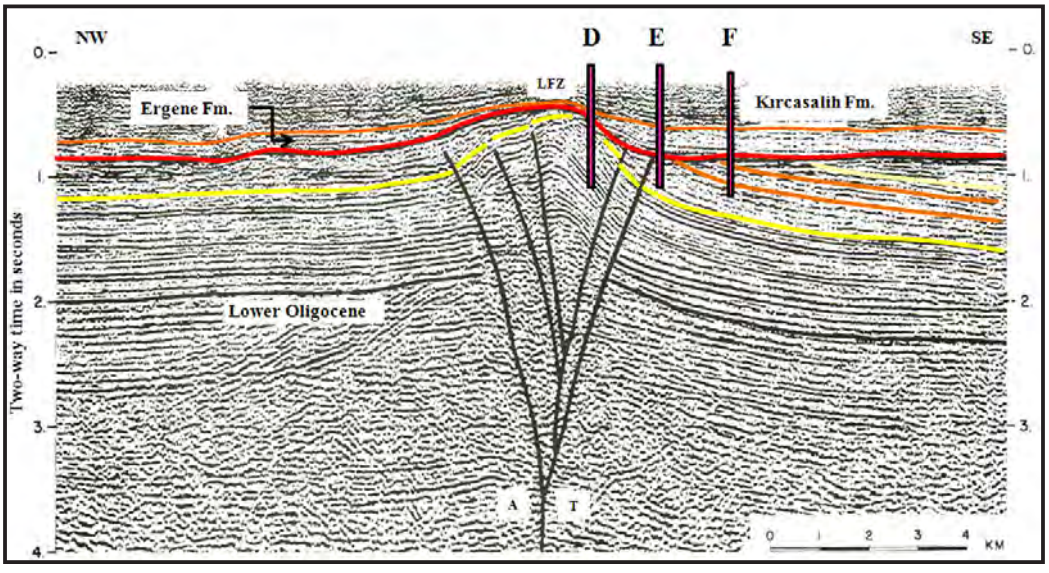

Figure 10 – Lüleburgaz Fault Zone (LFZ) is shown in seismic line (see Figure 5 for location). (Compiled from Perinçek, 1991; 2006).

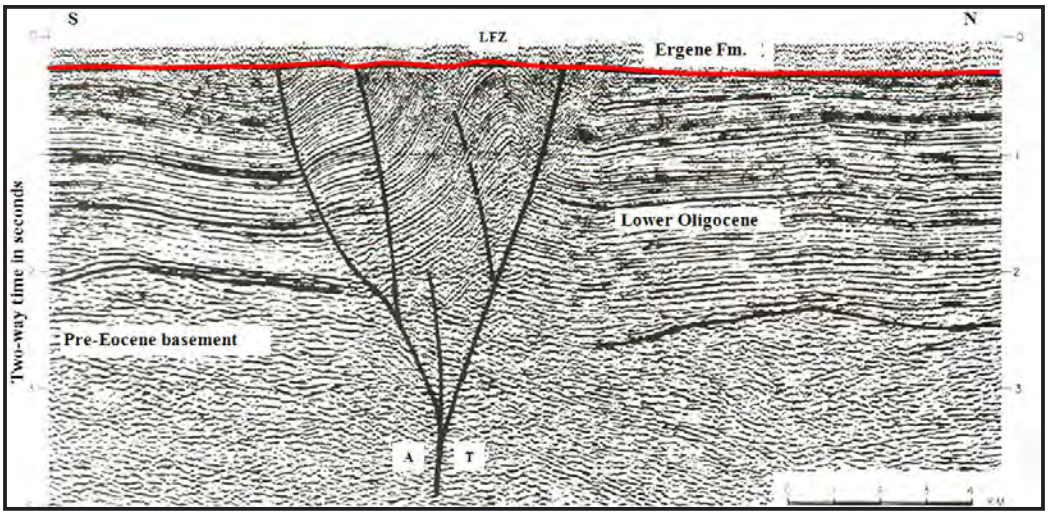

Figure 11 – A positive flower structure is shown around Havsa in western part of the Lüleburgaz Fault Zone (LFZ) (compiled from Perinçek, 1991; 2006).

the Mesutlu-1 well (Figure 8).

Danişmen Formation is thin around the Kızılcıkdere 1, Bayramdere 1, Kocadere 1, Ceylan 4, and Emirali 1 wells (Figure 8). The Kırklareli fault zone, which is northernmost branch of NAFZ at the end of Middle Miocene-Late Miocene (Figure 5) extends in the vicinity of above mentioned wells. This is another good example for uplift and erosion associated with this fault.

In seismic section given in figure 9, the Lüleburgaz fault zone (LFZ) is shown at the center (Perinçek, 1991). It was assumed that reflector indicated by yellow color represents a level close to the base of Danişmen Formation and two different levels in the same section indicated by orange color are the lignite layers. Approximate lignite depth is hypotheticial to explain erosion problem in the region. The reflector indicated by red color further above is an angular discontinuity at the base of Ergene Formation. An anticline at the left was formed concurrently with the fault activation and erosion was taken place along the anticline axis after the uplifting. The discordance plane that formed after the fault was not folded. This indicates that fault in this area did not move following the deposition of Ergene Formation. The erosion that occurred after the formation of anticline is quite noticeable in the seismic section. It is clearly shown in seismic section that in the well designated by B symbol first Ergene Formation is encountered and then Danişmen Formation is cut further below the discordance. At point B upper part of Danişmen Formation is completely eroded meanwhile lignite layers indicated by two orange lines are also removed. In conclusion, lignite will not be cut in the presumed B well. In well A at left of B hypotheticial well, lignite will be most probably encountered. In the presumed well C lignite layers will not be cut since Danişmen Formation is significantly eroded.

The flower structure shown in figure 10 was developed in compression buckling along the fault zone. Following the first activation of fault Ergene Formation was deposited in the Middle-Late Miocene and discordance at the base of this formation was folded and then Kırcasalih Formation was deposited in Pliocene and finally discordance plane comprising the Pliocene sequence was folded since fault system continued its activation. While Ergene and Kırcasalih Formations were deposited at east of Thrace basin the movement continued along the Thrace fault system. In seismic section given in figure 10 the level indicated by yellow color is assumed to represent reflector that is close to the base of Danişmen Formation. Two orange reflectors at right side of section represent proposed lignite levels. The angular unconformity at the base of Middle-Late Miocene Ergene Formation was marked with red color. Although this unconformity plane in figure 9 is not folded, discordance plane in red color in seismic section in figure 10 is shown to be folded. Folding of discordance plane is not common to western part of basin but around Vakıflar wells and Silivri in eastern part of basin. Following the deposition of Ergene Formation, the fault was reactivated and thus discordance plane was folded (Perinçek, 1991 and 2006). The positive flower structure shown at the center of figure 10 is related to compression buckling of lateral strike-slip faulting. When the seismic section is evaluated

by means of lignite potential, it is predicted that in well D following a thin layer of Ergene Formation directly Osmancık Formation is cut. In this case, in the proposed well D Danişmen Formation is probably completely eroded. In well E shown in Figure 10 after the Ergene Formation and discordance lower part of Danişmen Formation will be cut. Therefore, due to erosion no lignite level is expected in well E. In the proposed well F, after the Ergene Formation and discordance Danişmen Formation with lignite interbeds is possibly cut. From well F to southeast direction the thickness of Danişmen Formation above the lignite levels will be increased. Considering the thickness of overlying Ergene Formation, it seems difficult to find any lignite level at economic depths at right part of the section **(**Perinçek, 2010*a, b, c*).

In figure 11 uplifting along the fault zone, anticline formation and subsequent erosion are apparent. Due to erosion, in an area parallel to the fault zone thickness of Danişmen Formation is decreased and locally lowered to 100 m and occasionally become zero. In association with erosion, lignite levels in middle part of Danişmen Formation are also removed. As shown from figure 9, discordance plane in this section was not also folded. After the fault formation, no tectonic movement was occurred along the fault zone. Positive flower structure of Lüleburgaz fault zone is shown in figure 11. The area of positive flower structure (the area of Aktaş-1, Haznedar-1 and Mesutlu-1 wells between and around Havsa-Babaeski; Figures 6 and 10) is the upliftted part and erosion area along the Lüleburgaz fault zone. The interpretation for seismic section in figure 9 and 10 is also valid for this section. There is little possibility to cut any lignite layer at the center of the positive flower structure. Wings of this structure are potential sites for lignite. New license areas proposed by this study are at the wings of aforementioned structure.

4.4. Total thickness map of lignite for the Danişmen Formation

Thickness map of lignite, as expected, will be proper for the aim of study if it is made in the regional scale, therefore, thickness map was made for the whole Thrace region. This map may be regarded as a kind of facies map since it shows swamp and lake areas where lignite is accumulated. Due to facies change of lignite levels and erosion there is a discontinuity in the lateral direction.

During the construction of lignite thickness map, two different data sets were used. The first is total thickness map of lignite using TPAO well data. The second is lignite thickness map using MTA and TKİ well data. At the beginning of project these two maps were drawn separately. Considering the total lignite thickness there are inconsistencies between these maps.

Lignite thickness within the Danişmen Formation is controlled by 2 important factors. In thickness map using TPAO data (Figure 12) and revised thickness map using MTA and TKİ data (Figure 13) there is no lignite in areas shown by blue color. There are two reasons for the absence of lignite. The first is facies change in the Danişmen Formation.

During the deposition of Danişmen Formation lignite was formed in swamp and lake areas but not in the fluvial deposits where conglomerate and sandstone were accumulated. In figure 14 absence of lignite in blue colored areas is attributed to facies changes in the Danişmen Formation. The Danişmen Formation at north of Demirhanlı 1well is represented by siltstone, sandstone, and conglomerate which change to clay, siltstone and marl towards the east (Figure 14). As a result of decreasing of clastic content in the sequence marl was deposited in a low-energy environment which is represented by swamp areas. Therefore at south of Demirhanlı 1well lignite with thickness of 5 m was accumulated in clay and marls. In this map it is shown that lignite thickness is between 0 – 7 m. For instance, for a distance of 500 m, total lignite thickness might change from 0 to 7 m which create difficulties in the lignite exploration works.

In the area of Hayrabolu wells (Figures 12 and 13) no lignite was found because of unsuitable conditions of Danişmen Formation for the lignite formation. Although lignite is absent in this area the thickness of Danişmen Formation is 600-1000 m. This region is at south of Thrace fault system and therefore the reason for absent of lignite is not relate to erosion but deposition.

Another reason is related to structural evolution of the basin. Significant erosion was occurred along structural heights and faults that developed in Middle Miocene as a result of activity of Thrace Fault System. The thickness of Danişmen Formation on the structural heights becomes thin by erosion (Figure 8) and accordingly lignite layers were disappeared.

When the total lignite thickness map is prepared and well data of MTA, TKİ and TPAO are evaluated following issues were taken into account **(**Perinçek, Perinçek, 2010*a, b, c*);

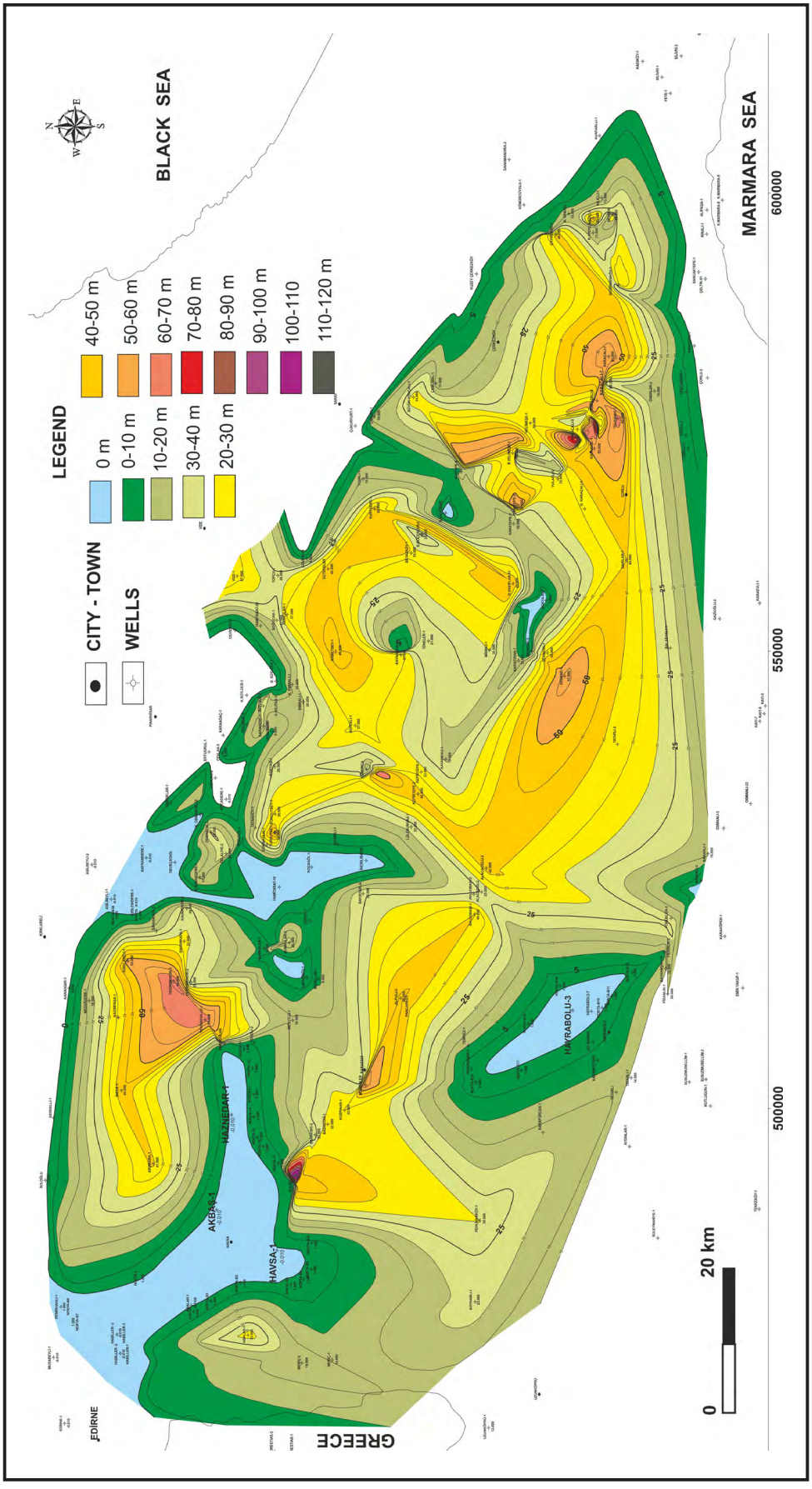

Figure 12 – Total thickness map of lignite layers within the Danişmen Formation; prepared using TPAO well data. There is no lignite layer in blue-colored areas. The map was drawn based on TPAO well data (Perinçek, 2010*b, c*).

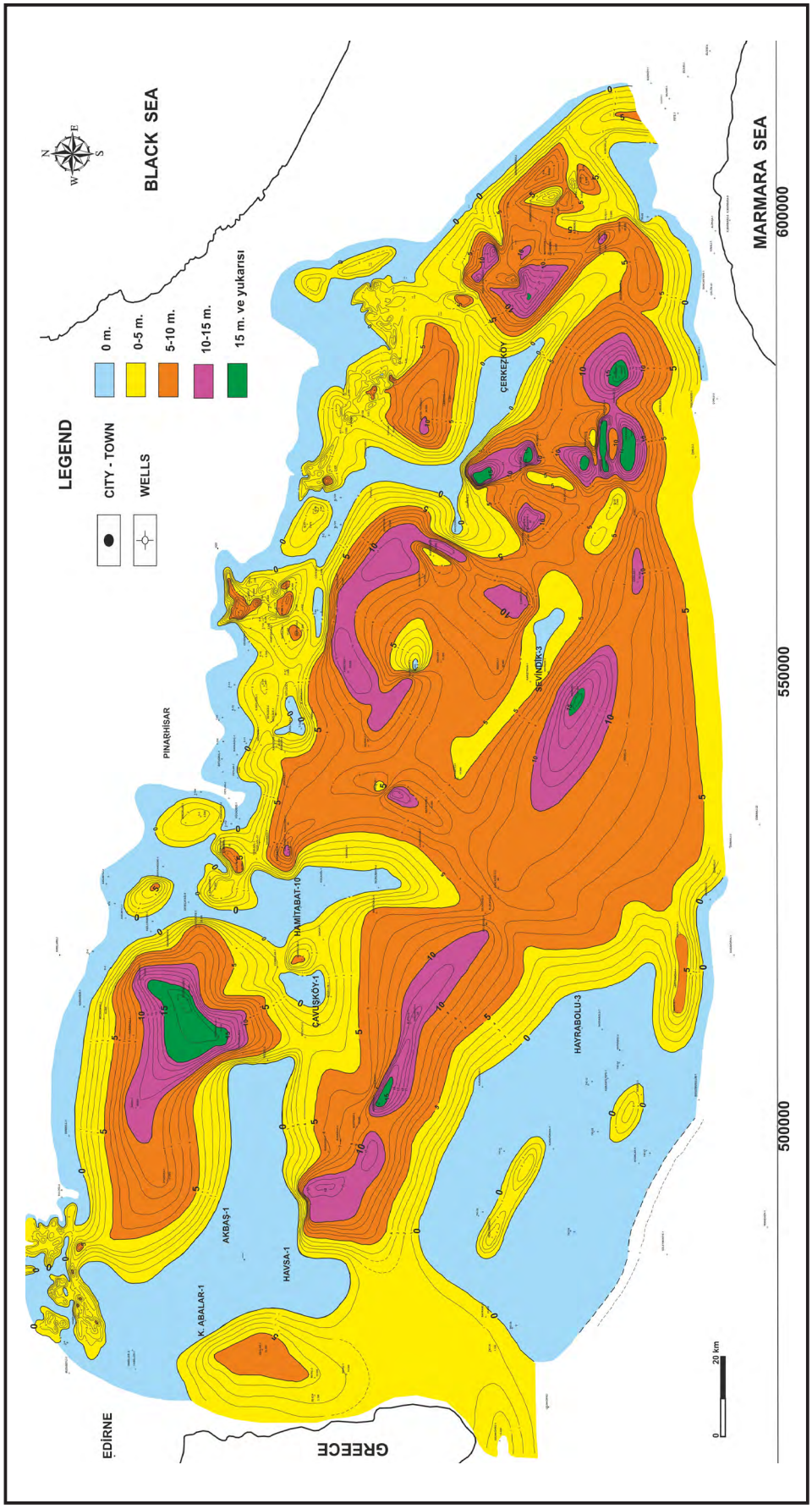

Figure 13 – Total thickness map of lignite. For this map TPAO, TKİ and MTA data were used (Perinçek, 2010*b*, *c*).

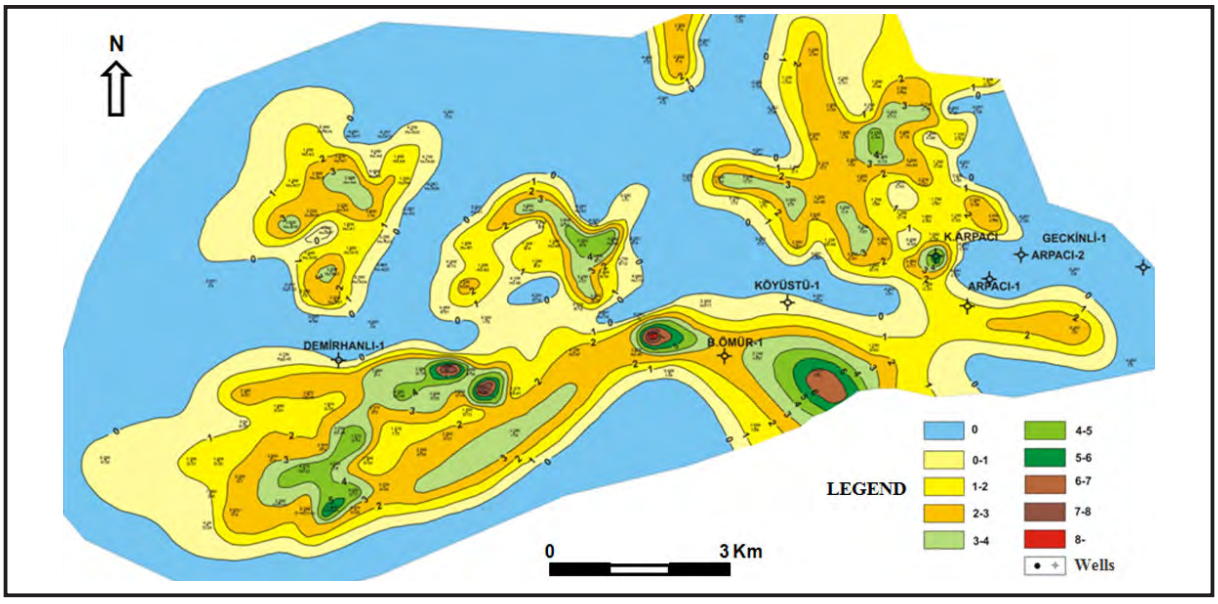

Figure 14 – Total thickness map of lignite levels within the Danişmen Formation between Süloğlu -1 and Musabeyli-1 wells at southeast of Edirne (Perinçek, 2010*b, c*).

1- The total lignite thickness map based on TPAO data contains some discrepancy since the area of interest of TPAO is not the coal. Therefore thickness values in this map do not properly serve the aim of study. Nevertheless the "Lignite Thickness Map" based on TPAO data was instructive at the beginning since it indicates the lignite-dense areas (Figure 12). In TPAO wells lignite thickness was generally shown higher because no core sample was taken from lignite levels since the Danişmen Formation is not the target formation. The Danişmen Formation was progressed with diamond drilling and only cutting off samples were taken. During the drilling following the progress of lignite level, failure occurs in the overlying lignite levels and the material fell down reaches at the bottom and recycled to the surface which makes an impression that lignite is continuously intercepted. In TPAO wells claystone levels with high lignite content, ligniferous shale and ligniferous claystone levels are also progressed as lignite. Consequently, lignite thickness cut in the wells is found much thicker in the composite well logs. In TKİ and MTA wells ligniferous levels are progressed with coring the thickness of lignite cut in the wells are reliable. Therefore lignite thickness map obtained from TPAO data was reviewed considering the geologic data of region and total lignite thickness map constructed with TPAO and TKİ-MTA well data was revised and integrated. Then the revised TPAO lignite thickness map (Figure 12) was combined with total lignite thickness map established by TKİ-MTA data. During this process, thicknesses in wells with coring were considered and lignite thicknesses in TPAO wells were reduced. The map used in this study (Figure 13) is the revised lignite thickness map. In areas where TKİ, MTA and TPAO wells are close to each other TPAO wells were compared with TKİ and MTA wells and the their ration was examined. It was shown from the results of this work that lignite thickness in TPAO wells is about 3-4 times greater than those of TKİ and MTA wells. The area which hosts wells of different organizations is in northeast part of Thrace basin. In these areas TPAO well data are compared with MTA and TKİ data and using the resulting ration TPAO thicknesses were evaluated by dividing 3 or 4 and the new total lignite thickness map was established (Figure 13). When making this proportioning process, these values were obtained by dividing lignite thickness in some TPAO wells by 2 or 5. In doing this, geologic information of the basin, particularly structural setting, was taken into account which greatly contributed to the map. Total lignite thickness map given in Figure 13 was constructed with solely interpretive contouring without using computer program. During the contouring thicknesses from TPAO data were reduced with respect to the closest MTA and TKİ well. Therefore, reduction rate is different for each well. During the interpretive contouring, structural setting of Kırklareli, Lüleburgaz and Babaeski fault zones was considered.

Thicknesses selected for above mentioned rations and used in the present thicknesses are given in table 1 and ordering in the list is from northwest to northeast of the basin. The first value in table is the one shown in TPAO wells and the second is calculated using a proportion.

Table 1- Thickness of lignite cut in TPAO wells and some examples for calculated thicknesses.

Well name	TPAO Thickness meter	Thickness used, meter	Well name	TPAO Thickness meter	Thickness used, meter
Adalar 1	33	5	**Kepirtepe 2**	42	9
Ağrızbaba 1	41	9	**Turgutbey 2**	52	10
İnece 1	44	10	**Ahmetbey 1**	49	11
Kırklareli 1	53	13	**Doğuvakıflar 1**	45	10
Değirmencik 3	86	17	**Sarılar 1**	40	10
Kozpınar 1	35	8	**Karatepe 1**	52	12
Babaeski 1	32	7	**Kurtdere 1**	42	9
Alpullu 1	46	12	**Üçtepeler 1**	42	9
Avluobası 1	40	10	**Büyükyoncalı 1**	34	10
Alacaoğlu 2	42	9	**Telkavak 1**	62	15
Lüleburgaz 1	22	5	**Karaçalı 1**	60	16

2- At the first stage of project, well correlation was made in the Thrace region and it was found that, because of insufficient well depth, lignite zones in some MTA and TKİ wells are not penetrated which are encountered in lower parts of TPAO wells. In the thickness map given in figure 13 lignite levels that are cut in lower parts of TPAO wells are not taken into account. Therefore total lignite thickness map given in Figure 13 represents minimum total lignite thickness. Based on data available, Figure 13 yields the pessimist thicknesses for the lignite levels.

3- The northern part of total lignite thickness map (Figure 13) could be processed in detail because of intense number of core samples and well data. In northern areas where intense well data are available areas without lignite layers are easily recognized. Thickness variations in these areas reflect facies distribution within depositional basin of Danişmen formation. For example, in blue areas in figure 14 absence of lignite is explained with facies characteristics. Structural factors controlling the lignite thickness is very limited. The kind of detail cannot be mentioned for central and southern Thrace regions. In central and southern Thrace regions, the areas where lignite levels are absent (blue areas in figure 13) are eroded and uplifted due to the Thrace Fault System (Kırklareli, Lüleburgaz and Babaeski Fault Zones) which is a continuation of NAF. Therefore lignite thickness in central and southern parts of this map does not truly reflect the facies changes in the Danişmen formation. In some areas lignite might not be widespread as shown.

4- Lignite levels within the Danişmen formation are mostly found in middle section. In areas where the formation is eroded lignite levels are also eroded. Consequently in total lignite thickness map given in Figure 13, the areas where lignite is absent correspond to thin levels of Danişmen formation in total lignite thickness map. In other words, there is no lignite in areas where Danişmen formation is thin. The Kuzey Abalar 1, Aktaş 1, Havsa-1, Çavuş Köyü 1, Hamidabat-10, Çerkezköy and Sevindik 3 TPAO wells do not have any lignite level (Figure 13).

5- Lignite layers mostly occur in marl. Pebbly, sandy and carbonaceous levels do not contain lignite. In addition, lignite is also absent in areas of widespread shale levels.

4.5. Total thickness map of Ergene and Kırcasalih formations:

Thickness of Ergene Formation is the first obstacle to access the lignite. In order to examine the change of thickness of this formation within the basin, thickness map of Ergene Formation was established throughout the Thrace Basin (Figure 15). In TPAO and some MTA and TKİ wells, the Ergene Formation and overlying Kırcasalih (Thrace) Formation could not be differentiated. Therefore thickness of Kırcasalih Formation was included to the thickness map of Ergene Formation. Consequently, when mentioned the thickness map of Ergene Formation total thickness map of both formations are meant. Examination of some seismic sections in the Thrace Basin reveals dicorformity between the two formations (Figure 10). This unconformity is not recognized everywhere. The lithologies of Kırcasalih (Thrace) and Ergene formations are similar which complicates distinguishing these units in the field. On the recent MTA and TPAO geology maps these units were mapped separately.

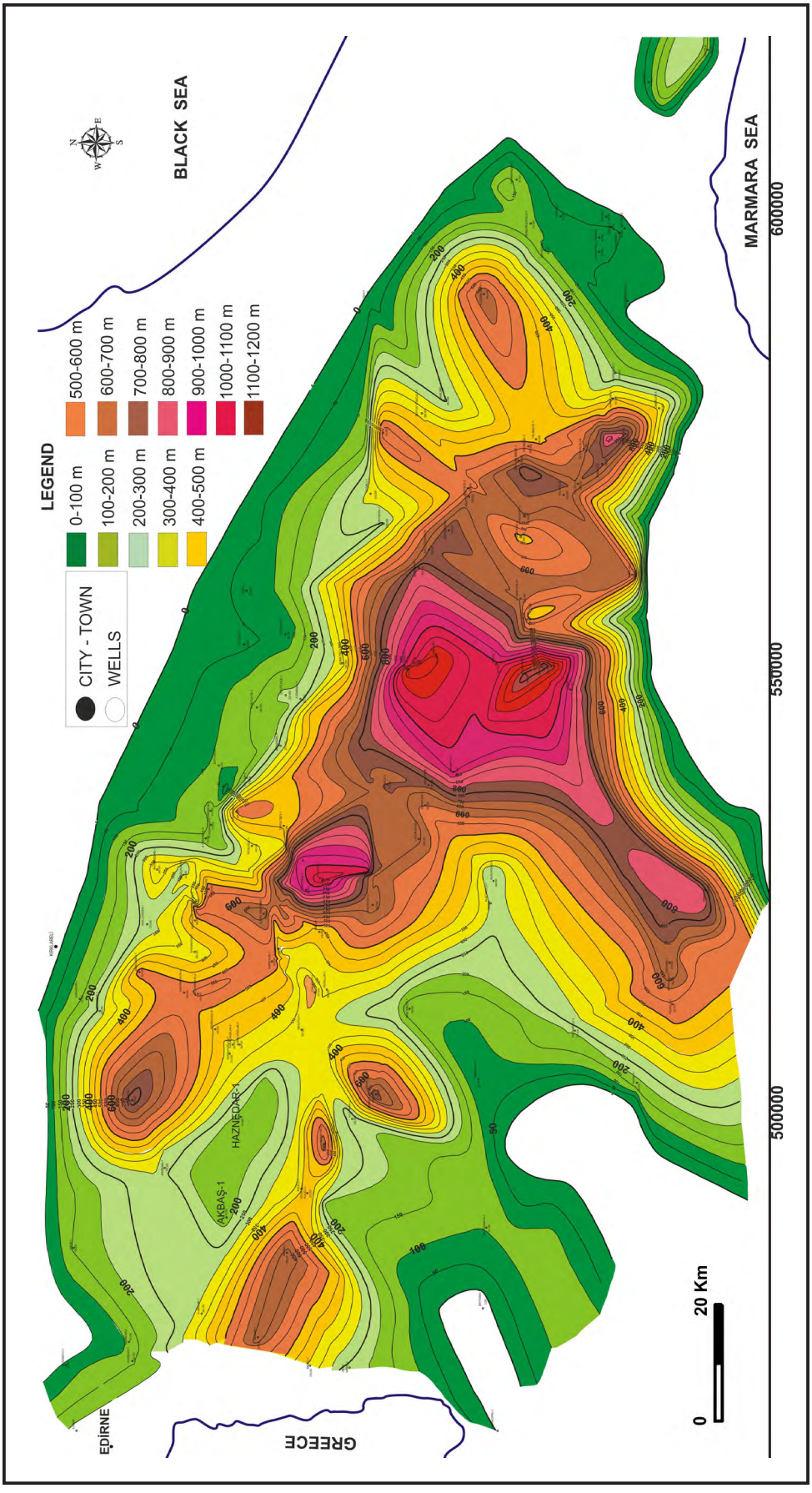

Figure 15 – Total thickness map of Ergene and Kırcasalih (Thrace) formations (Perinçek, 2010*b*, *c*).

In the green colored are shown in Figure 15 total thickness of Ergene and Kırcasalih formations is 0-300 m. yellow and dark yellow colors represent thickness of 300-500 m, orange color 500-800 m and brown and red colors represent 800-1200 m. The areas where Ergene Formation is thicker than 500 m are not suggested for obtaining permit and drilling. The thickness of Ergene Formation is controlled partly by the activity of NAF in the Thrace basin. In paleo-heights comprised by the fault (around Akbaş 1 and Haznedar 1 wells; Figure 15) the Ergene Formation is thin. In addition, it is known that Ergene Formation is also thin along the margins of Thrace basin. A few permits at south of Vize are suggested to be abandoned since Ergene Formation in these areas is thicker than 500 m. At these sites lignite thickness may be economic but not at feasible depths.

The Ergene Formation was deposited on paleo-heights which are formed by structural events occurring along the Thrace Fault System which is the oldest branch of NAF. During the deposition some paleo-heights that formed by the effect of NAF were coincided in the last stages of deposition of Ergene Formation and therefore in these areas the unit is thin (Perinçek, 2010*a, b, c*) (Figure 10). The Thrace Fault System was reactivated following the deposition of Ergene Formation between Vakıflar-1 and Istanbul at east of Thrace basin and discordance plain at the base of Ergene Formation was folded together with Ergene Formation (Figure 10) and as a result the formation was partly eroded. New paleo-heights occurring in erosional areas represent thin parts of the Kırcasalih formation. Following the deposition of Kırcasalih formation activity of fault was continued on the Thrace Fault System. Following this activity the Kırcasalih formation slightly inclined and folded. This activity is shown in eastern parts of the Thrace basin since this area is close to the Sea of Marmara where NAF is active.

5. Assessment of Seismic Data

Seismic sections provided to TKİ by TPAO were evaluated and areas where lignite layers close to the surface were identified (Perinçek 2010*a, b, c*). Assessment of these sections was done for the area (around Babaeski) between TKİ licenses at south of Pehlivanköy and licenses around the Karacaoğlan town. Section nos MAD-84-411 (Figure 16), MAD-84-432 (Figure 17) and MAD-84-413 (Figure 18) are included to this report. Well data (Babaeski 2, Minnetler 1) were transferred to the seismic sections using seismic-time data. Reflection plane shown with orange color in sections represents the base of Ergene formation (above the Danişmen Formation). Green levels in sections are the lignite layers. Reflection planes indicated with green may contain lignite around the well but green reflection continuing in lateral direction does not necessarily mean the presence of lignite along the seismic line. In other words, levels indicated by green colors and represented by lignite in the wells show lateral facies change and may change to marl or clay. In these sections, planes with lignite levels were traced and the areas where these layers get close to surface were identified. If there is no lateral facies change it is possible that green levels are

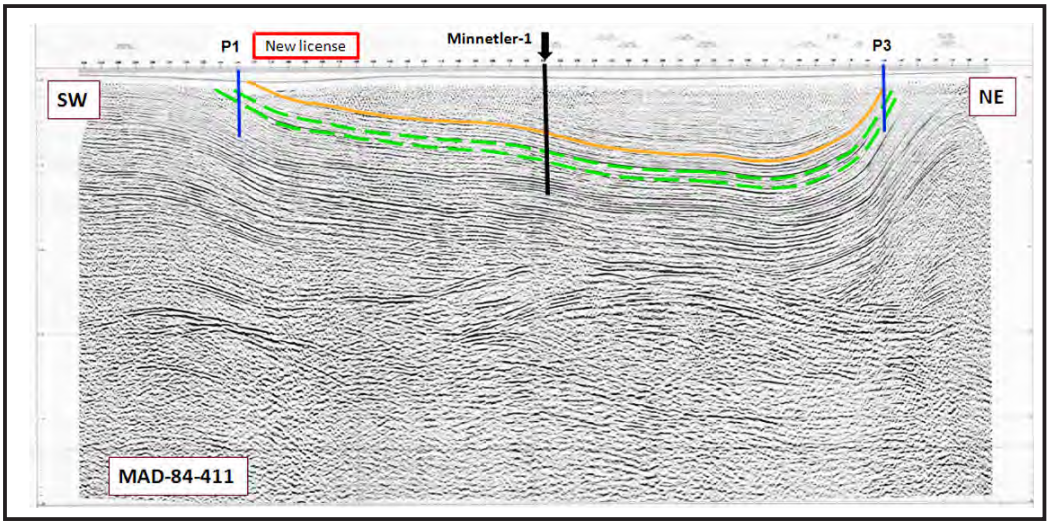

Figure 16 – Seismic section no MAD-84-411. Lignite layers (green) and the base (top of the Danişmen Formation) of Ergene Formation (orange) are marked on the section. Proposed P1 well is southwest of section and P3 well is at northeast (for locations see Figures 19, 20 and Figure 5).

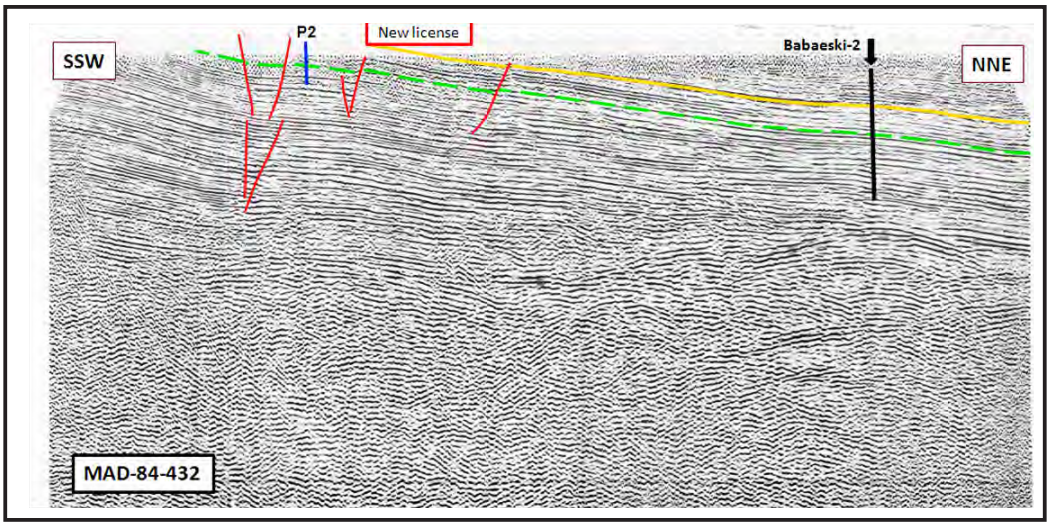

Figure 17 - Seismic section no MAD-84-432. Lignite layers (green) and the base (top of the Danişmen Formation) of Ergene Formation (orange) are marked on the section (for locations see Figures 19 and Figure 5).

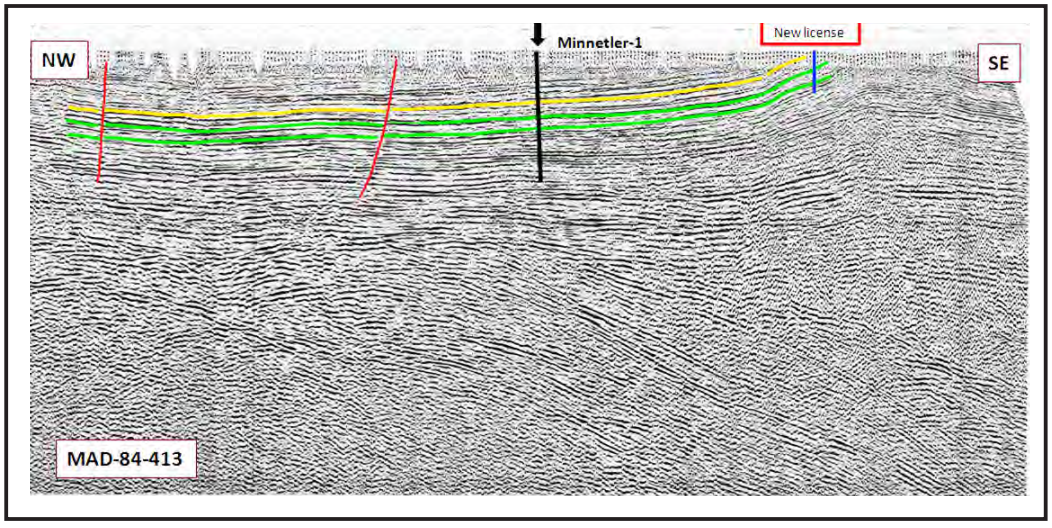

Figure 18 - Seismic section no MAD-84-413. Lignite layers (green) and the base (top of the Danişmen Formation) of Ergene Formation (orange) are marked on the section (for locations see Figures 19 and Figure 5).

cut in areas close to surface and they contain lignite. In the seismic sections red lines represent faults. The locations of TPAO wells (Minnetler 1, Babaeski 2) on the sections are shown with vertical black lines. The locations of wells proposed to be drilled by TKİ in 2011 are shown with vertical blue lines.

In figure 16, from Minnetler 1 well to SW and NE directions the reflection that is supposed to represent lignite content is shown to get closer to the surface. P1 well is projected at SW of section (for location see Figure 19). This well is in the license area that was owned in the past by TKİ. The P3 well shown at NE of figure 16 is within the license area owned by TKİ in 2010 (Figure 20). It is suggested that this well should be immediately drilled. In figure 17, the point indicated by P2 symbol at SW of section is within the TKİ license area owned in the past years (for location see Figure 19). This well is also preferentially drilled in the area.

6. Obtaining license and proposed wells

6.1. New license areas owned by TKİ

1 – Around Mesutlu 1 well (Figure 13): TKİ was suggested to own license around the Mutlu, Kadıköy, and Kuleli villages in the Karacaoğlan region at north of Babaeski and around Çavuşlu (Figure 12),

Karacaoğlan, and Oruçlu villages at the northeast (Perinçek et al., 2011). The promising results of maps produced for the Thrace Basin lead to taking these licenses. From these maps the thickness of Ergene Formation is expected to be around 350 m. The same maps also indicate that lignite levels in the Danişmen Formation are achieved at economic depths. In lignite thickness map prepared based on well data total thickness of lignite is expected to be around 10 m.

2 – Around Musulca at south of Süloğlu: TKİ took licenses around the Habiller, Musulca, Arpaç, Küküler, Akardere and Paşayeri villages (south of Süloğlu; Figure 14). In this area, total thickness of Ergene and Kırcasalih formations is nearly 300-400 m. Lignite bands within the Danişmen formation are expected to be cut at economic depths.

6.2. Wells proposed to be drilled in license areas of TKI

In the second stage of study conducted for TKİ, a supplementary work was carried out to maintain that reliable data is applied to drilling of wells in present licenses and licenses taken by TKİ in 2010. Before proposed drilling in permit data on TPAO wells around the license areas were taken into account.

Using the prepared maps constructed and other geologic and seismic data, the areas where lignite could be cut at shallow depths are estimated. The data to be achieved in this study contain important tips regarding the depth of lignite levels. As known due to facies changes within the Danişmen Formation lignite levels are discontinuous. Total lignite thickness may change in short distances and become zero.

Northern parts of license areas at S and SE of Pehlivanköy (Figure 19) where TKİ drilled wells in previous years are expected to have lignite levels at economic depths. It is thought that in these areas Danişmen Formation is exposed but Ergene Formation is not present or very thin. Seismic section given in figures 16 and 17 is included to support this opinion. For this area there are limited data to identify facies distribution of Danişmen Formation and the presence of lignite layers. In spite of this, these areas are needed to be tested. If facies is suitable, the number of wells in the license will be increased in north and south directions. In these licenses (Figure 19) wells

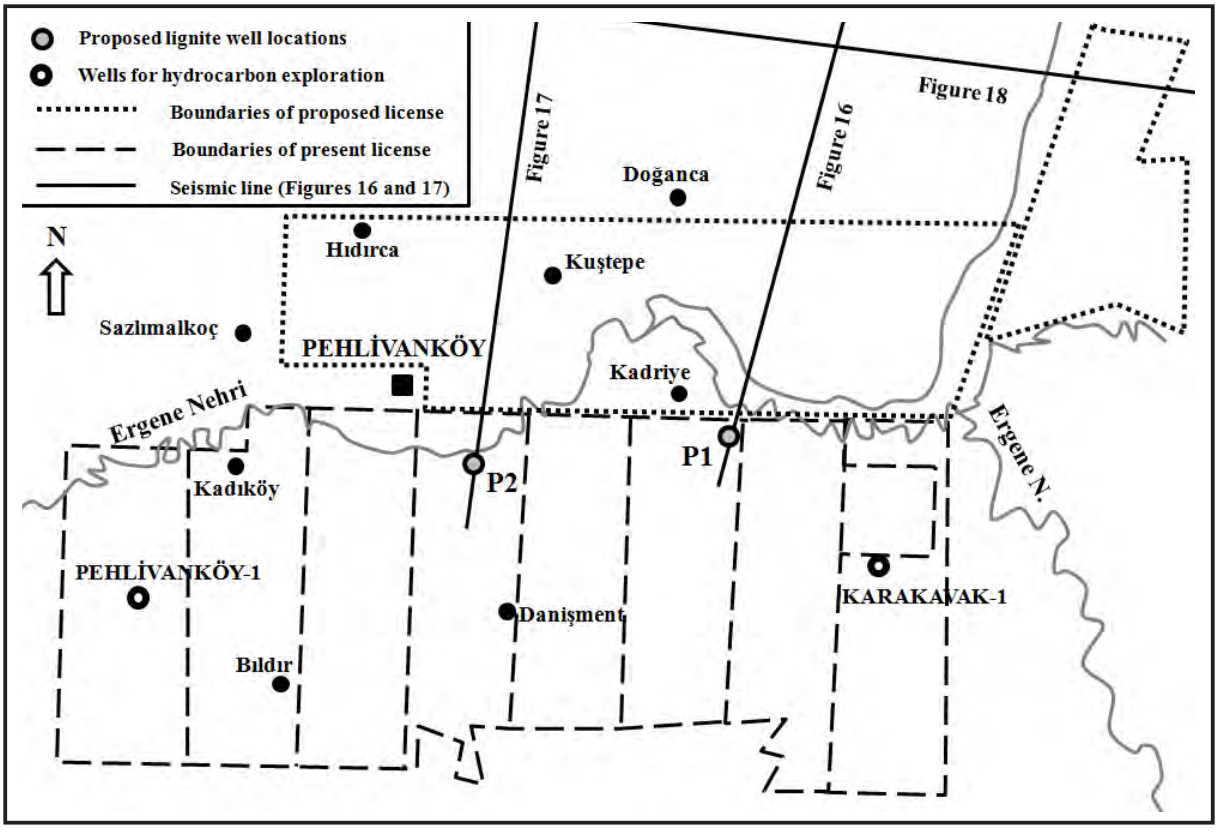

Figure 19 – Locations of wells (P1 and P2) to be drilled in northern parts of license areas of TKI at S and SE of Pehlivanköy. 2 new license areas to be taken around northeast of Pehlivanköy are marked with dashed line.

P1 (Figure 16) and P2 (Figure 17) are proposed to be drilled. In well P1 lignite level can be penetrated at depth of 100-200 m. Depth of well is proposed to be 400 m. In well P2 lignite level is expected to be encountered between 200-300 m. Depth of this well is suggested as 500 m. It is possible that in wells P1 and P2 (Figure 19) lignite levels can be penetrated much shallower depths.

Wells should be immediately drilled in license areas taken in 2010 around the Karacaoğlan town at north of Babaeski (Figure 20). Locations of proposed wells are shown in Figure 20. On this map P3, P4-A, P4-B, P5 and P6 symbols show the proposed well locations. Considering the results from P3 well (Figure 16), locations of these wells may be changed. It is thought that reflection planes, which are believed to represent lignite layers, are intercepted at depth of 200-300 m (Figure 16). In this well, first a thin part of Ergene formation will be cut and then Danişmen Formation will be progressed. It is possible that 2 different lignite levels will be intercepted in the P3 well. The lignite level below could be at depth of 300-400 m. Lignite layers and alternating litologies of Danişmen Formation are expected to have a high slope which results in cutting of a much thicker lignite layer.

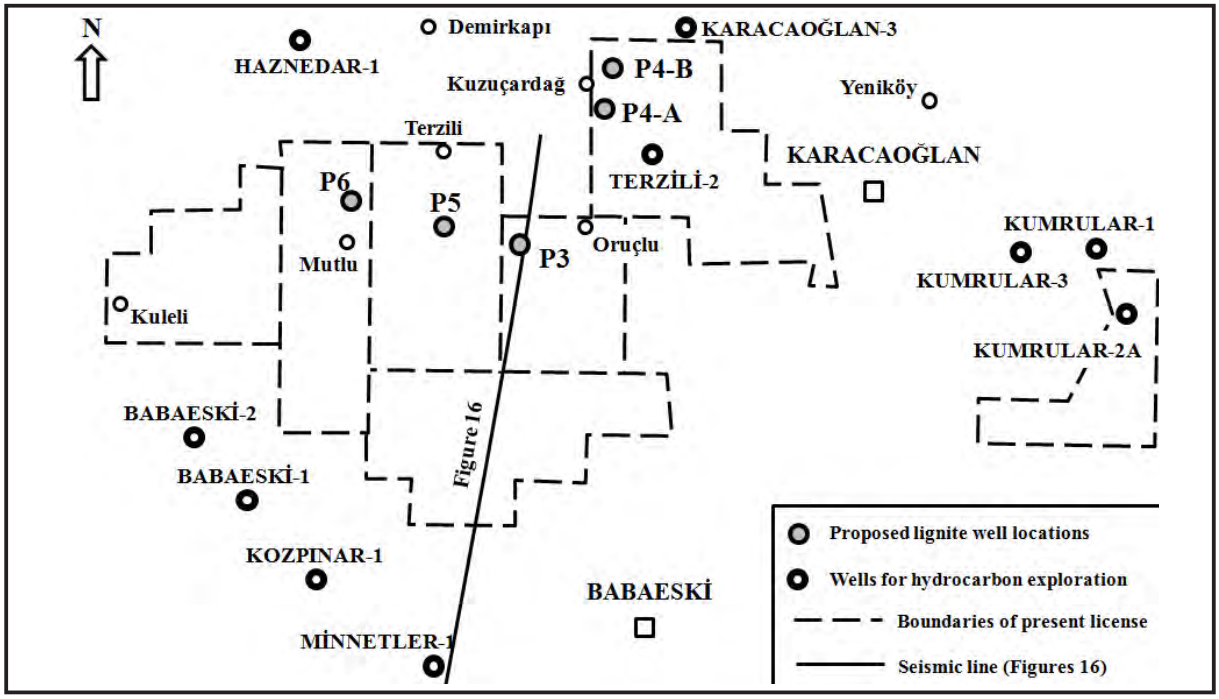

Figure 20 – Map showing the locations of wells to be drilled in license (taken in 2010) areas around Karacaoğlan town at north of Babaeski.

In license areas at south of Umur 1 well north of Hasköy, a number of 8 wells (H1, H2, H3, H4, H5, H6, H6, H7, H8) are proposed (Figure 21). For this area since no seismic data are available it is not possible to suggest a net figure for the depth of lignite layers. However geologic works conducted during the first stage of project indicate that he Ergene Formation is very thin in this area and lignite layers are shallowly seated since Danişmen Formation is eroded and for these reasons present licenses were taken. The locations and arrangement of wells to be drilled in this area may be changed in accordance with results from H1 well. At north of these licenses in Umur 1 well lignite was cut at depth of 225 m (Figure 21). In addition, around this well and in the Süloğlu lignite field at north thickness of lignite attains 7-8 m (Figure 14).

6.3. Proposed new license areas

Seismic data yields that lignite levels of the Danişmen Formation will be closer to the surface at east of Pehlivanköy. Therefore new licenses are suggested for this area. As shown from figures 16 and 17, reflectors which are presumably lignite layers get close to the surface. Just north of TKI license areas around Pehlivanköy at least 2 licenses are suggested. The new license area is marked with red rectangular on the seismic section in figure 16.

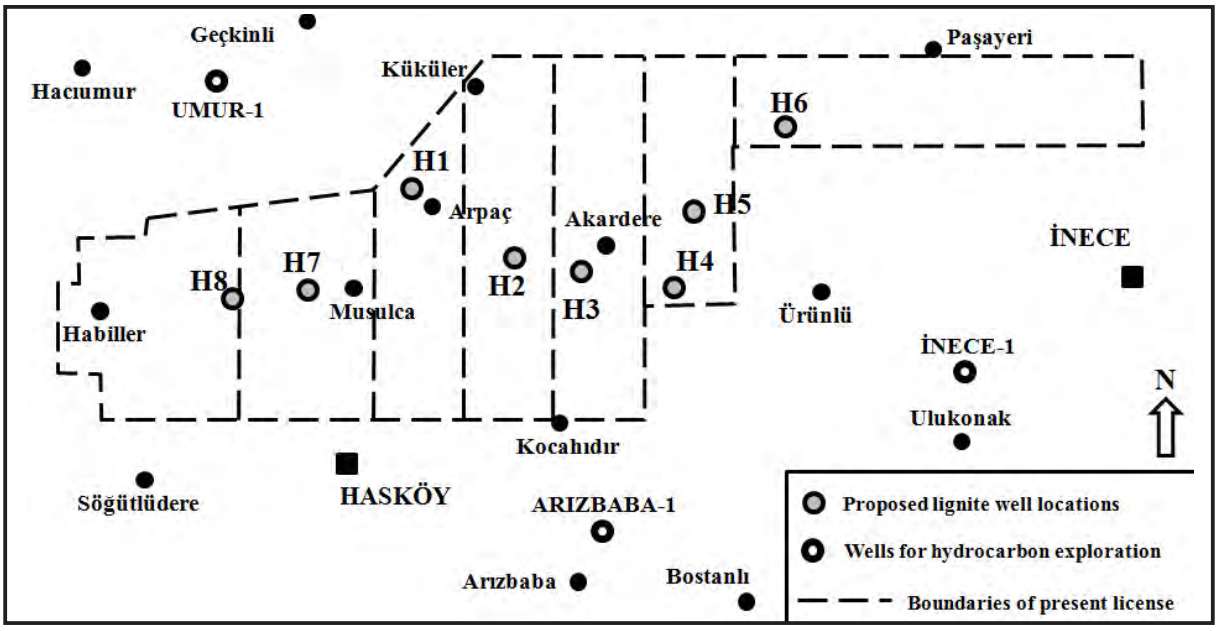

Figure 21 – Proposed wells to be drilled in license areas at north of Hasköy (H1, H2, H3, H4, H5, H6, H7, H8).

Seismic data (Figure 18) indicate that lignite-bearing Danişmen Formation at SE of Babaeski area gets close to the surface. It is believed that Ergene Formation will be thin-very thin within the proposed license area. Therefore new licence was suggested for NE of Pehlivanköy area (Figure 19). The proposed license area is marked with red rectangular on the seismic section in figure 18.

Results of this study show that there are areas suitable for taking new license around Pancarköy-Babaeski and based on these findings TKİ took new licenses in this area.

7. Results

Within the concept of project which started in April 2009 studies summarized below were implemented for the whole Thrace basin using TKİ, TPAO and MTA well data. In order to reveal lignite potential of Thrace basin maps of regional scale were established. From these maps information was gathered that is useful not only for TKİ but also for TPAO and MTA. It was aimed that results of project will contribute to all relevant governmental organizations (Perinçek 2010*a, b, c*).

The maps produced from this study are listed below:

1- Osmancık Formation structure map (Figure 6)

2- Danişmen Formation discordance plane "paleo-topography" map (Figure 7)

3- Danişmen Formation thickness map (Figure 8): Lignite levels within the Danişmen Formation are generally found in the middle and middle-upper parts of the unit. It is shown in the thickness map that the unit is changes its thickness between of 0-1650 m. The decrease in thickness is attributed to erosion process following an uplift that is triggered by the Thrace Fault System. In some areas, the Danişmen Formation is completely eroded. As a result, lignite layers within the unit are also eroded. Therefore it is suggested that during the lignite exploration the areas where unit is intensely eroded should be avoided. In areas where the formation is quite thick it is difficult to find lignite layers in the middle part of unit at economic depths. Therefore, in the unit areas with thickness exceeding 1000 m are risky which should be kept away.

4- For lignite levels within the Danişmen Formation 2 total thickness maps were prepared (Figures 12 and 13). First using the TPAO well data total lignite thickness map was prepared (Figure 12) then a second map was produced using well data from MTA and TKİ. Data in total lignite thickness map based on TPAO data may contain some mistakes since TPAO is not an organization specialized in lignite. Therefore, lignite thickness map produced by TPAO data (Figure 12) was reviewed using geological data from the region and combined with total lignite thickness map established by TKİ-MTA data. Thus a total lignite thickness map was obtained for the whole Thrace region (Figure 13). This study revealed that lignite distribution in

the Thrace region was partly developed under facies control and Thrace Fault System (Perinçek, 1987; 1991). Was controlling thickness of the lignite These new findings are important for the geology of Thrace region and may contribute to lignite and oil exploration works in the region.

5- In order to examine thickness of Ergene Formation within the basin, thickness map of this formation was prepared throughout the Thrace basin (Figure 15). It is shown on this map that the unit changes between 0-1250 m. Based on this map, in areas where thickness of Ergene Formation exceeds 400 m, it is difficult to find lignite layers of the Danişmen Formation at economic depths. Therefore areas where thickness of unit exceeds 400 m should be avoided.

6- In the Thrace region stratigraphic correlations were made considering the data from wells drilled by MTA and TKİ. Data from these correlations provided understanding the lateral and vertical facies change of lignite. These correlations were evaluated together with other maps and issues and as a result new licenses were suggested to be taken in areas of high lignite potential (Perinçek et al., 2011). Results of these correlations and similar works are scope of a different paper.

7- In areas with licenses taken by TKI in 2010 and previous years, locations of wells to be drilled in the coming years were determined. These wells will be drilled in a sequence. During the drilling stage, results of previous well will be taken into account and if necessary the order of drilling will be changed. When programming the drilling of wells around Pehlivanköy and Karacaoğlan areas (Figures 19 and 20) results of subsurface maps were used and there are geologic and seismic controls. However, locations of wells in areas at north of Hasköy (Figure 21) wells locations are based solely on geologic data from maps.

8- In the second stage of project, following the completion of maps based on geologic data and seismic assessment, based on the results acquired TKI obtained new licenses (Perinçek et al., 2011).

9- Using the results of this study that was conducted for the whole Thrace basin a new exploration strategy was established. In this respect, new licenses are suggested near by uplifted areas of the Thrace Fault System. The areas where the Danişmen Formation is partly eroded around the paleo-heights and the overlying Ergene Formation is quite thin are selected as the target. This new strategy is one of the important results of this study.

The maps and reports that prepared for the Thrace basin were submitted to TKI in 2010. As a result of findings from this report, a new exploration strategy was established to determine and own new license areas (Perinçek et al., 2011). When making such decisions, subsurface and surface geologic data were evaluated in conjunction with seismic data and exceptionally different method was pursued. Well locations were determined following the assessment of all data.

8. Studies planned in the coming years

1- If the results of chemical analysis of samples from wells drilled by TKİ and MTA are provided for the whole Thrace basin, calorie distribution maps are suggested. Numerous numbers of analyses is required for successful results from these maps and therefore reliable results cannot be achieved with limited data. These maps which will be established with chemical analyses may also provide information on facies characteristics of the Danişmen Formation.

2- Facies map of Danişmen Formation is another attempt to accurately reveal the lignite potential of Thrace basin. It is possible to examine lateral and vertical facies changes with well correlations. In order to see the vertical facies in map dimension (third dimension) facies maps should be constructed. Underground geology data of TPAO are important data set that should be used during preparation of facies maps. These data are well logs and composite well logs. Facies maps of Danişmen Formation can be made providing these data from TPAO. Geology maps are another data set for these maps. The facies maps should be supported with field works. When making maps sections in some exposures should be visited and surface and subsurface data must be combined. In the long term lignite potential of Thrace basin is thought to be transformed to gas by burning underground. In this case, rather than depth of lignite levels, lateral changes in association with facies distribution come into prominence. In order to minimize the drilling costs facies works are crucially important. Facies study is indispensable for the Thrace basin which requires a longsuffering work.

3- Thickness and structure maps produced so far should be continuously revised with data from new wells drilled by TKİ, MTA and TPAO and then wells for lignite production should be drilled on

reliable points. Data on wells to be drilled by various organizations must be evaluated simultaneously with other proposed works. Thus a complementary system will be established and works will be carried out in more coordinated way. Data of wells to be drilled in the Thrace basin by TKI and other relevant organizations will provide a great support in construction of facies maps. During the generation of facies maps, data on these wells will be evaluated and taking the results of each stage into consideration if necessary facies maps will be updated. Thus new wells to be drilled will be directed to areas of high expectation.

Acknowledgements

Subsurface geology data were provided by TKİ, MTA and TPAO. Without well data and other information given by TPAO to TKİ organization this study would not be possible. TKİ and ÇOMÜ team thank MTA and TPAO organizations and staff for providing access to data set. Special thanks go to Ayhan Kösebalaban, İsmail Ergüder and Yaşar Ünal who supported the project and made data flow possible.

Received: 28.06.2014
Accepted: 01.11.2014
Published: June 2015

References

Akartuna, M. 1968. Armutlu yarımadasının jeolojisi. *İstanbul Üniversitesi Fen Fakültesi Monografiler* 20, 105 s.

Alişan, C. 1985. Trakya "I" Bölgesi'nde Umurca-1, Kaynarca-1, Delen-1 kuyularında kesilen formasyonların palinostratigrafisi ve çökelme ortamlarının değerlendirilmesi. *TPAO. Araştırma Grubu Rapor No: 386,* 60 s. Ankara (unpublished)

Atalık, E. 1992. Depositional systems of the Osmancık formation in the Thrace Basin. Doktora Tezi, Orta Doğu Teknik Üniversitesi, 343 s. Ankara (unpublished).

Barka, A. 1981. Seismo-tectonic aspect of the North Anatolian Fault Zone: Ph.D thesis, University of Bristol, Bristol England, 333 p

Barka, A., Hancock, P. 1984. Neotectonic deformation patterns in the convex-northwards arc of the North Anatolian Fault Zone. In: Dixon, J.E., Robertson, A.H.F. (Eds), The Geological Evolution of the Eastern Mediterranean Region. *Geol. Soc. London,* pp. 763-773.

Batı, Z., Erk, S., Akça, N. 1993. Trakya Havzası Tersiyer Birimleri'nin Palinomorf, Foraminifer ve Nannoplankton Biyostratigrafisi. *TPAO Araştırma Grubu Rapor* No: 1947, 92 s. Ankara (unpublished).

Batı, Z., Alişan, C., Ediger, V.Ş., Teymur, S., Akça, N., Sancay, H., Ertuğ, K., Kirici, S., Erenler, M., Aköz, Ö. 2002. Kuzey Trakya Havzası'nın Palinomorf, Foraminifer ve Nannoplankton Biyostratigrafisi, *Türkiye Stratigrafi Komitesi Çalıştayı (Trakya Bölgesi'nin Litostratigrafi Adlamaları) Özleri*, s. 14.

Burke, W. F., Uğurtaş, G. 1974. Seismic interpretation of Thrace Basin, in H. Okay and E. Dileköz, eds., Proceeding of second petroleum congress of Turkey: *Association of Turkish Petroleum Geologists,* 227-248

Bürkan, K. 1992 1:50 000 ölçekli Trakya F29 c ve d paftaları jeoloji haritası, *Türkiye Petrolleri Anonim Ortaklığı Arama Grubu Arşivi.*

Çağlayan, M.A., Yurtsever, A. 1998. Burgaz-A3, Edirne-B2 ve B3; Burgaz-A4 ve Kırklareli-B4; Kırklareli-B5 ve B6; Kırklareli-C6 paftaları *Maden Tetkik ve Arama Genel Müdürlüğü*, 1:100 000 ölçekli açınsama nitelikli Türkiye jeoloji haritaları, No: 20, 21, 22, 23.

Doust, H., Arıkan, Y. 1974. The geology of the Thrace Basin, *Türkiye İkinci Petrol Kongresi Tebliğleri Kitabı*, s. 119-136.

Duman, T.M., Keçer, M., Ateş, Ş., Emre, Ö., Gedik, İ., Karakaya, F., Durmaz, S., Olgun, Ş., Şahin, H., Gökmenoğlu, O. 2004. İstanbul metropolü batısındaki (Küçükçekmece Silivri-Çatalca yöresi) kentsel gelişme alanlarının yer bilim verileri, *Maden Tetkik ve Arama Genel Müdürlüğü* Özel Yayın Serisi- 3.

Ediger, V. Ş. 1982. Kuleli Babaeski sırtının (KB Trakya) Paleo-ortamsal incelemesi ve Kuzey Trakya havzasının hidrokarbon potansiyelinin değerlendirilmesinde yeni yaklaşım: *Türkiye Petrolleri Anonim Ortaklığı Rapor* No: 1995, 194 s. Ankara (unpublished).

Ediger, V. Ş. 1988. Biga Yarımadası'ndaki kömürlü birimlerden alınan örneklerin palinolojik analizi, *Türkiye Petrolleri Anonim Ortaklığı Araştırma Merkezi Grubu Rapor* No: 809, Ankara (unpublished)

Ediger, V.Ş., Alişan, C. 1989. Tertiary fungal and algal palynomorph biostratigraphy of the northern Thrace basin, Turkey. *Review of Palaeobotany and Palynology* 58, 139-161.

Fourquin, C. 1979. L'Anatolie du nord-ouest, marge méridionale du continent Européen, historie paléogéographique, tectonique et magmatique durant le Secondaire et le Tertiaire: *Bulletin de la Société Géologique de France,* 17, 1059-1070.

Gerhard, J.E., Alişan, C. 1987. Palynostratigraphy, paleoecology, and visual organic geochemistry Turgutbey-2, Değirmencik-3 and Pancarköy-1, Thrace Basin, Turkey. *Türkiye Petrolleri Anonim Ortaklığı Araştırma Merkezi Grubu Rapor* No: 983, 33 s. Ankara (unpublished).

Gökçen, N. 1971. Güneydoğu Trakya'nın Paleojen stratigrafisinde ostracod'lar açısından yeni görüşler. *Türkiye 1. Petrol Kongresi Bildirileri Kitabı*, 81-85.

Görür, N., Okay, A.I. 1996. Fore-arc origin of the Thrace basin, northwest Turkey. *Geologische Rundschau,* 85, 662-668.

İmik, M. 1988. Kırklareli-C2-3 Paftası ve İzahnamesi. *Maden Tetkik ve Arama Genel Müdürlüğü* 1:100 000 ölçekli Türkiye Jeoloji Haritaları, , 10 s.

Kara, H., Tuncalı, E., Narin, R., Gürsoy, B., Dümenci, S. 1996. Trakya Tersiyer kömür havzası raporu. *Maden Tetkik ve Arama Genel Müdürlüğü Rapor* No: 9974, Ankara, (unpublished).

Kasar, S., Bürkan, K., Siyako M., Demir, O. 1983. Tekirdağ- Şarköy-Keşan-Enez bölgesinin jeolojisi ve hidrokarbon olanakları. *Türkiye Petrolleri Anonim Ortaklığı Arama Grubu Rapor* No: 1771, 71 s. Ankara (unpublished).

Kasar, S., Eren, A. 1986. Kırklareli-Saray-Kıyıköy bölgesinin jeolojisi. *Türkiye Petrolleri Anonim Ortaklığı Arama Grubu Rapor* No: 2208, 45 s. Ankara (unpublished)

Kasar, S. 1987. Edirne-Kırklareli-Saray (Kuzey Trakya) bölgesinin jeolojisi. *Türkiye 7. Petrol Kongresi Tebliğleri Kitabı,* 281-291.

Keskin, C. 1974. Kuzey Trakya Havzası'nın Stratigrafisi. *Türkiye İkinci Petrol Kongresi Tebliğleri Kitabı,* 137 – 163.

Ketin, İ. 1957. Kuzey Anadolu Deprem Fayı. *İstanbul Teknik Üniversitesi Dergisi*, İstanbul Türkiye, no. 15, 49-52

Ketin, İ. 1976. San Andreas ve Kuzey Anadolu fayları arasında bir karşılaştırma: *Türkiye Jeoloji Kurumu Bülteni,* 19, 149-154

Kopp, K.O., Pavoni, N., Schindler, C. 1969. Geologie Thrakiens IV: Das Ergene-Becken. Beih zum Geol. Jahrb., Heft 76, 136 s., Hannover.

Lebküchner, R.F., 1974. Orta Trakya Oligosen'nin jeolojisi hakkında. *Maden Tetkik ve Arama Enstitüsü Dergisi* 83, 1-29, Ankara.

N.V. Turkse Shell. 1969. AR/NTS/837, 838 ve 839 hak sıra no'lu arama ruhsatlarına ait terk raporu. *Türkiye Petrolleri Anonim Ortaklığı Arama Grubu Rapor* No: 1468. Ankara (unpublished).

Öztunalı, Ö., Üşümezsoy, Ş. 1979. Istranca Masifi'nin "Çekirdek" kayaçları ve petrojenetik evrimleri. *Türkiye Jeoloji Kurumu-İstanbul Üniversitesi Yerbilimleri Fakültesi, Altınlı Sempozyumu,* 37-44.

Perinçek, D. 1987. Trakya Havzası Renç Fay Zonunun Sismik Özellikleri. *Türkiye 7. Petrol Kongresi Bildirileri,* 11-20

Perinçek, D. 1991, Possible strand of the North Anatolian Fault in the Thrace Basin, Turkey – An Interpretation. *AAPG Bulletin* 75, 241 – 257.

Perinçek, D. 2006. Marmara - Trakya havzalarının Yapısal Evrimi ve Fayların Zamansal Gelişimi. Çanakkale Onsekiz Mart Üniversitesi, Genç Jeo (Jeoloji Öğrenci Topluluğu) Çanakkale, 27-38

Perinçek, D., Karslıoğlu, Ö. 2007. Çanakkale Boğazı'nın oluşumu ve Kuvaterner yaşlı birimlerin dağılımında fayların rolü. 60. *Türkiye Jeoloji Kurultayı Bildiri Özetleri,* 16-22 Nisan, Ankara, 478-479.

Perinçek, D. 2010*a*. Trakya Havzası'nın Linyit İmkanları *TKİ Rapor*, Ocak 2010, 55 s. Ankara (unpublished).

Perinçek, D. 2010*b*. Trakya Havzası'nın Linyit İmkanları *TKİ Rapor*, Mart 2010, 37 s. Ankara (unpublished).

Perinçek, D. 2010*c*. Trakya Havzası'nın Linyit İmkanları *TKİ Final Rapor*, Aralık 2010, 51 s. Ankara (unpublished).

Perinçek, D., Ataş, N., Erensoy, E., Karatut, Ş. Kösebalaban, A., Ergüder İ., Ünal., Y. 2011. Trakya Havzası'nın linyit potansiyeli ve bunu kontrol eden jeolojik faktörler. *64. Türkiye Jeoloji Kurultayı Bildiri Özetleri*, 16-25-29 Nisan 2011, Ankara, 93-94

Saner, S. 1985. Saros Körfezi dolayının çökelme istifleri ve tektonik yerleşimi, Kuzeydoğu Ege Denizi, Türkiye. *Türkiye Jeoloji Kurumu Bülteni*, 28, 1-10.

Saraç, G. 1987. Kuzey Trakya bölgesinde Edirne-Kırklareli-Saray-Çorlu-Uzunköprü Derekebir yörelerinin memeli paleo-faunası, Ankara Univ., Fen Bil. Enst., Jeo. Müh. Anabilim Dalı, Yük. Lisans Tezi. Ankara (unpublished).

Siyako, M. 2005. Trakya ve yakın çevresinin Tersiyer stratigrafisi. *Türkiye Petrolleri Anonim Ortaklığı Arama Grubu Rapor* No: 4608, 104 s. Ankara (unpublished)

Siyako, M. 2006*a*. Trakya Havzası'nın linyitli kumtaşları, *Maden Tetkik ve Arama Genel Müdürlüğü Dergisi*, 132, 63 – 73.

Siyako, M. 2006*b*. Trakya Bölgesi Litostratigrafi Birimleri (Tersiyer Bölümü). *Stratigrafi Komitesi, Litostratigrafi Birimleri Serisi-2. Maden Tetkik ve Arama Genel Müdürlüğü yayını*. 70 s

Siyako, M., Kasar, S. 1985. Edirne-Lalapaşa-Kırklareli bölgesinin jeolojisi. *Türkiye Petrolleri Anonim Ortaklığı Arama Grubu Rapor* No: 2062, 78 s. Ankara (unpublished)

Siyako, M., Bürkan, K., Okay, A.I. 1989. Biga ve Gelibolu yarımadalarının Tersiyer jeolojisi ve hidrokarbon olanakları. *Türkiye Petrol Jeologları Derneği Bülteni*, 1, 183-199.

Sümengen, M., Terlemez, İ. 1991. Güneybatı Trakya yöresi Eosen çökellerinin stratigrafisi. *Maden Tetkik Arama Dergisi,* 113, 17-30.

Sütçü, E., Paker, S., Nurlu, Y., Kumtepe, P., Cengiz, T. 2009. Tekirdağ-Malkara havzasında CBS yöntemleriyle potansiyel kömür sahalarının belirlenmesine yönelik iki değişkenli istatistiksel yaklaşım. *TMMOB Coğrafi Bilgi Sistemleri Kongresi*, 02-06 Kasım 2009, İzmir, 8 s.

Şengüler, İ. 2008. Trakya Havzası Kömür Aramaları Projesi Raporu (2005-2006-2007 Yılı Sondajları), *Maden Tetkik Arama Genel Müdürlüğü Rapor* No: 11069, Ankara, (unpublished).

Şengüler, İ. 2013. Ergene (Trakya) Havzası'nın jeolojisi ve kömür potansiyeli. *Maden Tetkik Arama Genel Müdürlüğü Doğal Kaynaklar ve Ekonomi Bülteni* Sayı 16, 109-114

Şengüler, İ., Toprak, S., Kara, H., Öner, A., Tuncalı, E., Kır, N. 2000. Güney Trakya Bölgesindeki Kömürlerin Petrografik İncelemesi ve Ortamsal Yorumu. *Türkiye 12. Kömür Kongresi Bildiriler Kitabı*, Karadeniz Ereğlisi, Zonguldak. 173-180.

Şengüler, İ., Akman, Ü., Taka, M., Dümenci, S., Kalkan, İ., Kır, N., Sulu, K. 2003. Güney Marmara Neojen Havzalarının Kömür Potansiyeli. *56. Türkiye Jeoloji Kurultayı Bildiri Özleri Kitabı*, Ankara, 212-213,

Şentürk, K. Sümengen, M., Terlemez, İ., Karaköse, C. 1998*a*. Çanakkale- D3 Paftası *Maden Tetkik ve Arama Genel Müdürlüğü,* 1:100 000 ölçekli açınsama nitelikli Türkiye jeoloji haritaları, 63.

Şentürk, K. Sümengen, M., Terlemez, İ., Karaköse, C. 1998*b*. Çanakkale D4 Paftası *Maden Tetkik ve Arama Genel Müdürlüğü,* 1:100 000 ölçekli açınsama nitelikli Türkiye jeoloji haritaları, 64.

Taner, F., Çağatay, A. 1983. Istranca masifindeki maden yataklarının jeolojisi ve minerolojisi. *Türkiye Jeoloji Kurumu Bülteni,* Ankara, Türkiye, v.26, 31-40

Temel, R.Ö. ve Çiftçi, N.B. 2002. Gelibolu Yarımadası, Gökçeada ve Bozcaada Tersiyer çökellerinin stratigrafisi ve ortamsal özellikleri. *Türkiye Petrol Jeologları Derneği Bülteni* 14, 17-40.

Turgut, S., Siyako, M., Dilki, A. 1983. Trakya Havzası'nın jeolojisi ve hidrokarbon olanakları. *Türkiye Jeoloji Kongresi Bülteni*, 4, 35-46.

Turgut, S., Türkaslan, M., Perinçek, D. 1991. Evolution of the Thrace sedimentary basinand its hydrocarbon prospectivity. Spencer AM (ed) Generation, accumulation, and production of Europe's hydrocarbons. *Special Publication of Eurapean Association of Petroleum Geoscientists*, 1, 415-437.

Turgut, S., Eseller, G. 2000. Sequence stratigraphy, tectonics and depositional history in Eastern Thrace Basin, NW Turkey. *Marine and Petroleum Geology*, 17, 61-100.

Türkecan, A., Yurtsever A. 2002. İstanbul Paftası, 1: 500 000 ölçekli Türkiye Jeoloji Haritası Serisi. *Maden Tetkik ve Arama Genel Müdürlüğü*, Ankara.

Umut, M, İmik, M., Kurt, Z., Özcan, İ., Sarıkaya H., Saraç, G. 1983. Tekirdağ, Silivri (İstanbul), Pınarhisar alanının jeolojisi. *Maden Tetkik ve Arama Genel Müdürlüğü Rapor No*: 7349. Ankara (unpublished).

Umut, M. 1988*a*. Kırklareli-C5 Paftası ve İzahnamesi, 1:100 000 ölçekli Türkiye Jeoloji Haritaları, *Maden Tetkik ve Arama Genel Müdürlüğü,* Ankara 10 s.

Umut, M. 1988*b*. Kırklareli-C4 Paftası ve İzahnamesi, 1:100 000 ölçekli Türkiye Jeoloji Haritaları, *Maden Tetkik ve Arama Genel Müdürlüğü,* Ankara 6 s.

Umut, M, İmik, M., Kurt, Z., Özcan, İ., Ateş, M., Karabıyıkoğlu M., Saraç, G. 1984. Edirne İli-Kırklareli İli-Lüleburgaz (Kırklareli İli)-Uzunköprü (Edirne İli) civarının jeolojisi.. *Maden Tetkik ve Arama Genel Müdürlüğü Rapor No:* 7604, 42 s. Ankara (unpublished).

Üşümezsoy, Ş. 1982. Igneous and metamorphic geology and mineralization of Istranca region (Geotectonic setting and mineralization of the Istranca masif). *İstanbul University Earth Sciences Review*, v.3, no. 1-2, 227-294

Ünal, O. T. 1967. Trakya jeolojisi ve petrol imkanları. *Türkiye Petrolleri Anonim Ortaklığı Arama Grubu Rapor* No: 391, 80 s. Ankara (unpublished)

Bull. Min. Res. Exp. (2015) 150: 109-120

Bulletin of the
Mineral Research and Exploration

http://bulletin.mta.gov.tr

ELEMENT ENRICHMENTS IN BITUMINOUS ROCKS, HATILDAĞ FIELD, GÖYNÜK/BOLU

Ali SARI[a*], Murad ÇİLSAL[b] and Şükrü KOÇ[a]

[a] *Ankara Üniversitesi Müh.Fak., Jeoloji Müh.Böl., 06100 Tandoğan/Ankara*
[b] *Ankara Üniversitesi Fen Bilimleri Enstitüsü Müdürlüğü İrfan Baştuğ Caddesi, 06110 Dışkapı/ANKARA*

Keywords:
C_{org}, Element Enrichment, Redox, Oxic, Suboxic, Anoxic, Sulfidic Environment.

ABSTRACT

In this study, element enrichments in bituminous rocks (bituminous shale, bituminous clays- tone and bituminous marl) of the Kabalar formation in the Hatıldağ field in Göynük town of the city of Bolu are investigated and their economic potential is discussed with regard to being a mineral deposit. Element analysis was conducted with ICP-ES (ICP emission spectrometry) and ICP-MS (ICP mass spectrometry) techniques. Organic carbon content in rocks was analyzed with Rock-Eval VI device. In pyrolysis analysis conducted on a total of 28 bituminous rocks that are collected from the Kayalık Dere measured stratigraphic section, Corg minimum and maximum are 0.40 %wt and 8.25 %wt, respectively (with average of 3,6 %wt). Major and trace elements analyzed were compared with those of Peru Continental Shelf Sediments, Namibia Continental Shelf Sediments, Gulf of California Sediments, Me- diterranean Sapropels, Black Sea Sapropels, Cenomanian/Turonian (C/T) Demerara Rise Anoxic Sediments and C/T Gubbio Anoxic Sediments which are known to be deposited under anoxic conditions. In the studied samples, enrichment levels of major and trace element con- tents are determined with respect to average shale. Fe, Mg, Ca and K of the major elements and As, Ba, Co, Cu, Ni, Rb, Sr, V, Zn and Zr of trace elements were found to be more enriched with respect to basins compared. Higher concentrations of Ca, Mg and Ba elements in the studied samples indicate that depositional environment in Hatıldağ is more carbonaceous and suboxic.

1. Introduction

The study area is located between Dağhacılar and Kabalar villages within boundaries of Göynük town, Bolu. In the field, Paleocene-Eocene units are exposed. Bituminous rocks cropping out in the study area are quite thick, reaching 290 meter in some places. This situation increases the economic value of the region in terms of petroleum and gas potential. It is also significant since these rocks accumulate plenty of major, trace and rare earth elements.

Some of the studies related to general geology, coal geology and bituminous shales are as follows; Şeker and Kesgin, 1991; Sarı and Sonel, 1995; Şener and Şengüler, 1998; Büyükutku et al., 2005; Sarı and Aliyev, 2005; Aliyev, et al., 2006; Sarı et al., 2007, Kara and Korkmaz, 2008; Şengüler, 2012.

The organic rocks, which are the source of today's oil deposits, were deposited in mild periods of the world history that correspond to Cambrian- late Devonian-Carboniferous, middle late Permian and

* *Corresponding author: Ali Sarı, sari@eng.ankara.edu.tr*

Cretaceous times. Bituminous rocks are deposited in much sulfurous, reducing environment, which was formed as a result of high organic productivity developing in the basin, and due to accumulation and decay of dead organisms at the bottom. In studies, it was seen that there was a systematical relationship between these bituminous rocks and the element enrichment. It was also observed that much sulfurous reducing environmental conditions that formed as a result of the accumulation and decay of dead organism at the bottom had the most significant role in element enrichments. Free metals in sulfidic environments are either bonded to an organic structure or deposited as metal sulfites and enriched in bituminous rocks. Metals that are taken into river bodies as the river flows into basin and detaches them from rocks, dissolved metals in sea water, hydrothermal solutions that comes from faults and fractures or volcanic ashes are shown as the source of metals in bituminous rocks (Mao et al., 2002; Cruse and Lyons, 2004).

The increasing oil prices in the world have forced the USA and other countries to find new sources for alternative energy within last 15 years. The need for the alternative energy have revived bituminous rocks (bituminous shale, bituminous marl and bituminous claystone) in recent years. Within this scope, the shale gas exploration, which takes important place in the agenda of big countries such as; the USA and China, have accelerated investigations in Turkey as well. In doing so; the fracturing process in Silurian Dadaş Formation of Shell Company in Diyarbakır has been completed and test studies are performed for production. Again, the oil production studies from bituminous rocks still continue in Hatıldağ/Göynük field within scope of a joint project which is carried out by Turkish Coal Enterprises (TKİ) and Turkish Petroleum Corporation (TPAO). It is especially possible to enrich elements from organic rich rocks using residual ashes which remain after retorting the oil at the surface. Bituminous rocks within this framework are very rich storage for Major, Trace and Rare Earth Elements (REE) and assessed like a mineral deposit. In near future, the source supply for elements, which will be needed by high technologies, will be spoken in the agenda of Turkey. When looking from these points of views, this investigation is important for element acquirements and source determinations. Remarkable enrichments in Si, Mn, Cr, Fe, Na, K, Ca, Mg and Ti elements and depletion in P element were observed in bituminous samples of Kayalık Stream measured stratigraphical section (MSS) in this study. Among trace elements, the enrichments of Ni, Sc, Ba, Be, Co, Cs, Hf, Sn, Sr, U, Th, Ta, V, W, Cu, Pb, As, Sb, Ag, and Se elements are generally in higher concentrations than average shale.

2. Material and Method

Bituminous rocks (bituminous shale, bituminous marl and bituminous shale) used in this study were taken from Kayalık Stream in Hatıldağ/Göynük field, and named as the Kayalık Stream MSS. 113 samples were systematically collected in Kayalık Stream MSS. Among these, 28 samples belong to bituminous rocks. Pyrolysis analysis was performed for 28 bituminous samples, which contain organic material, by using Rock-Eval VI instrument in TPAO laboratories. Minimum and maximum Total Organic Content (TOC) in rocks are 0.40 wt% and 8.25 wt%, respectively (with average value of 3.76 wt%). In order to better determine the element enrichments in the basin, both bituminous and non-bituminous rocks were separately subjected to element analyses. Inorganic chemical analyses of samples, which had been pulverized in agate mortar, were carried out in Acme Analytical Laboratories Ltd. (Canada) using ICP-ES (ICP emission spectrometry) and ICP-MS (ICP mass spectrometry) techniques. By using ICP-ES method, major and trace element concentrations were calculated in 113 samples. REE analyses were performed by ICP-MS method. Again, total sulfur, total carbon and inorganic carbon analyses were carried out in ACME Analytical Laboratories Ltd. (Canada) using Leco device in 113 samples. Element abundances obtained were compared and interpreted based on rocks; besides, their geochemical behaviors were investigated calculating correlation coefficients. Enrichment values in elements in our study area were compared with other elements in worldwide known reducing environments.

3. Geologic Setting

The basement of the study area is constituted by Lower Paleozoic Bolu granitoids which outcrops in south of Göynük basin and by metamorphic rock types (Blumenthal, 1948; Saner, 1978*a*). Blumenthal (1948) stated that Bolu granitoid basically developed in pre Upper Ordovician, but there had been other intrusions into this body. These rocks are massive, medium to fine grained granites enriched in potassium feldspar.

The oldest units in vicinity of the study area are Upper Cretaceous in age. These are formed by Seben

formation, which is composed of gray to greenish gray, limestone banded, marl and sandstone at the bottom, and by the conformably overlying Taraklı formation represented by shale, marl and sandstone. The Upper Cretaceous units are both laterally and vertically transitional with Paleocene-Eocene units. From bottom to top; these units are formed by Beşikkaya Formation Limestone Member (sandstone-marl member and limestone-marl member), Agsaklar Formation (conglomerate-sandstone member, marl member, limestone member), the overlying Hatıldağ Formation (productive bituminous shale member/ sterilized bituminous shale member), and by the Kabalar Formation (red marls consisting of sandstone and conglomerate lenses) at the top (Figure 1). Bituminous shales located in middle parts of the Hatıldağ Formation are brownish beige in color, and are sometimes intercalated with marl and claystone. Total thickness of bituminous shales is 290 m of which their thicknesses vary between 0.01-9 m.

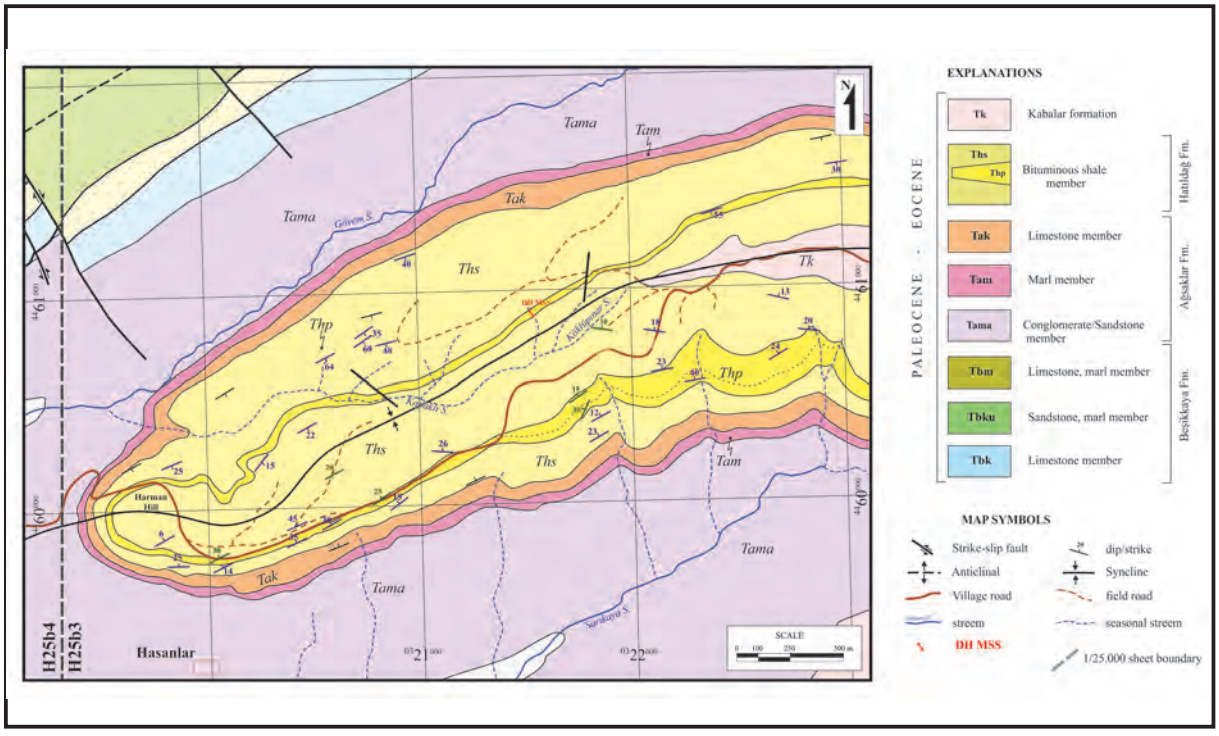

Figure 1- Geological map of the study area (Modified from Yanılmaz et al, 1980; Şengüler, 2012).

The regression of the sea which had started at the end of Upper Cretaceous from south to north also continued in Paleocene. Shallow marine limestones (Beşikkaya Formation) were deposited in Paleocene in the basin which became gradually shallow. Marine depositions have continued in a controlled way during Paleocene. Delta formations of the regressive marine and the coastal flat and coastal plain formations have controlled the rock deposition. Meandering river channel deposits, flood plain deposits and deposits with marine intercalations, which are observed in formations, indicate that the region was subjected to marine transgression in Paleocene-Eocene times. The marine transgression is distinctive by a typical sediment assemblage around Kabalar village in the study area (Saner, 1978*a*). The region also preserved its marine character in Eocene. The depth did not exceed 150-300 m in this period, and the deposition of bituminous shale, bituminous claystone and bituminous marl occurred in protected lakes behind barriers which had formed as a result of marine regression.

4. Findings and Discussion

4.1. Element Enrichments in Rocks enriched by Organic Material

Organic carbon content of bituminous rocks depends on biological productivity, prevention and sedimentation rate. Bituminous rocks are not only rich in organic material such as petroleum source rocks but also in important metals. The significant difference of metal bearing shales than petroleum sources is that they can form economic mineral deposits. Only 1%

organic carbon is enough for sulfate microorganisms to produce H_2S by breaking up the organic matter and make the environment anoxic. As a result of high amount organic matter entrance into sediment, the metal enrichments in significant amounts occur in the form of metal sulfides in periods when the groundwater is reducing/anoxic (Mao et al., 2002). Most major elements (Si, Al, Fe, K, Ca, Mg, Na, Ti, Mn and P; according to decreasing order in amount) are affected by biological processes and diagenesis. Silica is not only located in the structural lattice of clay minerals, feldspar or quartz, but also form an important component of plankton residuals such as amorphous opal. Iron is extremely sensitive in reducing environments and can participate into sediments as pyrite in the form of iron sulfide. Besides, the iron is observed as structural component on mineral grains and in the form of oxide/hydroxide layer (Canfield et al., 1992). They are located in calcium and few magnesium carbonate components. Manganese has a tendency to be reductive like iron at high Mn values of minimum oxygen water zone (Bender et al., 1977; Lewis and Luther, 2000). But it does not form stable sulfides except for special cases (Böttcher and Huckriede, 1997; Hucriede and Meischner, 1996). Trace element geochemistry of Namibia and Californian Gulf upwelling sediments have been investigated by Brongersma-Sanders et al. (1980) and Calvert and Price (1983). These investigators showed that certain trace elements such as; As, Ba, Cd, Cr, Cu, Mo, Ni, V, Zn had significantly been enriched.

Generally; metals exhibit a remarkable enrichment within laminated, organic rich facies deposited especially under euxinic conditions, and low enrichments in reverse bioturbated, organic poor facies. Based on temporal sea water data, the presence of trace element bio-accumulation in sediment composition by marine planktons and continuing regeneration processes were detected also for upwelling sediments of the Californian Gulf. As a result, the elements such as; V, U and Mo were derived from an early diagenetic source and intruded from water column into sediment by diffusion (Table 1).

Table 1- Major and Trace Element/Al Ratios on the Aged and Current Sedimentary Rocks (Brumsack, H-J., 2006).

Element	Averege Shale	Peruvian coast	Namibia mud	Gulf of California	Mediterranean sapropels	Black Sea-1	Black Sea-2	C/T Demerara rise	C/T Averege	C/T Gubbio
Si/Al	3,11	4,33	30,2	6,29	2,65	3,08	2,98	6,13	7,36	16,4
Ti/Al	0,053	0,052	0,08	0,049	0,061	0,048	0,044	0,053	0,05	0,044
Fe/Al	0,55	0,45	0,8	0,46	1,22	0,65	0,57	0,62	0,77	1,33
Mg/Al	0,18	0,28	0,38	0,2	0,39	0,3	0,28	0,24	0,22	0,23
Ca/Al	0,18	1,5	2	0,31	4,07	5,15	0,77	8,57	2,15	0,22
Na/Al	0,13	0,98	0,91	0,23	0,45	0,98	0,78	0,41	0,26	0,05
K/Al	0,34	0,28	0,39	0,29	0,25	0,3	0,3	0,26	0,28	0,37
P/Al	0,008	0,096	0,17	0,022	0,016	0,018	0,019	0,07	0,047	0,046
Ag/Al	0,008	0,12	0,148	0,042	0,12	0,079	0,076	0,73	0,73	0,78
As/Al	1,1	4,3	11	1,35	15,4	4,15	2,87	8,6	7,9	18
Ba/Al	66	69	298	121	341	174	260	155	204	3638
Bi/Al	0,015	0,045	0,08	0,03	0,044	0,07	0,06	0,042	0,065	0,39
Cd/Al	0,015	8,5	26	0,55	2,7	0,26	0,27	5,81	6,27	2,14
Co/Al	2,1	1,2	2,9	1,4	17,4	6,2	3,8	2,81	14,7	5,9
Cr/Al	10,2	24,4	72	9,4	28,3	12,2	12,8	57	41,4	33,9
Cu/Al	5,1	11,6	32	5,8	33,1	17,6	23,7	31,9	43,8	63
Mn/Al	96	52	28	41	202	129	56	42	125	23
Mo/Al	0,15	10,6	37	2,6	27,9	14,7	26,2	37,7	61,4	12,8
Ni/Al	7,7	20,2	41	8,1	54,6	16,7	24,5	60	65,2	52,4
Pb/Al	2,5	3,5	3,7	3,6	2,9	5,3	3,7	3	4,5	4
Rb/Al	16	12,3	22	15	12,1	15,6	15,7	11,2	18,1	16,7

Table 1- (continued)

Re/Al	0,11	1,12	2,25	n.d.	7,55	0,98	1,22	3,1	4,9	2,85
Sb/Al	0,17	0,5	n.d.	0,85	2,67	0,57	0,33	4,38	4	1,56
Sr/Al	34	86	181	35	200	271	59	318	106	122
Tl/Al	0,077	0,33	2,5	0,08	0,58	0,12	0,18	1,19	1,2	3,44
U/Al	0,42	2,3	28,6	1,21	4,1	3,2	3,3	4,87	6,4	2,9
V/Al	15	38	126	21,5	139	29	44	491	271	271
Zn/Al	11	24	29	18,7	25	19	18	246	459	249
Zr/Al	18	21	25,2	n.d.	24	18	15	15	18	19

4.2. Major Element Enrichments

In correlation studies of major oxides made by Al_2O_3, Al_2O_3 element gave very high positive correlation with SiO_2, Fe_2O_3, Na_2O and K_2O elements, indicating that all these elements were detritic and derived from the same source. However; Al_2O_3 gave a very high negative correlations with MgO and CaO indicating that these elements were derived from different origins, and the sources of MgO and CaO elements were carbonate in origin (Table 2).

Table 2- Correlation of major oxides of the study area.

Kayalık Stream MSS	**Corg**	**SiO_2**	**Al_2O_3**	**Fe_2O_3**	**MgO**	**CaO**	**Na_2O**	**K_2O**	**TiO_2**	**P_2O_5**	**MnO**
Corg	1,00	-0,16	-0,15	-0,25	0,10	-0,13	-0,14	-0,03	-0,16	0,07	-0,38
SiO_2		1,00	0,82	0,81	-0,50	-0,74	0,22	0,71	0,75	-0,09	0,06
Al_2O_3			1,00	0,93	-0,74	-0,44	0,67	0,56	0,97	0,05	0,27
Fe_2O_3				1,00	-0,78	-0,35	0,63	0,52	0,92	0,04	0,48
MgO					1,00	-0,13	-0,76	-0,21	-0,74	-0,41	-0,53
CaO						1,00	0,25	-0,69	-0,35	0,39	0,43
Na_2O							1,00	-0,15	0,72	0,25	0,55
K_2O								1,00	0,50	-0,19	-0,16
TiO_2									1,00	0,06	0,35
P_2O_5										1,00	0,11
MnO											1,00

The increase in Si/Al ratio expresses an increase in detritic quartz amount; however, the decrease in this amount could express an increase in clay amount. The increase in K/Al ratio presents more micaeous clay input and probably a fine grained K-feldspar increase. But, there was not observed any remarkable enrichment in K, among samples of the study area; on the contrary, there was observed some depletion in some samples. It indicates that, illite type clay in samples is niether much available, nor is the depositional environment a deep marine. In Kayalık Stream MSS samples, the enrichment of major elements with respect to Al normalized shales are in question; even, there is observed an enrichment more than 100 times in Ca and Mg elements (Figure 2). It shows that our sedimentary environment is in a system which is suitable for carbonate deposition. Similarly; high enrichments observed in Mn again originate from carbonate minerals. When major element enrichments of bituminous samples in Kayalık Stream MSS were totally studied, there were observed enrichments in Si, Mn, Cr elements ranging between 1 to 10 times. However; the enrichment amounts in Fe, Na, K and Ti elements range between 1 to 5 times, and there is depletion in P element. The remarkable point here is the enrichments up to 100 times in Ca and Mg elements. This shows that the sedimentary environment in Hatıldağ field is generally carbonated (suitable to limestone and dolomite deposition) (Figure 2). Low Si concentrations indicate that detritic silica input is extremely low in depositional environment, and the depositional environment of bituminous rock is a water column which is generally calm and stagnant.

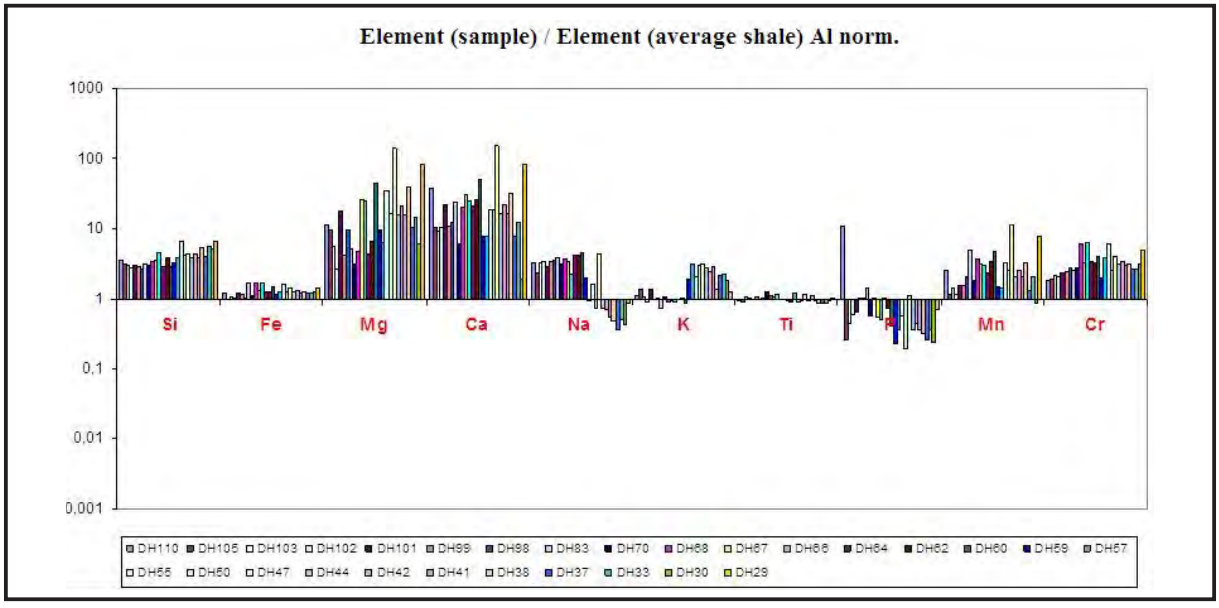

Figure 2- Enrichment of Kayalıkdere samples compared to the major elements shales which were normalized by Al.

4.3. Trace Element Enrichments

The chemical composition of the main rock is importantly affected from local or regional soil and water chemistry. Therefore; the atmospheric water in sedimentation becomes effective in element enrichment. Elements may be deposited in much sulfurous reducing depositional environments by being absorbed or as sulfides (FeS_2, PbS, CuS, CoS, ZnS, MoS_2). For this reason; some trace metals become enriched in organic rich rocks. Enrichment Factors (EF) are determined by normalizing clastic input of each trace element by Al and comparing these ratios with normal shale. This approach is used by many authors in assessing the trace element enrichments in accumulated sediments today and in the past (Calvert and Pedersen, 1993). EF is calculated as; $EF_{element}X=X/Al_{sample}$ / $X/Al_{average\ shale}$. If EF_X is greater than 1, then $X_{element}$ is enriched with respect to average shale, if it is less than 1, then it is depleted.

All trace elements (TE) are affected by stronger processes under low oxygen conditions like; the intense increase of organic carbon amount as it was in Mn/Fe redox cycle in the presence of H_2S within water column in sedimentary redox boundary or under euxinic conditions (Pratt and Davis, 1992; Calvert and Pedersen, 1993; Morse and Luther, 1999). The obtained results which are related with the characteristic trace element samples and redox environments are as follows; (1) while upwelling sediments generally become enriched in Cd and P, they become depleted in Co and Mn, (2) sapropels reflect strong sulfidization in anoxic water column and have a tendency of high enrichment in Ba, Mo, S, Re, As, Cu, Ni, Sb, and Fe, (3) upwelling systems, the distance of H_2S accumulation into sediment sea water interface, bio-accumulation intensity and its reproduction reflect the broad area of environmental conditions which play an important role for trace element accumulation, (4) the trace element content of anoxic basins is controlled by being based on the trace element presence in water column and sedimentation rate, (5) very high bio-production is the main key which transforms oxic environment into anoxic environment (Brumsack, 2006). One of the most significant discoveries related with trace element behaviors in oceans is that these elements occur within processes of biologic cycle (Bruland, 1983). Pleistocene sapropels consist of Co, Cu, Cr, Ni, and V metals, and Cd, Mo, Re, Sb, Tl and U metals in fewer amounts, and Bi element in much fewer amount (Brumsack 1989; Hatch and Leventhal, 1992; Calvert and Pedersen, 1993). These elements are deposited either as sulfides (especially iron sulfides) or as connected to an organic matter (Calvert et al., 1985; Jacobs et al., 1985). Some metals (Mo, U, V) may accumulate into the sediment by diffusion or after reduction during early diagenesis (Brumsack and Gieskes, 1983; Shaw et al., 1990).

In samples belonging to the study area, the enrichments of Ni, Sc, Ba, Be, Co, Cs, Hf, Sn, Sr, U, Th, Ta, V, W, Cu, Pb, As, Sb, Ag and Se elements mainly show an increase compared to average shale. In addition; Ni, Sr, W, As, Ag and Se elements become enriched 100 times more than average shale

in some samples (Figure 3). Some elements such as; Ni, Co, U, V, Pb, Cu elements to show very high enrichment probably depends on the presence of C_{org}. High Ag enrichments might be due to the retention in silicate bio-geochemical cycle, the particles in groundwater or due to the adsorption in sulfide and diagenetic Selenides (Ndung'u et al., 2001; McKay and Pedersen, 2002; Crusius and Thomson, 2003).

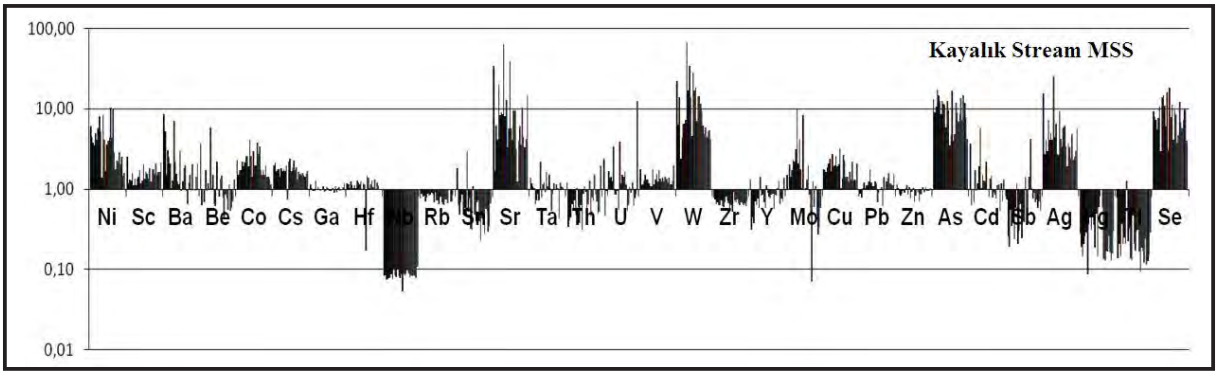

Figure 3- Enrichment of Kayalıkdere samples trace elements compared to the normalized shale which were normalized by Al.

4.4. The Comparison of Element Enrichments with Reducing Environments in the World

The enrichment values of major and trace elements of the Kayalık Stream MSS were compared with element enrichments of Peru Coastal Shelf Sediments, Namibia (Africa) Coastal Shelf Sediments, Mediterranean Sapropels, Black Sea Sapropels, Cenomanian/Turonian Demerara Rise Sediments and Cenomanian/Turonian Gubbio Sediments (Table 3, Figure 4). Considering average enrichments, it was seen that there were enrichments in different element accumulations of the regions, which had been deposited in organic matter rich, anoxic/euxinic environments. These differences are related with the variability of redox conditions of depositional environments. For instance; as the organic matter accumulation will be low or absent in oxic conditions, the conditions (organic matter or sulfides) in which metals would be accumulated will not develop. Elements in semi-sulfidic environments are deposited in the form of organic ligands by being attached to organic structures. Elements in sulfidic environments prefer being deposited in the form of sulfides (FeS_2, PbS, CuS, MoS_2 etc.). Especially; bituminous samples in the study area to display element enrichments in wide range indicates non-homogeneity of the depositional environment of Hatıldağ field and the frequent variation of redox environmental conditions. Elements like; Mo and Co, which generally show enrichment with organic carbon, in Hatıldağ field samples, are quite lower than enrichment rates of sediments in other regions. This indicates that, the depositional environment in Hatıldağ field is less sulfidic/anoxic compared to other environments.

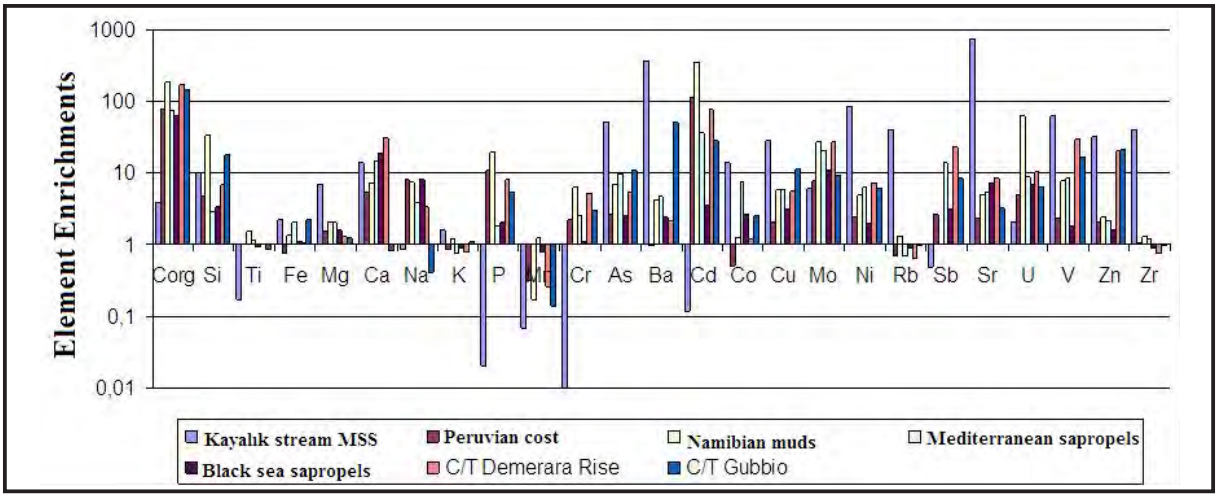

Figure 4- In Kayalıkdere major and trace element enrichment's averages in comparison with other reducing conditions of the world.

Table 3- Major and trace element enrichments of Peruvian Coast, Namibia muds, Mediterranean and Black Sea sapropels, C/T Demerara Rise and C/T Gubbio organic rich rocks of the studied samples.

Major Element	**Kayalık Stream MMS**	**Peruvian Coast**	**Namibian Muds**	**Mediterranean sapropels**	**Black Sea sapropels**	**C/T Demerara Rise**	**C/T Gubbio**
C_{org}	3,76	76,96	185,22	73,91	63,91	175,22	147,39
Si	10,1	4,75	33,10	2,90	3,38	6,72	17,97
Ti	0,17	0,98	1,51	1,15	0,91	1	0,83
Fe	2,2	0,76	1,36	2,07	1,10	1,05	2,25
Mg	6,98	1,49	2,03	2,08	1,6	1,28	1,23
Ca	13,84	5,43	7,24	14,73	18,64	31,02	0,80
Na	0,85	8,17	7,58	3,75	8,17	3,42	0,42
K	1,56	0,84	1,17	0,75	0,90	0,78	1,11
P	0,02	10,97	19,43	1,83	2,06	8	5,26
Mn	0,07	0,32	0,17	1,24	0,79	0,26	0,14
Cr	0,01	2,17	6,4	2,52	1,08	5,07	3,01
Trace Element	**Kayalık Stream MMS**	**Peruvian Coast**	**Namibian Muds**	**Mediterranean sapropels**	**Black Sea sapropels**	**C/T Demerara Rise**	**C/T Gubbio**
As	51	2,65	6,77	9,48	2,55	5,29	11,08
Ba	370	0,95	4,11	4,70	2,4	2,14	50,18
Cd	0,12	113,33	346,67	36	3,47	77,47	28,53
Co	14	0,51	1,22	7,33	2,61	1,18	2,48
Cu	29	2,06	5,69	5,88	3,13	5,67	11,2
Mo	6	7,71	26,91	20,29	10,69	27,42	9,31
Ni	85	2,38	4,82	6,42	1,96	7,06	6,16
Rb	40	0,70	1,26	0,69	0,89	0,64	0,95
Sb	0,5	2,67	n.d.	14,24	3,04	23,36	8,32
Sr	755	2,29	4,83	5,33	7,23	8,48	3,25
U	2	4,97	61,84	8,86	6,92	10,53	6,27
V	64	2,34	7,75	8,55	1,78	30,22	16,68
Zn	32	2,02	2,44	2,11	1,6	20,72	20,97
Zr	40	1,05	1,26	1,2	0,9	0,75	0,95

Major and trace elements in samples of the study area, normalized by Al, were compared with elements deposited under other anoxic/euxinic conditions in the world. Thus, there were observed enrichments generally in the concentration of Ca, Mg, K, Cr, Sr and Ba elements in Kayalık Stream MSS. Especially; the concentrations of Ca, Ba and Mg elements were estimated quite high (Figures 4 and 5, Table 4). This indicates that, redox conditions of the depositional environment in Hatıldağ field is generally subjected to oxic/dioxic conditions. The basin is quite carbonated and its redox condition is less sulfidic compared to other environments. The high carbonate and dolomite contents in studied bituminous samples also support this fact.

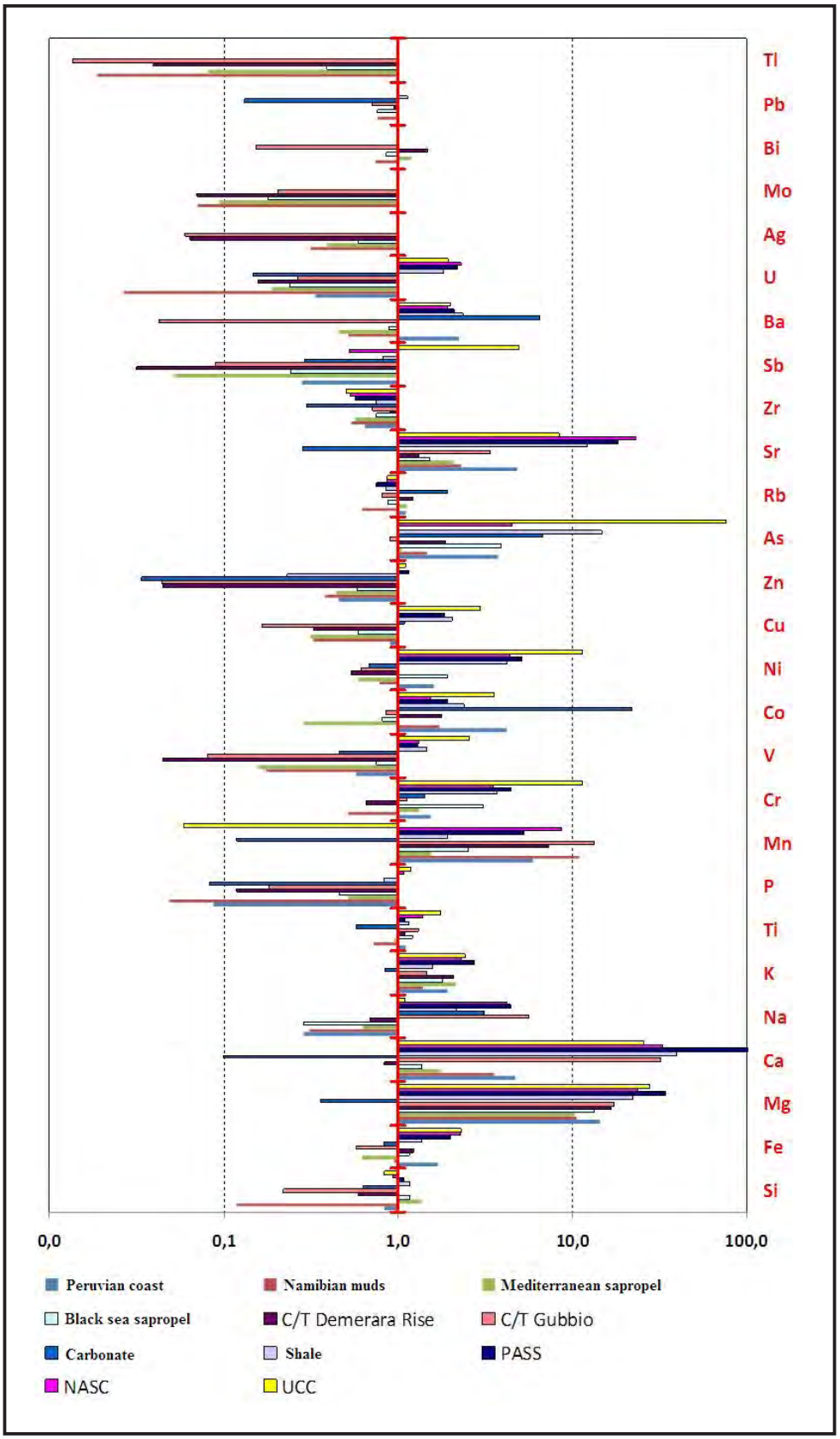

Figure 5- Kayalıkdere's bituminous samples enrichments based on Peruvian Coast, Namiby Mud, Mediterranean Sapropel, Black Sea Sapropel, the C/T Demerara Rise, C/T Gubbio, carbonate, shale, PASS, NASCAR and UCC enriched samples.

Table 4- Average enrichment values of elements in Kayalık Stream MSS with respect to other elements in reducing environment in the world.

	Elem./ Al	[Element (DH)/Al] / [Element (Other reducing environments)/Al]										
El.	**DH ÖSK**	**Peru Coast**	**Namibian mud.**	**Mediterranean sapropels**	**Black Sea sapropels**	**C/T Demera. Rise**	**C/T Gubbio**	**Carbonate**	**Shale**	**PASS**	**NASC**	**UCC**
Si	3,61	0,83	0,12	1,36	1,17	0,59	0,22	0,63	1,16	1,09	0,94	0,83
Fe	0,76	1,69	0,95	0,62	1,17	1,23	0,57	0,84	1,39	1,99	2,28	2,32
Mg	4,03	14,38	10,60	10,32	13,42	16,78	17,50	0,36	22,37	34,59	23,79	27,81
Ca	7,12	4,75	3,56	1,75	1,38	0,83	32,39	0,10	39,58	103,67	33,17	25,79
Na	0,28	0,29	0,31	0,63	0,29	0,69	5,65	3,14	2,17	4,45	4,19	1,10
K	0,54	1,93	1,39	2,16	1,80	2,08	1,46	0,85	1,59	2,76	2,30	2,42
Ti	0,06	1,11	0,72	0,95	1,21	1,09	1,32	0,58	1,16	1,09	1,40	1,76
P	0,01	0,09	0,05	0,52	0,46	0,12	0,18	0,08	0,83	0,99	1,09	1,18
Mn	0,03	5,92	11,00	1,54	2,57	7,33	13,39	0,12	1,92	5,29	8,69	0,06
Cr	0,00	1,55	0,52	1,33	3,10	0,65	1,13	1,43	3,72	4,44	3,50	11,50
V	21,91	0,58	0,17	0,16	0,76	0,04	0,08	0,46	1,46	1,29	1,33	2,59
Co	5,04	4,20	1,74	0,29	0,81	1,79	0,85	21,90	2,40	1,93	1,55	3,58
Ni	32,30	1,60	0,79	0,59	1,93	0,54	0,62	0,68	4,19	5,19	4,40	11,47
Cu	10,45	0,90	0,33	0,32	0,59	0,33	0,17	1,10	2,05	1,85	n.a.	2,97
Zn	11,03	0,46	0,38	0,44	0,58	0,04	0,04	0,03	0,23	1,15	n.a.	1,10
As	16,18	3,76	1,47	1,05	3,90	1,88	0,90	6,80	14,71	n.a.	4,50	76,63
Rb	13,66	1,11	0,62	1,13	0,88	1,22	0,82	1,91	0,85	0,75	0,86	0,87
Sr	414,11	4,82	2,29	2,07	1,53	1,30	3,39	0,29	12,18	18,29	23,04	8,41
Zr	2,66	0,65	0,54	0,57	0,75	0,91	0,72	0,30	0,75	0,57	0,54	0,51
Sb	13,59	0,28	n.a.	0,05	0,24	0,03	0,09	0,29	0,82	n.a.	0,53	4,96
Ba	155,14	2,25	0,52	0,45	0,89	1,00	0,04	6,52	2,35	2,11	1,93	2,00
U	0,77	0,34	0,03	0,19	0,24	0,16	0,27	0,15	1,84	2,20	2,29	1,96
Ag	0,05	n.a.	0,32	0,39	0,59	0,06	0,06	n.a.	n.a.	n.a.	n.a.	n.a.
Mo	2,64	n.a.	0,07	0,09	0,18	0,07	0,21	n.a.	n.a.	n.a.	n.a.	n.a.
Bi	0,06	n.a.	0,75	1,20	0,85	1,50	0,15	n.a.	n.a.	n.a.	n.a.	n.a.
Pb	2,84	n.a.	0,77	0,98	0,77	0,95	0,71	0,13	1,14	n.a.	n.a.	n.a.
Tl	0,05	n.a.	0,02	0,08	0,39	0,04	0,01	n.a.	n.a.	n.a.	n.a.	n.a.

5. Results

As a result of correlation studies of major oxides made by Al_2O_3, quite high positive correlations were obtained in SiO_2, Fe_2O_3, Na_2O and K_2O elements. This indicates that, all these elements are continental and derived from the same origin. Al_2O_3 to give quite high negative correlations with MgO and CaO shows that these elements are carbonate in origin.

The enrichments of Ni, Sc, Ba, Be, Co, Cs, Hf, Sn, Sr, U, Th, Ta, V, W, Cu, Pb, As, Sb, Ag, and Se elements among trace elements mostly show an increase with respect to average shale in bituminous samples of the Kayalık Stream MSS.

Enrichments in Ca and Mg elements in bituminous samples of the Kayalık Stream MSS are nearly 100 times. While there are observed variations in enrichments between 1 to 10 times in Si, Mn and Cr

elements, the enrichment values in Fe, Na, K and Ti elements vary between 1 to 5 times. However, there was observed depletion in P element.

Element enrichments of the Kayalık Stream MSS were normalized by Al and compared with Peruvian Coast, Namibia muds, Mediterranean sapropels, Black Sea sapropels, C/T Demerara Rise, C/T Gubbio, Carbonate average, Average Shale, PASS, NASC and with UCC rocks. As a result, enrichments generally in Mg, Ca, K, Cr, Sr and Ba concentrations were observed. It indicates that, the depositional environment in Hatıldağ Field is quite carbonated and its redox conditions are less sulfidic with respect to other anoxic/euxinic basin conditions. The high carbonate and dolomite contents in studied samples also support this fact.

Acknowledgements

This study has been carried out with contributions of Turkish Coal Enterprises (TKİ). We would like to thank to Vice General Director Dr. Abdurrahman Murat, Mustafa Özdingiş and to all other people who took part while performing this investigation.

Received: 13.02.2015
Accepted: 25.02.2015
Published: June 2015

References

Aliyev, S., Sarı A., Koç, S., 2006. Investigation of Organic Carbon and Iron Group Elements in the Bituminous Rocks. *Energy Sources*, part A. 28,1461-1472pp.

Bender, M.L., Klinkhammer, G.P., Spencer, D.W., 1977. Manganese in seawater and marine manganese balance. *Deep-Sea Res*. 24, 799– 812pp.

Böttcher, M.E., Huckriede, H., 1997. First occurence and stable isotope composition of authigenic g-MnS in the central *Gotland Deep (Baltic Sea). Mar. Geol.* 137, 201–205pp.

Brongersma-Sanders, M., Stephan, K.M., Kwee, T.G., de Bruin, M., 1980. Distribution of minor elements in cores from the Southwest Africa shelf with notes on plankton and fish mortality. Mar.Geol. 37, 91–132pp.

Bruland, K.W., 1983. Trace elements in sea water. In: Riley, J.P., Chester, R. (Eds.), *Chemical Oceanography.* Academic Press, London, UK, 398p.

Brumsack, H.J., 1989. Geochemistry of recent TOC-rich sediments from the Gulf of California and the Black Sea. *Geologische Rundschau*, 78, 851-882pp.

Brumsack, H.J., 2006. The trace metal content of recent organic carbon-rich sediments: Implications for Cretaceous black shale formation, Paleogeography, Paleoclimatology, *Paleoecology*. 232, 344-361pp.

Brumsack, H.J., Gieskes, J.M., 1983. Interstitial water trace-metal chemistry of laminated sediments from the Gulf of California, *Mexico. Mar. Chem.* 14, 89– 106pp.

Blumenthal, M., 1948. Bolu civarı ile Aşağı Kızılırmak mecrası arasındaki Kuzey Anadolu silsilelerinin jeolojisi: *Mine Research and Exploration Institute Publications*, B-13, Ankara, Turkey.

Büyükutku, A,G., Sarı, A., Karaçam,A., 2005. The reservoir potential of the Eocene carbonates in the Bolu Basin, West of Turkey . *Journal of Petroleum Science and Engineering.* 49, 79-91pp.

Calvert, S., Price, N.B., 1983. Geochemistry of Namibian shelf sediments. In: Suess, E., Thiede, J. (Eds.), Coastal Upwelling. *Plenum Press*, 337– 369pp.

Calvert, J. G., Lazrus, A. L., Kok, G. L., Heikes, B. G., Walega, J. G., Lind, J. A., Cantrell, C. A., 1985. Chemical mechanisms of acid generation in the troposphere. *Nature*. 317, 27-35pp.

Calvert, S.E., Pedersen, T.F., 1993. Geochemistry of Recent oxic and anoxic marine sediments: implications for the geological record. *Marine Geology*. 113, 67– 88pp.

Canfield, D.E., Raiswell, R., Bottrell, S., 1992. The reactivity of sedimentary iron minerals toward sulfide. *Am. J. Sci*. 292, 659– 683pp.

Cruse, A.M., Lyons, T.W., 2004. Trace metal records of regional paleoenvironmental variability in Pennsylvanian (Upper Carboniferous) black shales. *Chemical Geology.* 206, 319–345pp.

Crusius, J., Thomson, J., 2003. Mobility of authigenic rhenium, silver, and selenium during postdepositional oxidation in marine sediments. *Geochimica et Cosmochimica Acta*. 67, 265–273pp.

Hatch, J.R., Leventhal, J.S., 1992, Relationship between inferred redox potential of the depositional environment and geochemistry of the Upper Pennsylvanian (Missourian) Stark Shale Member of the Dennis Limestone, Wabaunsee County, Kansas, U.S.A. *Chemical Geology*. 99, 65–82pp.

Helz, G.R., Miller, C.V., Charnock, J.M., Mosselmans, J.F.W., Pattrick, R.A.D., Garner, C.D., Vaughan, D.J., 1996. Mechanism of molybdenum removal from the sea and its concentration in black shales: EXAFS evidence. *Geochimica et Cosmochimica Acta*. 60, 3631–3642pp.

Huckriede, H., Meisschner, D., 1996. Origin and environment of manganese-rich sediments within black-shale basins. Geochimica et Cosmochimica Acta. 60,1399-1413pp.

Jacobs, L., Emerson, S., Skei, J., 1985. Partitioning and transport of metals across the O2/H2S interface in a permanently anoxic basin: Framvaren Fjord, Norway. *Geochimica et Cosmochimica Acta*. 49, 1433–1444pp.

Kara,G. R., Korkmaz S., 2008. Element contents and organic matter-element relationship of The Tertiary oil shale deposits in Northwest Anatolia, Turkey", *Energu & Fuels,* 22,3164-3173pp.

Lewis, B.L., Luther, G.W., 2000. Processes controlling the distribution and cycling of manganese in the oxygen minimum zone of the Arabian Sea. *Deep-Sea Res.* Part II. 47, 1541– 1561pp.

Mao, J., Lehmann, B., Du, A., Zhang, G., Ma, D., Wang, Y., Zeng, M., and Kerrich, R., 2002, Re-Os dating of polymetallic Ni-Mo-PGE-Au mineralization in Lower Cambrian black shales of South China and its geological signifi cance: *Economic Geology and the Bulletin of the Society of Economic Geologists*. 97, 1051–1061pp.

McKay, J.L., Pedersen, T.F., 2002. Accumulation of redox-sensitive trace metals in continental margin sediments and their paleoapplications. Eos Trans. AGU, 83(4), *Ocean Sciences Meet. Suppl.* Abstract OS32B-124.

Morse, J.W., Luther III, G.W., 1999. Chemical influences on trace metal-sulfide interactions in anoxic sediments. *Geochimica et Cosmochimica Acta.* 63, 3373–3378pp.

Ndung'u, K., Thomas, M.A., Flegal, A.R., 2001. Silver in western equatorial and South Atlantic Ocean. *Deep-Sea Res*. Part II. 48, 2933–2945pp.

Pratt, L.M., Davis, C.L., 1992. Intertwined fates of metals, sulfur, and organic carbon in black shales. In: Pratt, L.M., Comer, J.B., Brassell, S.C. (Eds.), Geochemistry of Organic Matter in Sediments and Sedimentary Rocks. SEPM Short Course Notes. 27,1– 27pp.

Saner, S. 1978*a*. Geology and the environments of deposition of Geyve-Osmaneli- Golpazarı-Taraklı area. *Journal of the Faculty of Science of Istanbul University*, B 43, 63–91pp.

Sarı, A., Sonel, N., 1995. Kayabaşı (Göynük-Bolu) Yöresinin Bitümlü Şeyl İncelemeleri. *Türkiye Jeoloji Bülteni*. 2, 39-49pp.

Sarı, A., Aliyev,S.A., 2005. Source Rock Evaluation of The Lacustrine Oil Shale Bearing Deposits, Göynük/ Bolu,Turkey. *Energy Sources*.27, 271-279pp.

Sarı, A., Aliyev, S.A., Koralay,B., 2007. Source Rock Evaluation of the Eocene Shales in the Gökçesu Area (Bolu/Turkey). *Energy Sources*, Part A.29,1025-1039pp.

Şeker, H., Kesgin,Y., 1991. Geology and petroleum possibilities of around Nallıhan Mudurnu-Senen-Beypazarı regions. TPAO report no: 2907.

Şener, M., Şengüler, I. 1998. Geological, mineralogical and geochemical characteristics of oil shale bearing deposits in the Hatildag oil shale field, Göynük, *Turkey. Fuel*, 8, 871-880pp.

Şengüler, İ., 2012. Hatıldağ and Himmetoğlu (Göynük/ Bolu) Civarının Stratiğrafisi ve Bitümlü Şeyl Oluşumları. *TPJD Bülteni*, 24, 7-21pp.

Shaw, T.J., Gieskes, J.M., Jahnke, R.A., 1990. Early diagenesis in differing depositional environments: the response of transitions metals in pore water. *Geochimica et Cosmochimica Acta*, 54, 1233–1246pp.

Yanılmaz, E., Taka, M., Şengüler, İ. and Sümer, A., 1980. Göynük (Bolu) bitümlü şist sahası hakkında rapor. *Maden Tetkik ve Arama Genel Müdürlüğü Rapor* No: 6993, Ankara, (unpublished).

BULLETION OF THE MINERAL RESEARCH AND EXPLORATION

Foreign Edition 2015 150

CONTENTS

Bull. Min. Res. Exp. (2015) 150: 121-130

Bulletin of the
Mineral Research and Exploration

http://bulletin.mta.gov.tr

HALLOYSITE INTERCALATION OF NORTHWEST ANATOLIA

Bülent BAŞARA[a*] and Saruhan SAKLAR[a]

[a] *Maden Tetkik Arama Genel Müdürlüğü, Maden Analizleri ve Teknoloji Daire Başkanlığı, Ankara*

Keywords:
Intercalation, Halloysite, Kaolinite, Dimethyl Sulfoxide, Formamide.

ABSTRACT

In this study, the representative samples were taken from the halloysite deposits located in Çanakkale-Balıkesir regions, in NW Anatolia. At first, the dehydration temperatures of the samples were determined after sample preparation and characterization studies. It was found that halloysite samples began to lose their interlayer waters at 50°C and continued up to 70°C. The intercalation studies were carried out on dehydrated samples by using ethylene glycol, potassium acetate, dimethyl sulfoxide and formamide. Although there were negative results by ethylene glycol and potassium acetate, the satisfactory results were obtained by dimethyl sulfoxide and formamide. It was understood that the most effective reagent in terms of intercalation was formamide.

1. Introduction

Double layered (1:1) halloysite mineral, which is formed by the disintegration of aluminum silicate minerals, is generally associated with kaolinite. The chemical formula of its dehydrated structure is the same with that of kaolinite ($Al_2Si_2O_5(OH)_4$) and consists of nanometer sized tubes, in different prismatic shapes mainly the cylindrical type (Kirkman, 1981).

The halloysite mineral shows similar mineralogical and chemical characteristics with kaolinite, and it can absorb water molecules between its layers. This halloysite mineral is called as "halloysite (10 Å)" or "hydrated halloysite", and the layer distances are 10 Å as it contains water (Churchman and Carr, 1973). The ion exchange and reactivity etc. of the interlayer water in halloysite (10 Å) have important effects on the physical characteristics of the mineral (Jousssein et al., 2005). The distance between layers in halloysites, which lost their interlayer waters, is 7 Å and this value is the same as kaolinite. Actually; it is reported that this distance is 7.2 Å and the thickness of water molecules is 2.8 Å (Hiller and Ryan, 2002). Halloysites, which lost their interlayer waters, are named as "dehydrated" or "halloysite (7 Å)". In figure 1, the atomic structure for halloysite (7 Å) and (10Å) is given (Murray, 2007).

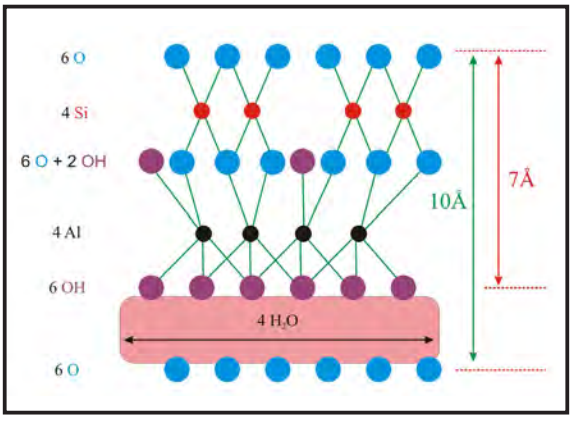

Figure 1- The atomic structure of halloysite (Murray, 2007).

When halloysite (10Å) structures are heated above low temperatures such as 35-40°C, they irreversibly lose their interlayer waters. It is also stated that the dehydration temperature depends on factors such as; the relative humidity (air) of the environment and the ore mineralogy-geology (Churchman et al.,

* *Corresponding author: Bülent Başara, b.basara@hacettepe.edu.tr*

1972). It was also pointed out that, samples in high relative humid environments could preserve their interlayer waters at higher temperatures. In other words; the relative humidity of the environment in which samples are preserved is important rather than the temperature in dehydration process (Harrison and Greenberg, 1962; Joussein et al., 2006). Such that, the dehydration begins under relative humidity conditions below 70%; therefore, the halloysite should carefully be stored.

The intercalation means, "intervene" or "forming a complex", and it is used as the intake of other atoms into crystal structure (cage) in mineralogy. Active guest molecules, during halloysite intercalation, destruct hydrogen bonds and enter layers of which waters have extruded. Thus, the interlayer distance again increases from 7Å to 10 Å (Horvarth et al., 2011). So, it is easily separated from kaolinite in XRD analysis.

The XRD patern of a halloysite mineral, between 5-15°, for 10 Å and 7 Å forms, which was taken from a halloysite mine in Balıkesir-Gönen region, is given in figure 2 (Başara et al., 2013). Dehydrated halloysites have the same basal peak with that of kaolinite in XRD analysis. Therefore, the intercalation method is necessary in order to distinguish them.

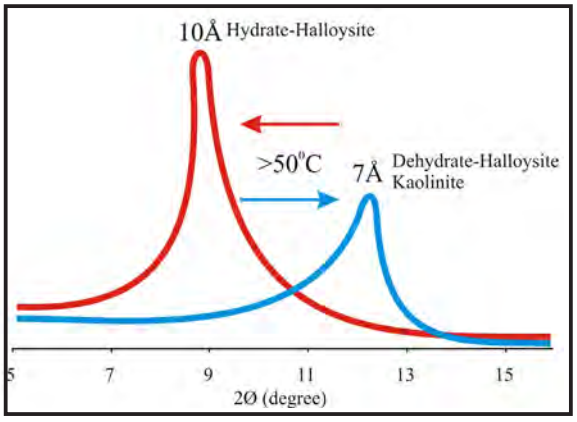

Figure 2- Basal XRD patern of both hydrated and dehydrated halloysite (Başara et al., 2013).

Many studies have been carried out on halloysite intercalation, and the fastest and effective intercalation reactive has been searched. The formamide is the first reactive which transform dehydrated halloysites into hydrated halloysites (Churchman and Theng, 1984; Churchman et al., 1984; Churchman, 1990). The usability of other reactives such as; dimethyl sulfoxide, potassium acetate, hydrazine, urea have also been investigated (Wada, 1961, Churchman and Carr, 1973; Mellouk, et al., 2009; Nicolini, et al., 2009; Horvath, et al., 2011).

It was effectively observed that, the use of formamide in intercalation is effective for naturally dehydrated halloysites which show different mineralogy and formation. However, successful results could not be taken by formamide in halloysites which were dried in ovens above 110°C. Moreover; it was stated that formamide had not been effective at all in some cases (Joussein et al., 2007).

In this study, the intercalation experiments were performed on representative samples taken from halloysite deposits which are traded and form in NW Anatolia in the country. Relative humid loss temperatures of samples, reactive of intercalation and the method were established. The results obtained by the intercalation method were used in the investigation of halloysite/kaolinite association in samples, and the sample description was carried out by XRF analysis.

2. Northwest Anatolian Halloysite Deposits

The economical halloysite deposits of Turkey are located in northwest, especially in Balıkesir – Çanakkale region (Saklar et al., 2011). The northwest Anatolian halloysite deposits are observed in the form of NE-SW extending tectonic zones (Duru et al., 2007; Duru et al., 2012). It is pointed out that, Halloysite formations are occur in Tertiary volcanic units (Ilgar et al., 2012). However, Uygun (2012) suggested that, halloysite deposits in the region had occasionally been emplaced into partly faulty contacts between Jurassic dolomitic limestones and andesitic volcanics. He also stated that, these deposits had been formed due to the effect of acidic volcanics such as; latite and rhyodasite or hypogenic hydrothermal melts. It is also emphasized that, halloysites were formed as a result of hydrothermal effects related with fault zones in low pH environments (2-3) due to dissolution-precipitation mechanism of andesitic tuffs (Akçay, et al., 2008; Dönmez et al., 2008; Erdoğan et al., 2012). Similar suggestions were also stated by other investigators saying that, NW Anatolian halloysite deposits were hydrothermally formed by low pH, silica and aluminum rich solutions (Laçin and Yeniyol, 2006; Ece and Schroeder, 2007).

New Zealand is the leader country in the production of halloysite, and the source of its deposits are hydrothermal which is similar to that of Turkey (Christie, et al., 2000; Murray, 2007; Christie, et al., 2011).

3. Material and Method

Halloysite deposits, in which representative samples were used, are respectively Balıkesir-Gönen-Alacaoluk limonitized halloysite deposit (BGL),

Balıkesir-Gönen-Alacaoluk pyritized halloysite deposit (BGP), Çanakkale-Yenice-Soğucak halloysite deposit (HAL) and Çanakkale-Yenice-Kırıklar (ALCL) halloysite deposit.

The chemical analyses were performed by Philips Axios XRF Spectrometer by making fire loss under 1050°C. XRD analyses were performed by Bruker D8 Advance X-ray diffractometer using Cu-Kα radiation, between 2-70° 2θ intervals, 40kV voltage and 40 mA current. In order to make more detailed reading in studies for intercalation, the XRD analysis was carried out between 1°/d, 5-30° goniometer velocity.

In order to perform XRD analyses of clay contents of pulverized samples more sensitive, the parts of raw materials thinner than 2 μm were obtained by decantation method using Stokes equation, and the oriented clay fraction samples were prepared (Wills and Napier-Munn, 2006).

In order to detect the dehydration temperature, samples were kept 1 hour under temperatures of 40°C, 50°C, 60°C, 70°C, 80°C and 100°C. Later on, samples dried under 100°C were used in intercalation experiments.

Merck brand glycol ($C_2H_6O_2$), potassium acetate (CH_3COOK), dimethyl sulfoxide ($(CH_3)_2SO$) and formamide (CH_3NO) were used in intercalation experiments. Ethylene-glycol samples were prepared by keeping them 2 hours under 70°C temperature in a desiccator in which there is lethylene-glycol in it. Potassium acetate, which is available in powder form, were heated and dissolved in pure water, then applied on samples nearly 10 seconds from a 20 cm distance by using a spray gun. However, formamide and dimethyl sulfoxide were directly sprayed on samples, because they were in liquid phase. As formamide is more poisonous compared to other agents, the experiments were carried out under fume cupboard. The XRD analyses for dimethyl sulfoxide and others were carried out resting them 3 and 1 hour, respectively after spraying.

4. Findings

The chemical compositions of samples (Table 1) indicate that, SiO_2, Al_2O_3 and fire loss ratios are close to each other and are in high quality when compared with exported products (Saklar et al., 2012). Iron amounts are few in BGL and BGS samples; however, there is SO_3 amount higher than 1% in BGP, and these originate from limonite, pyrite and alunite (Saklar et al., 2011). Although; XRF analyses were performed in the same region with the study of Saklar (2011) in some samples (BGP, ALCL), there are small differences between the previous study and the results of the analysis since samples used were collected from different locations of deposits.

Table 1- Chemical compositions of halloysite samples (%).

Sample	SiO_2	Al_2O_3	Na_2O	K_2O	MgO	P_2O_5	CaO	TiO_2	MnO	Fe_2O_3	SO_3	*F.L.
ALCL	47.8	35.5	<0.1	<0.1	0.1	0.3	0.1	<0.1	<0.1	0.6	0.11	15.35
BGL	46.7	35.0	<0.1	0.3	0.2	<0.1	<0.1	0.1	<0.1	1.6	0.14	14.75
HAL	47.3	35.9	<0.1	<0.1	0.1	0.6	<0.1	0.1	<0.1	0.2	0.31	15.20
BGP	45.1	34.7	<0.1	0.1	1.0	0.4	0.2	0.1	<0.1	1.0	1.17	15.95

*F.L: Fire Loss

XRD basal peak values of hydrated halloysite samples were published by Anthony et al. (1995). These are, respectively, 10,0 Å (100), 4,36 Å (70), 3,35 Å (40), 2,54 Å (35), 1,480 Å (30), 1,672 Å (14) and 1,281 Å (8). In figure 3, XRD results of unprocessed samples were given. In all samples, the halloysite peak is observed, and this peak in samples of BGP and ALCL is wider than samples HAL and BGL. Besides; 7 Å and 4.46 Å peaks showing the halloysite (7 Å) except for ALCL and 7 Å and 3.58 Å peak showing the kaolinite are observed in low intensities. Therefore; it can be considered that there is a few amount of kaolinite in samples except for ALCL.

In figures 4, 5, 6, 7, 8 and 9; XRD diffractograms of raw samples heated under 40°C, 50°C, 60°C, 70°C, 80°C and 100°C are given. When studying these graphics, there was not observed any change in samples at 40°C. However; it was seen that, hydrated halloysites lost most of their interlayer waters in samples BGL and HAL at 50°C, but there was not any change in other samples. At 60°C, it was observed that halloysites in samples ALCL and BGP began to lose their interlayer water; however, the halloysites in samples BGL and HAL had completely lost their interlayer water. It was detected that, halloysites in samples ALCL and BGP completely had lost their interlayer water at 70°C.

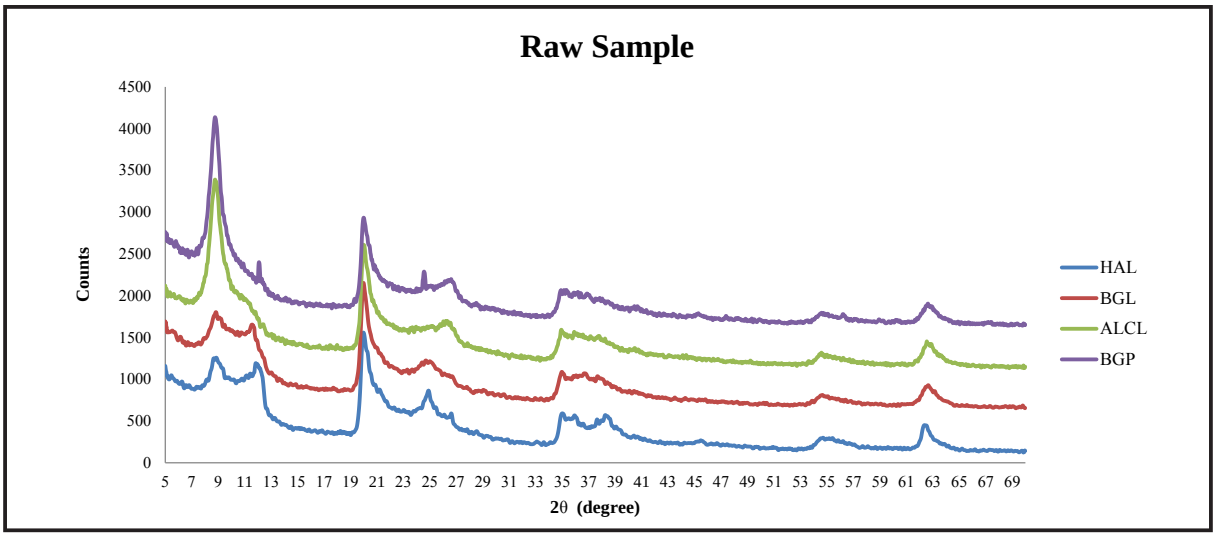

Figure 3- XRD diffractograms of raw samples.

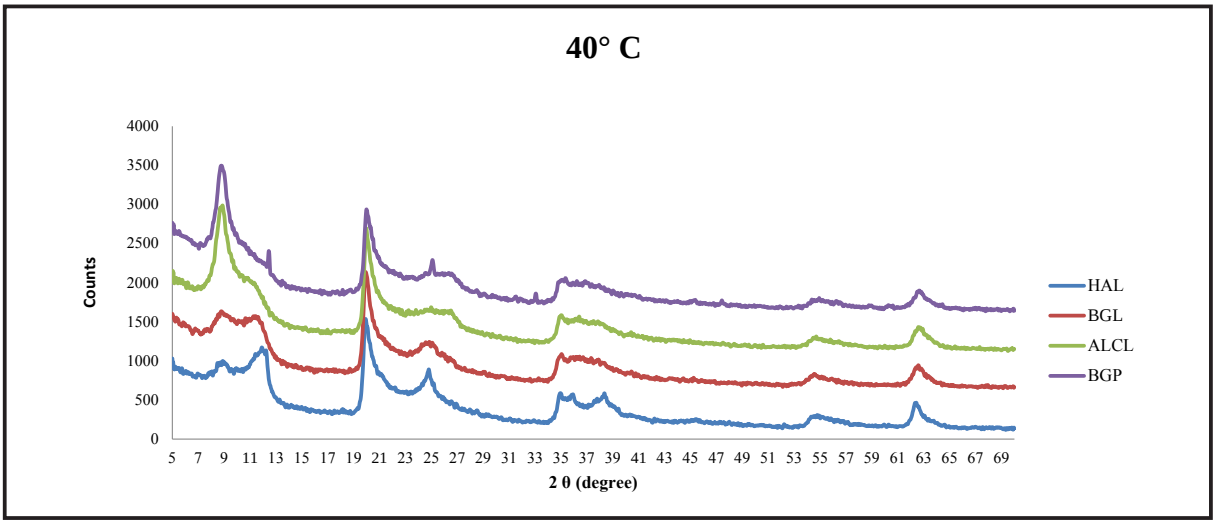

Figure 4- XRD diffractograms of raw halloysite samples heated up to 40°C.

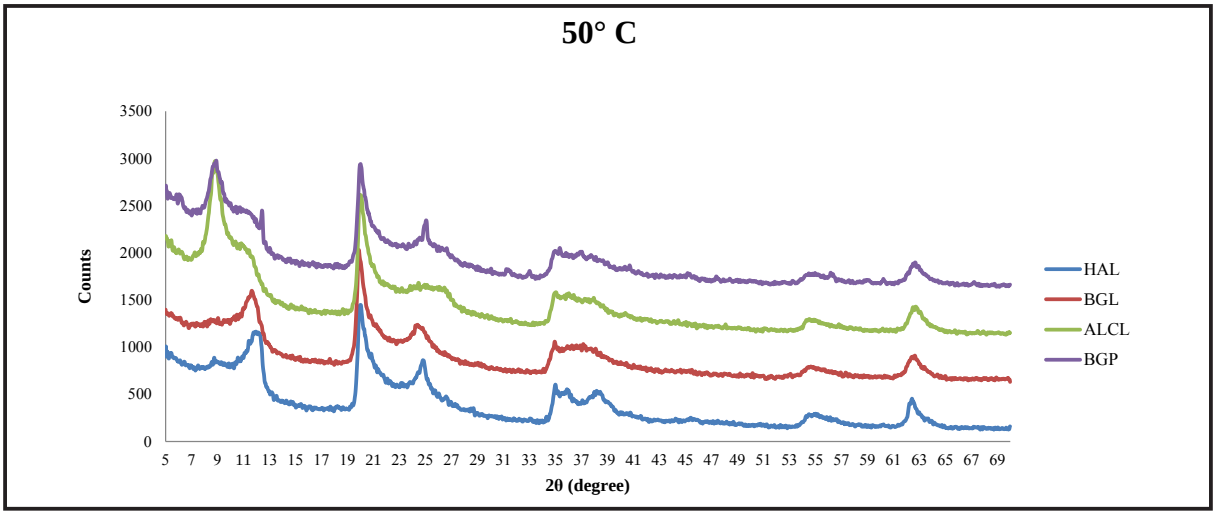

Figure 5- XRD diffractograms of raw halloysite samples heated up to 50°C.

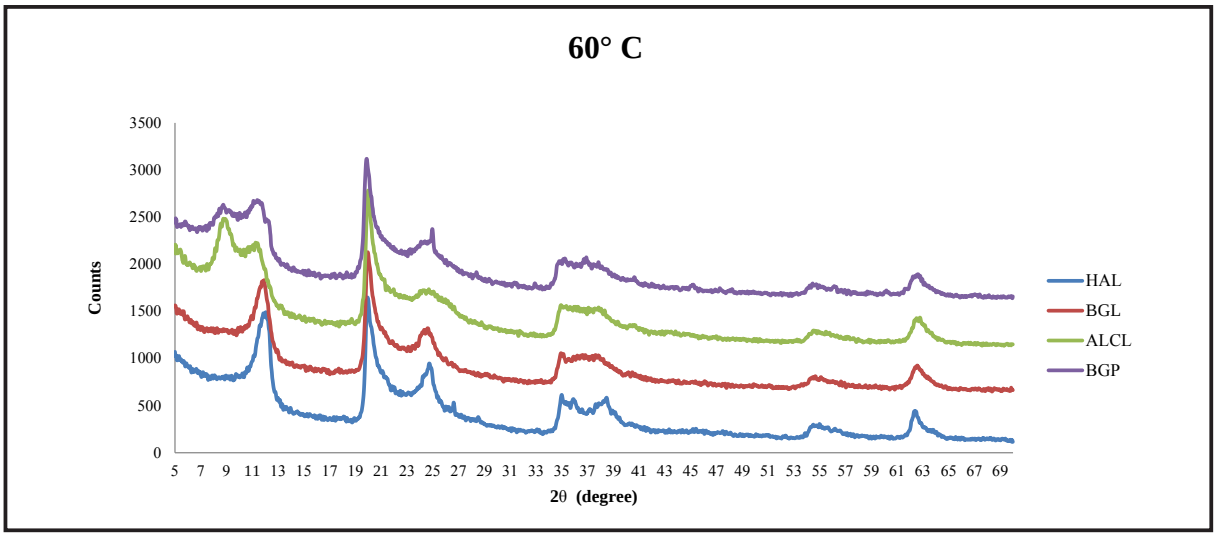

Figure 6- XRD diffractograms of raw halloysite samples heated up to 60°C.

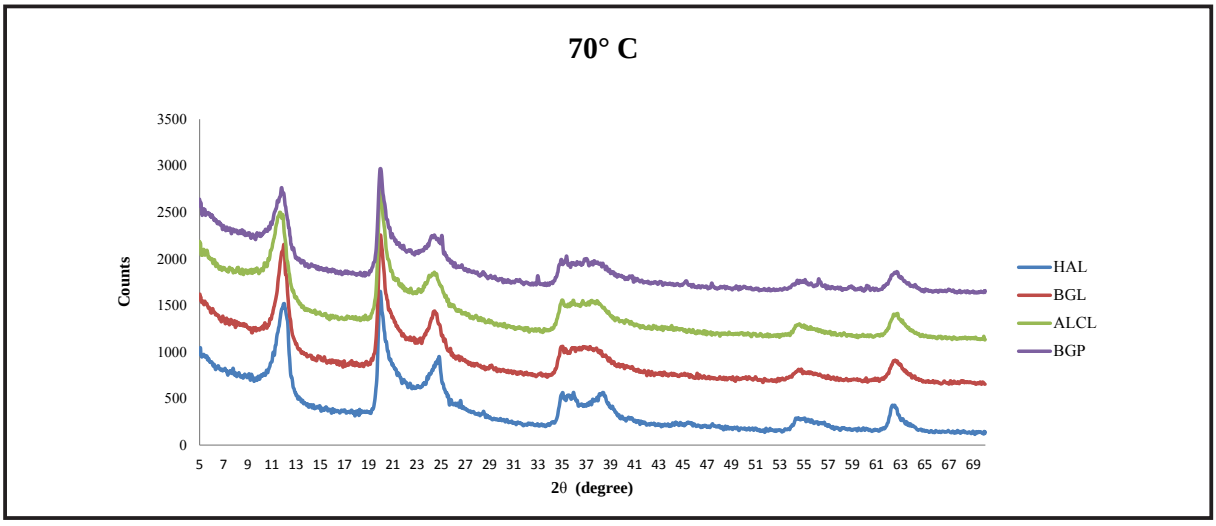

Figure 7- XRD diffractograms of raw halloysite samples heated up to 70°C.

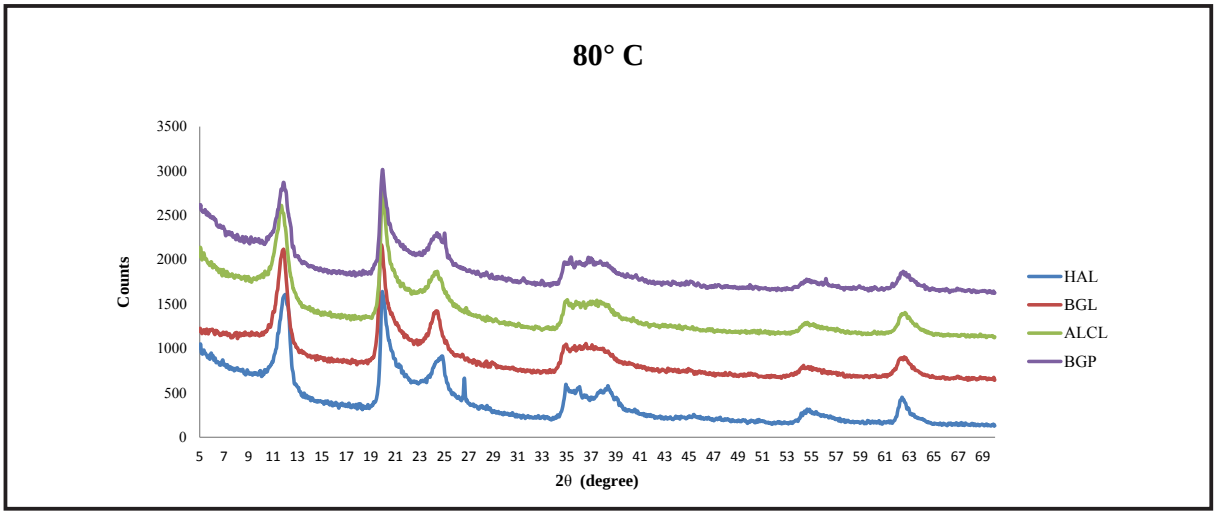

Figure 8- XRD diffractograms of raw halloysite samples heated up to 80°C.

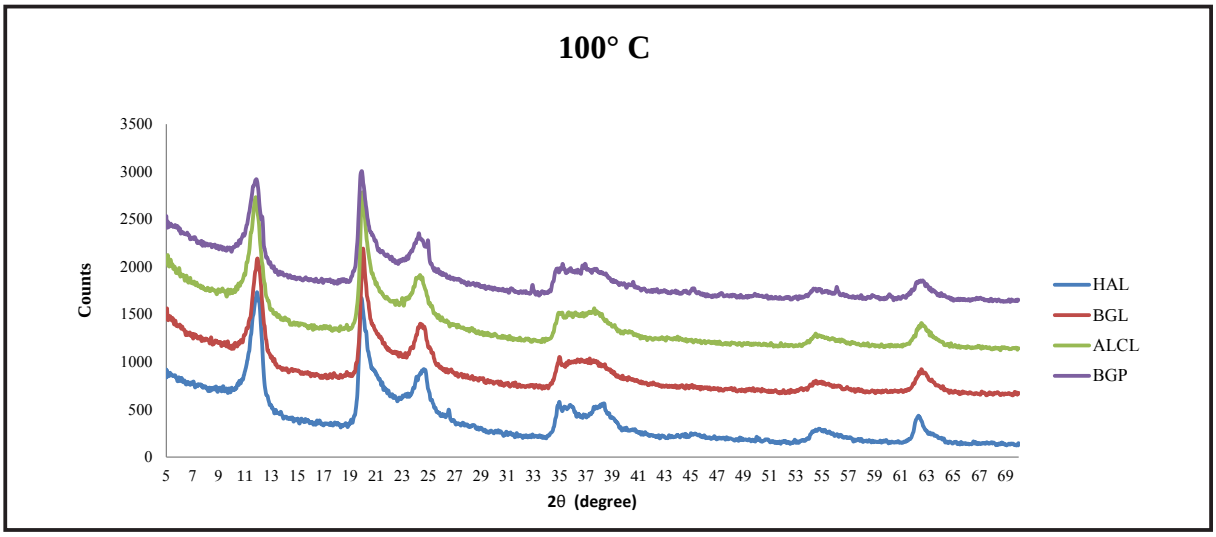

Figure 9- XRD diffractograms of raw halloysite samples heated up to 100°C.

In order to observe any change that might occur, the experiments were performed at 80°C and 100°C too, but there were not observed any change in XRD diffractograms. As a result of these analyses, halloysites in samples HAL and BGP, which had been collected from the study area, transformed into 7 Å (dehydrated) halloysite completely losing their water between 50-60°C. However; the halloysites in samples BGP and ALCL turned into 7Å (dehydrated) halloysites losing their water at 60-70°C. Results show that, halloysite minerals will not lose their interlayer water as long as they will be kept under normal room conditions. It is considered that, this is due to relative humidity ratios of the environment in which samples are present.

Halloysite (7Å) samples were used for intercalation experiments, and the result of analyses by ethylene-glycol treatment is given in figure 10. The vapor of ethylene-glycol, which can widen the interatomic distance by entering into bodies of smectite group clay minerals, were not successful in (7Å) halloysite samples, and there was not observed any change in XRD diffractograms. The similar result was also obtained for potassium acetate, and it was seen that this reactive was not effective for intercalation neither (Figure 11).

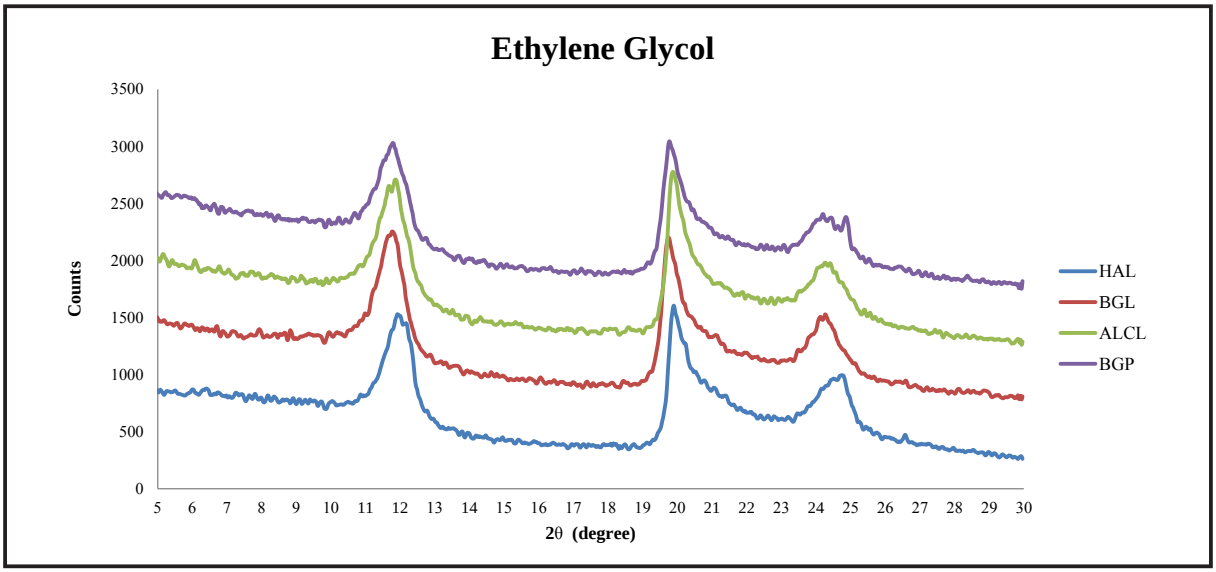

Figure 10- XRD diffractograms of halloysite samples (7Å) performed by ethylene-glycol.

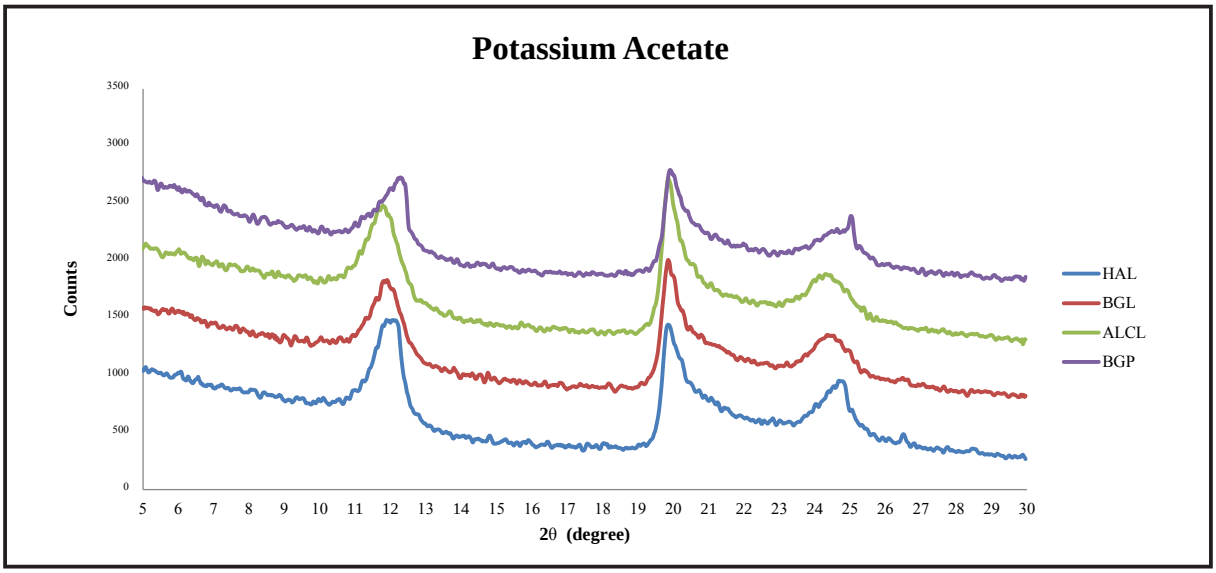

Figure 11- XRD diffractograms of halloysite samples (7Å) performed by potassium acetate.

Results obtained for dimethyl sulfoxide are given in figure 12. As seen, dimethyl sulfoxide intervene halloysite layers though partly and increases interlayer distance. In order to get the best result from the intercalation experiment using this reactive, it is necessary to wait more than 1 hour. When waited 3 hours after spraying, it was seen that halloysites (7Å) formed halloysite/dimethyl sulfoxide intercalate complex. (7Å) structure completely disappears in BGL and ALCL samples; however, it partly stops in samples BGP and HAL. So, more standby duration should be made after dimethyl sulfoxide treatment.

Results of the intercalation experiment for formamide is seen in Figure 13. In all of the dehydrated halloysites available in samples, the halloysite/formamide intercalation occurred. In other words, it was detected that, 7Å peaks had disappeared and 10 Å peaks had been formed again. This result indicates that the most effective reactive used for intercalation among the others is formamide.

The other result is that all reflections around 7 Å increase to around 10 Å. Samples (HAL, BGL, ALCL and BGP) used in tests fully contained 7 Å and 10 Å halloysites.

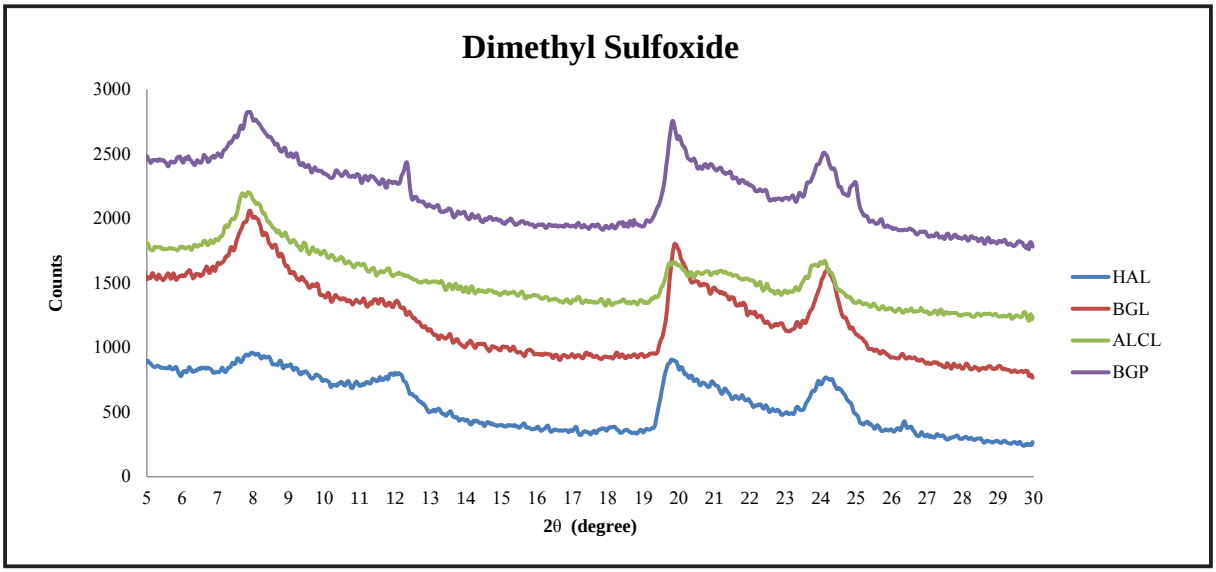

Figure 12- XRD diffractograms of 7Å halloysite samples treated by dimethyl sulfoxide.

5. Discussion and Results

Fire assay tests performed on samples taken in NW Anatolia region showed that these should be subjected to temperatures of 50°C or more for halloysite 10 Å structures to transform into 7 Å. This transformation is fully completed at 70°C. In conditions when halloysite minerals, which will be quarried from deposits in the region and stored, would be kept in room conditions (at temperatures below 50°C) and in less relative humidity ratios, hydrate halloysites might preserve their interlayer waters.

The transformation process from hydrate structure to dehydrate structure is irreversible under natural conditions. That is; halloysite minerals, which lose their waters at temperatures of 50°C or more, cannot retake this atomic water into their bodies which they lost from humidity and other water sources.

The ethylene-glycol, which is used to distinguish clay minerals, was tested in halloysite minerals in intercalation, but there was not achieved any success. Similar results were also taken for potassium-acetate, but there was not detected any effect of intercalation. There was achieved a successful result by spraying dimethyl-sulfoxide and formamide chemicals. A full transformation from 7 Å to 10 Å was determined especially in all samples studied with formamide. Therefore; it was understood that, the formamide was an effective reactive also for NW Anatolian halloysite as being compatible with literature.

Received: 02.09.2014
Accepted: 15.02.2015
Published: June 2015

References

Akçay, A.E., Dönmez, M., Ilgar, A., Duru, M., Pehlivan, Ş. 2008. 1:100.000 ölçekli Türkiye jeoloji haritaları, Bandırma H 19 paftası No 103, *Maden Tetkik ve Arama Genel Müdürlüğü*, 26p. Ankara.

Anthony, J.W., Bideaux, R.A., Bladh, K.W., Nichols, M.C., 1995. Handbook of Mineralogy, Vol. II. Silica, Silicates, *Mineral Data Publishing,* Tucson, Arizona. (http://www.handbookofmineralogy.org/pdfs/halloysite.pdf)

Başara, B., Saklar, S., Ağrılı, H., Kibar, U., 2013., Türkiye Halloysit Ve Kaolenlerinin Mineralojik Tanımlanmasında İnterkalasyon Yönteminin Araştırılması proje sonuç raporu, *Maden Tetkik Arama Genel Müdürlüğü*, Rapor No: 11705. Ankara, (unpublished)

Christie, A. B., Douch, C. J., Winfeld, B. J., Thompson, B. N., 2000, New Zealand's *industrial mineral potential*, Industrial Minerals, July, 66p.

Christie, T., Thompson, B., Brathwaite, B., 2011, *Mineral Commodity Report* 20- Clays, http://www.nzpam.govt.nz/cms/pdf-library/minerals/publications/

Churchman, G.J. 1990. Relevance of different intercalation tests for distinguishing halloysite from kaolinite in soils. *Clays and Clay Minerals*, 38, 591–599.

Churchman, G. J., Aldridge, L. P., Carr, R. M. 1972. The relationship between the hydrated and dehydrated states of an halloysite. *Clays and Clay Minerals*, 20, 241-246.

Churchman, G. J., Carr, R. M. 1973. Dehydration of the washed potassium acetate complex of halloysite. *Clays and Clay Minerals*, 21, 423-424.

Churchman, G. J., Theng, B. K. G. 1984. Interactions of halloysites with amides: mineralogical factors affecting complex formation. *Clay Minerals*, 19, 161-175.

Churchman, G. J., Whitton, J. S., Claridge, G. G. C., Theng, B. K. G. 1984. Intercalation method using formamide for differentiating halloysite from kaolinite. *Clays and Clay Minerals*, 32, 241–248.

Dönmez, M., Akçay, A.E., Duru, M., Ilgar, A., Pehlivan, Ş. 2008. 1:100.000 ölçekli Türkiye jeoloji haritaları, Çanakkale H 17 paftası No 101, *Maden Tetkik ve Arama Genel Müdürlüğü*, 27 p. Ankara.

Duru, M., Pehlivan, S., Dönmez, M., Ilgar, A., Akcay, A.E. 2007. 1:100.000 ölçekli Türkiye jeoloji haritaları, Bandırma H 18 paftası No 102, *Maden Tetkik ve Arama Genel Müdürlüğü,* 50 p. Ankara.

Duru, M., Pehlivan, Ş., Okay, A.İ., Şentürk, Y., Kar, H.,2012. Biga Yarımadası'nın Tersiyer Öncesi Jeolojisi, s.7-74, Biga Yarımadası'nın Genel ve Ekonomik Jeolojisi, Editörler: Erdoğan Yüzer, Gürkan Tunay, *Maden Tetkik ve Arama Genel Müdürlüğü Özel Yayın Serisi*, No: 28, Ankara.

Ece, Ö. İ., Schroeder, P. A. 2007. Clay mineralogy and chemistry of halloysite and alunite deposits in the Turplu area-Balıkesir-Turkey. *Clays and Clay Minerals*, 55, 1, 18-35.

Erdoğan, M., Gençoğlu, H., Mahmutoğlu, Y., 2012. Biga Yarımadası'nın Endüstriyel Hammadde Olanakları, s.273-289, Biga Yarımadası'nın Genel ve Ekonomik Jeolojisi, Editörler: Erdoğan Yüzer, Gürkan Tunay, *Maden Tetkik ve Arama Genel Müdürlüğü Özel Yayın Serisi*, No: 28, Ankara

Harrison, J.L., Greenberg, S.S., 1962. Dehydration of fully hydrated halloysite from Lawrence County, Indiana., *9th National Conference on Clays and Clay Minerals* 374-377.

Hillier, S., Ryan, P.C. 2002. Identification of halloysite (7 Å) by ethylene glycol solvation: the 'MacEwan effect'. *Clay Minerals* 37, 487–496.

Horvath, E., Kristof, J., Kurdi, R., Mako, E., Khunova, V. 2011. Study of urea intercalation into halloysite

by thermoanalytical and spectroscopic techniques. *Journal of Thermal Analysis and Calorimetry* 105, 53–59.

Ilgar, A., Demirci, E.S., Demirci, Ö., 2012. Biga Yarımadası Tersiyer İstifinin Stratigrafisi ve Sedimantolojisi, s.75-122, Biga Yarımadası'nın Genel ve Ekonomik Jeolojisi, Editörler: Erdoğan Yüzer, Gürkan Tunay, *Maden Tetkik ve Arama Genel Müdürlüğü Özel Yayın Serisi* No: 28, Ankara

Joussein, E., Petit, S., Churchman, G. J, Theng, B. K. G., Righi, D., Delvaux, B. 2005. Halloysite clay minerals-a review. *Clay Minerals*, 40, 383–426.

Joussein, E., Petit, S., Fialips, C.I., Vieillard, P., Righi, D., 2006. Difference in the dehydration–rehydration behavior of halloysites: new evidence and interpretations. *Clays and Clay Minerals* 54, 473–485.

Joussein, E., Petit, S., Delvaux, B. 2007. Behavior of halloysite clay under formamide treatment. *Applied Clay Science* 35, 17–24.

Kirkman, J.H.,1981. Morphology and structure of halloysite in New Zeland tephras, *Clays and Clay Minerals* 29 (1), 1-9.

Lacin, D., Yeniyol, M. 2006. An example to the halloysite deposits formed associated with the andesitic pyroclastics: Soğucak halloysite deposit (Yenice-Çanakkale). *Istanbul Üniv. Yerbilimleri Dergisi* 19, 1, 27-41.

Mellouk, S., Cherifi, S., Sassi, M., Marouf-Khelifa, K., Bengueddach, A., Schott, J. and Khelifa, A. 2009. Intercalation of halloysite from Djebel Debagh (Algeria), adsorption of copper ions. *Applied Clay Science*, 44, 230–236.

Murray, H. H. 2007. Applied Clay Mineralogy-Developments in Clay Science 2. *Elsevier*, 180p.

Nicolini, K. P., Fukamachi, C. R. B., Wypych, F., Mangrich, A. S. 2009. Dehydrated halloysite intercalated mechanochemically with urea: Thermal behavior and structural aspects. *Journal of Colloid and Interface Science* 338, 474–479.

Saklar, S., Ağrılı, H., Zimitoğlu, O., Başara, B., Bayrakdar, H., 2011. Türkiye halloysit kaynaklarının değerlendirme olanaklarının araştırılması proje sonuç raporu, *Maden Tetkik Arama Genel Müdürlüğü Rapor No*: 11467, 122 p. Ankara, (unpublished)

Saklar, S., Ağrılı, H., Zimitoğlu, O., Başara, B., Kaan, U. 2012. Kuzeybatı Anadolu halloysit/kaolinitlerinin karakterizasyon çalışmaları, *Maden Tetkik Arama Genel Müdürlüğü Dergisi* 145, 48-61.

Uygun, A. 1999. KB - Anadoluda karbonat kayaları içine yerleşmiş bazı halloysit yataklarının jeolojisi ve oluşumu. *Maden Tetkik Arama Genel Müdürlüğü Dergisi* 121, 141-151.

Wada, K. 1961. Lattice expansion of kaolin minerals by treatment with potassium acetate. *American Mineralogist* 46, 78-91.

Wills, B.A., Napier-Munn, T.J., 2006. Wills Mineral Processing Technology, 7th Edition, *Elsevier*, Amsterdam.

BULLETION OF THE MINERAL RESEARCH AND EXPLORATION

Foreign Edition 2015 150

CONTENTS

Bull. Min. Res. Exp. (2015) 150: 131-144

Bulletin of the
Mineral Research and Exploration

http://bulletin.mta.gov.tr

REFINEMENT OF THE REVERSE EXTRUSION TEST TO DETERMINE THE TWO CONSISTENCY LIMITS

Kamil KAYABALI[a*], Ayla Bulut ÜSTÜN[b] and Ali ÖZKESER[a]

[a] *Ankara Üniversitesi, Jeoloji Mühendisliği Bölümü, Ankara*

[b] *Maden Tetkik ve Arama Enstitüsü Genel Müdürlüğü, Jeoloji Etütleri Dairesi Başkanlığı, Ankara.*

Keywords:
Liquid Limit, Plastic Limit, Fall-cone Method, Rolling-Device Method, Reverse Extrusion Test

ABSTRACT

Liquid limit (LL) and plastic limit (PL) are the two most commonly used index properties of fine-grained soils. They have been used in not only classification of soils but also in correlation with certain engineering properties. Therefore, they have been subjected to numerous researches since they were first introduced by Atterberg in 1911. While their mechanisms were well defined in many codes and they have been in use for decades, criticisms often arose pertinent to the uncertainties inherent to them. Incredible amount of effort has been exerted to invent more rational testing methods in place of both the Casagrande's cup and bead rolling methods. Part of those efforts has been on devicing a single tool to measure the two relative index properties together. Recently, the reverse extrusion test was brought into the use of geotechnical engineers. It was shown that this tool has a potential of measuring LL, PL, and even the shrinkage limit (SL). The aim of this investigation is to reassess the ability of the reverse extrusion test to determine LL and PL with further refinement. In this regard 70 fine-grained soils covering a large range of plasticity were employed. Fall-cone method and rolling-device method were employed to determine LL and PL, respectively. The reverse extrusion tests were carried out at least five different water contents per soil sample. Extrusion pressures were plotted against water content and a curve fitting was applied to data pairs, from which the y-intercept (the coefficient a) and the slope (the coefficieent b) of the curve were determined. Those reverse extrusion coefficients were utilized to determine the representative extrusion pressures corresponding to LL and PL, as was done by the earlier researchers; however, the degree of success for the prediction of LL and PL using the representative extrusion pressures was not encouraging. Different from the previously proposed approaches, the reverse extrusion coefficients (i.e., a and b) were subjected to a multiple regression analysis along with the results of the conventional testing methods of fall-cone and rolling-device to determine the LL and PL as functions of the reverse extrusion parameters. It was shown that LL and PL can be predicted with a great degree of success using the reverse extrusion coefficients. While a great majority of the liquid limits found by using the fall-cone method were predicted with a ±10% error, almost all of the plastic limits found by the rolling device were predicted with a ±10% error. This refined investigation on the reverse extrusion test confirmed and proved that the reverse extrusion test is a simple, robust and inexpensive method capable of predicting both of two fundamental consistency limits using a single device.

1. Introduction

Atterberg limits namely liquid limit and plastic limit are the most commonly used and most easily defined index properties of fine-grained soils. They were first proposed in 1911 by Atterberg for agricultural purposes to establish the range of moisture content of soils at the plastic phase (Casagrande, 1932). They determine interrelationships between the solid and liquid phases of soils. They have

* *Corresponding author: Kamil Kayabalı, kayabali@ankara.edu.tr*

been used extensively in classifying soils of similar mechanical properties. Whilest most researchers defined Atterberg limits as water holding capacity of soils, which is the basic physical meaning, another group of scientists considered them as critical states of undrained shear strength in terms of water content. The standardization of these limits for the purpose of soil classification were done by Casagrande (1932, 1958). Since then, these limits of consistence have been the focus of interest because they involve a number of uncertainties, they are defined by different equipments and, more importantly, they are not based on a rational basis for quantifying the consistency limits, particluarly the plastic limit.

The most common procedure for defining the liquid limit of a soil uses the Casagrande's cup test as currently defined in ASTM (2010) D4318-10. In this test, a brass cup is raised by a snail-shaped cam and then dropped from a distance of 10 mm onto a rubber base. The soil sample in the brass cup is grooved by special tool and the liquid limit is defined as the water content corresponding to 25 blows to close groove for a length of 13 mm. Because the chances are very low to catch the 25 blows at first attempt, the test is repeated several times at different water contents each having a different number of blows. A semilogaritmic plot is constructed with the water content is on the linear axis and the number of blows is on the logarithmic axis. A straight curve is fitted to the data points and the water content corresponding to 25 blows is read off. The liquid limit is the water content of a soil when 25 blows cause 13 mm of closure of the groove at the base of the cup.

The uncertainties and/or the factors affecting the results of Casagrandes's cup method have been addressed as (Johnston and Strom, 1968; Wroth and Wood, 1978; Whyte, 1982; Clayton et al., 1995; Lee and Freeman, 2007; Haigh, 2012):

1) The hardness of the base of the apparatus (i.e. hard rubber in ASTM D4318 versus soft rubber in British Standards),

2) Physical properties of the bench on which the Casagrande's cup stands,

3) Changes in drop height due to lacking of regular calibration of the drop height,

4) The performance of the operator,

5) The tendency of halves to slide together,

6) The migration of water in dilatant soils,

7) Incorrect frequency of drops,

8) Soil type,

9) Use of worn grooving tools,

10) Incorrect forming of soil groove,

11) Dynamic effects inherent to the equipment.

The range of results reported for Casagrande's cup method is rather alarming, particularly in view of the fact that it was known by the participating organizations that their results would be compared with those of rival organizations. Sherwood (1970) commented that Transport and Road Research Laboratory (UK) attempts to assess the amount of error attributable to defective or worn apparatus in the liquid limit test indicated that majority of error was due to operator technique (Clayton et al., 1995). It was reported that the incorrect frequency of drops caused some 15% moisture content error in determining the liquid limit using the Casagrande's cup method (Clayton et al., 1995).

The test has been carried out worldwide with little variations from that proposed by Casagrande. For instance, while ASTM D4318 standard utilized hard rubber base, the British and Indian codes still enforces the use a soft rubber base. The grooving tool used in this test also comes two variants in ASTM and AASHTO. While the one by AASHTO yields unsatisfactory grooves, its use nevertheless persisted (Haigh, 2012).

Plastic limit was defined by Atterberg as the water content at which the soil paste cannot be rolled into a thread (Casagrande, 1932). This method requires a soil mass to be rolled into a thread by hand with a specified pressure. The moisture content, expressed as a percentage of the weight of oven dried soil at which the soil mass begins to crumble when rolled into a thread of about 3 mm is defined as the plastic limit. Commonly known as the "bead rolling" test, this procedure has the following uncertainties and/or factors affecting the plastic limit test results (Whyte, 1982; Sivakumar et al., 2009):

1) The pressure applied to the soil bead,

2) The geometry (e.g. width of the hand contact to bead diameter),

3) The friction between the soil, hand, and base plate,

4) The speed of rolling,

5) The risk of contaminating the soil sample,

6) The vagueness of the guidelines on the test.

The amount of finger pressure used and the shape of the fingers varies to a great extent and, in addition, operators frequently do not perform the test using the tips of the fingers since these are eminently suited to the task (Clayton et al., 1995). Even if the test is performed by strictly following the guidelines specified in the related codes, its repeatability by the same operator and reproducibility amongst different agencies are low because it does not include a commonly accepted quantifiable procedure. For instance, because the operator visually inspects the diameter of the thread at the time of crumbling and usually uses no caliper to measure it, small variations in the diameter of the thread may cause considerable differences on the resulting PL value, which in turn may result in a different level of plasticity for the same soil or in a major shift from silt to clay or viceversa.

Regarding a number of limitations of the Casagrande's cup method outlined above, many researchers proposed the use of the fall-cone method to determine the liquid limit (Sherwood and Ryley, 1970; Wood, 1982; Belviso et al., 1985; Wasti and Bezirci, 1986) and the same has been included in several national codes of practice such as British standars (BSI, 1990), Canadian standards (CAN/BNQ, 1986) and Indian standards (ISI, 1985) (Prakash and Sridharan, 2006). In spite of the main advantages of fall-cone test such as simplicity, ease of operation and comparative reproducability, the American Society for Testing and Materials (ASTM), one of the worldwide used standards, has not included the fall-cone method (Prakash and Sridharan, 2006). Attempts have been made so that the fall-cone can be employed to determine the plastic limit as well (e.g. Belviso et al., 1985; Prakash and Sridharan, 2006; Lee and Freeman, 2007). Lee and Freeman (2007) compared eight non-ASTM test methods to the Casagrands's cup liquid limit method and did the same for ten non-ASTM alternatives to the bead-rolling plastic limit method on three cohesive soils. They reported that only one non-ASTM method (i.e. the unified or "dual-weight" fall-cone apparatus) yield within 10% of the ASTM liquid and plastic limit values.

One of the attempts for devising a single tool capable of determining both consistency limits is the development of soil extrusion test. Extrusion is a technique whereby materials such as metals, plastics or food stuff are induced to flow plastically through a die by a ram (Medhat and Whyte, 1986). It was first brought into attention by Timar (1974) who was able to have partial success to determine the most common two Atterberg limits (i.e., LL and PL) using the direct extrusion method. Difficulties were reported in interpreting the results due to the influence of friction as the billet is forced along the container of the die. Whyte (1982) first used the reverse extrusion test in soil mechanics extensively. He reported that the reverse extrusion technique is a reliable method for determining soil plasticity that promises to be rapid, simple and economical. Medhat and Whyte (1986) extended the use of the reverse extrusion test to relate the shear strength to extrusion pressures. They obtained plastic limit values with a reasonable repeatability and reported that the reverse extrusion method appears to offer potential as an index test method.

In an attempt to determine the most common two consistency limits using the same and less operator-dependent instrument, Kayabalı and Tüfenkçi (2007) employed the reverse extrusion test by following the guidelines outlined by Whyte (1982). For the twenty soils they tested, they set two extrusion pressures of 2250 kPa and 30 kPa for the plastic limit and liquid limit, respectively. Kayabalı and Tüfenkçi (2010) further refined the reverse extrusion test to determine consistency limits. They determined plastic limit and liquid limit as the water contents corresponding to the extrusion pressures of 3000 kPa and 35 kPa, respectively, based upon tests performed on 30 soil samples. Kayabalı (2012), based on about some 4000 consistency tests on 100 soils with different levels of plasticity, determined that the liquid limit, plastic limit and the shrinkage limits are the water contents corresponding to the extrusion pressures of 20 kPa, 2000 kPa and 12000 kPa, respectively.

Research conducted by the senior author (i.e., Kayabali and Tüfenkçi, 2007; Kayabalı and Tüfenkçi, 2010 and Kayabalı, 2012) reveals that the extrusion pressures corresponding to liquid an plastic limits are not unique.

Therefore, the determination of consistency limits as the water contents corresponding to the certain values of the extrusion pressure does not appear to be a viable approach. Nevertheless, the potential of the reverse extrusion test to determine the consistency limits can be addressed using a different analysis method.

The scope of this investigation is two-folds: 1) Re-examination of the relation between the results of the reverse extrusion test and those of the consistency

limits by testing a new set of soil data representing a reasonably large range of soil plasticity. 2) Introduction of an alternative method and comparison between the methodology previously employed by the senior author and the newly proposed statistical approach.

2. Materials

As part of the evaluation of the consistency limits via the reverse extrusion test 70 fine-grained soil samples were prepared. Because an investigation such a present study needs to cover a range of plasticity as wide as possible, the soil samples used for the investigation were prepared in the laboratory. The difficulty of obtaining a number of natural soil samples covering a large range of plasticity should be appreciated. Accordingly, the test materials were prepared using the mixtures of a natural soil sample with fine-grained sand and commercially available bentonite. The natural soil sample had a liquid limit and plastic limit of 54 and 26, respectively. In order to obtain soil samples of lower liquid limits than 54, a fine-grained sand sieved through a #40 mesh was added to the natural sample at varying proportions. A similar procedure was applied to obtain soil samples with higher liquid limits than 54 by adding commercial bentonite to the natural soil at certain increments. This way, a series of soil samples were constituted whose liquid limit ranged from 29 to 105. It should be noted that the natural soil samples was oven-dried, pulverized and sieved through #40 mesh prior to mixing with fine sand and bentonite.

3. Methods

The testing methods employed for this investigation include the fall-cone, the rolling-device and the reverse extrusion. Whilest the Casagrande's percussion method is a more common method than the fall-cone test, it has long been recognized that the Casagrande liquid limit test is not very repeatable. In contrast, the fall-cone test has been shown to give a much lower standard deviation of the results than the cup test when identical samples are tested at multiple laboratories (Sherwood, 1970; Haigh, 2012). Upon this fact, the fall-cone method was selected to determine the liquid limit of soil samples. The setup employed for this purpose has a cone of 80 g mass and a cone angle of 30 degrees. The wet soil sample with a moisture content somewhat higher than its liquid limit was first homogeneously mixed and placed into the container of the setup with a smoothly leveled surface. The cone was released and let it penetrate into the specimen for 5 seconds. It was ensured that there was zero air gap between the tip of the cone and the upper surface of the specimen. The depth of penetration of the cone was measured by a digital gage. Following this, the moisture content of the specimen was determined. The second specimen was prepared in a manner so that the mositure content was higher than the previous stage. The specimen was homogeneously mixed again and subjected to cone penetration. Another moisture content determination was performed and this process was repeated on several specimens with different water contents. The cone penetration versus water content data were plotted on a linear graph and the water content corresponding to the penetration depth of 20 mm was determined as the liquid limit of the soil sample.

As for the plastic limit test the rolling-device shown in figure 1 was utilized. While the common practice has long been the employment of hand rolling of a soil bead, introduction of a rolling-device and thus further standardization of the plastic limit eliminated some of the uncertainties pertinent to the performance of the plastic limit test by bead rolling by hand. In this test the top and bottom plates have smooth unglazed paper attached to them against sticking of the soil bead to those plates. The soil bead is placed between these two plates and the top plate is moved back and forth with a slight pressure. This action is continued until the top plate comes to contact with the side rails, which are 3.2 mm higher than the base plane of the bottom plate. The plastic limit is determined as the water content when the thread of soil breaks into a series of cylynder-shaped pieces about 3.2 to 9.5 mm in length. This process is repeated for at least three times and the average water content is fixed as the plastic limit.

Figure 1- The rolling-device used to determine the plastic limit of soil samples.

The testing apparatus used for the reverse extrusion test is mainly composed of a container and a rammer (Figure 2). The inner diameter of container

Figure 2- The reverse extrusion apparatus.

is 38 mm and its height is 150 mm. The rammer has a die orifice of 6 mm in the middle. There is a clearance of 0.2 mm between the rammer and the inner surface of the container. Oven-dried, pulverized and sieved soil sample of about 150g is required for this test. Approximately 100g of soil specimen is first wetted by an amount of water slightly lower than its liquid limit and mixed homogeneously. The wet mixture is divided into a few chunks of about the same size. Each chunk is then dropped into the container and tapped with a piston. This way, all chunks of wet soil are filled into the container somewhat in a compacted manner to ensure that there is not large vugs in between. Then, the rammer is driven into the container, which are placed together in a uniaxial load frame with a digital load cell. The soil inside the container is loaded at a rate of 1 mm/min and the compression force is recorded. The soil is compressed until it fails in the form of soil worm as shown in figure 3. The compression force continues to increase until the compressed soil extrudes from the die orifice and then becomes steady as shown in figure 4, which consists of 5 experimental curves, each obtained at different water contents. The flat portion of curves in figure 4 corresponds to the extrusion pressures at failure, which are then plotted in a semi-logarithmic graph against water content. A sample graph is shown in figure 5. The logarithm of extrusion pressure versus the water content results in a perfectly linear relationship. An attempt to investigate the operator dependence of the reverse extrusion test by employing several unexperienced people revealed that the test is not operator dependent and eliminates many uncertainties pertinent to Casagrande's cup liquid limit and bead-rolling techniques.

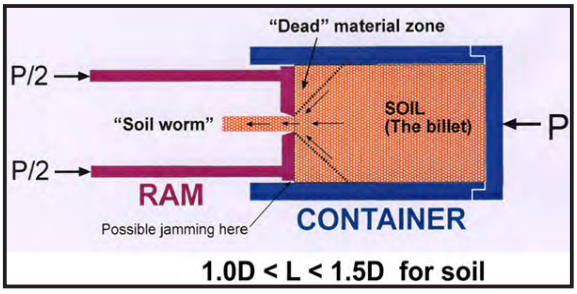

Figure 3- Schemmatical illustration of how the reverse extrusion method works (L = the length and D = the diameter of the soil billet).

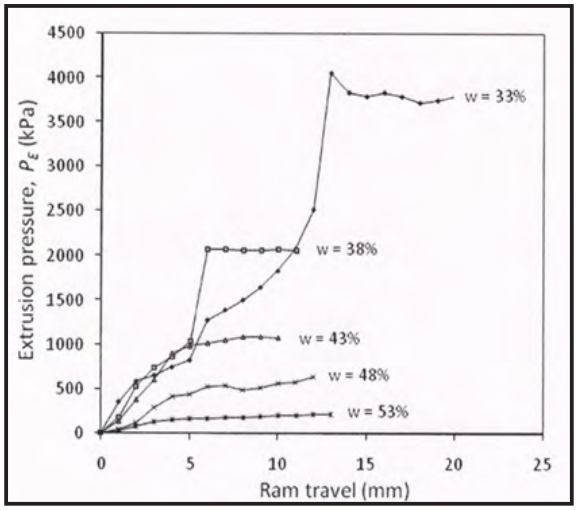

Figure 4- Reverse extrusion test results for different water contents. The flat portion of curves develops after the soil worm forms.

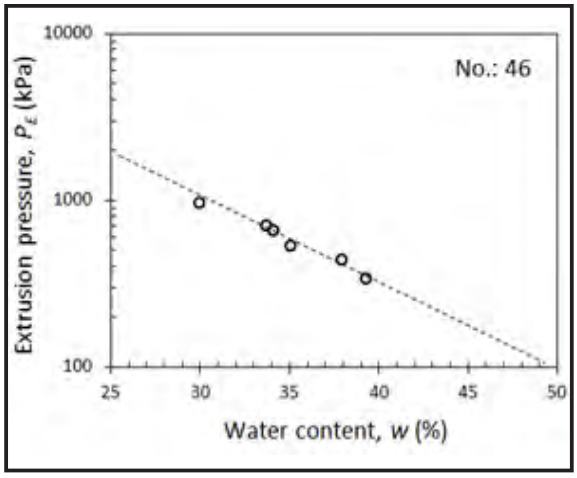

Figure 5- Example plot for the extrusion pressures at failure versus water contents.

4. Results and Discussion

A comprehensive laboratory experiment program was followed towards predicting the two fundamental consistency limits of fine-grained soils. To determine the liquid limits of soil samples, at least five data pairs of cone penetration depth versus water content were constituted. The overall results obtained from the fall-cone liquid limit tests are given in table 1 for 70 soil samples.

Concerning the plastic limits of the same set of samples, the rolling-device method was employed as explained before. The plastic limit tests were repeated 5 times for each soil sample and the averages were taken and listed in table 1.

Table 1- The liquid limits determined using the fall-cone method, the plastic limits determined using the rolling device method, and the reverse extrusion coefficients for 70 fine-grained soils used in this investigation.

No.	LL	PL	a	b		No.	LL	PL	a	b
1	29.3	16.9	6.07	6.7		36	51.5	26.3	5.25	13.8
2	30.7	16.4	5.97	6.9		37	51.5	23.8	5.61	11.5
3	30.8	15.4	5.96	6.9		38	53.2	23.6	5.25	13.8
4	31.6	16.5	6.01	6.8		39	53.5	25.6	5.30	13.5
5	32.2	16.9	5.85	7.5		40	53.5	25.8	5.53	12.0
6	32.2	18.1	5.86	7.2		41	54.5	25.3	5.17	14.1
7	32.9	17.3	5.15	9.9		42	55.0	23.9	4.68	18.3
8	33.2	17.2	5.85	7.5		43	55.0	24.9	5.03	15.0
9	33.5	18.1	5.86	7.6		44	55.9	26.0	4.67	18.7
10	34.5	18.6	6.03	7.4		45	57.5	25.4	4.88	16.5
11	35.2	18.3	6.08	7.4		46	59.4	25.5	4.56	19.3
12	35.3	18.0	5.53	8.7		47	60.5	24.7	5.14	15.3
13	36.8	18.9	5.74	8.5		48	62.0	26.0	4.94	17.0
14	37.0	17.8	5.88	8.3		49	62.8	25.3	4.64	19.3
15	37.2	19.1	5.30	10.2		50	63.0	24.4	4.79	17.8
16	37.8	19.5	5.51	9.5		51	65.0	26.5	5.08	15.7
17	39.0	19.5	5.69	9.3		52	67.0	26.1	4.67	18.9
18	40.3	19.1	5.79	8.9		53	69.0	24.4	4.99	16.4
19	41.2	21.0	5.53	10.0		54	69.5	25.9	4.89	17.3
20	42.0	20.0	5.34	10.6		55	72.0	25.7	4.60	20.2
21	42.2	21.3	5.73	9.3		56	75.0	26.4	4.91	17.4
22	42.4	21.6	5.64	9.5		57	77.0	26.9	4.57	21.0
23	43.5	21.8	4.93	13.3		58	79.5	26.4	4.83	18.0
24	44.0	21.0	6.37	7.9		59	80.0	27.8	4.68	19.8
25	44.2	23.2	5.34	11.6		60	83.0	27.3	4.95	17.1
26	44.5	23.0	5.52	11.5		61	84.0	26.7	4.80	18.4
27	44.8	20.7	5.18	11.5		62	84.5	26.1	4.59	20.7
28	45.0	23.4	6.00	9.0		63	88.5	26.7	4.78	18.2
29	45.3	22.8	5.64	10.7		64	90.5	27.8	4.39	23.3
30	45.9	22.9	5.53	10.9		65	92.5	26.5	4.62	20.4
31	48.1	25.8	5.52	11.5		66	93.0	28.2	4.57	20.6
32	48.8	23.5	5.52	11.5		67	95.0	28.1	4.69	19.9
33	49.6	24.7	5.76	10.7		68	101.0	27.5	4.31	24.6
34	49.6	25.1	5.44	11.7		69	102.0	27.8	4.50	22.8
35	50.2	25.0	5.75	11.1		70	105.0	29.1	4.50	22.8

As for the reverse extrusion tests, at least five experiments were conducted on each soil sample at varying moisture contents. The extrusion pressure versus water content data pairs at the time of failure were plotted as shown in figure 5. The best fit curve for the data pairs was drawn upon visual inspection for each soil sample. The y-intercept (the coefficient a) and the slope (the coefficient b) of the best fit curve were determined for all 70 soil samples. These reverse extrusion coefficients (i.e. a and b values) for each soil were presented in table 1. The major reason for establishing the y-intercept and the slope of extrusion pressure versus water content plots is to analytically determine the spesific values of extrusion pressures at plastic and liquid limits.

The extrusion pressures corresponding to the liquid limit values determined from the fall-cone test are calculated using the a and b coefficients and listed in table 2. Then, they are plotted as a histogram in figure 6(a). The histograms published by the senior author for the similar purposes are also included in figure 6 for comparison. A close look at figure 6(a) reveals that there is not a distinct range of extrusion pressures dramatically different from the others. Rather, it is observed that most extrusion pressures corresponding to liquid limits fall into a range from 0-30 kPa. To assign a representative extrusion pressure for the liquid limit as was done by Kayabalı and Tüfençki (2010) the arithmetic mean of all extrusion pressure values in this range can be taken, which is aproximately 15 kPa. Coincidently, the median value is also 15 kPa for this interval of extrusion pressures.

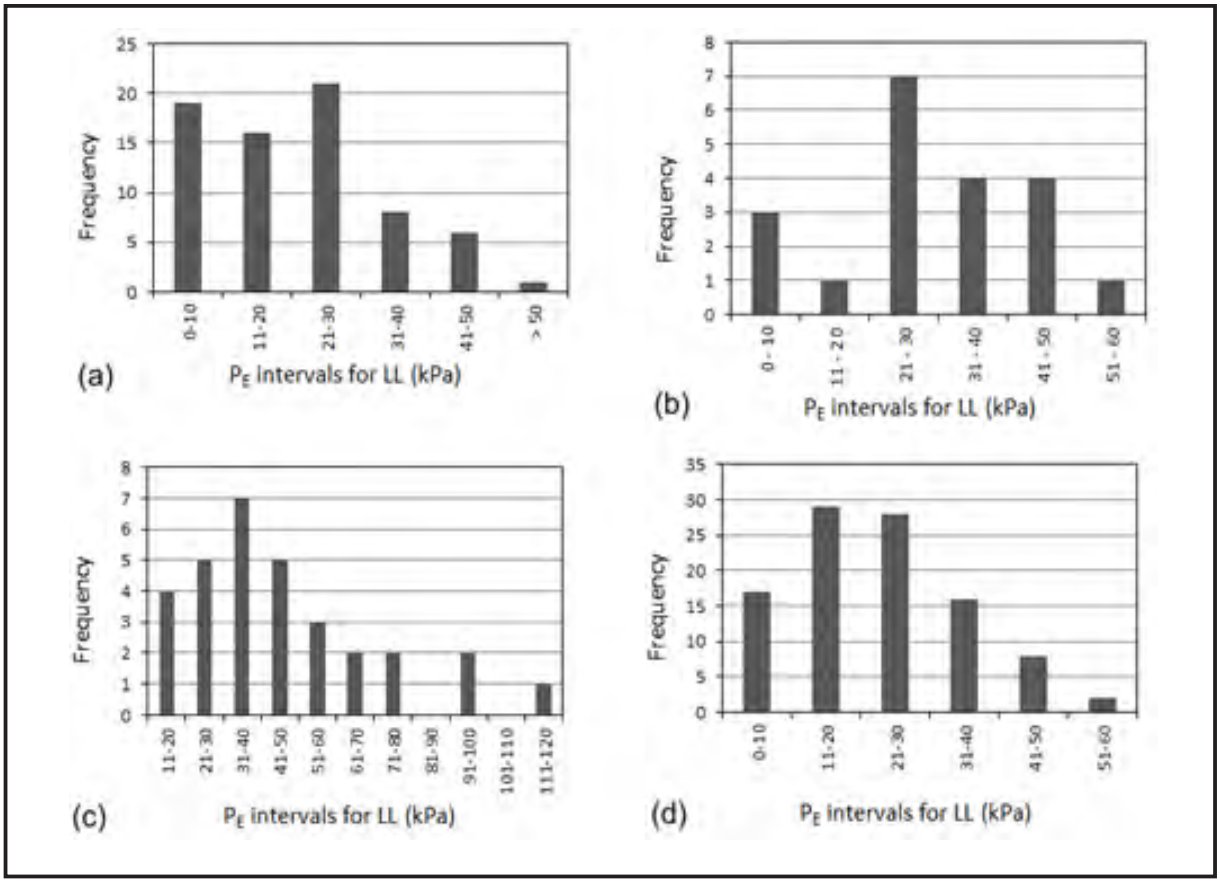

Figure 6- Extrusion pressure distribution for liquid limit: a) This study, b) from Kayabalı and Tüfenkçi (2007), c) from Kayabalı and Tüfenkçi (2010) and d) from Kayabalı (2012).

In order to predict the liquid limit using the representative extrusion pressure of 15 kPa determined above, a series of computations were carried out using the a and b coefficients. The results are listed in table 2. The liquid limit values predicted using the representative extrusion pressure of 15 kPa versus the original liquid limit values determined from the fall-cone test are plotted in figure 7 which

yields a moderately good coefficient of regression (R^2 =0.62). It is observed that the liquid limit can be predicted with a great success up to 70; beyond that, the predicted LL becomes increasingly smaller as the measured LL increases. The most likely reason for this deviation is the fact that the extrusion pressure corresponding to the liquid limit is not the same for all soils.

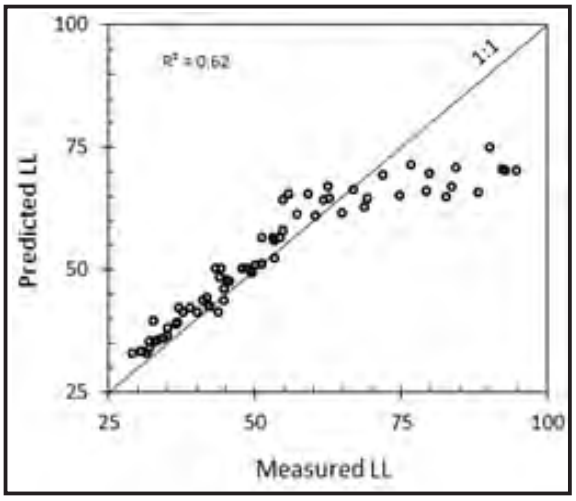

Figure 7- The predicted liquid limits using the representative extrusion pressure of 15 kPa versus the liquid limits determined from fall-cone method.

The extrusion pressures corresponding to the plastic limits determined from the rolling-device method were calculated using the a and b coefficients as well. The newly predicted plastic limits are listed in table 2. Then, the predicted plastic limits are grouped into certain intervals to constitute a histogram in figure 8(a), which also includes previously published histograms of similar nature by the senior author for comparison purposes. It is observed that the extrusion pressures corresponding to plastic limits from the rolling-device method predicted using the a and b coefficients fall mostly into the interval of 2000-2500 kPa; the mean of the extrusion pressures in this interval is approximately 2300 kPa. Using this representative value of 2300 kPa along with the two coefficients, plastic limits for each sample were predicted and listed in table 2. A correlation between the predicted plastic limits using the representative extrusion pressure of 2300 kPa and plastic limits from the rolling-device method is obtained with a moderate value of regression coefficent (R^2 = 0.71) (Figure 9). The degree of scatter around the plastic limit values of about 24-28 appears to be high; which is also considered to be the results of assuming that the extrusion pressure corresponding to plastic limit is the same for all soils.

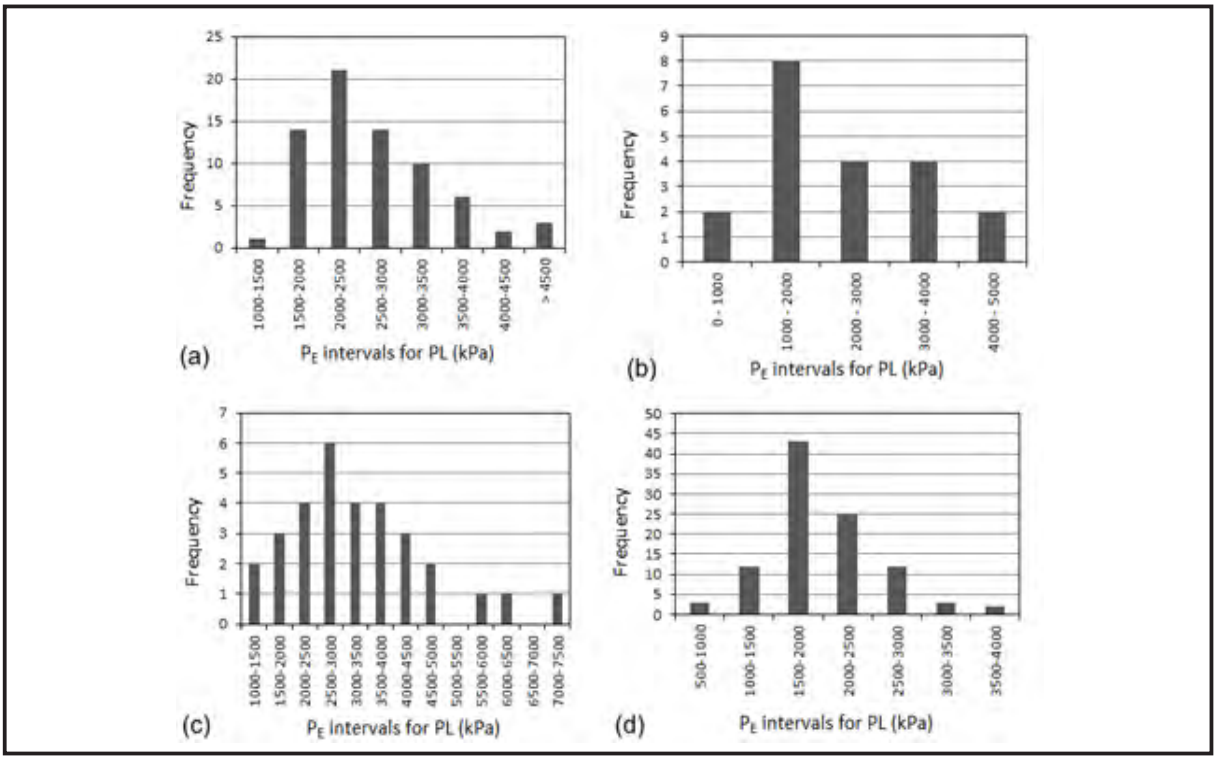

Figure 8- Extrusion pressure distribution for plastic limit: a) This study, b) from Kayabalı and Tüfenkçi (2007), c) from Kayabalı and Tüfenkçi (2010) and d) from Kayabalı (2012).

Table 2- The computed extrusion pressures for liquid limit [$P_{E(LL)}$] and plastic limit [$P_{E(PL)}$], the predicted liquid limit and plastic limit using the representative extrusion pressures ($LL_{PE=15\ kPa}$ and $PL_{PE=2300\ kPa}$), the predicted liquid limit and plastic limit using the reverse extrusion coefficients in the empirical relationships ($LL_{a\&b}$ and $PL_{a\&b}$), and the amount of errors involved in predicting LL and PL with the empirical relationships (DLL and DPL).

No.	$P_{E(LL)}$ (kPa)	$P_{E(PL)}$ (kPa)	$LL_{PE=15\ kPa}$	$PL_{PE=2300\ kPa}$	$LL_{a\&b}$	$PL_{a\&b}$	DLL (%)	DPL (%)
1	50	3529	32.8	18.1	35.9	17.2	22.5	2.0
2	33	3919	33.1	18.0	34.9	17.1	13.5	4.1
3	31	5347	33.0	17.9	34.7	17.0	12.5	10.4
4	23	3833	32.9	18.0	35.2	17.1	11.3	3.6
5	36	3951	35.1	18.7	35.2	17.7	9.2	4.5
6	24	2219	33.7	18.0	34.0	17.0	5.7	5.9
7	67	2527	39.3	17.7	31.3	17.2	4.9	0.4
8	27	3603	35.1	18.7	35.2	17.7	5.9	2.7
9	28	3009	35.6	19.0	35.8	18.0	6.9	0.7
10	23	3285	35.9	19.7	38.4	18.7	11.2	0.6
11	21	4046	36.3	20.1	39.4	19.1	12.0	4.2
12	30	2891	37.9	18.9	34.0	17.9	3.7	0.4
13	26	3285	38.8	20.2	37.5	19.1	1.9	1.1
14	26	5438	39.0	20.9	39.6	19.7	7.0	10.9
15	45	2676	42.1	19.8	35.7	19.0	3.9	0.7
16	34	2867	41.2	20.4	37.2	19.4	1.6	0.7
17	31	3919	42.0	21.7	40.3	20.4	3.4	4.8
18	18	4405	41.1	21.6	40.6	20.4	0.7	6.8
19	26	2692	43.5	21.7	40.1	20.5	2.7	2.2
20	24	2839	44.1	21.0	38.5	20.0	8.2	0.2
21	16	2752	42.4	22.0	41.3	20.8	2.2	2.4
22	15	2324	42.4	21.6	40.2	20.5	5.3	5.3
23	46	1954	49.9	20.9	41.7	20.8	4.2	4.7
24	6.3	5150	41.0	23.8	49.0	22.7	11.4	7.9
25	34	2188	48.3	22.9	43.7	21.9	1.0	5.6
26	45	3311	50.0	24.8	48.2	23.5	8.3	2.0
27	19	2399	46.0	20.9	39.1	20.2	12.8	2.3
28	10	2512	43.4	23.7	46.2	22.4	2.7	4.3
29	25	3230	47.8	24.4	46.7	23.0	3.2	0.8
30	21	2686	47.5	23.6	44.9	22.4	2.1	2.4
31	22	1890	50.0	24.8	48.2	23.5	0.2	9.1
32	19	2996	50.0	24.8	48.2	23.5	1.3	0.2
33	13	2829	49.0	25.7	50.1	24.1	1.0	2.3
34	16	1971	49.9	24.3	47.1	23.1	5.0	8.1
35	17	3146	50.8	26.5	52.4	24.9	4.4	0.3
36	33	2209	56.2	26.1	54.6	25.0	6.1	5.1
37	14	3471	51.0	25.9	50.8	24.4	1.3	2.3
38	25	3466	56.2	26.1	54.6	25.0	2.7	5.7
39	22	2533	55.7	26.2	54.3	25.0	1.5	2.5
40	12	2399	52.2	26.0	51.6	24.6	3.5	4.8
41	20	2375	56.3	25.5	54.0	24.6	1.0	2.8
42	47	2366	64.1	24.1	66.1	25.2	20.2	5.3
43	23	2344	57.8	25.0	55.2	24.5	0.4	1.6

Table 2- (contınued)

44	48	1904	65.3	24.5	69.1	25.6	23.5	1.6
45	25	2191	61.1	25.1	60.4	25.1	5.1	1.3
46	30	1733	65.3	23.1	68.9	25.0	16.0	2.1
47	15	3354	60.6	27.2	61.6	26.3	1.8	6.4
48	20	2574	64.0	26.8	67.0	26.6	8.1	2.2
49	24	2134	66.9	24.7	72.9	26.0	16.2	2.7
50	18	2626	64.3	25.4	67.0	25.9	6.4	6.0
51	8.7	2467	61.3	27.0	62.4	26.2	4.1	1.0
52	13	1946	66.0	24.7	70.8	25.9	5.7	0.9
53	6.1	3178	62.5	26.7	64.2	26.3	6.9	7.6
54	7.5	2471	64.3	26.4	67.3	26.4	3.1	1.9
55	11	2127	69.2	25.0	79.4	26.6	10.3	3.7
56	4.0	2470	65.0	26.9	69.1	26.8	7.8	1.5
57	8.0	1946	71.3	25.4	86.0	27.3	11.7	1.3
58	2.6	2309	65.8	26.4	70.6	26.7	11.2	1.0
59	4.4	1888	69.4	26.1	79.9	27.2	0.1	2.2
60	1.2	2257	64.5	27.2	68.3	26.8	17.7	1.7
61	1.7	2233	66.7	26.5	72.8	26.8	13.3	0.5
62	3.2	2134	70.7	25.4	84.0	27.1	0.6	4.0
63	0.8	2056	65.6	25.8	70.0	26.3	20.9	1.5
64	3.2	1574	74.9	24.0	100.8	27.5	11.4	1.2
65	1.2	2094	70.3	25.7	82.7	27.2	10.6	2.5
66	1.1	1589	69.9	24.9	81.8	26.7	12.1	5.2
67	0.8	1896	69.9	26.4	81.5	27.5	14.2	2.3
68	1.6	1556	77.1	23.3	111.9	27.8	10.8	1.0
69	1.1	1909	75.8	26.0	102.7	28.5	0.7	2.5
70	0.8	1674	75.8	26.0	102.7	28.5	2.2	2.1

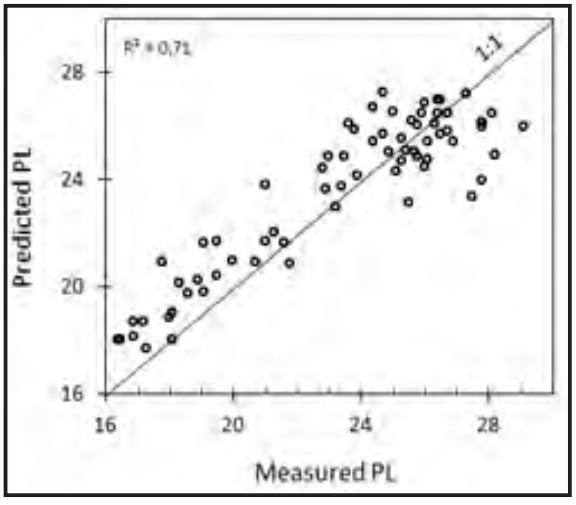

Figure 9- The predicted plastic limits using the representative extrusion pressure of 2300 kPa versus the plastic limits determined from rolling-device method.

Both regression coefficients for the correlations between the representative extrusion pressures from the reverse extrusion test and the liquid limits from the fall-cone method and the plastic limits from the rolling-device method, respectively, are rather encouraging; however, the authors' perception is that neither the correlation between the predicted and laboratory-determined liquid limits nor the correlation between the predicted and the laboratory-determined plastic limits can be utilized for practical purposes because the amounts of error involved in both predictions would be unacceptably high. The most likely reason for the imperfect match between the predicted- and laboratory-determined Atterberg limits are the variations of predominant range of extrusion pressures in histograms of figures 6 and 8. For instance, the predominant intervals for the extrusion pressures corresponding to liquid limits are 21-30 kPa for this study, 21-30 kPa for Kayabalı and Tüfenkçi

(2007) data, 31-40 kPa for Kayabalı and Tüfenkçi (2010) data and 11-20 kPa for Kayabalı (2012) data (Figure 6). The range of plasticity for soils used in this investigation and those in the previously published papers are not the same. Apparently, the extrusion pressures are plasticity dependent; for instance, while the soil samples with liquid limits higher than 75 have extrusion pressures corresponding to liquid limits less than 5 kPa, the soil samples with liquid limits around 30 or so have extrusion pressures corresponding liquid limits greater than roughly 30 kPa, indicating that the extrusion pressures corresponding liquid limits of low-plastic soils may be as high high as ten times that the extrusion pressures corresponding to liquid limits of high-plastic soils (see, for instance, table 1).

A similar conclusion can be drawn from figure 8, where the predominant intervals of extrusion pressures corresponding to the experimentally determined plastic limits are 2000-2500 kPa for this study, 1000-2000 kPa for Kayabalı and Tüfenkçi (2007) data, 2500-3000 kPa for Kayabalı and Tüfenkçi (2010) study and 1500-2000 kPa for Kayabalı (2012) data. There is not a unique extrusion pressure to represent soils' plastic limit either. The bottomline is that assigning a single extrusion pressure value for all liquid limits is not realistic; the same is true for plastic limit.

In an attempt to seek a more meaningful relationship between the reverse extrusion characteristics of fine-grained soils and consistency limits a multiple regression analysis was carried out. For this purpose the liquid limit or the plastic limit were tried to be determined to be the functions of reverse extrusion coefficients (i.e., a and b).

The multiple regression between the reverse extrusion coefficients and the liquid limits determined using the fall-cone method resulted in the following empirical relationship with $R^2 = 0.92$:

$$LL = 0.04(a^{3.3})1.135^{b} \quad (1)$$

Likewise, the multiple regression analysis between the reverse extrusion coefficients and the plastic limits determined using the rolling-device method yield the following empirical relationship with $R^2 = 0.94$:

$$PL = 0.04(a^{2.33})\, b^{0.98} \quad (2)$$

At the next step the liquid and plastic limits are predicted with the empirical relationships given by equations (1) and (2), respectively. For instance, the liquid limit of any soil sample can be predicted by plugging the reverse extrusion coefficients of that soil sample into Eq. (1). Table 2 includes liquid limits and plastic limits for all soil samples predicted by the empirical relationships given in Eq. (1) and (2).

Figure 10 illustrates the correlation between the predicted liquid limit by Eq. (1) and the liquid limit determined through the fall-cone method. The matching of the predicted data with the laboratory data is superior (with $R^2 = 0.91$) to the correlation between the liquid limits predicted by the representative extrusion pressure of 15 kPa (Figure 7). It appears that there is some scatter of data pairs in figure 10. One possible reason for this may be due to the uncertainties inherent to the fall-cone test itself. Further analyses may be required to asses this thoroughly. The correlation between the predicted PL using the reverse extrusion coeeficients [i.e., Eq. (2)] provided better matching with the laboratory data from the rolling-device (see Figure 11; $R^2 = 0.91$) than that did the representative extrusion pressure of 2300 kPa (Figure 9).

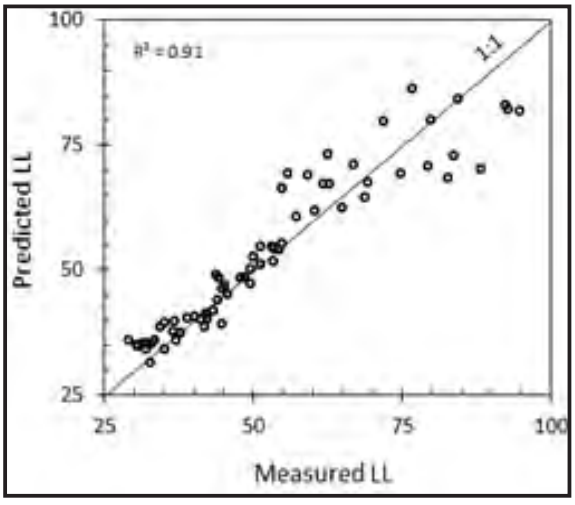

Figure 10- The predicted liquid limits using Eq. (1) versus versus the liquid limits determined from fall-cone method.

In order to assess the ability of the newly proposed equations to predict the liquid limit and plastic limit, a series of error analysis was performed. For instance, the amount of error involved in predicting the liquid limit with the proposed relationship (i.e., Eq. 1) was

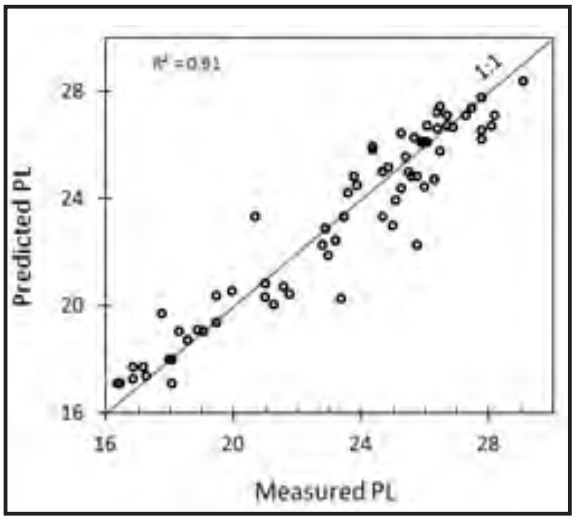

Figure 11- The predicted plastic limits using Eq. (2) versus versus the plastic limits determined from rolling-device method.

calculated as the ratio of the absolute value of the difference between the experimentally determined value and the predicted value to the experimentally determined value. The results are presented in table 2 as percentages. The same approach was employed to calculate the amounts of error for plastic limit and the results were listed in table 2.

To examine the distribution of percent errors for predicting the liquid limit the histogram in figure 12 was constructed. It is observed that more than 70% of experimentally determined liquid limits were predicted with an error less than 10%. The mean of all error values is 7.2% with a standard deviation of 5.8%. The percent error distribution for the plastic

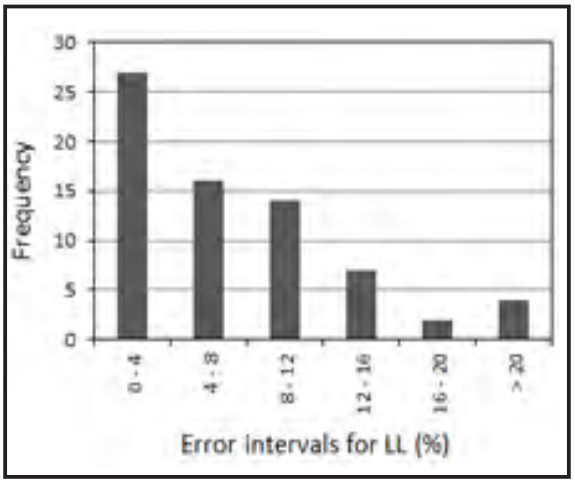

Figure 12- Percent error distribution for the predicted liquid limits using Eq. (1) with respect to the liquid limits determined from fall-cone method.

limit is shown in figure 13 as a histogram. The ability of the newly proposed equation to predict the plastic limit using the reverse extrusion coefficients appears to be remarkably good. About all plastic limits were predicted with an error of 10% and more than 80% of the plastic limits obtained from the rolling-device method can be found with a ±5% error.

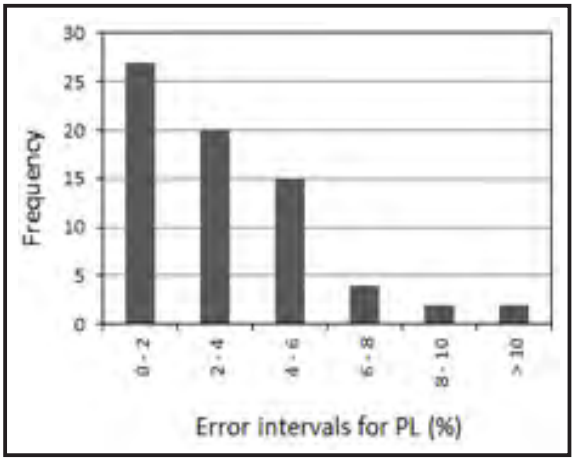

Figure 13- Percent error distribution for the predicted plastic limits using Eq. (2) with respect to the plastic limits determined from rolling-device method.

5. Conclusions

Following conclusions were drawn from this investigation:

1) The liquid limits and plastic limits predicted using the representative extrusion pressures of 15 kPa and 2300 kPa for the liquid limit and plastic limit, respectively, yield moderate- to good-level of correlations with the experimentally-determined consistency limits.

2) The imperfect match between the predicted consistency limits using the representative extrusion pressures and the experimentally determined consistency limits are attributed to the fact that the extrusion pressure corresponding to liquid limit is not constant for all soils. The same is true for plastic limit. It was observed that the extrusion pressures at either liquid limit or plastic limit for low-plasticity soils are many times those of high-plasticity soils. Therefore, the selection of representative extrusion pressures for liquid limit and plastic limit for the definition of those consistency limits proved not to be a good reference.

3) An alternative using the coefficents obtained from the fitted curves to the extrusion pressure versus water content data (i.e. a and b) in a multiple regression analysis showed that there exists a very

good level of correlation between the reverse extrusion coefficents and the two consistency limits.

4) The success obtained from a new series of predictions using the emprical equations using the multiple regression analysis is much better. The average of absolute errors for plastic limit and liquid limit are 3% and 7%, respectively.

5) The previous researchers indicated that the reverse extrusion test is robust, simple and highly inexpensive method. This fact is confirmed herein and it is proposed that the reverse extrusion method can be reliably used for the prediction of two of the most commonly used consistency limits together.

6) The proposed method is limited to the soils with the liquid limit range of 29-105. Precaution should be taken when applied to soils outside this range. Further analyses are recommended to cover the soils of very low plasticity as well as very high plasticity.

Received: 02.09.2014
Accepted: 15.02.2015
Published: June 2015

References

American Society for Testing Materials, 2010. Standard test methods for liquid limit, plastic limit, and plasticity index of soils: ASTM D4318-10, West Conshohocken, PA.

Belviso, R., Ciampoli, S., Cotecchia, V., and Federico, A., 1985. Use of the cone penetrometer to determine consistency limits. *Ground Engineering*, 18(5), 21-22.

BSI, 1990. Methods of test for civil engineering purposes classification tets (BS1377-2): British Standard Institution (BSI), London, UK.

CAN/BNQ, 1986. Soils – determination of liquid limit by the Swedish fall-cone penetrometer method and determination of plastic limit: CAN/BNQ 2501-092-M-86, Canadian Standards Asspciation and Bureau de Normalization du Quebec, Rexdale, Ont.

Casagrande, A, 1932. Research on the Atterberg limits of soils: *Public Roads*, 13, 3, 121-130.

Casagrande, A, 1958. Notes on the design of liquid limit device: *Geotechnique*, 8, 2, 84-91.

Clayton, C. R. I., Matthews, M. C. and Simons, N. E., 1995, Site investigation: Blackwell Science, 584 p.

Dolinar, B., 2010. Predicting the normalized, undrained shear strength of saturated fine-grained soils using plasticity-value correlations: *Applied Clay Science,* 47, 428-432.

Haigh, S. K., 2012. Mechanics of the Casagrande liquid limit test: *Canadian Geotechnical Journal*, 49, 1015-1023.

ISI, 1985. Determination of liquid and plastic limits (2270)I In Indian Standard Method of Test for Soils, Part 5, Indian Standards Institution (ISI), New Delhi, India.

Johnston, M. M., Strom, W. E. Jr., 1968. Results of second division laboratory testing program on standard soil samples: Misc. Paper, 3-978, U.S. army Engineer Waterways Experiment Station, Vicksburg, MS.

Kayabalı, K., 2012. An alternative testing tool for plastic limit: *Electronic Journal of Geotechnical Engineering* 17(O), 2107-2114.

Kayabalı, K., Tüfenkçi, O. O., 2007. A different perspectıve for the determination of soil consistence limits: International Symposium on Geotechnical Engineering, Ground Improvement and Geosynthetics for Human Security and Environmental Preservation, Bangkok, Thailand, 423-432.

Kayabalı K., Tüfenkçi, O. O., 2010. Determination of plastic and liquid limits using the reverse extrusion technique: *Geotechnical Testing Journal* 33(1), 14-22.

Lee, L. T., Freeman, R. B., 2007. An alternative test method for assessing consistency limits. *Geotechnical Testing Journal*, 30(4), 1-8.

Medhat, F., Whyte, I. L., 1986. An appraisal of soil index tests. *Geological Society, Engineering Geology Special Publication* 2, 317-323.

Prakash, K., Sridharan, A., 2006. Critical appraisal of the cone penetration method of determining soil plasticity. *Can. Geotech. J.* 43, 884-888.

Sherwood, P. T., 1970. The reproducibility of the results of soil classification and compaction tests: Report LR 339, Crowthorne, Road Research Laboratory.

Sherwood, P. T., Ryley, M. D., 1970. An investigation of a cone-penetrometer method for the determination of the liquid limit. *Geotechnique*, 20, 2, 203-208.

Sivakumar, V., Glynn, D., Cairns, P., Black, J. A., 2009. A new method of measuring plastic limit of fine materials. *Geotechnique*, 59, 10, 813-823.

Timar, A., 1974. Testing the plastic properties of cohesive and intermediate-type soils by extrusion. *Acta Tech. Ac. Sci. Hungary* 76 (3-4), 355-370.

Wasti, Y., Bezirci, M. H., 1986. Determination of the consistency limits of soils by the fall-cone test. *Canadian Geotechnical Journal* 23, 241-246.

Whyte, I. L., 1982. Soil plasticity and strength – a new approach for using extrusion. *Ground Engineering*, 15(1), 16-24.

Wood, D. M., 1982. Cone penetrometer and liquid limits. *Geotechnique*, 32, 2, 152-157.

Wroth, C. P., Wood, D. M., 1978. The correlation of index properties with some basic engineering properties of soils. *Canadian Geotechnical Journal* 15(2), 137-145.

BULLETION OF THE MINERAL RESEARCH AND EXPLORATION

Foreign Edition 2015 150

CONTENTS

Bull. Min. Res. Exp. (2015) 150: 145-162

Bulletin of the
Mineral Research and Exploration

http://bulletin.mta.gov.tr

INVESTIGATION OF IRRIGATION WATER QUALITY OF SURFACE AND GROUNDWATER IN THE KÜTAHYA PLAIN, TURKEY

Berihu Abadi BERHE[a*], Mehmet ÇELİK[b] and Uğur Erdem DOKUZ[a]

[a] *Ankara Üniversitesi, Fen Bilimleri Enstitüsü, Jeoloji Mühendisliği Anabilim Dalı, 06100, Tandoğan, Ankara*
[b] *Ankara Üniversitesi, Mühendislik Fakültesi, Jeoloji Mühendisliği ABölümü, 06100, Tandoğan, Ankara*

Keywords:
Water Chemistry, Water Quality, Hydrochemical Facies, Chemical Index, Agricultural Irrigation, Kütahya Plain

ABSTRACT

The Kütahya plain is one of the plains in Kütahya/Turkey, where drinking, agricultural and industrial water supplies are highly dependent on groundwater resources. The local population largely depends on water from alluvial shallow aquifer waters and some on the Felent and Porsuk rivers. Appraisal of surface and groundwater quality is extremely important to make sure the sustainable use of it for drinking, agricultural, and industrial purposes. The chemical quality of surface and groundwater of Kütahya plain has been studied in detail in order to have better understanding of potential water quality. A total of 21 groundwater samples and 6 surface water samples were collected in and around the plain. The relative abundance of major ions (meq/l) for most of the water samples were $Ca^{2+} > Mg^{2+} > (Na^{+}+K^{+})$ for cations and $HCO_3^{-} > SO_4^{2-} > Cl^{-}$ for anions. Five hydrochemical facies have been identified based on the major ion chemistry of the surface and groundwater of this area. However, based on hydrochemical facies, the type of water that predominates in the study area is Ca-Mg/Mg-Ca-HCO_3 type during both December 2013 and June 2014. There is no significant change in the hydrochemical facies noticed during the two sampling periods. The chemical Index such as Sodium Absorption Ratio (SAR), Residual Sodium Carbonate (RSC), Sodium Percentage (%Na), Permeability Index (PI), Kelley Index (KI), Magnesium Ratio (MR), Potential Salinity (PS) and Total Hardness (TH) were calculated. The results indicated that SAR, RSC and KI values revealed 100%, %Na value revealed 92.6%, PI and PS values revealed 85.2% and MR value revealed 66.7% of water samples are within the safe limit suitable for irrigation. To sum up, the quality of surface and groundwater of Kütahya plain in general was suitable for irrigation.

1. Introduction

Groundwater plays an important role in human life and development. The Safe portable water is absolutely essential for healthy living. About 80% diseases of the world population and more than one-third of the deaths in the developing countries are due to contamination of water (WHO 1993). Subsurface water is ultimate and most suitable fresh water resource for human consumption in both urban as well as rural areas. Rapid growth of population, development of agriculture and industrial activities especially in alluvial plain aquifers caused an intense increase in water consumption. The chemical constituents of irrigation water can affect plant growth directly through toxicity or deficiency, or indirectly by altering plant availability of nutrients (Ayers and Westcot, 1985; Rowe and Abdel-Magid 1995). Capillary pressure is the main cause for increasing amount of salty waters in vadoz zone and hence the nature of upper part of the soil zone changes into more saline (Çelik et al., 2008).

Irrigation water quality is generally evaluated by some determining factors such as Sodium Absorption Ratio (SAR), Residual Sodium Carbonate (RSC), Sodium Percentage (%Na), and Electrical Conductivity (EC). Along with the these indicators,

* *Corresponding author: Berihu Abadi Berhe, berhag2000@gmail.com*

some additional indices to categorize the waters for irrigation like Permeability Index (PI), Kelley Index (KI) and Total Hardness (TH) are also important.

The location of this study area was Kütahya district of Kütahya plain. It is located in downstream of Köprüören plain and upstream of Porsuk dam where the people of Eskişehir and Kütahya use as main source of water for both irrigation and domestic purposes. In the study area, people of this district and surrounding villages are the pioneer users of surface and groundwater for drinking and irrigation Purpose.

The interactions between agricultural irrigation, surface water and groundwater resources are always very close. The agricultural activities and industrial establishments in Kütahya city such as: sugar factories, nitrogen factories and leather industries are responsible for disposing treated and untreated effluents in the natural drainage system of Felent and Porsuk rivers. This paper describes the surface and subsurface water chemistry of shallow aquifers affected by agricultural activities and industrial establishments at Kütahya plain, Kütahya, Turkey.

Therefore, the present study was mainly conducted to measure and analyze the irrigation water quality parameters of Felent and Porsuk Rivers and groundwater of Kütahya plain that could potentially impact food safety of irrigation crops.

1.1. Study Area

The study area, Kütahya plain including its catchment is bounded by (UTM) coordinates 225000 – 268000 E longitude and 4345000 – 4380000 N latitude with an area of around 93 km^2 and its cathment covers about 530 km^2. Location map of study area shows in figure 1. The area is characterized by hills in the southwest and western parts. The highest elevation in the hilly area is 1764 m above sea level, whereas, much of the plain flat-lying, with height, typically, 920 to 950 m above sea level. The maximum length between the northwestern to southeastern tips and width of the plain is about 25.0 km and 5.5 km respectively. The natural surface drainage within the study area is generally towards the two dominant and perennial rivers: Felent and Porsuk Rivers. Felent River is fed by Enne dam located on the northwest of the Kütahya plain.

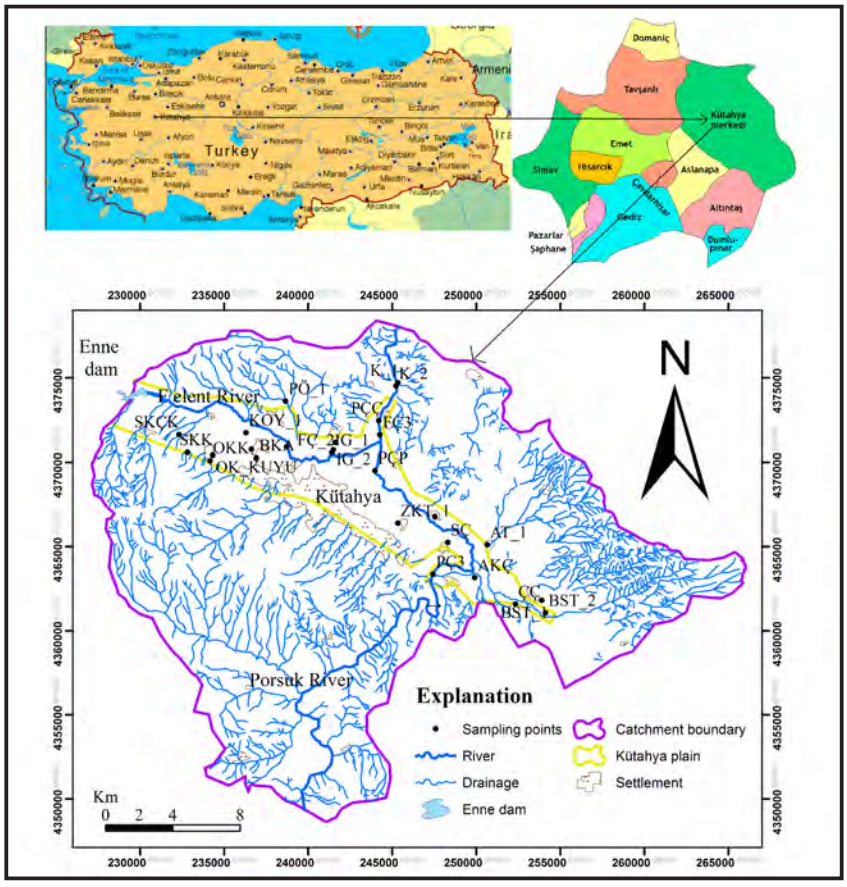

Figure 1- Location map of the study area and the sampling sites.

Kütahya has a warm summer continental climate, with cold and snowy winters and warm and dry summers. Rainfall occurs mostly during the spring and autumn. According to the data recorded at Kütahya Meteorological Station between the years 1975 and 2011, 75% of total rainfall occurs during the period of November - May and the annual average precipitation is about 543.85 mm. The average annual air temperature is 10.8°C with a maximum in July to August and a minimum in December to January.

1.2. Geological and Hydrogeological situation

The basment of of the study area Paleozoic age rocks. On top of these rocks Mesozoic, Neogene and Quatrernary rocks are exposed (Figure 2).

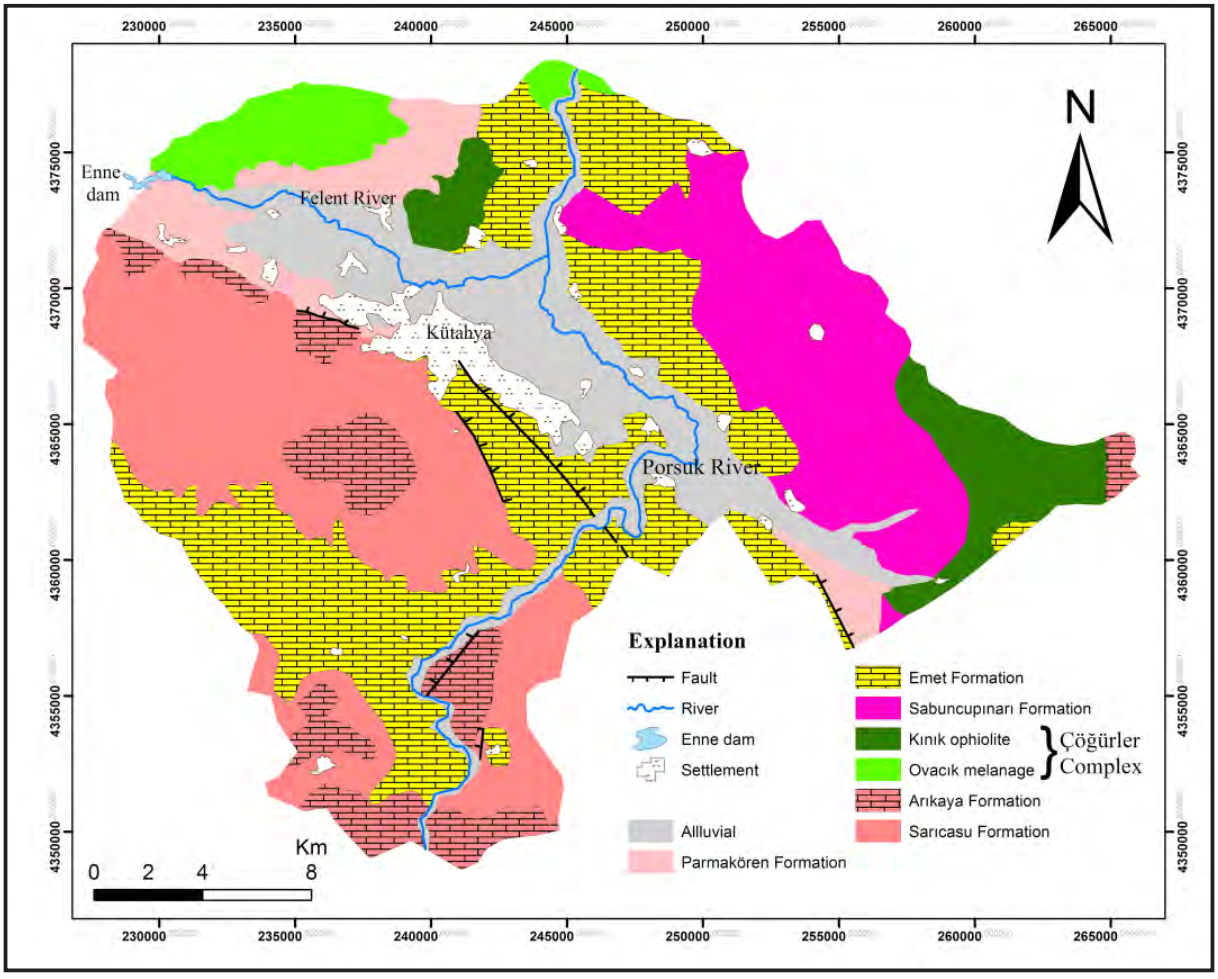

Figure 2- Geological map of the study area (modified from DSİ 1981, 2003; Özburan, 2009).

The oldest lithologic unit cropping out in the south west part of study area is the Sarıcasu formation of Paleozoic age, composed of schists, calc schist, quartz schist and crystallized limestone. At the top of the Sarıcasu formation is the Arıkaya formation of Upper Permian-Lower Triassic age, Marble. Unconformably overlying these Paleozoic schists and marble, are the outcropping Mesozoic age of Çöğürler Comlexes which is composed of low-grade regional metamorphism, and schistserpentinizated periodite and ophiolite-greenschist (DSI 1981 and 2003, Özburan, 2009). Crystalline limestones which we ascribe to the Mesozoic, unconformably overlie the Çayca Tuf and at the top, it is also unconformably covered by Plieistocene age of Parmakören Formation and Alluvials. Quaternary alluvium, consisting of fluviatile pebble, gravel, sand, clay, and silt, is widely distributed in this plain and has a maximum depth of 100 meters.

Quaternary sediments are the most important formations over a greater part of the study area specially for irrigation purpose. The groundwater occurs in the unconsolidated quaternary sediments dominated by gravel and sand.

In the plain the quaternary aquifer's hydraulic conductivity (K) and transmissivity (T) ranges 0.01- 336 m/day and 1.61 - 1010 m^2/day and with a mean values of 44.42 m/day and 213.48 m^2/day, respectivelly (Berhe et al., 2014).

The Parmakören formation is also another water bearing formation exposed in western part of the plain. The sandstone and gravelstone of this formation has hydraulic conductivity that ranges from 0.02 to 0.44 m/day with a mean value of 0.11m/day, and transmissivity varies from 1.56 to 26.92 m^2/day and its mean value is 8.59 m^2/day (Berhe et al. 2014).

In some boreholes the hydraulic characteristics of limestone aquifer of Emet formation within the area is affected by the dominance of marl lithology. Yield values show that some wells gave very small amount of water: for example 0.7 L/sec. However, the overall yield and values of aquifer constants are generally high as compared to other aquifers of the study area. In this aquifer there is well that can provide about 84.27 L/sec and The calculated hydrualic conductivity (K) and transmissivity (T) of these wells of this formation are ranging between 0.003 – 26.3 m/day and 1.11 - 2662.01 m^2/day with a mean value of 2.8 m/day and 350.81 m^2/day, respectivelly (Berhe et al., 2014).

The well opened in Çöğürler Complex in the ophiolitic material and has a yield of 7 l/sec. According to the results calculated from pumping test of residual drawdown data, the transmissivity and hydrualic conductivity values were 6.64 m^2/day and 0.034 m/day, respectively (Berhe et al., 2014).

2. Material and Method

Felent and Porsuk rivers were used to collect surface water samples and hand pumps, and wells opend by private and state hydrualic works Turkey were used to collect groundwater samples. A total of 6 surface river samples 3 from each were collected downstream and 21 groundwater samples were collected seasonally from Kütahya alluvial plain and sorrounding in December 2013 and June 2014. In-situ measurements of physicochemical parameters were done in the field using Multi 350i multi-parameter.

Water samples were filtered using 0.45 micron disposable capsule filter and collected in 250 ml polyethylene bottles with poly-seal caps for chemical analysis which have been done at Hacettepe University Water Chemistry Laboratory in Ankara, Turkey, using DIONEX LC25 and ICS-1000 High Performance Ion Chromotgraphy system and Automatic acid titration burette (for HCO_3^- and CO_3^{2-}) using the Standard Methods suggested by the American Public Health Association (APHA, 1989).

Aquachem Version 5.1 software was used to generate some of the important figures presented in this study.

In Arc GIS 10 software, geo-database was used to generate the spatial distribution maps of the chemical indices. The present work used the Inverse Distance Weighted (IDW) method for spatial interpolation of the chemical indices. Inverse Distance Weighted (IDW) is an interpolation technique in which interpolated estimates are made based on values at nearby locations weighted only by distance from the interpolation location (Naoum and Tsanis, 2004).

The parametres which were used in determination of irrigation water quality were all calculated using established standard equations (Table 1).

Electrical conductivity, at 25 °C, can be estimated by multiplying of the sum cations or anions (both in meq/l) by 100 where the accuracy of major ions is less than 5% (Appelo and Postma, 1994). In this study, electrical conductivity was not done in the field and the EC values of water samples collected during December 2013 was determined according this method (Table 2).

3. Results

3.1. Hydrogeochemistry

The result of hydrochemical analyses of surface and ground water samples are given in tables 2 and 3. The dominant major ions (meq/l) for most of the water samples were $Ca^{2+} > Mg^{2+} > (Na^+ + K^+)$ for cations and $HCO_3^- > SO_4^{2-} > Cl^-$ for anions (Table 4, 5 and Figure 4).

The concentration of cations- Ca^{2+}, Mg^{2+}, Na^+, K^+ ions ranged from 21.93 to 165.4; 6.89 to 237.91; 0.05 to 105.54; 0.52 to 105.4 mg/1 and anions (HCO_3^-, SO_4^{2-},Cl^-) varied from 275.39 to 731.41, 0.11 to 649.43; and 1.63 to 173.94 mg/l, respectively. The analytical precision for measurement of ions was determined by calculating the ionic balance error, which falls within the acceptable limits of ± 5%. The temperature of the groundwater ranged from 8.5 °C to 19.5 °C with an average value of 14.28 °C (Tables 2 and 3).

Table 1- Standard equations used to calculate different irrigation water quality indices (All concentrations are in meq/l, TH is in mg/l).

Parameter	Formula	Source
Sodium Adsoption Ratio	$SAR = \frac{Na^+}{\sqrt{\frac{Ca^{2+}+Mg^{2+}}{2}}}$	Hem (1991)
Permeability Index	$PI = (\frac{Na^+ + HCO3^-}{Ca^{2+}+Mg^{2+}+Na^+})x100$	Doneen (1964)
Residaul Sodium Carbonate	$RSC = (CO_3^{-} + HCO_3^{-}) - (Ca^{2+} + Mg^{+2})$	Ragunath (1987)
Magnesium Ratio	$MR = \frac{Mg^{2+}X100}{Ca^{2+}+Mg^{2+}}$	Paliwal (1972)
Sodium Percentage	$Na\% = (\frac{Na^+ + K^+}{Ca^{2+}+Mg^{2+}+K^+ + Na^+})x100$	Tank and Chandel (2010)
Kelley Index	$KI = \frac{Na^+}{Ca^{2+}+Mg^{2+}}$	Kelly (1963)
Potential Salinity	$PS = Cl^- + 0.5SO_4^{2-}$	Doneen (1964)
Total Hardness	$TH = (2.497Ca^{2+}) + (4.11Mg^{2+})$	Todd (1980)

Table 2- Results of chemical analyses of the surface and groundwater samples of the study area (Date of sampling: December 2013); Explanation: EC (µS/cm), concentrations (mg/l), temperature (°C),*surface water, ▪ spring water, ▲ shallow groundwater,▼deep groundwater.

Sample No	pH	T	EC	K^+	Na^+	Mg^{2+}	Ca^{2+}	Cl^-	SO_4^{2-}	HCO_3^-	%Error
PÇ-3*	8.23	13.8	613.0	2.61	9.74	21.32	83.25	2.36	9.05	337.57	4.75
PÇP*	8.53	13.3	665.0	3.01	10.71	22.72	85.36	6.93	24.00	355.34	0.32
PÇÇ*	7.70	14.9	844.5	6.29	31.97	24.92	81.02	22.16	31.79	438.25	-0.82
FÇ-1*	9.67	11.7	1104.5	6.88	23.81	59.38	106.53	28.63	79.17	479.71	3.31
FÇ-2*	8.72	10.3	1105.5	5.85	24.49	63.95	102.71	31.40	90.03	461.94	4.94
FÇ-3*	7.72	15.2	1111.0	30.51	31.55	39.79	119.66	26.42	22.34	574.47	4.15
SKK▪	8.83	10.6	483.0	0.86	2.27	22.15	59.32	1.78	6.50	275.39	1.89
OKK▪	8.12	13.7	539.5	1.21	3.37	52.94	21.93	3.66	16.77	284.86	4.71
SÇ▲	7.49	17.1	664.5	2.89	9.06	24.12	86.99	5.20	18.03	355.34	2.31
AKÇ▲	8.15	14.4	813.0	4.71	17.16	33.96	95.26	15.43	34.63	396.8	3.78
ÇÇ▲	8.18	13.4	654.0	4.59	7.37	37.75	65.00	6.20	13.43	343.49	4.10
BST-1▲	7.89	13.2	719.5	3.63	4.43	38.22	82.52	8.14	12.79	384.95	4.98
BST-2▲	7.71	12.8	858.5	2.49	5.45	62.23	71.37	4.63	16.12	456.02	4.59
AT-1▲	7.99	13.8	2071.5	158.99	68.35	105.53	118.56	94.36	153.18	621.84	4.51
İYKT-1▲	9.11	14.0	1985.0	129.99	69.88	82.66	152.28	92.05	187.18	586.31	4.68
ZKT-1▲	8.00	13.3	868.0	0.86	20.33	6.89	146.16	13.88	52.54	417.52	1.01
KOY-1▲	7.73	8.5	864.5	2.61	10.91	45.26	92.35	15.62	27.53	417.52	3.14
BK-A▲	8.34	13.0	720.0	1.25	5.53	41.38	76.77	11.35	13.84	355.34	4.58
İG-1▲	7.87	14.2	1352.5	4.38	43.86	76.79	114.77	60.99	184.30	441.21	4.53
İG-2▲	8.57	13.5	891.0	2.57	19.71	55.3	75.61	16.94	54.38	420.49	4.24

Table 2- (continued)

İG-3▲	8.93	14.5	3135.0	8.02	105.54	237.91	154.30	173.94	649.43	731.41	2.83
KOYM▲	7.74	12.2	1139.0	14.09	16.08	51.91	123.41	35.50	51.42	538.93	1.58
K-1▼	7.92	14.5	704.5	6.53	19.94	22.95	86.74	25.48	41.09	296.12	3.34
K-2▼	8.00	14.1	793.5	7.45	19.78	40.49	76.82	20.86	60.19	331.65	4.25
PÖ-1▼	8.46	13.8	576.5	1.85	16.4	29.78	50.16	6.33	9.39	313.88	-0.05
SKÇK▼	8.39	10.1	795.0	1.19	5.78	16.36	133.31	6.51	9.72	432.33	4.52
OKKuyu▼	8.45	12.7	517.0	0.60	3.12	24.67	60.26	3.19	2.73	302.04	0.44

Table 3- Results of chemical analyses of the surface and groundwater samples of the study area (Date of sampling: June 2014); Explanation: EC (µS/cm), concentrations (mg/l), temperature (°C),*surface water, ▪ spring water, ▲ shallow groundwater,▼deep groundwater.

Sample No	pH	T	EC	K^+	Na^+	Mg^{2+}	Ca^{2+}	Cl^-	SO_4^{2-}	HCO_3^-	%Error
PÇ-3*	7.58	16.9	548	2.30	8.55	25.03	82.40	4.98	20.16	331.65	4.29
PÇP*	7.54	18.5	608	3.82	15.64	27.33	85.61	11.58	24.20	361.26	3.70
PÇÇ*	7.24	18.4	762	6.53	23.87	32.04	82.95	21.68	38.14	393.83	4.78
FÇ-1*	7.42	15.5	690	5.70	17.06	33.35	86.03	14.60	52.29	373.11	4.59
FÇ-2*	7.52	15.4	556	4.16	12.12	27.75	72.38	11.48	40.29	302.04	3.43
FÇ-3*	7.34	19.2	672	7.03	19.74	30.96	78.65	18.71	54.64	343.49	4.76
SKK▪	7.62	12.8	431	0.52	1.24	26.71	59.24	1.63	6.06	284.27	3.60
OKK▪	7.35	13.9	694	0.85	2.82	57.99	81.00	3.10	16.56	479.71	3.82
SÇ▲	7.20	17.1	559	2.19	7.54	21.41	93.36	5.11	16.95	343.49	4.38
AKÇ▲	7.32	15.9	672	3.44	14.25	35.31	91.09	11.61	32.62	393.83	3.69
ÇÇ▲	7.47	15.4	542	3.63	6.01	43.46	60.63	5.21	12.59	367.18	3.02
BST-1▲	7.55	16.4	629	2.26	3.68	43.18	77.69	5.96	12.62	384.95	3.78
BST-2▲	7.32	16.2	681	2.15	5.15	57.10	75.63	3.87	12.93	456.02	4.50
AT-1▲	7.15	17.1	2050	165.99	63.35	100.53	120.56	95.36	140.18	630.84	4.51
İYKT-1▲	7.10	19.5	1677	105.40	57.44	85.59	146.58	89.27	173.05	581.10	3.78
ZKT-1▲	7.04	18.6	822	0.60	16.73	12.42	165.40	17.00	50.88	444.17	4.72
KOY-1▲	7.25	12.6	756	1.87	9.00	48.95	97.81	14.79	24.54	444.17	3.67
BK-A▲	7.20	14.6	625	0.89	4.39	42.40	75.78	11.48	13.40	364.22	3.58
İG-1▲	7.16	14.3	1226	3.29	39.84	83.02	128.86	83.41	231.92	438.25	2.12
İG-2▲	7.21	12.3	767	2.10	18.59	54.37	82.82	15.96	60.84	432.33	3.54
İG-3▲	7.19	12.5	1822	5.04	73.71	173.39	124.55	110.99	430.32	651.45	2.20
KOYM▲	7.01	12.0	789	9.44	8.18	47.64	101.53	18.54	25.58	467.86	3.73
K-1▼	7.13	17.6	832	6.88	29.65	34.13	102.73	76.57	50.57	319.80	3.35
K-2▼	7.49	19.0	580	5.64	11.00	36.61	59.71	13.59	27.25	296.12	3.95
PÖ-1▼	7.31	18.7	516	1.44	14.74	33.37	53.68	6.26	9.06	313.88	3.03
SKÇK▼	7.11	13.5	667	0.73	5.42	21.79	120.93	8.38	5.21	432.33	3.06
OK Kuyu▼	7.08	12.2	555	0.78	4.28	30.34	71.13	6.29	10.24	337.57	1.32

The evolution of hydrochemical parameters of groundwater can be understood by plotting the concentration of major cations and anions in the Piper's and Schoeller's diagrams. The most acceptable method to classify and compare water types based on ionic composition is proposed by Piper (1944) by plotting the chemical data on a trilinear diagram (Figure 3). Schoeller (1967) diagram is semi-logarithmic diagram was developed to represent major ion analyses in meq/l and to demonstrate different hydrochemical water types on the same diagram (Figure 4). This type of graphical representation has the advantage that, unlike the Piper diagram, actual water sample concentrations are displayed and compared.

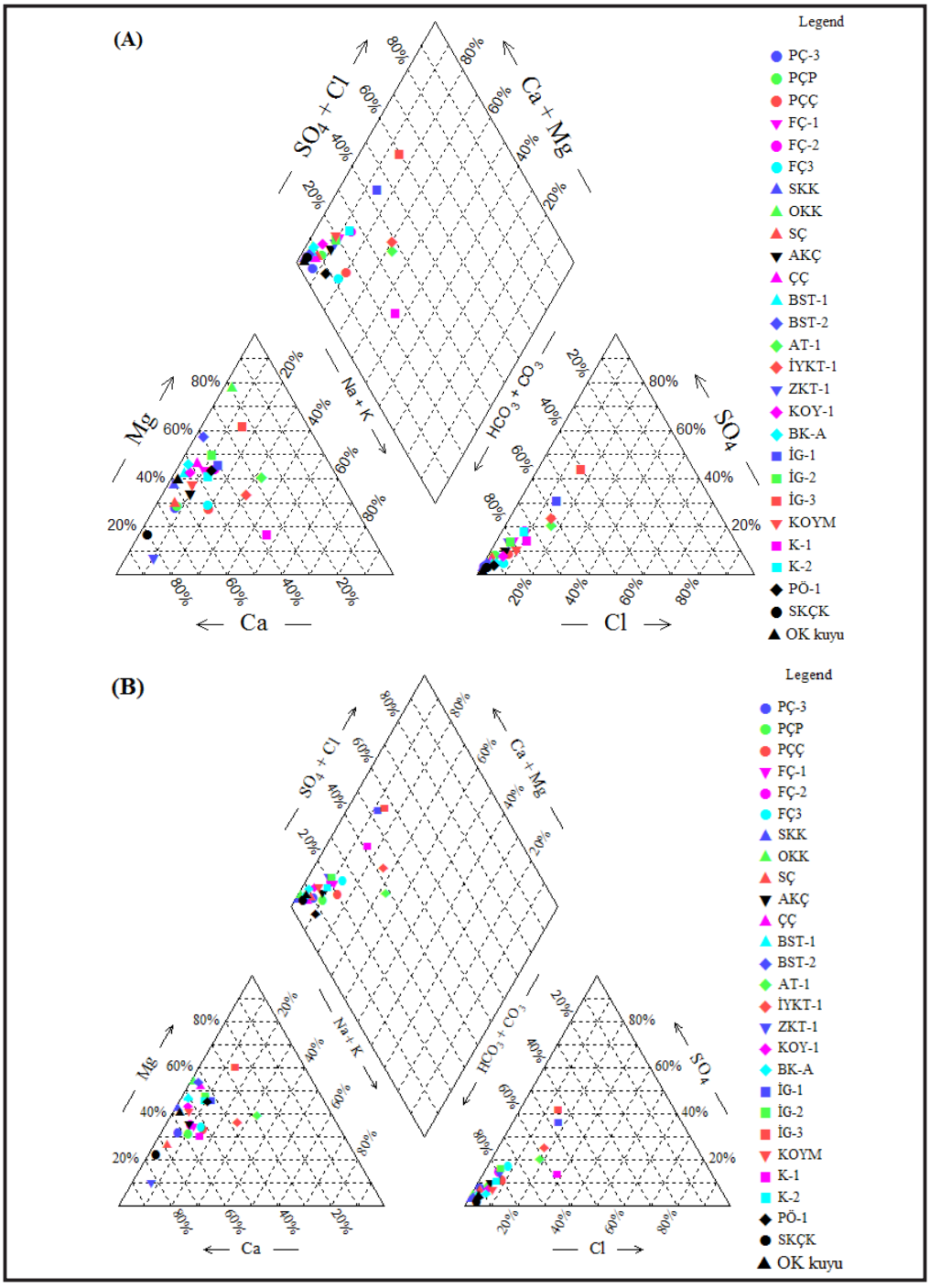

Figure 3- Piper's diagram of surface and groundwater samples (Sampling date- A: December 2013 and B: June 2014).

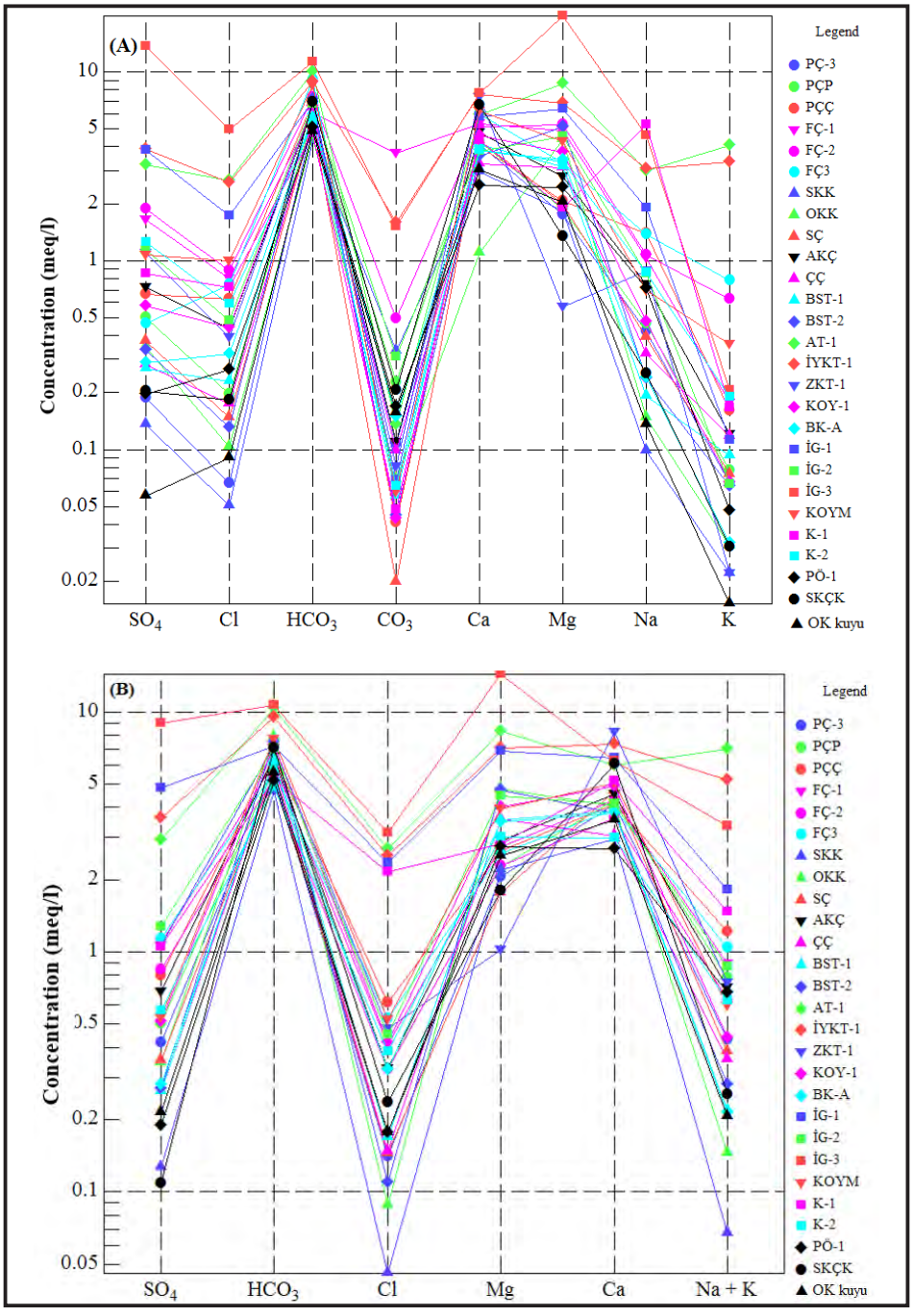

Figure 4- Schoeller diagram of surface and groundwater samples (Sampling date- A: December 2013 and B: June 2014).

The concentration of major ions of surface and groundwater of the study area were plotted in the Piper trilinear diagram to determine the Hydrochemical facies/water type. Hydrochemical facies are, district zones that posses cation and anion concentration categories, a result of rock-water interactions, geology and natural or anthropogenic contamination sources used to describe the type of water that differ in their chemical composition.

Five hydrochemical facies have been identified based on the major ion chemistry of the surface and groundwater of this area. However, based on hydrochemical facies, the type of water that predominates in the study area is Ca-Mg/Mg-Ca-HCO_3 type during both December 2013 and June 2014. Most of the waters of the two seasons are similar types but three water samples (IG-1, IG-3 and K-1) resulted in mixed water types (Tables 4, 5, Figure 3 and 4).

Table 4- Hydrochemical facies of surface and groundwater samples based on major ions (December 2013 samples).

Sample No	Cations	Anions	Hydrochemical facies
Surface waters			
PÇ-3, PÇP, PÇÇ, FÇ-1	$Ca^{2+}>Mg^{2+}>(Na^{+}+K^{+})$	$HCO_3^{-}>SO_4^{2-}>Cl^{-}$	Ca-Mg-HCO_3
FÇ-2	$Mg^{2+}>Ca^{2+}>(Na^{+}+K^{+})$	$HCO_3^{-}>SO_4^{2-}>Cl^{-}$	Mg-Ca-HCO_3
FÇ-3	$Ca^{2+}>Mg^{2+}>(Na^{+}+K^{+})$	$HCO_3^{-}>Cl^{-}>SO_4^{2-}$	Ca-Mg-HCO_3
Spring waters			
SKK	$Ca^{2+}>Mg^{2+}>(Na^{+}+K^{+})$	$HCO_3^{-}>SO_4^{2-}>Cl^{-}$	Ca-Mg-HCO_3
OKK	$Mg^{2+}>Ca^{2+}>(Na^{+}+K^{+})$	$HCO_3^{-}>SO_4^{2-}>Cl^{-}$	Mg-Ca-HCO_3
Shallow groundwaters			
SÇ, AKÇ, ÇÇ, BST-1, İYKT-1, KOY-1, KOYM	$Ca^{2+}>Mg^{2+}>(Na^{+}+K^{+})$	$HCO_3^{-}>SO_4^{2-}>Cl^{-}$	Ca-Mg-HCO_3
BST-2, AT-, İG-2	$Mg^{2+}>Ca^{2+}>(Na^{+}+K^{+})$	$HCO_3^{-}>SO_4^{2-}>Cl^{-}$	Mg-Ca-HCO_3
İG-1	$Mg^{2+}>Ca^{2+}>(Na^{+}+K^{+})$	$HCO_3^{-}>SO_4^{2-}>Cl^{-}$	Mg-Ca-HCO_3-SO_4
ZKT-1	$Ca^{2+}>(Na^{+}+K^{+})>Mg^{2+}$	$HCO_3^{-}>SO_4^{2-}>Cl^{-}$	Ca-HCO_3
BK-A	$Ca^{2+}>Mg^{2+}>(Na^{+}+K^{+})$	$HCO_3^{-}>Cl^{-}>SO_4^{2-}$	Ca-Mg-HCO_3
İG-3	$Mg^{2+}>Ca^{2+}>(Na^{+}+K^{+})$	$SO_4^{2-}>HCO_3^{-}>Cl^{-}$	Mg-Ca-SO_4-HCO_3
Deep groundwaters			
K-1, K-2, PÖ-1	$Ca^{2+}>Mg^{2+}>(Na^{+}+K^{+})$	$HCO_3^{-}>SO_4^{2-}>Cl^{-}$	Ca-Mg-HCO_3
SKÇK	$Ca^{2+}>Mg^{2+}>(Na^{+}+K^{+})$	$HCO_3^{-}>SO_4^{2-}>Cl^{-}$	Ca-HCO_3
OK Kuyu	$Ca^{2+}>Mg^{2+}>(Na^{+}+K^{+})$	$HCO_3^{-}>Cl^{-}>SO_4^{2-}$	Ca-Mg-HCO_3

Table 5- Hydrochemical facies of surface and groundwater samples based on major ions (June 2014 samples).

Sample No	Cations	Anions	Hydrochemical facies
Surface waters			
PÇ-3, PÇP, PÇÇ, FÇ-1, FÇ-2, FÇ-3	$Ca^{2+}>Mg^{2+}>(Na^{+}+K^{+})$	$HCO_3^{-}>SO_4^{2-}>Cl^{-}$	Ca-Mg-HCO_3
Spring waters			
SKK	$Ca^{2+}>Mg^{2+}>(Na^{+}+K^{+})$	$HCO_3^{-}>SO_4^{2-}>Cl^{-}$	Ca-Mg-HCO_3
OKK	$Mg^{2+}>Ca^{2+}>(Na^{+}+K^{+})$	$HCO_3^{-}>SO_4^{2-}>Cl^{-}$	Mg-Ca-HCO_3
Shallow groundwaters			
SÇ, AKÇ, BST-1, İYKT-1, KOY-1, KOYM	$Ca^{2+}>Mg^{2+}>(Na^{+}+K^{+})$	$HCO_3^{-}>SO_4^{2-}>Cl^{-}$	Ca-Mg-HCO_3
BST-2, AT-1, İG-2, ÇÇ,	$Mg^{2+}>Ca^{2+}>(Na^{+}+K^{+})$	$HCO_3^{-}>SO_4^{2-}>Cl^{-}$	Mg-Ca-HCO_3
İG-1, İG-3	$Mg^{2+}>Ca^{2+}>(Na^{+}+K^{+})$	$HCO_3^{-}>SO_4^{2-}>Cl^{-}$	Mg-Ca-HCO_3-SO_4
ZKT-1	$Ca^{2+}>Mg^{2+}>(Na^{+}+K^{+})$	$HCO_3^{-}>SO_4^{2-}>Cl^{-}$	Ca-HCO_3
BK-A	$Ca^{2+}>Mg^{2+}>(Na^{+}+K^{+})$	$HCO_3^{-}>Cl^{-}>SO_4^{2-}$	Ca-Mg-HCO_3
Deep groundwaters			
K-1	$Ca^{2+}>Mg^{2+}>(Na^{+}+K^{+})$	$HCO_3^{-}>Cl^{-}>SO_4^{2-}$	Ca-Mg-HCO_3-Cl
K-2, PÖ-1	$Mg^{2+}>Ca^{2+}>(Na^{+}+K^{+})$	$HCO_3^{-}>SO_4^{2-}>Cl^{-}$	Mg-Ca-HCO_3
OK Kuyu, SKÇK	$Ca^{2+}>Mg^{2+}>(Na^{+}+K^{+})$	$HCO_3^{-}>Cl^{-}>SO_4^{2-}$	Ca-Mg-HCO_3

3.2. Assessment of Waters for Irrigation Purpose

Enormous amounts of dissolved ions in irrigation water affect both agricultural soil physically and chemically and plants growth, thus reducing the productivity. Parameters such as Sodium Adsorption Ratio (SAR), Electrical Conductivity (EC), Residual Sodium Carbonate (RSC), Percent of Sodium (%Na), Magnesium Ratio (MR), Permeability Index (PI), Kelley Index (KI) and Potential Salinity (PS) were used to investigate the suitability of Felent and Porsuk rivers and groundwaters for irrigation. The average values of different parameter indices for rating surface and groundwater quality and its sustainability in irrigation for two differnt seasons were calculated (Table 6) and quality of irrigation water in relation to the different parameters is given by table 7.

Table 6- Values of different indices used for the assessment of the suitability of surface and groundwaters for irrigation.

Sample No	SAR			RSC (meq/l)			Na % (%)			MR			PI			KI			TH (mg/l)			PS (meq/l)			EC (µS/cm)		
	December 2013	June 2014	Average	December 2013	June 2014	Average	December 2013	June 2014	Average	December 2013	June 2014	Average	December 2013	June 2014	Average	December 2013	June 2014	Average	December 2013	June 2014	Average	December 2013	June 2014	Average	December 2013	June 2014	Average
PÇ3	0,25	0,21	0,23	-0,37	-0,73	-0,55	7,67	6,53	7,10	29,68	33,36	31,52	94,10	88,79	91,45	0,07	0,06	0,07	295,49	308,62	302,06	0,16	0,35	0,26	613,00	548,00	580,50
PÇP	0,27	0,38	0,32	-0,30	-0,60	-0,45	8,14	10,67	9,40	30,49	34,48	32,48	95,41	91,70	93,56	0,08	0,10	0,09	306,52	326,09	316,31	0,45	0,58	0,51	665,00	608,00	636,50
PÇÇ	0,80	0,56	0,68	1,09	-0,32	0,39	20,30	15,11	17,71	33,64	38,90	36,27	114,60	95,93	105,26	0,23	0,15	0,19	316,37	338,82	327,60	0,96	1,01	0,98	544,50	762,00	653,25
FÇ-1	0,46	0,40	0,43	-2,33	-0,92	-1,63	10,62	11,21	10,91	47,88	38,99	43,43	79,22	88,18	83,70	0,10	0,11	0,10	510,03	351,90	430,97	1,63	0,96	1,29	1104,50	690,00	897,25
FÇ-2	0,47	0,31	0,39	-2,81	-0,94	-1,88	10,48	9,71	10,09	50,65	38,72	44,68	75,44	85,32	80,38	0,10	0,09	0,10	519,30	294,79	407,04	1,82	0,74	1,28	1106,50	556,00	831,25
FÇ-3	0,64	0,48	0,56	0,17	-0,84	-0,33	18,90	13,83	16,37	35,40	39,35	37,38	101,64	88,54	95,09	0,15	0,13	0,14	462,33	323,65	392,99	0,98	1,10	1,04	1111,00	672,00	891,50
SKK	0,06	0,03	0,05	-0,27	-0,49	-0,38	2,46	1,29	1,87	38,10	42,63	40,37	94,53	90,53	92,53	0,02	0,01	0,02	239,16	257,71	248,43	0,12	0,11	0,11	453,00	431,00	442,00
OKK	0,09	0,06	0,07	-0,78	-0,95	-0,86	3,16	1,61	2,39	79,91	54,13	67,02	86,08	89,39	87,74	0,03	0,01	0,02	272,36	440,61	356,49	0,28	0,26	0,27	539,50	694,00	616,75
SÇ	0,22	0,18	0,20	-0,50	-0,79	-0,64	6,90	5,64	6,27	31,37	27,43	29,40	92,56	88,32	90,44	0,06	0,05	0,06	316,37	321,11	318,74	0,33	0,32	0,33	664,50	559,00	611,75
AKÇ	0,38	0,32	0,35	-1,04	-0,99	-1,02	10,31	8,68	9,50	37,01	38,98	38,00	87,45	87,70	87,57	0,10	0,08	0,09	377,41	372,55	374,98	0,80	0,67	0,73	513,00	672,00	592,50
ÇÇ	0,18	0,14	0,16	-0,72	-0,58	-0,65	6,45	5,10	5,77	48,91	54,16	51,53	89,25	91,54	90,40	0,05	0,04	0,05	317,46	330,01	323,73	0,31	0,28	0,30	654,00	542,00	598,00
BST-1	0,10	0,08	0,09	-0,95	-1,12	-1,03	3,79	2,85	3,32	43,29	47,81	45,55	87,25	85,28	86,26	0,03	0,02	0,02	363,13	371,46	367,30	0,36	0,30	0,33	719,50	629,00	674,25
BST-2	0,11	0,11	0,11	-1,20	-0,99	-1,10	3,35	3,19	3,27	58,97	55,44	57,21	86,50	88,56	87,53	0,03	0,03	0,03	433,97	423,54	428,76	0,30	0,24	0,27	858,50	681,00	769,75
AT-1	1,10	1,11	1,10	-4,40	-4,40	-4,40	32,54	32,61	32,58	59,46	59,46	59,46	74,95	74,98	74,96	0,20	0,21	0,20	729,76	714,21	721,99	4,26	4,16	4,21	2072,50	2071,50	2072,00
IYKT-1	1,13	0,93	1,03	-4,79	-4,83	-4,81	30,66	26,58	28,62	47,22	49,04	48,13	72,56	71,36	71,96	0,21	0,17	0,19	719,96	717,79	718,88	4,55	4,32	4,43	1985,00	1677,00	1831,00
ZKT-1	0,45	0,34	0,39	-1,02	-1,99	-1,50	10,34	7,42	8,88	7,21	11,01	9,11	88,39	80,07	84,23	0,11	0,08	0,10	393,27	464,04	428,66	0,94	1,01	0,97	868,00	822,00	845,00
KOY-1	0,23	0,19	0,21	-1,49	-1,62	-1,56	6,11	4,70	5,40	44,68	45,20	44,94	83,13	82,52	82,83	0,06	0,04	0,05	416,60	445,41	431,01	0,73	0,67	0,70	864,50	756,00	810,25
BKA	0,13	0,10	0,11	-1,41	-1,30	-1,35	3,63	2,86	3,25	47,04	47,97	47,51	81,16	82,61	81,88	0,03	0,03	0,03	361,75	363,48	362,61	0,46	0,46	0,46	720,00	625,00	672,50
İG-1	0,78	0,67	0,73	-4,81	-6,07	-5,44	14,37	12,06	13,21	52,44	51,50	51,97	65,53	59,49	62,51	0,16	0,13	0,14	602,17	662,96	632,57	3,64	4,77	4,20	1352,50	1226,00	1289,25
IG-2	0,42	0,39	0,41	-1,43	-1,52	-1,47	9,99	9,11	9,55	54,66	51,97	53,31	84,45	83,88	84,17	0,10	0,09	0,10	416,05	430,26	423,16	1,04	1,08	1,06	891,00	767,00	829,00
İG-3	1,24	1,00	1,12	-15,28	-9,80	-12,54	14,96	14,01	14,49	71,76	69,65	70,70	52,05	58,64	55,34	0,17	0,16	0,16	1363,09	1023,65	1193,37	11,67	7,61	9,64	3135,00	1822,00	2478,50
KOYM	0,31	0,17	0,24	-1,59	-1,31	-1,45	9,22	6,24	7,73	40,95	43,61	42,28	85,69	85,93	85,81	0,07	0,04	0,05	521,51	449,32	485,42	1,54	0,79	1,16	1139,00	789,00	964,00
OK well	0,09	0,11	0,10	-0,08	-0,51	-0,30	2,90	3,30	3,10	40,29	41,28	40,78	98,37	91,80	95,09	0,03	0,03	0,03	251,84	302,32	277,08	0,12	0,28	0,20	519,00	555,00	537,00
K-1	0,49	0,65	0,57	-1,36	-2,69	-2,03	14,27	15,60	14,94	30,37	35,38	32,88	80,78	70,83	75,80	0,14	0,16	0,15	310,93	396,81	353,87	1,15	2,69	1,92	704,50	832,00	768,25
K-2	0,45	0,28	0,37	-1,73	-1,14	-1,43	12,80	9,42	11,11	46,49	50,26	48,38	78,48	82,43	80,46	0,12	0,08	0,10	358,25	299,59	328,92	1,21	0,67	0,94	793,50	580,00	686,75
PÖ-1	0,45	0,39	0,42	0,19	-0,28	-0,04	13,32	11,11	12,22	49,46	50,61	50,04	103,42	95,42	99,42	0,14	0,12	0,13	247,63	271,20	259,41	0,28	0,27	0,27	576,50	516,00	546,25
SKÇK	0,13	0,12	0,12	-0,91	-0,74	-0,82	3,40	3,15	3,27	16,82	22,90	19,86	88,96	90,83	89,90	0,03	0,03	0,03	400,12	391,51	395,81	0,28	0,29	0,29	795,00	667,00	731,00

Table 7- Irrigation water quality according to different indices.

Parameter	Range	Class	Source
EC	< 250	Excellent	Richard (1954)
	250-750	Good	
	750-2000	Permissible	
	2000-3000	Doubtful	
	> 3000	Unsuitable	
Na%	< 20	Excellent	Todd (1960)
	20-40	Good	
	40-60	Permissible	
	60-80	Doubtful	
	> 80	Unsuitable	
MR	< 50	Suitable	Paliwal (1972)
	> 50	Unsuitable	
TH	< 60	Soft	Durfor and Becker (1964)
	60-120	Moderately	
	120-180	Hard	
	> 180	Very hard	
RSC	< 1.25	Safe	Aghazadeh and Mogaddam (2010)
	1.25-2.5	Marginally suitable	
	> 2.5	Not suitable	
SAR	< 20	Excellent	Todd (1960)
	20-40	Good	
	40-60	Permissible	
	60-80	Doubtful	
	> 80	Unsuitable	
PI	<25 (Class III)	Unsuitable	Doneen (1966)
	25-75 (Class II)	Good	
	> 75 (Class I)	Excellent	
KI	< 1	Suitable	Kelley (1940) and Paliwal (1967)
	> 1	Unsuitable	
PS	< 3	Suitable	Doneen (1964)
	> 3	Unsuitable	

3.2.1. *Sodium Adsorption Ratio (SAR)*

Whenever there is high sodium ion and low in calsium ion concentration in a water used for irrigation purpose, the ion-exchange complex may become saturated with sodium ion which destroys the nature of soil structure, due to the dispersion of the clay particles (Todd, 1980) and affects the plant growth. As indicated in table, the computed SAR values for two different seasons range from 0.03 to 1.24 and all values are within the excellent class (Table 6 and 7). According to the graph of sodium hazard versus salinty hazard (Wilcox, 1950) all the water sample collected in December 2013 and June 2014 fall into category C2-S1 and C3-S1, indicating low alkali hazards and excellent irrigation water. However, one shallow well water sample collected during december 2013 categorized as C4-S1 type indicating high salinity hazard and low alkali hazard (Figures 5A, B). The average spatial distribution maps of the two seasons is given in figure 6A and Northwest of the study area is the safest.

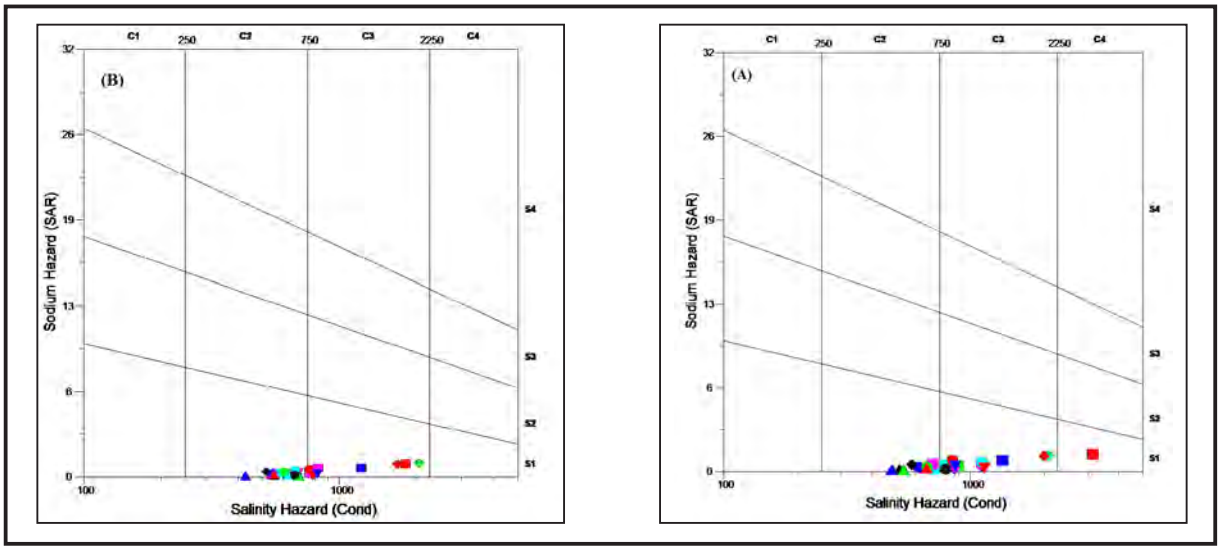

Figure 5- Classification of water samples with respect to salinity and sodium hazard: A) December 2013 and B) June 2014.

3.2.2. *Electrical Conductivity (EC)*

The most important water quality guideline on crop productivity is the salinity hazard as measured by electrical conductivity (Johnson and Zhang, 1990). Figure 6B illustrates the spatial distribution of EC over area of study. Majority of the area is characterized by good water quality. The average EC for the two seasons ranges from 442.38 to 2469.69 µS/cm (Figure 6B). According to the the spatial distribution map of EC, the waters in the northwest and southeast of Kutahya plain have a lower salinity hazard.

Based on standard classification systems (Richards, 1954; Todd, 1980), 59% of the samples falling into the good; 33% falling into permissible; and the remaining 8% falling into the doubtful, highly saline signifying high salinity hazard.

3.2.3. *Residual Sodium Carbonate (RSC)*

RSC has been calculated to determine the hazardous effect of carbonate and bicarbonate on the quality of water for agricultural purpose (Aghazadeh and Mogaddam, 2010). Table 6 indicated that the computed RSC values range from -15.28 to 0.39 meq/l and water samples are within the safe water category. The spatial distribution of the RSC value are given in Figure 6C and northwestern part of the plain have the lowest RSC values.

3.2.4. *Percent of sodium (%Na)*

Percent of sodium (Wilcox,1955) has been used in determination of groundwater suitability for irrigation, because the concentarion of sodium ion reacts with soil to reduce its permeability (Todd, 1980). The computed Na% for the study area ranged from 1.29 to 32.61%. Based on Table 7; and Figure 7D indicate that 92.6% of the waters from study area are within the excellent class and the rest 7.4% are within good class. Generally, Northwest of the Kütahya plain is the safest area.

3.2.5. *Magnesium Ratio (MR)*

Magnesium ratio is considered to be one of the most important parametr in determining the suitability of water for irrigation. Excess amount of magnesium in water reduces the growth and yields as the soil becomes more saline (Joshi et al, 2009). The values of MR for all water samples of the study area vary from 7.21 to 79.91 and spatially northwest part of the plain has the lowest values. According to the results 70.4% of the samples are suitable for irrigational practice (Tables 6, Figure 7E).

3.2.6. *Permeability Index (PI)*

The soil permeability is influenced by long term use of irrigation water and sodium (Na^+), calcium (Ca^{2+}) , magnesium (Mg^{2+}), bicarbonate (HCO_3^-) content of the soil (Raju, 2007). Doneen (1964) has evolved a formula, permeability index (PI) to measure the soil permeability for assessing the suitability of water for irrigation purposes (Table 1). The PI values range from 52.05 to 114.60 (Table 6) and the results indicate that 85.2% and 14.8% of the water samples of the study area fall within class I and class II respectivelly which make the water suitable for irrigation purposes. The

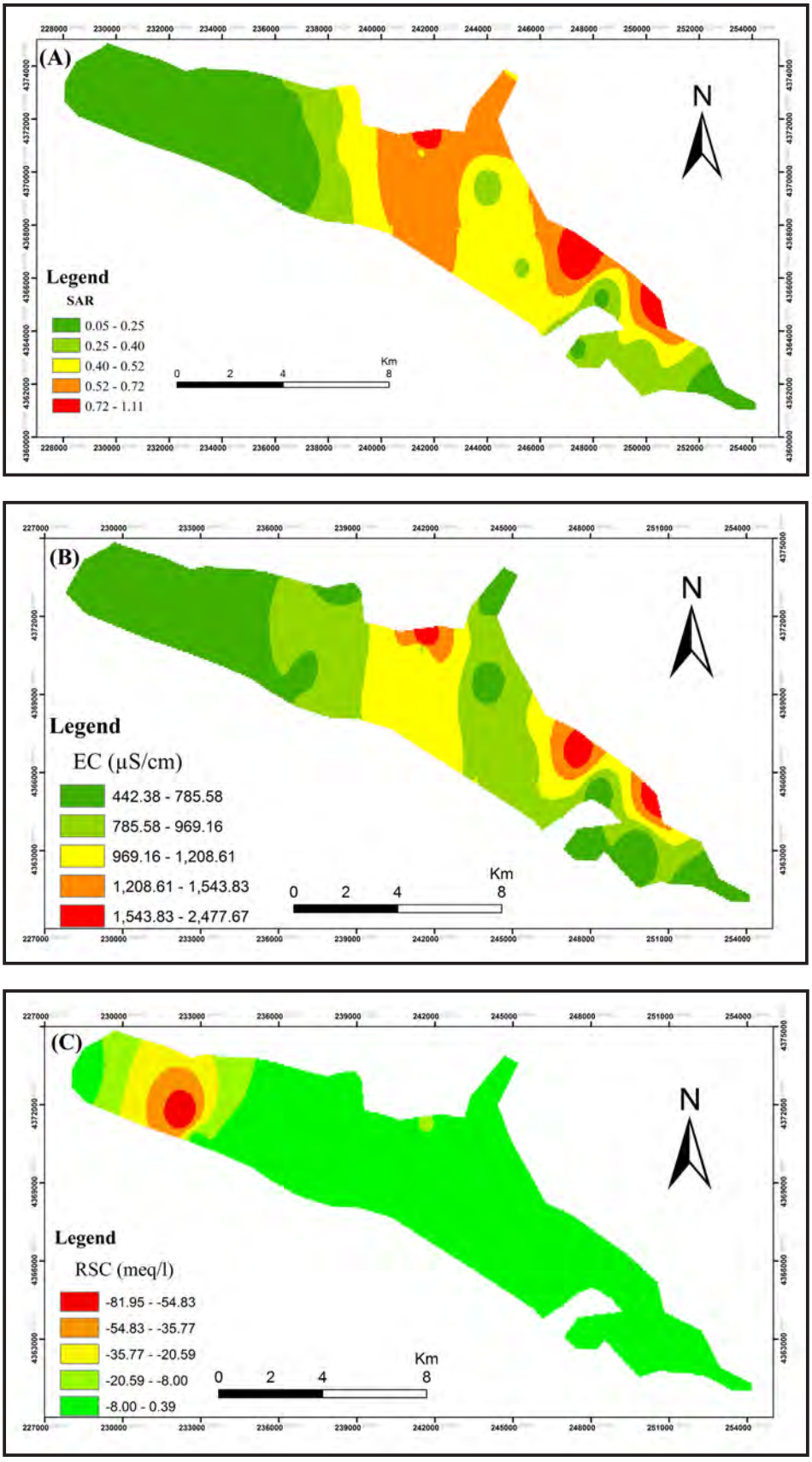

Figure 6- Spatial distribution of average values of two sampling seasons: (A) SAR, (B) EC (µS/cm) and (C) RSC (meq/l).

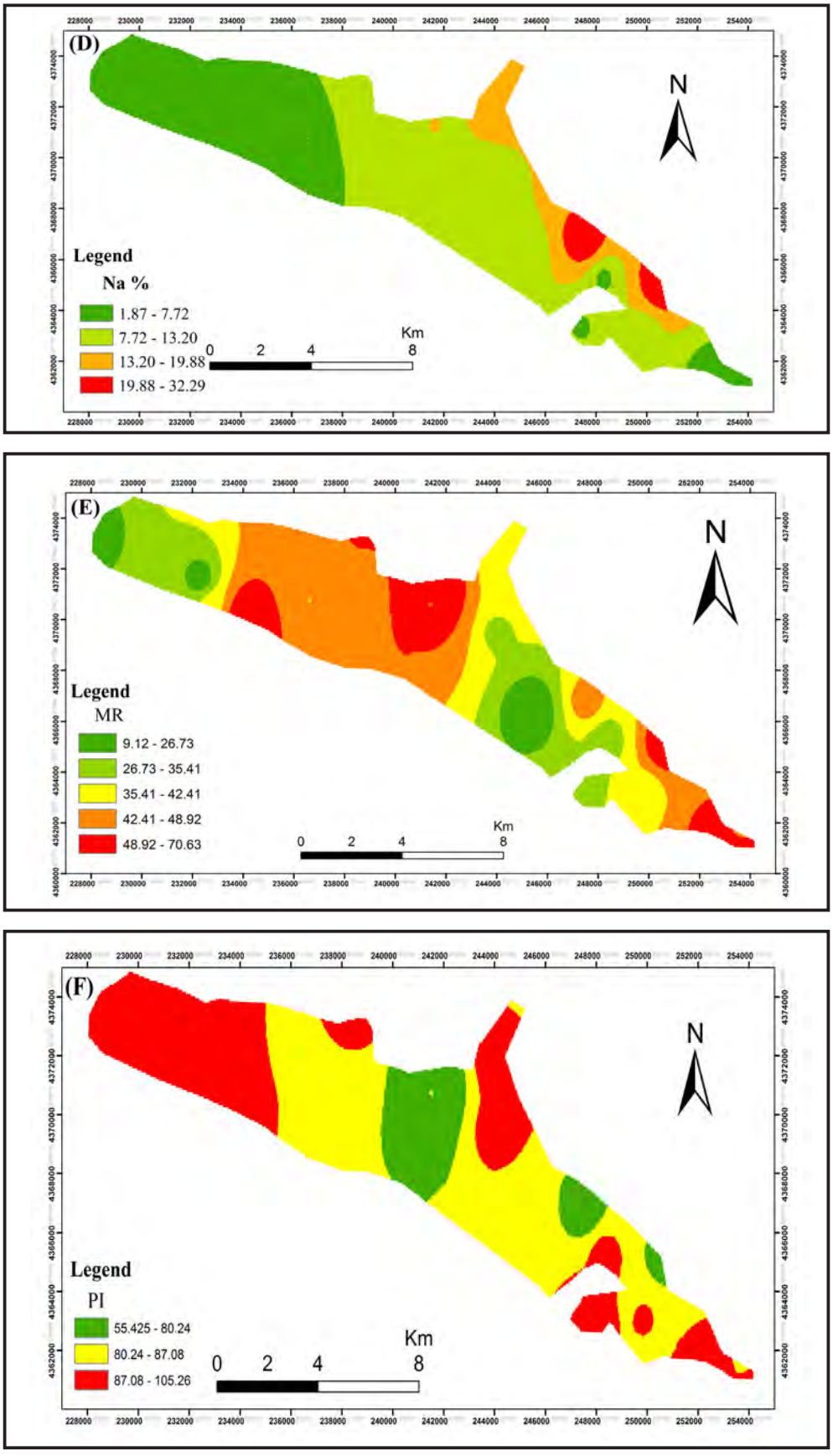

Figure 7- Spatial distribution of average values of two sampling seasons: (D) %Na, (E) MR and (F) PI.

spatial distribution map of average PI values of the two different seasons is given in figure 7F below and Northwest part of the plain is the safest.

3.2.7. *Kelley Index (KI)*

Kelley Index is expressed as the level of sodium ion measured against calsium and magnesium ions, and it is used to rate irrigation waters (Kelley, 1940; Paliwal, 1967). All the tested samples of the present study area classified as good because 100% of the KI values fall within the permissible limit of 1, indicating the good quality of the groundwater for irrigation purpose (Tables 6 and 7). The Spatial distribution map of average KI value for two sampling seasons is given by figure 8G below and the safest part of the area is shown in Northwest .

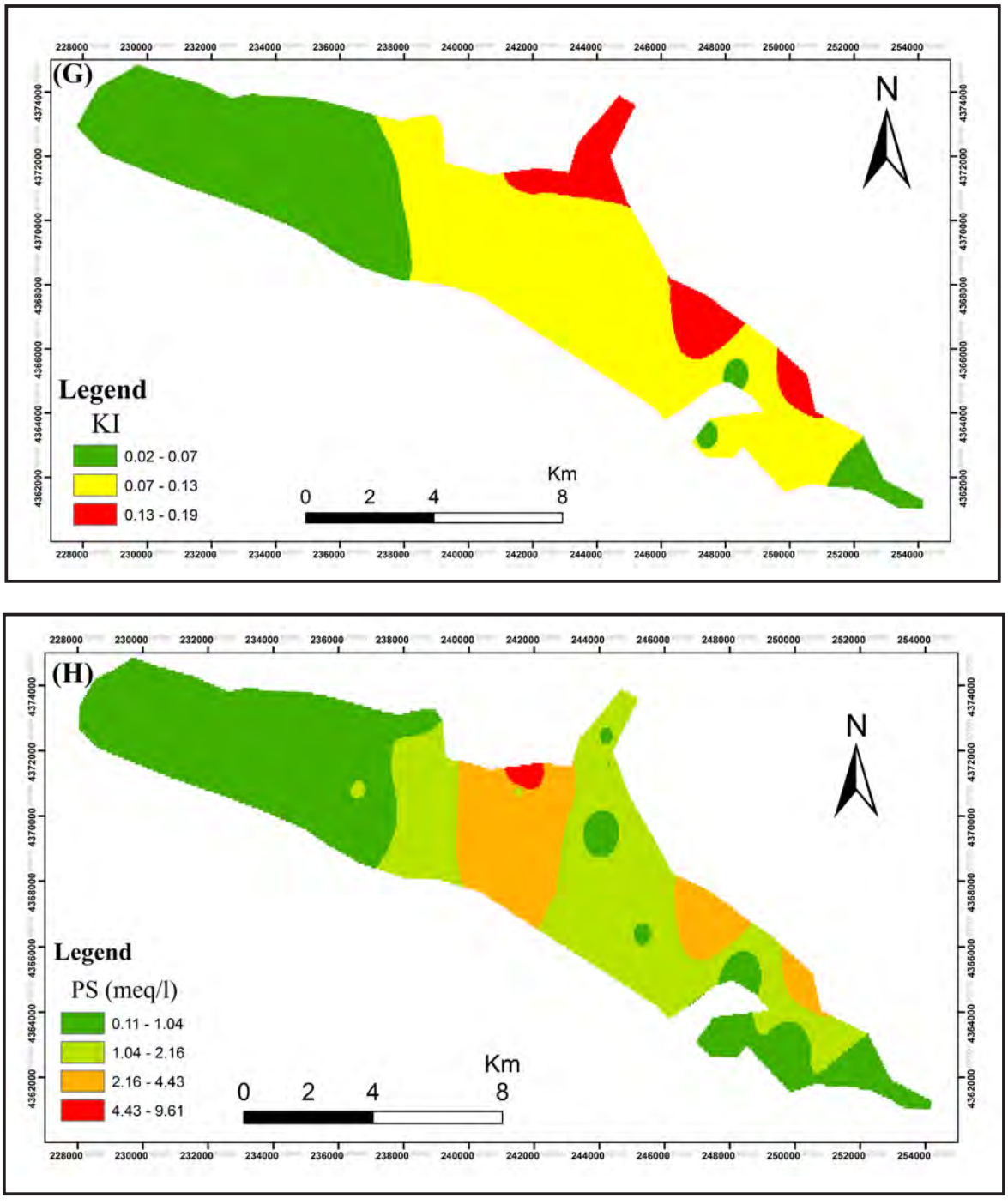

Figure 8- Spatial distribution of average values of two sampling seasons: (G) KI, (H) PS (meq/l) and (I) TH (mg/l).

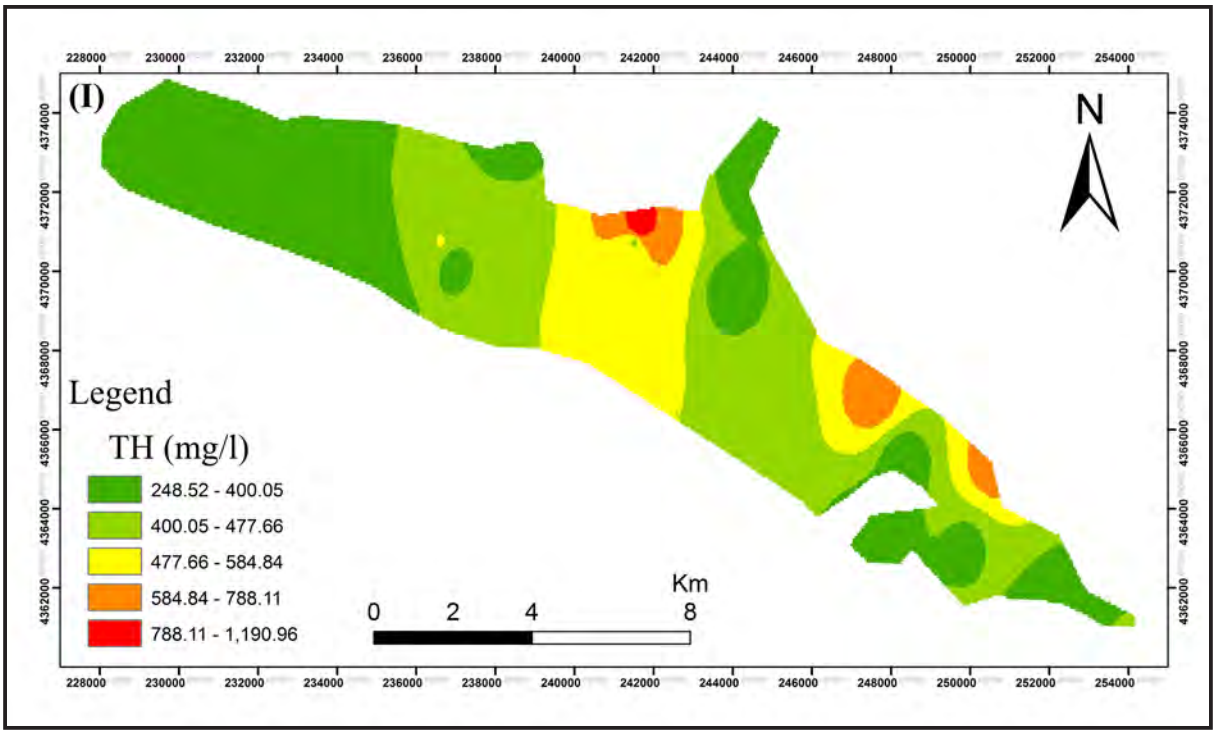

Figure 8- (continued)

3.2.8. *Potential Salinity (PS)*

Potential salinity is another parameter used for the classification of water for irrigation purpose. Potential salinity value less than 3 meq/l is suitable for irrigation purpose. Results from study area ranged from 0.11 to 11.67 meq/L (Table 6). The results of PS suggest that 85.2% of waters of the study area are suitable for irrigation. The average potential salinity spatial distribution map of two sampling seasons is produced for the area (Figure 8H).

3.2.9. *Total Hardness ($TH_{mg/l}$)*

Hard water is caused by high levels of calcium and magnesium carbonates. It is expressed as the total concentration of Ca^{2+} and Mg^{2+} as milligrams per liter equivalent $CaCO_3$ (Todd, 1980) The values of total hardness ranged from 247.63 to 1363.09 mg/l measured for the two different seasons (Table 6). It was witnessed that there was direct correlation TH with Ca^{2+} and Mg^{2+} values as the surface and groundwater in this area was very hard in nature indicating the presence of HCO_3^-, Ca^{2+} and Mg^{2+} ions concentrations. The plain's spatial distribution map of average TH (mg/l) value for two sampling seasons is given in figure 8I here under and the total hardness of the water increases towards northwest of the plain.

4. Discussion

Most of Kütahya plain groundwaters are Ca-Mg/Mg-Ca-HCO_3 water types which shows that geology appears to have greater influence on the chemical transformation of the groundwater resources, compared to any possible effects due to the anthropogenic activities within the study area.

The high value hardness in the waters is resulted from the alluvial and limestone aquifer of Emet formation, which is the main aquifer in the study area.

The Mg^{2+} ratio values 29.6 % of the water samples are unsuitable for irrigation. This can be explained by excess amount of Mg^{2+} in the samples. The observed high Mg^{2+} ion concentration resuled from the dolomite rocks and alluvial aquifer alkalinization of groundwater by leaching from organic fertilisers in weathered soils.

According to the calculated parameters (SAR, RSC, %Na, PI, KI, MR, PS ve TH) surface and groundwaters of northwest of the study area are less affected by urban wastewater, industrial wastewater and agricultural activities than other area and is good for irrigation purpose than waters from the rest part of the study area. In addition, northwest of the study area is constantly fed by Enne Dam which results in decreasing of ion concentration of surface and shallow groundwater.

The water chemistry of Kütahya plain is very important and needs care because the Porsuk Dam which uses as drinking water for both Kütahya and Eskişehir cities is situated in downstream. So any activities such as: agricultural activities, use of fertilizers, agricultural spraying, factory wastes and waste storage done in Kütahya plain should be controled.

Acknowledgements

This paper constitutes part of an on-going PhD research of the corresponding author, sponsored by the Ankara University Reaserch Institute. The author would like to express his thank and gratitude to the Reaserch Institute Office.

Received: 31.10.2014
Accepted: 11.02.2015
Published: June 2015

References

Aghazadeh, N., Mogaddam, A.A. 2010. Assessment of groundwater quality and its suitability for drinking and agricultural uses in the Oshnavieharea, Northwest of Iran. *Journal of Environmental Protection* 1, 30-40.

APHA, 1989. Standard methods for the examination of water and wastewater. 17th edition, *American Public Health Association,* Washington D.C., 1,268 p.

Appelo, C.A.J., Postma, D. 1994. Geochemistry. Groundwater and Pollution. *Rotterdam, A.A. Balkema*, 521 p.

Ayers, R.S., Westcot, D.W. 1985. Water quality for agriculture. Irrigation and drainage paper No. 29. Food and agriculture organization of the United Nations. Rome, 1-117.

Berhe, B.A., Çelik, M., Dokuz, U.E. 2014. Determination of aquifer properties of the Kütahya plain from a pumping and recovery test data. *67th Geological Congress of Turkey*, 14-18 April 2014, Ankara, 324-325.

Çelik, M., Ünsal, N., Tüfenkçi, O.O., Bolat, S. 2008. Assessment of water quality of the Lake Seyfe basin, Kırşehir, Turkey, *Environmental Geology*, 55, 559-569.

Doneen, L.D. 1964. Notes on water quality in agriculture. Published as a water science and engineering paper 4001, Department of Water Science and Engineering, University of California.

Doneen, L.D. 1966. Water quality requirement for agriculture. Proc. National Sym. Quality Standards for Natural Waters. University of Michigan, Ann. Report, 213- 218.

DSİ, 1981. Kütahya ve Köprüören Ovaları Hidrojeolojik Etüt Raporu, 65, say, *Devlet Su İşleri Genel Müdürlüğü*, 64 s, Ankara.

DSİ, 2003. Kütahya Ovası Karst Hidrojeolojisi Ara Raporu, *Devlet Su İşleri*, 41 s, Eskişehir.

Dufor C.N., Becker, E., 1964. Public water supplies of the 100 largestcities in the United States, 1962: U.S. Geological Survey, Water-Supply Paper 1812.

Hem, J.D. 1991. Study and interpretation of the chemical characteristics of natural waters. Book 2254, third edition. Scientific Publishers, Jodhpur.

Johnson, G., Zhang, H. 1990. Classification of Irrigation Water Quality, Oklahoma cooperative extension fact sheets (available at http://www.osuextra.com).

Joshi, D.M., Kumar, A., Agrawal. N. 2009. Assessment of the irrigation water quality of river Ganga in Haridwar District India. *Journal of Chemistry* 2(2), 285-292.

Kelley, W.P. 1940. Permissible composition and concentration of irrigation waters, Proc. ASCE 66.

Kelley, W.P. 1963. Use of saline irrigation water. *Soil science*., 95(6), 385-391.

Naoum, S., Tsanis, I.K. 2004. Ranking of spatial interpolation techniques using a GIS-based DSS. *Global Nest: the International journal* 6(1), 1-20.

Özburan, M. 2009. Neotectonic investigation of Kütahya and its surrounding. Ph.D. thesis, Kocaeli University, 227 p. Izmit (Unpublished).

Paliwal, K.V., 1967. Effect of gypsum application on the quality of irrigation waters. *The Madras agricultural journal* 59, 646–647.

Paliwal, K.V. 1972. Irrigation with saline water. New Delhi, *IARI*, 198p.

Piper, A.M. 1944. A graphical procedure in the geochemical interpretation of water analysis. Transactions, *American Geophysical Union* 25, 914–928.

Ragunath, H.M., 1987. Groundwater, second ed. *Wiley Eastern Ltd*, New Delhi, 456p.

Raju N.J., 2007. Hydrogeochemical parameters for assessment of groundwater quality in the upper Gunjanaeru River basin, Cuddapah District, Andhra Predesh, South India*, Environmental Geology*, 52, 1067-1074.

Richards, L.A., 1954. Diagnosis and Improvement of saline and alkali soils. Agric. Handbook 60, *USDA & IBH Publishing Company Limited*, New Delhi, India. 98- 99.

Rowe, D.R., Abdel-Magid, I.M., 1995. Handbook of Wastewater Reclamation and reuse. *CRC Press*, Inc. 550p.

Schoeller H., 1967. Geochemistry of groundwater. An international guide for research and practice, *UNESCO*, 15, 1-18.

Tank, D.K., Chandel, C.P.S., 2010. Analysis of the major ion constituents in groundwater of Jaipur City. *Nature and Science*, 8(10), 1-7.

Todd, D.K., 1960. Groundwater Hydrology. 1st ed., John Wiley and Sons, Inc,, 336p.

Todd, D.K., 1980. Groundwater Hydrology. 2nd ed., John Wiley and Sons, New York, 535p.

WHO, 1993. Guidelines for Drinking-Water Quality - 2nd Edition -Volume 1 - Recommendations, Geneva.

Wilcox, L.V. 1950. Classification and Use of Irrigation Waters. Department of Agriculture, United States, Circular No. 696, 16 p, Washington D.C.

Wilcox, L.V. 1955. Classification and use of Irrigation Waters. U.S. Dept. of Agric., Circular No. 696, 19 p, Washington D.C.

BULLETION OF THE MINERAL RESEARCH AND EXPLORATION

Foreign Edition 2015 150

CONTENTS

Bull. Min. Res. Exp. (2015) 150: 163-168

Bulletin of the
Mineral Research and Exploration

http://bulletin.mta.gov.tr

BRIEF NOTE ON NEOGENE VOLCANISM in KEMALPAŞA–TORBALI BASIN (İZMİR)

Fikret GÖKTAŞ[a*]

[a] *Maden Tetkik ve Arama Genel Müdürlüğü, Ege Bölge Müdürlüğü, İzmir*

This study was made in order to introduce Neogene volcanics the first time, which its presence has not been mentioned in previous investigations (Akdeniz et al., 1986; İnci, 1991; Kaya et al., 2007; Sözbilir et al., 2011), in Kemalpaşa–Torbalı basin corresponding to Torbalı section of the Akhisar Depression (Kaya, 1979; 1981) and to state their K/Ar ages (Figure 1).

Kemalpaşa group (Sözbilir et al., 2011) consisting of lower-middle Miocene deposits of Kemalpaşa–Torbalı basin from bottom to top is formed by Kesmedağı formation (Akdeniz et al., 1986), deposited in alluvial fan delta, Vişneli Formation (Sözbilir et al., 2011) which is made up of alluvial-fluvial deposits and by lacustrine Gökyaka formation (Göktaş, 2012) which has lateral equivalence (Figure 2). In upper parts of the Kesmedağı formation which reflects early-early middle Miocene sedimentation, the fauna of small mammal belonging to MN4 biozone (17-18 Ma: Steininger, 1999) was described (Kaya et al., 2007). Vişneli and Gökyaka formations overlying with a probable unconformity represent the middle Miocene sedimentation. Extrabasinal felsic tuff interlayers take place in upper parts of the lacustrine shale sequence (Aşağıvişneli member: Göktaş, 2012) which was distinguished in Gökyaka formation. 13.8±0.1 my Ar^{40}/Ar^{39} age was taken from those tuffs which are in ash fall facies (Sözbilir et al., 2011). Intrabasin Miocene volcanism represented by small lava extrusions from different origins is formed by Yukarıkızılca volcanic which was distinguished in middle Miocene deposit of the Kesmedağı formation and by Korucuk volcanic which intruded into Gökyaka formation (Göktaş, 2012).

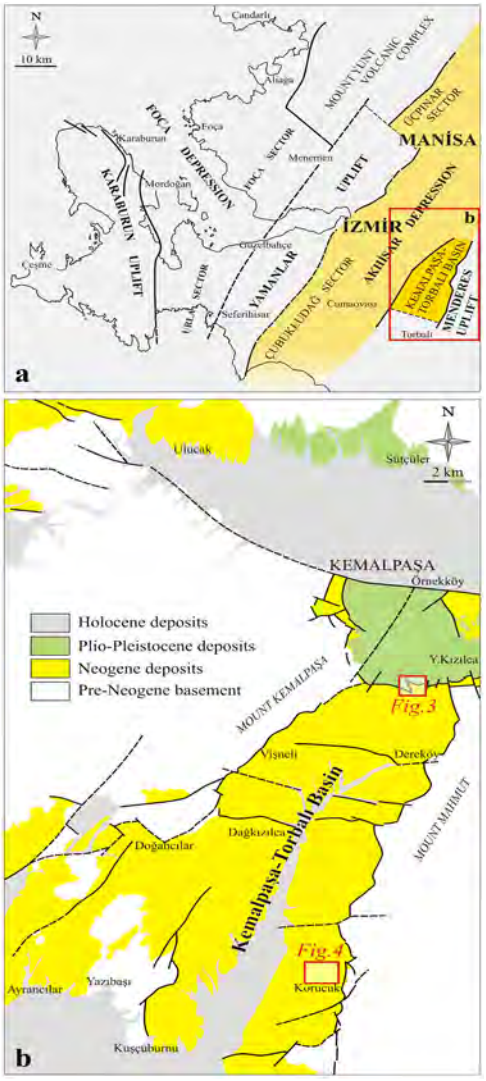

Figure 1- a) Tectonic setting of the Kemalpaşa-Torbalı basin in the Akhisar depression (modified after Kaya, 1979, 1981), b) Location map of investigated areas.

* *Corresponding author: Fikret Göktaş, fikretgoktas50@gmail.com*

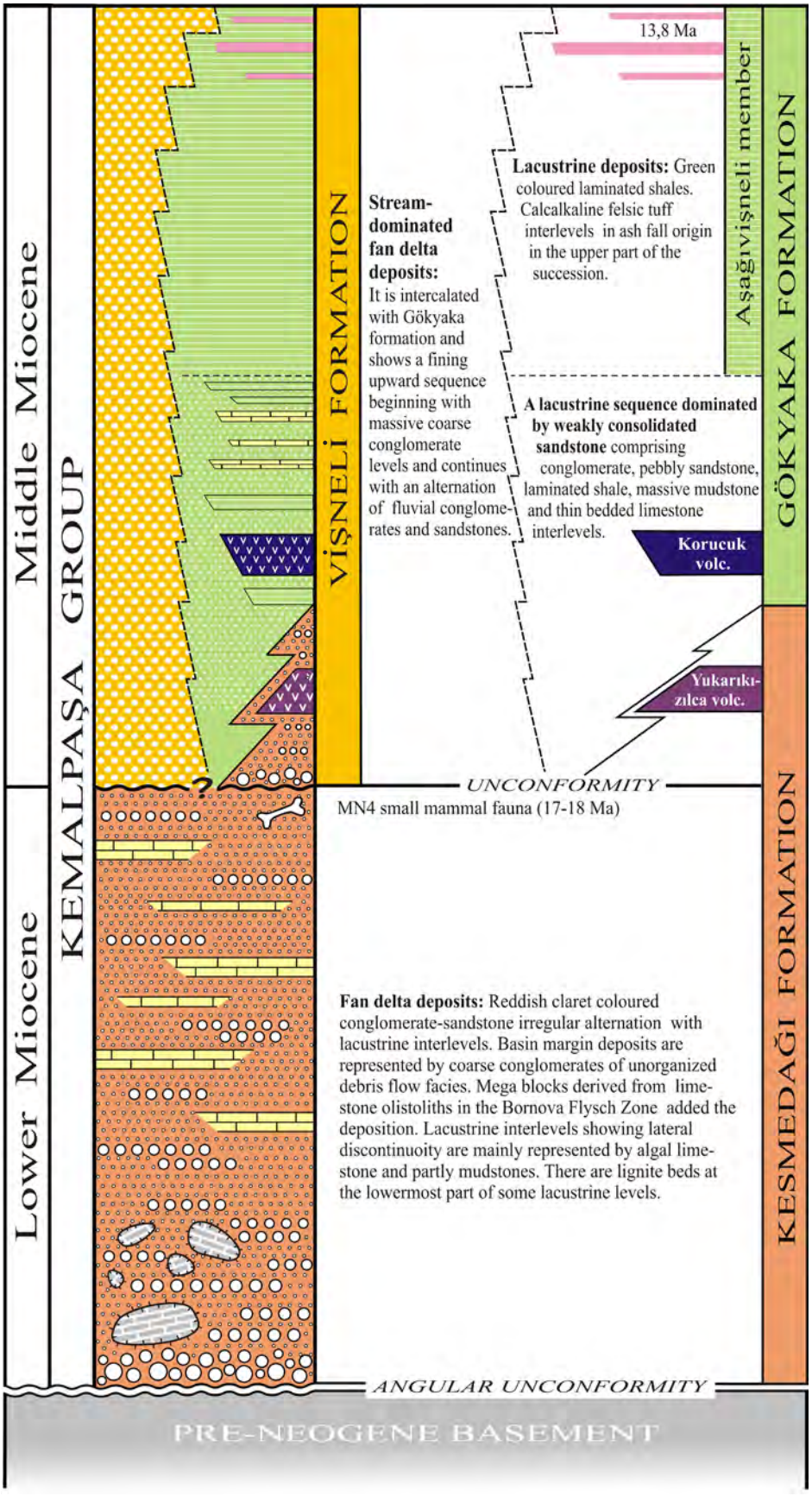

Figure 2- Generalized stratigraphy of the Kemalpaşa group litho-units (Modified after Sözbilir et al., 2011 and Göktaş, 2012).

1. Yukarıkızılca Volcanic

Bluish gray, altered lavas observed in reddish brown conglomerate-sandstone dominant sequence of the Kesmedağı formation were first defined by Göktaş (2012). At approximately 2.5 km SW of Yukarıkızılca village the lava mass distinguished around Karamolgediği Hill crop out in the section which was offset by strike slip and/or oblique slip faults of the detachment fault of Gediz Graben (Figure 3). Porphyry textured lavas of which its phenocrystal content is represented by plagioclase, amphibole, biotite, pyroxene and quartz were named as "andesite". Sheeted plagioclase phenocrysts show polysynthetic twinning and zoning. Some crystals display the characteristics of sieve and glomeroporphyritic textures. Some of amphibole phenocrysts have glomeroporphyritic texture, twinning and zoning. Sheetlike, anhedral ortho/clinopyroxene phenocrysts are occasionally observed in glomeroporphyritic texture. Quartz crystals are large, fractured and embayed. Within completely crystallized groundmass plagioclase, biotite microliths and opaque minerals are observed.

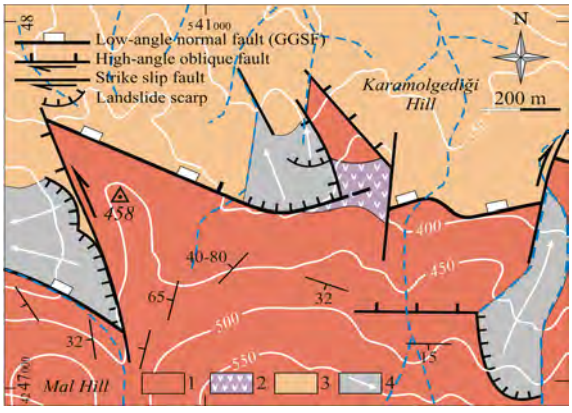

Figure 3- Geological map of the Yukarıkızılca volcanics and surrounding area (Göktaş, 2012). 1) Kesmedağı formation, 2) Yukarıkızılca volcanics, 3) Kızılca formation, 4) Landslide. GGSF: Gediz Graben Detachment Fault.

2. Korucuk Volcanic

The unit consisting rocks of mafic lava was first defined by Göktaş (2012) and distinguished as map unit. The main outcrop of the lava extrusion which is supposed to be deposited synchronous with the sedimentation in poor consolidated and massive sandstone sequence of the Gökyaka formation is around Yatan Hill in northeast of Korucuk village (Figure 4).

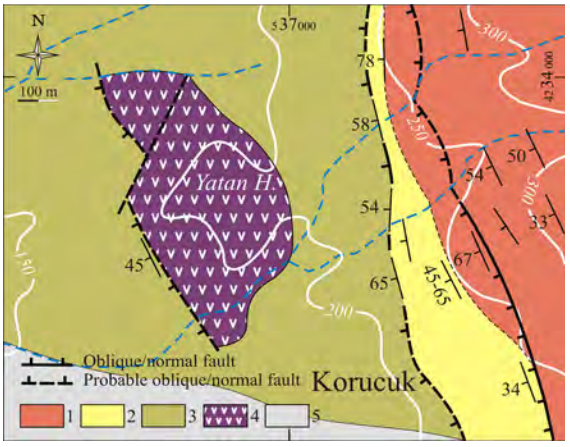

Figure 4- Geological map of the Korucuk volcanics and surrounding area (Göktaş, 2012). 1) Kesmedağı formation, 2) Kireçdere member, 3) Gökyaka formation, 4) Korucuk volcanics, 5) Alluvial fan deposits (Holocene).

Blackish, dark gray colored lava mass is extremely fractured in outer zones, with highly vesicular and altered. Porphyry textured lavas which their phenocrystal contents are represented by olivine, biotite and pyroxene were named as "olivine basalt". Euhedral-subhedral olivines which form glomeroporphyritic texture with each other and other phenocrysts have partly or fully turned into magnesium and iron carbonates starting from edges and fractures. Euhedral-subhedral clinopyroxenes are glomeroporphyritic in texture and display twining and zoning occasionally. Biotites and amphiboles which had transformed from clinopyroxene have become opaque starting from edges and cleavages. Fully crystallized groundmass material is formed by plagioclase microliths, microcrystals of biotite and pyroxene and opaque minerals. Quartz xenocrytals which are intensely observed in samples and have sizes larger than 5 mm reflect the magma mixing. As most of them were subjected to magmatic corrosion, embayed quartz crystals were surrounded by microliths and microcrystals of clinopyroxene.

3. Major Element Geochemistry

Major element composite of the Yukarıkızılca volcanic (Table 1) was assessed in TAS diagram which was suggested by Le Bas et al. (1986). Lava sample located between regions of andesite-dacite and sub alkaline section is "calc-alkaline" according to Irvine and Baragar (1971) (Figure 5a).

Korucuk volcanic falls into trachydacite region in TAS diagram of Le Bas et al. (1986) in which major

Table 1- Major element contents of Yukarıkızılca and Korucuk volcanics (%)

Sample	SiO_2	Al_2O_3	Fe_2O_3	MgO	CaO	Na_2O	K_2O	TiO_2	P_2O_5	MnO	Cr_2O_3	LOI
Yukarıkızılca	60.74	16.12	5.42	2.83	5.44	2.73	2.31	0.77	0.37	0.09	0.003	2.8
Korucuk	60.18	12.61	4.60	4.28	4.56	2.11	6.27	1.28	0.77	0.08	0.029	2.8

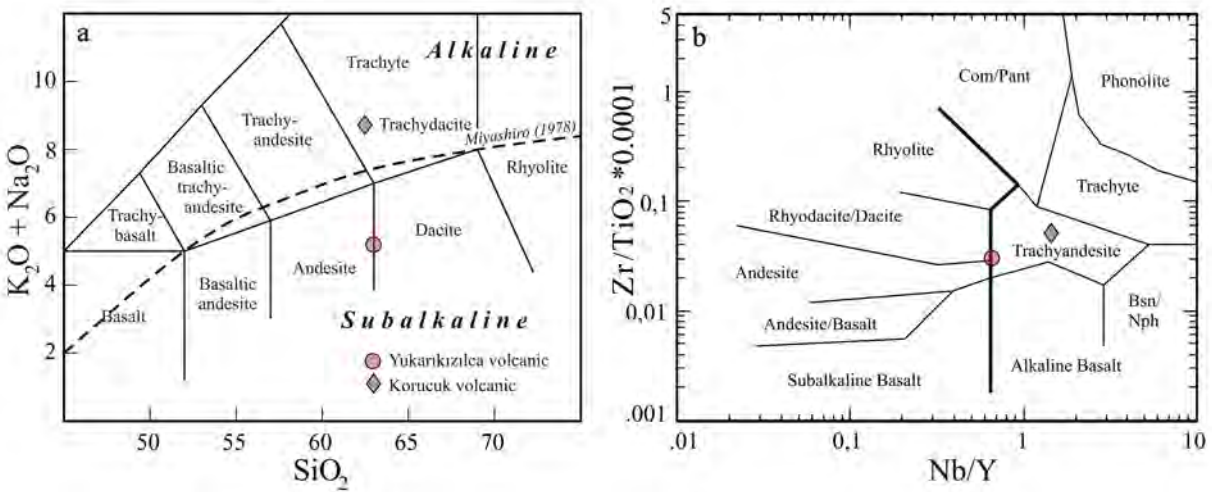

Figure 5- (a) TAS (Le Bas et al., 1986) and (b) Zr/TiO2 versus Nb/Y (Winchester and Floyd, 1977) diagrams of Yukarıkızılca and Korucuk volcanics.

element composite is assessed (Table 1) (Figure 5a). It was evaluated that this diagram gave confusing result, due to SiO_2 content (60.18%), which was oxidised by quartz xenocrytstals that had been gained by the magma mixing. In Winchester and Floyd 1977 nomenclature diagram based on stable elements (Zr: 650.0, Nb: 29.6, Y:20.2 ppm; TiO_2: %1.28), Korucuk volcanic plotted on trachyandesite region (Figure 5b) is ultrapotassic (K_2O>3%, MgO>3%, K_2O/Na_2O>2%; Foley et al.,1987) and could be named as latite.

4. Geochronology

K/Ar ages of Yukarıkızılca and Korucuk volcanics were detected as 15,6±0.6 Ma and 15,0±0,4 Ma (Table 2). Radiometric ages reflect that the intrabasin volcanism which is in similar ages activated in middle Miocene though they have different characters.

Table 2- Results of radiometric analyses of the samples taken from Yukarıkızılca and Korucuk volcanics.

Sample	Material	(%)K	$^{40}Ar_{rad(nl/g)}$	(%)$^{40}Ar_{air}$	Age (Ma)
Yukarıkızılca	%30 K-spar, %70 plagioclase	1.48	0.886	89.4	15.6±0.6
Korucuk	Biotite	7.63	4.380	62.0	15.0±0.4

Acknowledgement

This study was made within the scope of MTA Project named as "The Stratigraphy and Paleogeographic Evolution of Neogene and Quaternary Basins in Çeşme, Urla, Kemalpaşa-Torbalı Depressions; 2008-30-14-01.g". I would like to thank to Murat Yükünç (Geol. Eng., MS) who assisted during field studies and to Assoc. Prof. E. Yalçın Ersoy and Dr. H. Yavuz Hakyemez for their contributions. Major element and K/Ar analyses of samples taken from Yukarıkızılca and Korucuk volcanics were carried out in ACME laboratories (Vancouver – Canada).

Received: 24.02.2014
Accepted: 10.10.2014
Published: June 2015

References

Akdeniz, N., Konak, N., Öztürk, Z., Çakır, M.H. 1986. İzmir-Manisa dolayının jeolojisi. *Maden Tetkik ve Arama Genel Müdürlüğü* Rapor No: 7929, Ankara, (unpublished).

Foley, S.F., Venturelli, G., Green, D.H., Toscani, L. 1987. The ultrapotassic rocks: characteristics, classification and constraints for petrogenetic models. *Earth Science Reviews* 24, 81-134.

Göktaş, F. 2012. Kemalpaşa-Torbalı (İzmir) havzası ile yakın çevresindeki Neojen-Kuvaterner tortullaşması ve volkanizmasının jeolojik etüdü. *Maden Tetkik ve Arama Genel Müdürlüğü Rapor* No: *11569*, Ankara, (unpublished).

İnci, U. 1991. Torbalı (İzmir) kuzeyindeki Miyosen tortul istifinin fasiyes ve çökelme ortamları. *Maden Tetkik ve Arama Dergisi* 112, 13-26.

Irvine, N., Baragar, W.R.A., 1971. A guide to the chemical classification of the common volcanic rocks. *Canadian Journal of Earth Sciences* 8, 523–548.

Kaya, O. 1979. Orta Doğu Ege çöküntüsünün (Neojen) stratigrafisi ve tektoniği. *Türkiye Jeoloji Kurumu Bülteni* 22(1), 35-58.

Kaya, O. 1981. Miocene reference section for the coastal parts of West Anatolia. *Newsletters on Stratigraphy* 10, 164–191.

Kaya, O., Ünay, E., Göktaş, F., Saraç, G. 2007. Early Miocene stratigraphy of Central West Anatolia, Turkey: implications for the tectonic evolution of the Eastern Aegean area. *Geological Journal* 42, 85-109.

Le Bas, M.J., Le Maitre, R.W., Streckeisen, A., Zanettin, B. 1986, A chemical classification of volcanic rocks based on total alkali-silica diagram. *Journal of Petrology* 27, 745-750.

Sözbilir, H., Sarı, B., Uzel, B., Sümer, Ö., Akkiraz S. 2011. Tectonic implications of transtensional supradetachment basin development in an extension-parallel transfer zone: the Kocaçay Basin western Anatolia, Turkey. *Basin Research* 23(4), 423-448.

Steininger, F.F. 1999. Chronostratigraphy, geochrnology and biochronology of the Miocene "European Land Mammal Mega-Zones" (ELMMZ) and the Miocene "Mammal-Zones (MN-Zones)". Rössner, G. and Heissig, K. (eds). The Miocene Land Mammals of Europe, 9-24.

Winchester, J.A., Floyd, P.A. 1977. Geochemical discrimination of different magma series and their differentiation products using immobile elements. *Chemical Geology* 20, 325-343.

BULLETIN OF THE MINERAL RESEARCH AND EXPLORATION NOTES TO THE AUTHORS

1. Aims

The main aims of the journal are

- To contribute to the providing of scientific communication on geosciences in Turkey and the international community.
- To announce and share the researches in all fields of geoscience studies in Turkey with geoscientists worldwide.
- To announce the scientific researches and practices on geoscience surveys carried out by the General Directorate of Mineral Research and Exploration (MTA) to the public.
- To use the journal as an effective media for international publication exchange by keeping the journal in high quality, scope and format.
- To contribute to the development of Turkish language as a scientific language

2. Scope

At least one of the following qualifications is required for publishing the papers in the *Bulletin of Mineral Research and Exploration*.

2.1. Research Articles

2.1.1. Original Scientific Researches

- This type of articles covers original scientific research and its results related to all aspects of disciplines in geoscience.

2.1.2. Development Researches

- The studies using new approaches and methods to solve any problems related to geosciences and/or the researches using new approaches and methods to solve any problems related to the science of engineering performed in the General Directorate of Mineral Research and Exploration.

2.1.3. Review articles

- This type of papers includes comphrehensive scholarly review articles that summarize and critically assess previous geoscience reseach with a new perspective and it also reveals a new approach.

2.2. Discussion/Reply

- This type of article is intended for discussions of papers that have already been published in the latest issue of the *Bulletin.*
- The discussion/reply type articles that criticize all or a part of a recently published article, are published in the following first issue, if it is submitted within six months after the distribution of the *Bulletin*.
- The discussions are sent to the corresponding author of the original paper to get their reply, before publication. So that, the discussion and reply articles can be published at the same time, if they can be replied within the prescribed period. Otherwise, the discussion is published alone. Re- criticising of the replies is not allowed. The authors should keep the rules of scientific ethics and discussions in their discussion/reply papers. The papers in this category should not exceed four printed pages of the journal including figures and tables etc. The format of the papers should be compatible with the "Spelling Rules" of the *Bulletin.*

2.3. Short Notes

- Short notes publishing in the *Bulletin* covers short, brief and concisely written research reports for papers including data obtained from ongoing and/ or completed scientific researches and practices related to geoscience and new and/or preliminary factual findings from Turkey and worldwide.
- The short notes will follow a streamlined schedule and will normally published in the following first or second issue shortly after submission of the paper to the *Bulletin*. To meet this schedule, authors should be required to make revisions with minimal delay.
- This type of articles should not exceed four printed pages of the journal including figures, tables and an abstract.

3. Submission and Reviewing of Manuscripts

Manuscript to be submitted for publishing in the Journal must be written clearly and concisely in Turkish and/or English and it should be prepared in the *Bulletin of Mineral Research and Exploration* style guidelines. All submissions should be made online at the **http://bulletin.mta.gov.tr** website.

The authors, having no facility for online submission can submit their manuscript by post-mail to the

address given below. They should submit four copies of their manuscript including one original hard copy, and CD. The files belonging to manuscript should be clearly and separately named as "Text", "Figures" and "Tables" at the CD.

Address:
Maden Tetkik ve Arama Genel Müdürlüğü
Redaksiyon Kurulu Baflkanlığı
Üniversiteler Mah. Dumlupınar Bulvarı, No: 139
06800 Çankaya-Ankara

- The manuscript submitted for reviews has not been partially or completely published previously; that it is not under consideration for publication elsewhere in any language; its publication has been approved by all co-authors.
- The rejected manuscripts are not returned back to author(s) whereas a letter of statement indicating the reason of rejection is sent to the corresponding author.
- Submitted manuscripts must follow the *Bulletin* style and format guidelines. Otherwise, the manuscript which does not follow the journals' style and format guidelines, is given back to corresponding author without any reviewing.
- Every manuscript which passes initial Editorial treatise is reviewed by at least two independent reviewers selected by the Editors. Reviewers' reports are carefully considered by the Editors before making decisions concerning publication, major or minor revision or rejection.
- The manuscript that need to be corrected with the advices of reviewer(s) is sent back to corresponding author(s) to assess and make the required corrections suggested by reviewer(s) and editors. Authors should prepare a letter of well-reasoned statement explaining which corrections are considered or not.
- The Executive editor (Editorial Board) will inform the corresponding author when the manuscript is approved for publication. Final version of text, tables and figures prepared in the *Bulletin of Mineral Research and Exploration* style and format guidelines, will need to be sent online and the corresponding author should upload all of the manuscript files following the instructions given on the screen. In the absence of online submission conditions, the corresponding author should send four copies of the final version of the manuscript including one original hard copy, and CD by post-mail. The files belonging to manuscript should be clearly and separately named as "Text", "Figures" and "Tables" at the CD.
- To be published in the *Bulletin of Mineral Research and Exploration,* the printed lenght of the manuscript should not exceed 30 printed pages of the journal including an abstract, figures and tables. The publication of longer manuscripts will be evaluated by Editorial Board if it can be published or not.

4. Publication Language and Periods

- *The Bulletin of Mineral Research and Exploration* is published at least two times per year, each issue is published both in Turkish and English. Thus, manuscripts are accepted in Turkish or English. The spelling and punctuation guidelines of Turkish Language Instution are preferred for the Turkish issue. However, technical terms related to geology are used in accordance with the decision of the Editorial Board.

5. Spelling Draft

Manuscripts should be written in word format in A4

(29.7 x 21 cm) size and double-spaced with font size Times New Roman 10-point, margins of 25 mm at the sides, top and bottom of each page. Authors should study carefully a recent issue of the *Bulletin of Mineral Research and Exploration* to ensure that their manuscript correspond in format and style.

- The formulas requiring the use of special characters and symbols must be submitted on computer.
- Initial letters of the words in sub-titles must be capital. The first degree titles in the manuscript must be numbered and left-aligned, 10 point bold Times New Roman must be used. The second degree titles must be numbered and left-aligned, they must be written with 10 point normal Times New Roman. The third degree titles must be numbered and left-aligned, they must be written with 10 point italic Times New Roman. The fourth degree titles must be left-aligned without having any number; 10 point italic Times New Roman must be used. The text must continue placing a colon after the title without paragraph returns (See:Sample article: http://bulletin.mta.gov.tr).
- Line spacing must be left after paragraphs within text.
- Paragraphs must begin with 0.5 mm indent.
- The manuscript must include the below sections respectively;

  – Title Page

  – Abstract

– Key Words
– Introduction
– Body
– Discussion
– Conclusion
– Acknowledgements
– References

5.1-2. Title Page and Author's Adress

The title page should include:

A short, concise and informative title

The name(s) of the author(s)

The affiliation(s) and address(es) of the author(s)

The e-mail address, telephone and fax numbers of the corresponding author

The title must be short, specific and informative and written with capital letters font size Times New Roman 10-point bold. The last name (family name) and first name of each author should be given clearly. The authors' affiliation addresses (where the actual work was done) are presented below the names and all affiliations with a lower-case superscript letter is indicated immediately after the author's name and in front of the appropriate address. Provide the full postal address of each affiliation, including the country name and, if available, the e-mail address of each author.

The author who will handle correspondance at all stages of refereeing and publication, also post-publication are to be addressed (the corresponding author) should be indicated and the telephone, FAX and e-mail address given.

Please provide a running title of not more than 50 characters for both Turkish and English issue.

5.3. Abstract

- The article must be preceded by an abstract, which must be written on a seperate page as one paragraph, preferably. Please provide an abstract of 150 to 200 words. The abstract should not contain any undefined or non-standard abbreviations and the abstract should state briefly the overall purpose of the research, the principle results and major conclusions. Please omit references, criticisms, drawings and diagrams.
- Addressing other sections and illustrations of the text or other writings must be avoided.
- The abstract must be written with 10-point normal Times New Roman and single-spaced lines.
- "Abstract" must not be given for the writings that will be located in "Short Notes" section.
- English abstract must be under the title of "Abstract".

5.4. Key Words

Immediately after the abstract, please provide up to 5 key words and with each word seperated by comma. These key words will be used for indexing purposes.

5.5. Introduction

- The introdution section should state the objectives of the work, research methods, location of the study area and provide an adequate and brief background, avoiding a detailed literature survey.
- Non-standard or un-common classifications or abbreviations should be avoided but if essential, they must be defined at their first mention and used consistently thereafter.
- When needed reminder information for facilitating the understanding of the text, this section can also be used (for example, statistical data, bringing out the formulas, experiment or application methods, and others).

5.6. Body

- In this chapter, there must be data, findings and opinions that are intended to convey the reader about the subject. The body section forms the main part of the article.
- The data used the other sections such as "Abstract", "Discussions", and "Results" is caused by this section.
- While processing subject, care must be taken not to go beyond the objective highlighted in "Introduction" section. The knowledge which do not contribute to the realization of the purpose of the article or are useless for conclusion must not be included.
- All the data used and opinions put forward in this section must prove the findings obtained from the studies or they must be based on a reference by citation.
- Guidance and methods to be followed in processing subjects vary according to the characteristics of the subjects dealt with. Various phased topic titles can be used in this section as many as necessary.

5.7. Discussions

- This section should explore the significance of the results of the work, not repeat them. This must be written as a seperate section from the results.

5.8. Conclusions

- The main conclusion of the study provided by data and findings of the research should be stated concisely and concretely in this section.
- The subjects that are not mentioned sufficiently and/or unprocessed in the body section must not be included in this section.
- The conclusions can be given in the form of substances in order to emphasize the results of the research and be understandable expression.

5.9. Acknowledgements

Acknowledgement of people, grants, funds, etc should be placed in a seperate section before the reference list. While specifying contributions, the attitude diverted the original purpose of this section away is not recommended. Acknowledgments must be made according to the following examples.

- This study was carried out under the.....project.
- I/we would like to thank to …… for contributing the development of this article with his/her critiques.
- Academic and / or authority names are written for the contributions made because of ordinary task requirement.

For example:

– "Prof. Dr. ‹. Enver Altınlı has led the studies".

– "The opinions and warnings of Dr. Ercüment Sirel are considered in determining the limits of ilerdiyen layer."

- The contributions made out of ordinary task requirement:

For example:

– "I would like to thank to Professor Dr. Melih Tokay who gives the opportunity to benefit from unpublished field notes"; "I would like to thank to State Hydraulic Work 5. Zone Preliminary-Plan Chief Engineer Ethem Göğer." Academic and /or task-occupational titles are indicated for this kind of contributions.

- The contributions which are made because of ordinary task requirement but do not necessitate responsibility of the contributor must be specified.

For example:

– Such sentences as "I would like to thank to our General Manager, Head of Department or Mr. /Mrs. President ……who has provided me the opportunity to research"must be used.

5.10. References

- All references cited in the text are to be present in the reference list.
- The authors must be sure about the accuracy of the references. Publication names must be written in full.
- Reference list must be written in Times New Roman, 9-point type face.
- The reference list must be alphabetized by the last names of the first author of each work.
- If an author's more than one work is mentioned, ranking must be made with respect to publication year from old to new.
- In the case that an author's more than one work in the same year is cited, lower-case alphabet letters must be used right after publication year (for example; Saklar, 2011*a, b*).
- If the same author has a publication with more than one co-author, firstly the ones having single author are ranked in chronological order, then the ones having multiple authors are ranked in chronological order.
- In the following examples, the information related to works cited is regulated in accordance with different document/work types, considering punctuation marks as well.
- If the document (periodic) is located in a periodical publication (if an article), the information about the document must be given in the following order: surnames of the author/authors, initial letters of author's/ authors' first names. Year of publication. Name of the document. Name of the publication where the document is published (in italics), volume and/ or the issue number, numbers of the first and last pages of the document.

For example:

– Pamir, H.N. 1953. Türkiye'de kurulacak bir hidrojeoloji enstitüsü hakkında rapor. *Türkiye Jeoloji Bülteni* 4, 1, 63-68.

– Barnes, F., Kaya, O. 1963. ‹stanbul bölgesinde bulunan Karbonifer'in genel stratigrafisi. *Maden Tetkik ve Arama Dergisi* 61,1-9.

– Robertson, A.H.F. 2002. Overview of the genesis and emplacement of Mesozoic ophiolites in the Eastern Mediterranean Tethyan region. *Lithos* 65, 1-67.

- If more than one document by the same authors is cited, firstly the ones having single name must be placed in chronological order, then the ones having two names must be listed in accordance with chronological order and second author's surname, finally the ones having multiple names must be listed in accordance with chronological order and third author's surname.

- If the document is a book, these are specified respectively: surnames of the author/authors, initial letters of author's/authors' first names. Year of publication. Name of the book (initial letters are capital). Name of the organization which has published the book (in italics), name of the publication wherethe document is published, volume and/ or the issue number, total pages of the book.

For example

– Meric, E. 1983. Foraminiferler. *Maden Tetkik ve Arama Genel Müdürlüğü Eğitim Serisi* 23, 280p.

– Einsele, G. 1992. Sedimentary Basins. *Springer-Verlag*, p 628.

- If the document is published in a book containing the writings of various authors, the usual sequence is followed for the documents in a periodic publication. Then the editor's surname andinitial letters of their name /names are written. "Ed." which is an abbreviation of the editor word is written in parentheses. Name of the book containing the document (initial letters are capital). Name of the organization which has published the book (*in italics*). Place of publication, volume number (issue number, if any) of the publication where the document is published, numbers of the first and last page of the document.

For example:

– Göncüoğlu, M.C., Turhan, N., fientürk, K., Özcan, A., Uysal, fi., Yalınız, K. 2000. A geotraverse across northwestern Turkey. Bozkurt, E., Winchester, J.A., Piper, J.D.A. (Ed.). Tectonics and Magmatism in Turkey and the Surrounding Area. *Geological Society of London* Special Publication 173, 139-162.

– Anderson, L. 1967. Latest information from seismic observations. Gaskell, T.F. (Ed.). The Earth's Mantle. Academic Press. London, 335-420.

- If name of a book where various authors' writings have been collected is specified, those must be indicated respectively: book'seditor/editors' surname/surnames, and initial letters of their name/names. "Ed." which is an abbreviation of the editor word must be written in parentheses. Year of Publication. Name of the book (initial letters are capital). Name of the organization which has published the book (*in italics*), total pages of the book.

For example:

– Gaskel, T.F.(Ed.)1967. The Earth's Mantle. *Academic Press*, 520p.

- If the document is an abstract published in a Proceedings Book of a scientific activity such as conference/symposium/workshop …etc., information about the document must be given in the following order: surnames of the author/ authors, initial letters of author's/authors' first names. Year of publication. Title of the abstract. Name (in italics), date and place of the meeting where the Proceedings Book is published, numbers of the first and last pages of the abstract in the Proceedings Book.

For example:

– Yılmaz, Y. 2001. Some striking features of the Anatolian geology. *4. International Turkish Geology Symposiums,* 24-28 September 2001, London, 13-14.

– Öztunalı, Ö., Yeniyol, M. 1980. Yunak (Konya) yöresi kayaçlarının petrojenezi. *Türkiye Jeoloji Kurumu 34. Bilim Teknik Kurultayı*, 1980, Ankara, 36

- If the document is unpublished documents as report, lecture notes, and so on., information about the document must be given by writing the word "unpublished" in parentheses to the end of information about the document after it is specifiedin accordance with usual order which is implemented for a document included in a periodic publication.

For example:

– Özdemir, C. Biçen, C. 1971. Erzincan ili, İliç ilçesi ve civarı demir etütleri raporu. *General Directorate of Mineral Research and Exploration Report No: 4461*, 21 p. Ankara (unpublished).

– Akyol, E. 1978. Palinoloji ders notları. *EÜ Fen Fakültesi Yerbilimleri Bölümü*, 45 p., ‹zmir (unpublished).

- The followings must be specified for the notes of unpublished courses, seminars, and so on: name of the document and course organizer. Place of the meeting. Name of the book, corresponding page numbers.

For example:

– Walker, G. R. Mutti, E. 1973. Turbidite facies and facies associations. Pacific Section Society for Sedimentary Geology Short Course. Annaheim. Turbitides and Deep Water Sedimantation, 119-157.

- If the document is a thesis, the following are written: surname of the author, initial letter of the author's first name. Year of Publication. Name of the thesis. Thesis type, the university where it is given, the total number of pages, the city and "unpublished" word in parentheses.

For example:

– Seymen, ‹. 1982. Kaman dolayında Kırflehir Masifi'nin jeolojisi. Doçentlik Tezi, ‹TÜ Maden Fakültesi, 145 s.‹stanbul (unpublished).

- Anonymous works must be regulated according to publishing organization.

For example:

– MTA. 1964. 1/500.000 ölçekli Türkiye Jeoloji Haritası, ‹stanbul Paftası. Maden Tetkik ve Arama Genel Müdürlüğü, Ankara.

- The date, after the name of the author, is not given for on-printing documents; "in press" and / or "on review" words in parenthesis must be written. The name of the article and the source of publication must be specified, volume and page number must not be given.

For example:

– Ishihara, S. The granitoid and mineralization. Economic Geology 75th Anniversary (in press).

- Organization name, web address, date of access on web address must be indicated for the information downloaded from the Internet. Turkish sources must be given directly in Turkish and they must be written with Turkish characters.

For example:

– ERD (Earthquake Research Department of Turkey). **http://www.afad.gov.tr**. March 3, 2013.

- While specifying work cited, the original language must be used; translation of the title of the article must not be done.

6. Illustrations

- All drawings, photographs, plates and tables of the article are called "illustration".

- Illustrations must be used when using them is inevitable or they facilitate the understanding of the subject.

- While selecting and arranging the illustrations' form and dimensions, page size and layout of the *Bulletin* must be considered, unnecessary loss of space must be prevented as much as possible.

- The pictures must have high quality, high resolution suitable for printing.

- The number of illustrations must be proportional to the size of the text.

- All illustrations must be sent as separate files independent from the text.

- While describing illustrations in the text, abbreviations must be avoided and descriptions must be numbered in the order they are mentioned in the text.

- Photographs and plates must be given as computer files containing EPS, TIFF, or JPEG files in 600 dpi and higher resolutions (1200 dpi is preferred) so that all details can be seen in the stage of examination of writing.

6.1. Figures

- Drawings and photos together but not the plate in the text can be evaluated as "Figure" and they must be numbered in the order they are mentioned in the text.

- The figures published in the Bulletin of Mineral Research and Exploration must be prepared in computing environment considering the dimensions of single-column width 7.4 cm or double-column width 15.8 cm. Figure area together with the writing at the bottom should not exceed a maximum 15.8x21.

- Figures must not be prepared in unnecessary details or care must be taken not to use a lot of space for information transfer.
- Figures must be arranged to be printed in black-and-white or colored. The figure explanations being justified in two margins must be as follows: Figure 1 -Sand›kl› Town (Afyon); a) Geological map of thesouth-west, b) general columnar section of the study area (Seymen 1981), c) major neotectonic structures in Turkey (modified from Koçyiğit 1994).
- Drawings must be drawn by well-known computer programs painstakingly, neatly and cleanly.
- Using fine lines which can disappear when figures shrinks must be avoided. Symbols or letters used in all drawings must be Times New Roman and not be less than 2 mm in size when shrink.
- All the standardized icons used in the drawings must be explained preferably in the drawing or with figure caption if they are very long.
- Linear scale must be used for all drawings. Author's name, figure description, figure number must not be included into the drawing.
- Photos must have the quality and quantity that will reflect the objectives of the subject**.**

6.2. Plates

- Plates must be used when needed a combination of more than one photo and the publication on a special quality paper.
- Plate sizes must be equal to the size of available magazine pagespace.
- Figure numbers and linear scale must be written under each of the shapes located on the Plate.
- The original plates must be added to the final copy which will be submitted if the article is accepted.
- Figures and plates must be independently numbered. Figures must be numbered with Latin numerals and plates with Roman numerals (e.g., Figure1, Plate I).
- There must be no description text on Figures.

6.3.Tables

- Tables must be numbered consecutively in accordance with their appearence in the text.
- All tables must be prepared preferably in word format in Times New Roman fonts.
- Tables together with table top writing must not exceed 15x8 cm size.
- The table explanations being justified in two margins must be as follows:
- Table 1- Hydrogeochemical analysis results of geothermal waters in the study area.

7. Nomenclature and Abbreviations

- Non-standard and uncommon nomenclature abbreviations should be avoided in the text. But if essential, they must be described as below: In cases where unusual nomenclatures and unstandardized abbreviations are considered to be compulsory, the followed way and method must be described.
- Full stop must not be placed between the initials of words for standardized abbreviations (MER, SHW, etc.).
- Geographical directions must be abbreviated in English language as follows: N, S, E, W, NE …etc.
- The first time used abbreviations in the text are presented in parenthesis, the parenthesis is not used for subsequent uses.
- The metric system must be used as units of measure.
- Figure, plate, and table names in the article must not be abbreviated. For example, "as shown in generalized stratigraphic cross-section of the region (Figure 1……..."

7.1. Stratigraphic Terminology

Stratigraphic classifications and nomenclatures must be appropriate with the rules of International Commision on Stratigraphy and/or Turkey Stratigraphy Committee. The formation names which has been accepted by International Commision on Stratigraphy and/or Turkey Stratigraphy Committee should be used in the manuscript.

7.2. Paleontologic Terminology

Fossil names in phrases must be stated according to the following examples:

- For the use authentic fossil names:
- When the authentic fossil name is not used.
- Other examples of use;

  e.g. The type and species of Alveolina/ Alveolina type and species

- Taxonomic ranks must be made according to following examples:

Super family: Alveolina Ehrenberg, 1939 Family: Borelidae Schmarda, 1871 Type genus: *Borelis* de Montfort, 1808 Type species: *Borelis melenoides de Montfort, 1808*; *Nautilus melo* Fitchel and Moll, 1789	*Not reference, Not stated in the Reference section*
Borelis vonderschmitti (Schweighauser, 1951) (Plate, Figure, Figure in Body Text)	*Schweighauser, 1951 not reference*
1951 *Neoalveolina vonderschmitti* Schweighauser, page 468, figure 1-4	*Cited Scweighauser (1951), stated in the Reference section.*
1974 *Borelis vonderschmitti* (Schweighauser), Hottinger, page, 67, plate 98, figure 1.7	*Cited Hottinger (1974), stated in the Reference section.*

- The names of the fossils should be stated according to the rules mentioned below:
  - For the first use of the fossil names, the type, spieces and the author names must be fully indicated

    Alveolina aragoensis Hottinger

    Alveolina cf. Aragoensis Hottinger
  - When a species is mentioned for the second time in the text:

    A.aragoensis

    A.cf.aragoensis

    A.aff.aragoensis
  - It is accepted as citiation if stated as *Alveolina aragoensis* Hottinger (1966)
- The statment of plates and figures (especially for articles of paleontology):
  - for statment of the species mentioned in the body text

Borelis vonderschmitti (Schweighauser, 1951). (plate, figure, figure in the body text).

- When citing from other articles

  1951 Neoalveolina vonderschmitti Schweighauser, page 468, figure 1-4, figure in body text

  1974 *Borelis vonderschmitti* (Schweighauser), Hottinger, page 67, plate 98, figure 1-7
- For the citiation in the text
- (Schweighauser, 1951, page, plate, figure, figure in the body text) (Hottinger, 1974, page, plate, figure 67, plate 98, figure 1-7, figure in the bodytext.)

8. Citations

All the citiations in the body text must be indicated by the last name of the author(s) and the year of publication, respectively. The citations in the text must be given in following formats.

- For publications written by single author:
  - It is known that fold axial plain of Devonian and Carboniferious aged units around Istanbul is NS oriented (Ketin, 1953, 1956; Altınlı, 1999).
  - Altınlı (1972, 1976) defined the general characteristics of Bilecik sandstone
- For publications written by two authors:
  - The upper parts of the unit contain Ilerdian fossils (Sirel and Gündüz, 1976; Keskin and Turhan, 1987, 1989).
- For publications written by three or more authors:

According to Caner et al. (1975) Alıcı formation reflects the fluvial conditions.

The unit disappears wedging out in the East direction (Tokay et al., 1984).

- If reference is not directly obtained but can be found in another reference, cross-reference should be given as follows:

– It is known that Lebling has mentioned the existance of Lias around Çakraz (Lebling, 1932: from Charles, 1933).

9. Reprints

The author(s) will receive 5 free reprints and two hard copies of the related issues

10. Copyright and Conditions of Publication

- It is a condition of publication that work submitted for publication must be original, previously unpublished in whole or in part.
- It is a condition of publication that the authors who send their publications to the *Bulletin of Mineral Research and Exploration* hereby accept the conditions of publication of the Bulletin in advance.
- All copyright of the accepted manuscripts belong to MTA. The author or corresponding author on behalf of all authors (for papers with multiple authors) must sign and give the agreement under the terms indicated by the Regulations of Executive Publication Committee. Upon acceptance of an article, MTA can pay royalty to the authors upon their request according to the terms under the "Regulations of Executive Publication Committe" and the "Regulations of Royalty Payment of Public Office and Institutions"

All the information and forms about the *Bulletin of Mineral Research and Explorations* can be obtained from http://bulletin.mta.gov.tr